Technische Universität München

Wissenschaftszentrum Weihenstephan für Ernährung, Landnutzung und Umwelt
Holzforschung München, Professur für Holz-Bioprozesse

Plant polysaccharide perception and its molecular regulation – with a focus on pectin degradation – in *Neurospora crassa*

Nils Thieme, M.Sc.

Vollständiger Abdruck der von der Fakultät Wissenschaftszentrum Weihenstephan für Ernährung, Landnutzung und Umwelt der Technischen Universität München zur Erlangung des akademischen Grades eines

Doktors der Naturwissenschaften

genehmigten Dissertation.

Vorsitzender:	Prof. Dr. Klaus Richter
Prüfer der Dissertation:	1. Prof. Dr. J. Philipp Benz
	2. Prof. Dr. Wolfgang Liebl
	3. Prof. Dr. André Fleißner

Die Dissertation wurde am 18. April 2019 bei der Technische Universität München eingereicht und durch die Fakultät Wissenschaftszentrum Weihenstephan für Ernährung, Landnutzung, und Umwelt am 06. Juni 2019 angenommen.

Summary

The interest towards lignocellulosic biomass as an alternative feedstock to fossil oils for (bio-)refinery rose over the last decades, since the ever increasing energy demands cannot be sustainably and ecologically met by the limited deposits of crude oil. Lignocellulosic material is mostly comprised of plant cell walls, which contain the polysaccharides cellulose, hemicellulose and pectin. These polysaccharides can be broken down into fermentable sugars and converted into platform chemicals by microorganisms like filamentous fungi. However, utilization of these carbon sources is economically challenging, since their recalcitrance and complexity are hampering their fast and complete depolymerization. Rational genetic engineering can help to generate strains of filamentous fungi that can depolymerize plant cell wall polysaccharides much more efficiently. To find suitable target genes for genetic modification, our limited knowledge about fungal polysaccharide perception as well as plant cell wall degradation has to be expanded.

During this thesis work, the saprotrophic ascomycete and classical genetic model organism *Neurospora crassa* was used to examine fungal plant cell wall perception on a transcriptional level. Data of the 'Fungal Nutritional ENCODE Project', a large-scale transcriptomics study, was analyzed for patterns related to plant polysaccharide perception. The results of these analyses showed that *N. crassa* was able to differentiate the majority of the 46 tested plant cell wall-related carbon sources, with mannan(-derived saccharides) and xyloglucan as a notable exceptions. By identifying carbon catabolite repression (CCR) as well as starvation as two opposing driving forces shaping the gene expression responses in *N. crassa*, it was possible to determine the apparent nutritional value of most carbon sources by their induced transcriptional fingerprint. Moreover, using polysaccharide category (PolyCat) scores as a novel analysis method on the ENCODE data, it was possible to discern and easily visualize to which extend *N. crassa* can detect polysaccharides inside complex plant biomass. These results indicated that additional factor besides the chemical composition of the plant cell wall are affecting carbon source perception of *N. crassa*, such as substrate bioavailability, the physicochemical properties of plant biomasses and *Neurospora*'s own regulatory mechanisms.

The second part of this thesis focused on the identification and characterization of novel regulatory elements that modulate pectin degradation in *N. crassa*. By utilizing the ENCODE data together with genetic analyses, three novel $Zn(II)_2Cys_6$ transcription factors related to pectin degradation were identified. PDR-1 and PDR-2 are homologs to RhaR and GaaR in the *Aspergilli*, respectively, although they exhibited a much greater overlap in the regulation of genes involved in pectin degradation, such as those encoding pectinases, rhamnose catabolism and galacturonic acid catabolism enzymes. PDR-1 was furthermore found to be

regulated by nuclear exclusion until rhamnose is available, leading to post-translational activation and translocation into the nucleus. Besides PDR-1 and PDR-2, the orthologue to *Magnaporthe oryzae* Ara1 was found to be conserved in *N. crassa*. *Neurospora* ARA-1 is the main regulator of arabinose and galactose catabolism, even though PDR-1 and PDR-2 were found to be at least partially involved in the regulation of these processes.

In addition to the three transcription factors, a transporter protein and an F-box protein were identified to be involved in pectin perception and degradation in the present study. FRT-1 is the main transporter of the 6-deoxy-hexoses rhamnose and fucose in *N. crassa*, and it was found to be regulated on the level of expression in CCR-inducing conditions. Finally, a mutation in the F-box protein-encoding gene *frp-1* was identified to be causative for the CCR-independent pectinase hyper-secretion phenotype of the classical *N. crassa* mutant strain *exo-1* and might thus be involved in the proteolytic degradation of pectinase regulators. The additional hyper-secretion of α-amylases and invertases (but not pectinases) in Δ*frp-1* was found to be dependent on the starch regulator COL-26.

In summary, this thesis work provided novel insights into fungal polysaccharide perception and plant cell wall degradation. Based on the results of this study, the physicochemical composition of lignocellulosic biomasses significantly influences how efficiently they can be utilized by fungi. It is therefore important to determine suitable substrates based on the preferences of industrially used microorganisms to achieve the best rate of polysaccharide depolymerization. Furthermore, the identified regulatory elements are suitable targets for rational strain engineering. The transcription factors are possible targets to alter global regulation of pectinases, while a more specialized regulation can be achieved through manipulation of F-box and transport proteins.

Zusammenfassung

Das Interesse an lignocellulosischer Biomasse als Alternative zu fossilem Öl für die (Bio-)Raffinerie ist in den letzten Jahrzehnten gewachsen, da der konstant steigende Energiebedarf durch die begrenzten Vorkommen von Rohöl nicht nachhaltig und ökologisch gedeckt werden kann. Lignocellulose-haltiges Material besteht hauptsächlich aus Pflanzenzellwänden, welche die Polysaccharide Cellulose, Hemicellulose und Pektin enthalten. Diese Polysaccharide können in fermentierbare Zucker zerlegt und durch Mikroorganismen wie filamentöse Pilze in Plattformchemikalien umgewandelt werden. Die Nutzung dieser Kohlenstoffquellen ist jedoch wirtschaftlich schwierig, da ihre Rekalzitranz und Komplexität eine schnelle und vollständige Depolymerisation verhindern. Rationale Gentechnik kann helfen, Stämme von filamentösen Pilzen zu erzeugen, die Polysaccharide aus pflanzlichen Zellwänden effizienter depolymerisieren können. Um geeignete Zielgene für die genetische Modifikation zu finden, muss unser Wissen über die pilzliche Wahrnehmung von Polysacchariden sowie den Abbau von Pflanzenzellwänden erweitert werden.

Während dieser Arbeit wurde der saprotrophische Ascomycet und klassische genetische Modellorganismus *Neurospora crassa* verwendet, um die pilzliche Wahrnehmung von pflanzlichen Zellwänden auf transkriptioneller Ebene zu untersuchen. Die Daten des ‘Fungal Nutritional ENCODE Project’, einer groß angelegten Transkriptomic-Studie, wurden auf Muster im Zusammenhang mit der Wahrnehmung von pflanzlichen Polysacchariden analysiert. Die Ergebnisse dieser Analysen zeigten, dass *N. crassa* in der Lage war, die Mehrzahl der 46 getesteten pflanzenzellwandbezogenen Kohlenstoffquellen, mit Ausnahme von Mannan(-abgeleiteten Sacchariden) und Xyloglucan, zu unterscheiden. Die Identifizierung von *carbon catabolite repression* (CCR) sowie *starvation* als zwei gegensätzliche Triebkräfte der Genexpression in *N. crassa* ermöglichte es, den scheinbaren Nährwert der meisten Kohlenstoffquellen durch ihren induzierten transkriptionellen Fingerabdruck zu bestimmen. Darüber hinaus konnte mit Hilfe von *polysaccharide categories* (PolyCat) als neuartige Analysemethode für die ENCODE-Daten festgestellt und leicht visualisiert werden, inwieweit *N. crassa* Polysaccharide in komplexer pflanzlicher Biomasse detektieren kann. Diese Ergebnisse zeigten, dass zusätzliche Faktoren neben der chemischen Zusammensetzung der Pflanzenzellwand die Wahrnehmung von *N. crassa* beeinflussen, z.B. die Bioverfügbarkeit des Substrats, die physikalisch-chemischen Eigenschaften von Pflanzenbiomassen und die eigenen Regulationsmechanismen von *Neurospora*.

Der zweite Teil dieser Arbeit konzentrierte sich auf die Identifizierung und Charakterisierung neuer regulatorischer Elemente, die den Pektinabbau in *N. crassa* modulieren. Durch die

Verwendung der ENCODE-Daten in Verbindung mit genetischen Analysen wurden drei neue $Zn(II)_2Cys_6$-Transkriptionsfaktoren im Zusammenhang mit dem Pektinabbau identifiziert. PDR-1 und PDR-2 sind Homologe zu RhaR und GaaR in *Aspergillus*. PDR-1 und PDR-2 zeigten jedoch eine große Überschneidung bei der Regulation von Genen, die Pektinasen, Rhamnosekatabolismus- und Galakturonsäurekatabolismus-Enzyme kodieren und am Pektinabbau beteiligt sind. Darüber hinaus wurde festgestellt, dass PDR-1 durch den Ausschluss aus dem Nucleus reguliert ist, solange keine Rhamnose verfügbar ist. Anwesenheit von Rhamnose führt zu einer post-translationalen Aktivierung und Nucleus-Translokation von PDR-1. Neben PDR-1 und PDR-2 wurde das Ortholog zu *Magnaporthe oryzae* Ara1 in *N. crassa* identifiziert. *Neurospora* ARA-1 ist der Hauptregulator des Arabinose- und Galaktosekatabolismus, die jedoch zumindest teilweise auch von PDR-1 und PDR-2 mitreguliert werden.

Zusätzlich zu den drei Transkriptionsfaktoren wurden ein Transporterprotein und ein F-box-Protein in der vorliegenden Studie identifiziert. Diese Proteine sind ebenfalls an der Wahrnehmung und dem Abbau von Pektin beteiligt. FRT-1 ist der Haupttransporter der 6-Deoxyhexosen Rhamnose und Fucose in *N. crassa*. Die Aktivität dieses Transportproteins wird auf der Ebene der Expression reprimiert, solange CCR-induzierenden Bedingungen vorherrschen. Weiterhin wurde eine Mutation im F-box-Protein kodierenden Gen *frp-1* als ursächlich für den CCR-unabhängigen Pektinase-Hypersekretionsphänotyp der klassischen *N. crassa*-Mutante *exo-1* identifiziert. FRP-1 könnte somit am proteolytischen Abbau von Pektinase-Regulatoren beteiligt sein. Die zusätzliche Hypersekretion von α-Amylasen und Invertasen (aber nicht von Pektinasen) in Δ*frp-1* ist abhängig von COL-26, einem Regulator des Stärkeabbaus.

Zusammenfassend lässt sich sagen, dass diese Arbeit neue Erkenntnisse über die pilzliche Wahrnehmung von Polysacchariden und den Abbau von Pflanzenzellwänden lieferte. Die physikalisch-chemische Zusammensetzung von lignocellulosischen Biomassen beeinflusst maßgeblich, wie effizient diese von Pilzen genutzt werden können. Daher ist es wichtig, geeignete Substrate basierend auf den Präferenzen von industriell eingesetzten Mikroorganismen zu benutzen, um die beste Rate der Polysaccharid-Depolymerisation zu erreichen. Darüber hinaus sind die identifizierten regulatorischen Elemente geeignete Ziele für eine rationale genetische Modifikation von Produktionsstämmen. Die Transkriptionsfaktoren sind mögliche Ziele um eine Veränderung der globalen Regulation von Pektinasen zu erreichen, während die Manipulation von F-box- und Transportproteinen eine spezifischere Manipulation der pilzlichen Regulation ermöglicht.

Table of contents

List of figures

List of tables

1. Introduction

1.1. Utilizing lignocellulosic biomass for second generation biorefinery

About 50 % of the total biomass on this planet is comprised of lignocellulosic matter, a renewable organic compound that consists primarily of plant cell walls and has an estimated annual reserves of approximately 10–50 billion tons (Sánchez *et al.*, 2008; Demain, 2009; Somerville *et al.*, 2010). Therefore, lignocellulose is the most abundant biopolymer on earth and currently utilized in food, fiber, and paper industries, to name just a few. However, the interest towards lignocellulosic biomass as an alternative for crude oil extracts rose over the last decades (Werpy *et al.*, 2004; Ragauskas *et al.*, 2006; Sims *et al.*, 2010), since the ever increasing energy demands cannot be met by the limited deposits of fossil fuels (Fulton *et al.*, 2015). In addition, the societal demands for renewable and greenhouse gas neutral production of fuels, chemicals, and energy became more prominent in recent years. The production of CO_2-neutral platform chemicals could be achieved by utilizing lignocellulosic biomass in second generation biorefinery approaches (Werpy *et al.*, 2004; Fernando *et al.*, 2006; Sims *et al.*, 2010).

First generation biorefinery ferments sucrose derived from sugar cane or sugar beet, or simple sugars derived from starch to ethanol with yeast. This process has been utilized to making potable and technical alcohol for decades, but requires potential foodstuffs or animal feed as base material for the conversion (Naik *et al.*, 2010). To avoid the utilization of such material, second generation biorefinery employs lignocellulolsic feedstocks that are either agricultural waste/side products or special energy crops (Jäger and Büchs, 2012). The sugars of these feedstocks, which consists mostly of cell wall polysaccharides, can be obtained through total depolymerization of the plant cell wall by chemical and/or enzymatic hydrolysis. Afterwards, platform chemicals can be generated by specialized fermentation processes using suitable microorganisms (see Fernando *et al.*, 2006; Jäger and Büchs, 2012 for a review). However, lignocellulose rich plant cell walls have evolved to be recalcitrant to biological and physical attack. This property impedes their usage and makes the bioconversion of lignocellulosic biomass expensive (Himmel *et al.*, 2007; Lynd *et al.*, 2017). To achieve a good and economic yield of platform chemicals, all sugars of the plant cell wall have to be converted during second generation biorefinery (Naik *et al.*, 2010; Sims *et al.*, 2010).

1.2. Composition of lignocellulosic plant cell walls

Lignocellulosic plant cell walls are composed of the polyphenolic substance lignin, the three major polysaccharides cellulose, hemicellulose, and pectin, as well as numerous proteoglycans and structural proteins (Figure 1-1) (Somerville, 2004). Of the three polysaccharides, cellulose it the most abundant one (Varner and Lin, 1989). It forms highly ordered linear microfibrils, which are composed of long unbranched chains of β-1,4-linked D-glucose units that are crosslinked by hydrogen bonds (Frey-Wyssling, 1954). These microfibrils give the cell wall its tensile strength, but also increase its recalcitrance (Himmel *et al.*, 2007).

The second most abundant polysaccharides are hemicelluloses (Varner and Lin, 1989), which are branched polysaccharides that can form hydrogen bonds to the surface of cellulose fibrils (Somerville, 2004). Hemicelluloses are a group of heterogeneous polymers, e.g. xylan, xyloglucan, glucomannan and galactomannan, that contain backbones of neutral sugars. Xylan represents a major fraction of this polysaccharide group and is formed by chains of β-1,4-linked xylose, which can be substituted with arabinose, glucuronic acid, or other hexose sugars (Bastawde, 1992). The glucomannan polymer consists of β-1,4-linked D-mannopyranose and D-glucopyranose units distributed in a ratio of about 1.6:1 (Man:Glc) (Teramoto and Fuchigami, 2000). Xylans are the most abundant hemicelluloses in hard-woods, while glucomannan represents the major hemicellulose in softwoods (Timell, 1967).

The structurally and functionally most complex polysaccharides in plant cell walls are pectins, which form a matrix that embeds cellulose microfibrils and hemicellulose (Mohnen, 2008; Harholt *et al.*, 2010; Bonnin *et al.*, 2014). This makes pectin the main interconnector between plant cell wall polysaccharides and allows this structure to be load baring (Dick-Pérez *et al.*, 2011). The most abundant backbone monosaccharide of pectin it the charged D-galacturonic acid, which can comprise up to 70% of this polysaccharide (Caffall and Mohnen, 2009). A polymer of α-1,4-linked galacturonic acid is called homogalacturonan (HG), while xylogalacturonans (XGA) are HG polymers decorated by D-xylose residues. The most structurally complex HG derivative is called rhamnogalacturonan-II (RG-II), which comprises four conserved side chains formed by 12 different monosaccharide constituents (O'Neill *et al.*, 2004). Rhamnogalacturonan-I (RG-I), the second most abundant pectin domain, is formed by alternating D-galacturonic acid and L-rhamnose residues, which are decorated to about 50% with side chains made of L-arabinose, D-galactose or both (arabinogalactan) (Caffall and Mohnen, 2009; Harholt *et al.*, 2010).

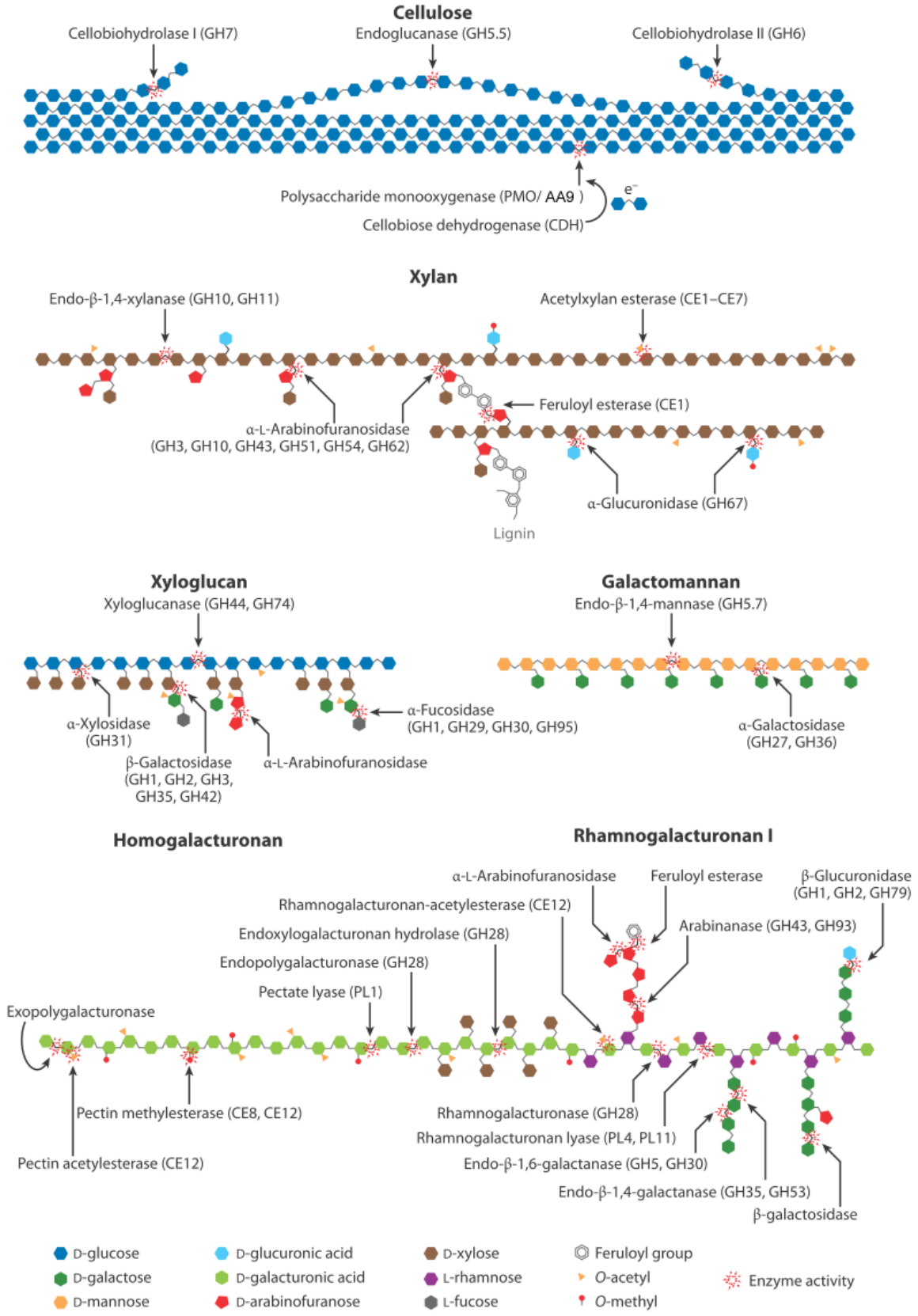

Figure 1-1: Chemical composition of plant cell wall polysaccharides and the enzyme activities required for their degradation.

Enzyme activities are represented by major CAZy classes on the plant cell wall polysaccharides cellulose, hemicellulose (xylan, xyloglucan, galactomannan), and pectin (homogalacturonan and rhamnogalacturonan I). This figure was modified from Glass *et al.*, 2013b.

In addition to their heterogenicity in monosaccharide composition, pectins are further modified by associated (Qi *et al.*, 1995) or structural proteoglycans (Tan *et al.*, 2013). Moreover, the domain-ratio and the number of modifications of pectin are highly variable (Vincken *et al.*, 2003; Chung *et al.*, 2014).

Plant cell walls are commonly differentiated into two developmental stages, primary and secondary plant cell walls (Keegstra, 2010). Primary cell walls are rich in pectin and can be found in still growing cells as well as fruits and leaves. Secondary plant cell walls are thickened structures that contain lignin and are composed predominantly of cellulose and hemicelluloses (Albersheim *et al.*, 1996). A connecting layer between plant cells is formed by the middle lamella, which is integral for cell growth and morphogenesis. The major polysaccharides of the middle lamella are pectins (Daher and Braybrook, 2015; Anderson, 2016). Together, the plant polysaccharides form a complex meshwork that confers rigidity to the plant cell wall and allows it to fulfil its multiple essential functions for the plant (Somerville, 2004; Popper *et al.*, 2011).

1.3. *Neurospora crassa* as plant cell wall degrading organism

Only a small fraction of microorganisms is capable of efficiently degrading lignocellulosic biomass. Among fungi, basidiomycete and ascomycete species play a dominant role in the biodegradation of plant cell wall polysaccharides. A suitable organism to study plant cell wall degradation is the saprotrophic ascomycete *Neurospora crassa* (Figure 1-2), which is able to enzymatically depolymerize plant cell walls and utilize the released monosaccharides as its sole carbon source (Tian *et al.*, 2009). This filamentous fungus is part of the Sordariomycetes and has been described some years ago as endophyte and opportunistic pathogen of Scots pine (*Pinus sylvestris*) (Kuo *et al.*, 2014). *N. crassa* is well established in research, as it was already used by Beadle and Tatum to prove the Nobel Prize winning “one-gene-one-enzyme” hypothesis (Beadle and Tatum, 1941). To this day, *N. crassa* research provides valuable new insights in genome defense systems (Selker, 1990), mitochondrial genetics (Griffiths *et al.*, 1995), photobiology and circadian rhythms (Linden *et al.*, 1997; Dunlap and Loros, 2006), cell

Figure 1-2: Growth phenotype of *N. crassa* wild-type strain on sucrose medium.

development and differentiation (Davis, 2000), DNA methylation (Freitag and Selker, 2005), cell-cell fusion (Fleissner *et al.*, 2008) as well as polar growth (Riquelme *et al.*, 2011).

The fully sequenced haploid genome of *N. crassa* has a size of more than 40 megabases (Galagan *et al.*, 2003) and is comprised of approximately 10,000 protein-coding genes, which have little redundancy (Borkovich *et al.*, 2004; Galagan and Selker, 2004). In addition, a nearly full genome deletion strain set of *N. crassa* (Dunlap *et al.*, 2007) is publicly available at the Fungal Genetics Stock Center (FGSC) (McCluskey *et al.*, 2010; Roche *et al.*, 2014). These resources have proven to be invaluable tools for the research of plant cell wall degradation in *N. crassa*.

Neurospora has the ability to secrete all necessary enzymes for a complete degradation of lignocellulose biomass (Dogaris *et al.*, 2013) and an updated list of carbohydrate-active enzymes (CAZy; Cantarel *et al.*, 2009) acting on plant cell wall polysaccharides was recently been published (Wu, 2017; Wu *et al.*, 2019). The following section contains a brief overview of the lignocellulolytic enzyme classes secreted by *N. crassa* during plant cell wall degradation (Figure 1-1).

Cellulose is depolymerized by endo- and exo-glucanases/cellobiohydrolases through hydrolytical cleavage inside the glucose chain (endo-glucanases) or the release of cellobiose form the terminal region of the polymer (exo-glucanases). The released cellobiose molecules are cleaved into single glucose molecules by β-glucosidases (van den Brink and de Vries, 2011). Additionally, polysaccharide monooxygenases (PMOs) cleave cellulose oxidatively rather than hydrolytically and can function on all parts of the glucan chain. They require copper, molecular oxygen and an election donor for proper function (Harris *et al.*, 2010; Phillips *et al.*, 2011; Beeson *et al.*, 2012).

Xylanases act on the xylan portion of hemicelluloses and are comprised of endo-xylanases that cleave inside the backbone and β-xylosidases that cleave xylose oligomers into xylose. Acetyl moieties that decorate the xylan backbone are processed by acetyl xylan esterases (van den Brink and de Vries, 2011). Glucomannan is hydrolyzed by glucanases and endo-mannanases into (gluco-)mannodextrins, which are further cleaved into their constituent monosaccharides by β-mannosidases (Moreira and Filho, 2008). Besides these enzymes, a number of additional enzymatic activities are required during hemicellulose and pectin degradation, including endo- and exo-arabinanases, β-arabinosidases, α-arabino-furanosidases, arabinogalactan endo-1,4-β-galactosidases, β-galactosidases, endo-β-1,6-galactanases, β-glucuronidases, α-glucuronidases as well as feruloyl esterases (van den Brink and de Vries, 2011; Glass *et al.*, 2013b).

Endo- and one exo-polygalacturonases are active on the HG-backbone of pectin by cleaving either inside the polymer or at accessible non-reducing ends, respectively. Endo-polygalacturonases release oligogalacturonides, while exo-polygalacturonases generate

galacturonic acid monosaccharides through enzymatic hydrolysis. Pectin methylesterases catalyze the de-esterification of pectin into pectate and methanol. Pectate and pectin lyases perform an eliminative cleavage of either pectate or pectin, respectively (van den Brink and de Vries, 2011; J. P. Benz *et al.*, 2014). While endo-and exo-polygalacturonases have their optimum catalytic activity in acidic pH, pectate and pectin lyases exhibit optimal performance at alkaline pH levels. Rhamnogalacturonan lyases, rhamnogalacturonan acetylesterases and unsaturated rhamnogalacturonyl hydrolases are required to break down the RG-I backbone of pectin (van den Brink and de Vries, 2011; J. P. Benz *et al.*, 2014).

1.4. Polysaccharide perception and regulation of plant cell wall degradation

Plant cell wall degradation is an immense commitment for fungi, since they have to allocate vast quantities of resources to its degradation. For that reason, if an easier to metabolize substrate like glucose is available, it will be utilized preferentially, while the polysaccharide degradation machinery will be turned off (Ronne, 1995; Ruijter and Visser, 1997; Gancedo, 1998; Aro *et al.*, 2005). This process is accordingly named carbon catabolite repression (CCR) and is present in most fungi, including *N. crassa* (Ebbole, 1998; Sun and Glass, 2011; Sun *et al.*, 2011). The conserved zinc-finger transcription factor Mig1/CreA/CRE1/CRE-1 mediates CCR in ascomycetes and basidiomycetes primarily through the repression of lignocellulolytic genes (Nehlin and Ronne, 1990; Dowzer and Kelly, 1991; Ilmén *et al.*, 1996; Ruijter *et al.*, 1997; Ebbole, 1998; Janus *et al.*, 2008; Sun and Glass, 2011; Yoav *et al.*, 2018). In *N. crassa*, CRE-1 regulates genes involved in cellulose and xylan utilization by directly binding to motifs in promoter regions of its regulated genes (Sun and Glass, 2011; Sun *et al.*, 2012; Znameroski *et al.*, 2012), which probably leads to a promoter binding competition between CRE-1 and positive regulatory factors (Sun and Glass, 2011). Furthermore, it is hypothesized that CRE-1 and its orthologues in other ascomycetes act in a so called “double-lock” manner by repressing the expression of genes encoding lignocellulolytic enzymes as well as the genes encoding their transcriptional activators (Kulmburg *et al.*, 1993; Mathieu and Felenbok, 1994; Orejas *et al.*, 1999; Tamayo *et al.*, 2008; Sun and Glass, 2011).

The degradation of complex organic matter like plant cell walls requires the release of large quantities of enzymes with different catalytic activities. However, the present carbon sources, e.g. polysaccharides, have to be identified and differentiated before fungi can express the necessary enzymes. The perception of plant polysaccharides in the extracellular space around the fungi is a three phase process (Tian *et al.*, 2009; Delmas *et*

al., 2012; Ries *et al.*, 2013). When switching fungi from one nutritional condition to another, such as from glucose to lignocellulose, fungi will initially enter a state of carbon starvation, in which the transcriptome has to be released from CCR, leading to **(1) de-repression** of a large array of genes including lignocellulolytic enzymes and various sugar transporters (Figure 1-3) (Sun and Glass, 2011; Znameroski *et al.*, 2012). These enzymes and transporter proteins will be expressed in low quantities and, in the case of lignocellulolytic enzymes, will then be secreted into the environment, where they act as 'scouts' to detect new carbon sources (Znameroski *et al.*, 2012; Coradetti *et al.*, 2013; Cai *et al.*, 2014; J. P. Benz *et al.*, 2014). If the enzymes come into contact with plant biomass during this **(2) scouting phase**, they start to slowly degrade it, releasing small soluble mono- and disaccharides in the process. These soluble sugars can be taken up by the expressed sugar porters and can then act as inducing molecules, informing the fungus about the carbon sources in its proximity and inducing transcription of corresponding degradation pathways (Sun and Glass, 2011; Sun *et al.*, 2012; Znameroski *et al.*, 2012, 2014; J. Benz *et al.*, 2014; J. P. Benz *et al.*, 2014). During this **(3) initiation phase**, the fungus adapts its metabolic response towards the detected polysaccharides, for example by strongly up-regulating the expression of specific enzymes and transporter proteins (Sun *et al.*, 2011, 2012; Znameroski *et al.*, 2012; Znameroski and Glass, 2013; J. P. Benz *et al.*, 2014; Lian *et al.*, 2014).

The information that a new carbon source was detected during the scouting phase gets transmitted by so far unknown signaling cascades to transcription factors. These transcription factors act as regulators that either enhance or repress gene expression based on the information received (Aro *et al.*, 2005). *N. crassa* encodes about 200 predicted transcription factors (Galagan *et al.*, 2003; Borkovich *et al.*, 2004; Shiu *et al.*, 2005), of which 178 contain a known DNA-binding motif, while the remaining 22 transcription factors may contain a non-canonical DNA-binding motif. These motifs can be divided into six families: the basic helix-loop-helix (bHLH), bZIP, C2H2 zinc finger, GATA factor, Myb and zinc binuclear cluster families (Tian *et al.*, 2011). The majority of published transcription factors involved in plant cell wall degradation are part of the $Zn(II)_2Cys_6$ (zinc binuclear cluster) family (see Huberman *et al.*, 2016; Seibert *et al.*, 2016; Benocci *et al.*, 2017 for a review).

Genes involved in the degradation of cellulose are regulated by three transcription factors of the $Zn(II)_2Cys_6$ family in *N. crassa* (Figure 1-4) (Coradetti *et al.*, 2012; Liu *et al.*, 2018). Two of these transcriptional activators, named cellulose degradation regulators 1 and 2 (CLR-1 and CLR-2), act together to regulate the majority of the cellulase gene expression (Coradetti *et al.*, 2012). The activity of CLR-1 is repressed in the absence of an inducer molecule by the repressor protein CLR-3 through an so far unknown mechanism

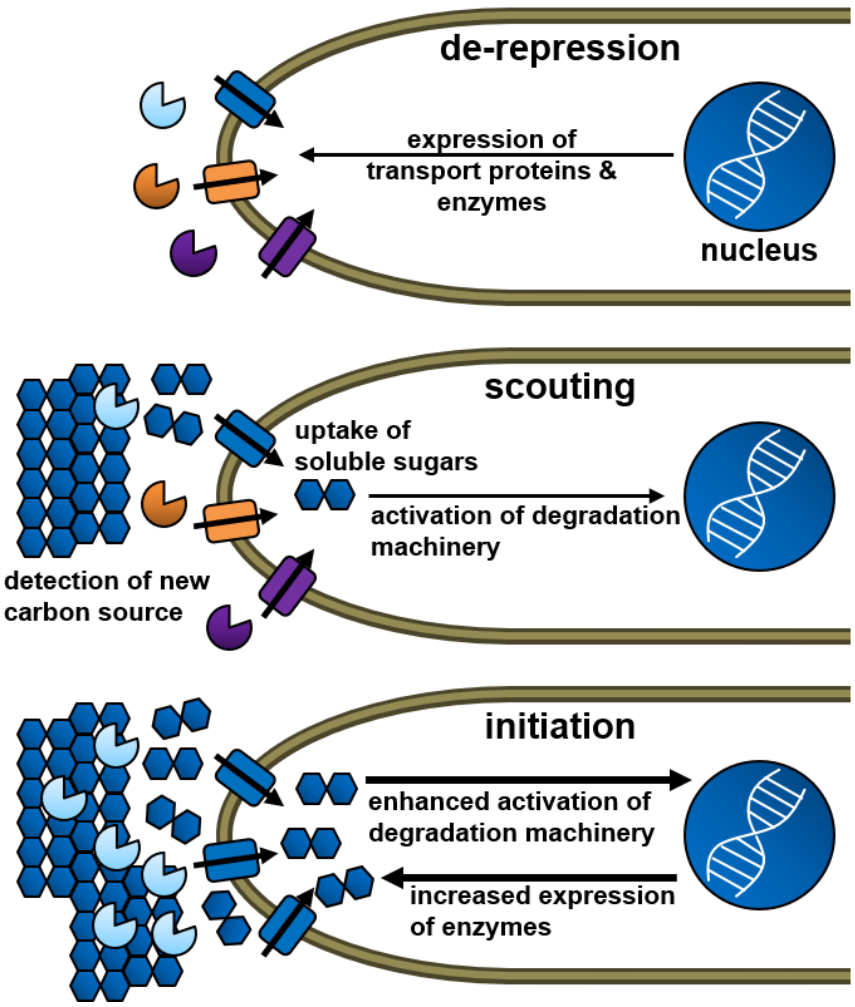

Figure 1-3: Schematic depiction of the three phases during fungal carbon source perception. During a phase of starvation, a small set of genes encoding transport proteins and lignocellulolytic enzymes get de-repressed. The secreted enzymes act as 'scouts' by depolymerizing any suitable carbon source in the environment of the fungus. They release soluble sugars that are transported into the cell where they induce the respective degradation machinery. This initiation process increases the expression of more genes related to the depolymerization of the found polysaccharide(s).

(Huberman *et al.*, 2017). Cellobiose, an inducer of lignocellulolytic enzyme expression (Znameroski *et al.*, 2012), is released during cellulose degradation and afterwards transported into the cell through the cellodextrin transporters 1 and 2 (CDT-1 and CDT-2) (Tian *et al.*, 2009; Galazka *et al.*, 2010; Ha *et al.*, 2010), which might act as transceptors to activate CLR-1 (Znameroski *et al.*, 2014). Moreover, presence of cellobiose releases CLR-1 from CLR-3 repression (Huberman *et al.*, 2017). CLR-1 then enhances the expression of its target genes, which include several genes necessary for efficient import and utilization of cellobiose as well as *clr-2* (Coradetti *et al.*, 2012; Craig *et al.*, 2015). CLR-2 is a constitutively active transcription factor that enhances the expression of the majority of cellulase as well as some hemicellulase genes (Coradetti *et al.*, 2012, 2013; Craig *et al.*, 2015). Recently, CLR-4 was described as an additional activator of cellulase transcription

in *N. crassa* (Liu *et al.*, 2018). This transcription factor directly binds to the promoter regions of *clr-1* as well as the cAMP signaling pathway adenylyl cyclase gene *cr-1*. This suggests that CLR-4 is a pivotal regulator for cellulolytic gene expression as well as the cAMP

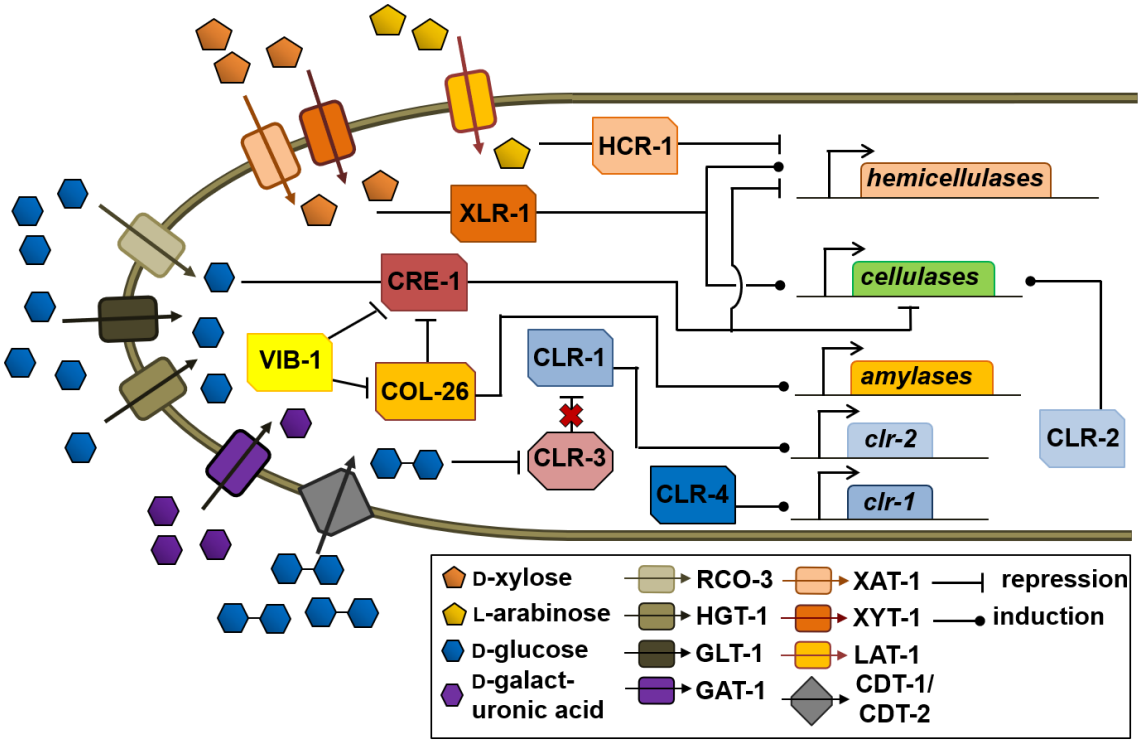

Figure 1-4: Model of regulators that mediate plant cell wall degradation in *N. crassa*. Glucose is taken up by the transport proteins RCO-3, GLT-1, HGT-1 and HGT-2, which leads to CRE-1 mediated CCR (down-regulation of cellulase and hemicellulase gene expression). Cellobiose is transported into the cell through CDT-1/CDT-2 and stops the repression of CLR-1 through CLR-3. CLR-1 activates the expression of CLR-2, which in turn enhances the expression of cellulase genes. CLR-4 directly binds the promoter region of *clr-1*, which leads to elevated expression levels of this gene. XLR-1 and HCR-1 regulate the expression of hemicellulases as activator or repressor, respectively. The activity of these transcription factors may be induced by the presence of arabinose or xylose, respectively. These monosaccharides are transported into the cell through XYT-1 and XAT-1 (xylose) or LAT-1 (arabinose). VIB-1 represses CRE-1 mediated CCR together with COL-26. COL-26 also enhances the expression of starch degradation genes (e.g. amylases). COL-26 also influences cellulase expression according to glucose levels, which is modulated by VIB-1. There are no transcription factors described in literature that regulate pectin degradation, although a galacturonic acid transporter (GAT-1) is published for *N. crassa* and the organism is able to utilize pectin as sole carbon source. This figure was modified from Seibert *et al.*, 2016.

pathway.

A Zn binuclear cluster transcription factor called xylan degradation regulator 1 (XLR-1) was essential for hemicellulose degradation in *N. crassa* (Sun *et al.*, 2012). XLR-1 is activates the expression of xylanases and was also necessary for a wild-type-like utilization of xylose. In contrast, the C2H2 family transcription factor hemicellulase regulator 1 (HCR-1) is a repressor of hemicellulase gene expression, as a deletion strain of *hcr-1* showed a significant up-regulation of a small number of hemicellulase genes (Li *et al.*, 2014).

Intriguingly, no regulator of (gluco-/galacto-)mannan degradation was found in *N. crassa* to this date. Expression studies by Tian *et al.* showed that mannanase genes were instead expressed after induction with the micro-crystalline cellulose Avicel (Tian *et al.*, 2009).
The transcription factors vegetative incompatibility blocked 1 (VIB-1) and colonial 26 (COL-26) influence CCR and cellulase gene expression in *N. crassa* (Xiong *et al.*, 2014). VIB-1 was originally described as a regulator of extracellular protease secretion in response to both carbon and nitrogen starvation as well as a mediator of non-self-recognition and cell death (Xiang and Glass, 2002; Dementhon *et al.*, 2006). COL-26 was described to be involved in glucose sensing of *N. crassa* as well as being essential for starch degradation and integration of carbon and nitrogen metabolism (Xiong *et al.*, 2014, 2017). Xiong *et al.* hypothesized that VIB-1 and COL-26 act at the induction stage of the cellulolytic response as negative regulators of CRE-1 mediated CCR (Xiong *et al.*, 2017). Later on, the glucose released during cellulose degradation leads to a repression of the cellulolytic response through COL-26. This regulation is then counteracted by VIB-1. Therefore, COL-26 may influence the strength of cellulase expression based on cytosolic glucose levels, while VIB-1 could be a global repressor of CCR by suppressing CRE-1 and COL-26 activity.
There are no regulators for pectin degradation described for *N. crassa* in published literature. However, the complexity of pectin as substrate indicates that an equally complex regulatory system is required to achieve complete depolymerization of this polysaccharide (Martens-Uzunova and Schaap, 2009). Indeed, over the last few years a number of specialized transcription factors were identified in other fungi, which regulate parts of the pectin degradation machinery. TRC1 and RhaR regulate rhamnose catabolism in *Pichia stipitis*, *Aspergillus niger* and *Aspergillus nidulans* (Koivistoinen *et al.*, 2012; Gruben *et al.*, 2014; Pardo and Orejas, 2014). Furthermore, *Aspergillus* RhaR also regulates some rhamnosidases (Gruben *et al.*, 2014; Pardo and Orejas, 2014). The transcription factor GaaR is a regulator of HG degradation and galacturonic acid utilization in *Botrytis cinerea* and *A. niger* (Alazi *et al.*, 2016; Zhang *et al.*, 2016), while the arabinose catabolism is either regulated by AraR in *A. niger* (Battaglia *et al.*, 2011a) or Ara1 in *Magnaporthe oryzae* (Klaubauf *et al.*, 2016).

1.5. Aims of this study

The complete depolymerization of lignocellulosic biomass is necessary for an economically affordable production of platform chemicals through biorefinery. To this date, the majority of fungal strains used for the production of hydrolytical enzymes were created by random mutagenesis. Although their production yields were further refined through process engineering, the rate of improvements is slowing down. Increasing the production of

hydrolytic enzymes in these organisms by further undirected evolution is difficult due to the accumulation of undesired secondary effects in the background. A rational engineering of production strains is advisable, because not only could this method lead to improved production yields, but it may also make the production process more manageable. Understanding how fungi detect new carbon sources and modulate their metabolism to utilize them is therefore crucial for further genetic modification of industrially used strains.

However, fungal polysaccharide perception as well as plant cell wall degradation are complex processes and our knowledge about them is still limited. To address these issues, the 'Fungal Nutritional ENCODE Project' was funded in 2013 by the Joint Genome Institute (Glass *et al.*, 2013a). This project comprised large-scale analyses of the transcriptional changes elicited in *N. crassa* by over 45 different plant cell wall related carbon sources. The vast amounts of data generated by this transcriptomics study were analyzed to identify polysaccharide specific expression patterns and novel regulatory elements as potential targets for rational strain engineering.

In the present study, the ENCODE data are going to be analyzed to determine major driving forces of plant biomass perception in *N. crassa* as well as visualize the response of *Neurospora* to cell wall polysaccharides. To achieve these tasks, principal component analyses (PCA) coupled with correlation analyses will be applied to the ENCODE data, which should reveal if there are carbon source specific responses elicited in *N. crassa*. Furthermore, these methods should show if there are major driving forces of expression across the used carbon sources that affect *Neurospora*. In addition, a novel method called polysaccharide category (PolyCat) scores will be utilized in this work to visualize which polysaccharides *N. crassa* is able to perceive inside complex plant cell walls. To corroborate the results that are based on transcriptome data, hierarchical clustering using either Pearson's correlation or Euclidean distance will be performed in addition to any other method.

The second part of this thesis is focused on the identification and characterization of novel regulatory elements that modulate pectin degradation. By utilizing the ENCODE data together with genomics approaches and the large genetic toolbox of *N. crassa*, so far unknown factors that influence pectin depolymerization should be determined. The *N. crassa* gene deletion strain set will be tested to find mutant strains that exhibit growth defects on pectin or pectin related carbon sources. Co-expression analyses and phylogenetic studies will be employed to determine regulatory elements that are coregulated with published pectinase genes. Detected regulators of pectin degradation will be rigorously tested through biochemical assays, monosaccharide uptake studies as well as real-time quantitative PCR. In addition, complementation and subcellular localization studies will be performed to further characterize regulatory elements where necessary.

2. Results

2.1. Transcriptional response during perception of carbon sources by *N. crassa*

Applying a large-scale transcriptomic approach, the 'Fungal Nutritional ENCODE Project' was aimed to create high-resolution models of the gene regulatory network steering the metabolic response of the model filamentous fungus *Neurospora crassa* to plant biomass (Glass *et al.*, 2013a). As such, it presents a wealth of information about the transcriptional adaptation of *N. crassa* to mono-, di-, and polysaccharides, as well as lignocellulosic biomass from grasses and woods (OTable 01). To gather these data, the *N. crassa* WT strain was induced for 4 h with one of 49 different carbon sources, such as plant polysaccharides or mono- and disaccharides that are building blocks of these polysaccharides, prior to RNA-Seq. In addition, the transcriptional starvation response of *N. crassa* (induction on medium with no carbon source) and response to an abundance of easy to metabolize sugars (2% sucrose) were measured as control conditions. While first results from these data have already been published (Hurley *et al.*, 2014; Thieme *et al.*, 2017), the most detailed analyses so far were performed by Vincent Wu (Wu, 2017), focusing on several main regulators of plant cell wall degradation (Wu *et al.*, 2019).

2.1.1. Determination of identifier genes using ENCODE data

The fungal transcriptional ENCODE data were used to analyze how the transcriptional response of *N. crassa* changes when it is confronted with complex plant biomass (e.g. grasses and woods). Since most of the plant cell wall polysaccharides are present in different concentrations (Varner and Lin, 1989), expression changes in *N. crassa* may be focused around the most abundant carbon source. Moreover, the bio-availability of these carbon sources could play a crucial role during detection of different substrates (Mansfield *et al.*, 1999; Peciulyte *et al.*, 2014; Hassan *et al.*, 2017). Concealed or recalcitrant polysaccharides may release fewer inducing molecules, masking their own presence in the biomass to the fungus.

Customarily, the transcriptional reaction of a fungus to lignocellulosic material is characterized by genes coding for lignocellulose-degrading enzymes, sugar transporters and transcription factors to a small set of related carbon conditions (Gruben *et al.*, 2017; Samal *et al.*, 2017; Wu *et al.*, 2019). However, the precise conditions leading to expression of these genes across the "chemical space" of plant cell wall components are not known for the majority of them. Moreover, the function of most of these proteins is usually inferred

through annotation based on protein domains, structure and/or sequence (Ashburner *et al.*, 2000; Lombard *et al.*, 2014; Weirauch *et al.*, 2014; Saier *et al.*, 2016; The Gene Ontology Consortium, 2017; El-Gebali *et al.*, 2019), with the function of some proteins being confirmed through physiological, bio-chemical or systems-level analyses (Samal *et al.*, 2017).

Taken together, the marker genes for polysaccharide perception that are described in literature are not sufficient to achieve a complete overview of how *N. crassa* perceives complex plant biomass. Therefore, the data generated by the 'Fungal Nutritional ENCODE Project', covering most of the sugar-based "chemical space" present in the plant cell wall, were screened *de novo* for genes that could be used to visualize the expression response ("perception") of *N. crassa* to plant biomass, irrespective of their putative function or role. To determine these **identifier genes**, the following prerequisites were applied:

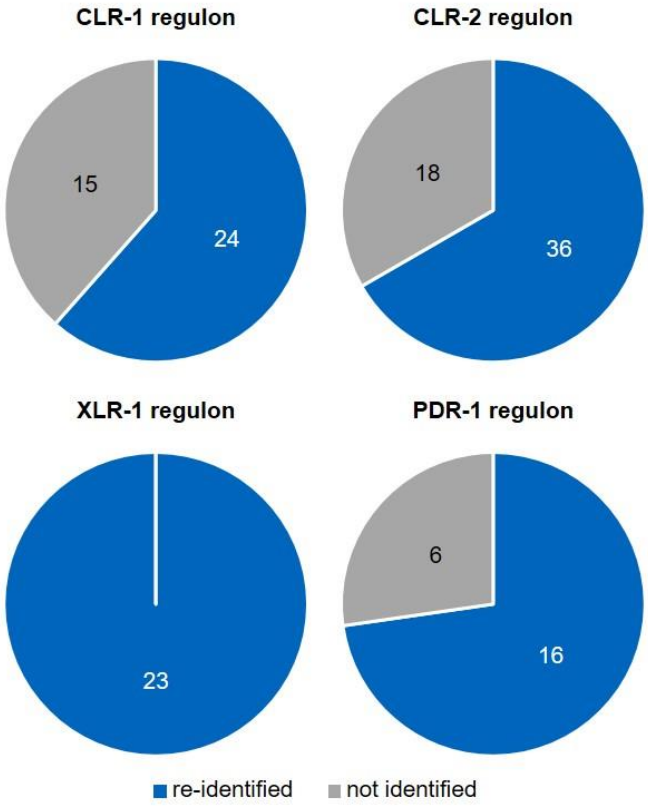

Figure 2-1: Overlap between known regulons and corresponding identifier genes.
The published target genes of CLR-1, CLR-2, XLR-1 and PDR-1 were compared against PolyCat identifier genes. CLR-1 and CLR-2 target genes were compared with identifier genes of the cellulose PolyCat. XLR-1 target genes were compared with xylan PolyCat identifier genes and PDR-1 target genes were compared to pectin PolyCat identifier genes.

Firstly, these identifier genes should be strongly expressed and their relative expression compared to no carbon (NoC) control should be significantly increased after induction with a relevant carbon source. Furthermore, the expression of these genes should be up-regulated specifically on carbon sources related to one specific polysaccharide. Application of these parameters should enrich the identifier gene sets for genes encoding proteins involved in other relevant processes that are activated during plant cell wall degradation besides polysaccharide catabolism, e.g. signaling, secretion or homeostasis.

Secondly, fungi can differentiate between polysaccharides and adapt their metabolism on transcriptional and protein levels. While most of the signaling cascades leading to

expression changes are unknown in fungi, specific regulators for cellulose, hemicellulose, pectin and starch degradation are described in published literature (Glass *et al.*, 2013b; Huberman *et al.*, 2016; Benocci *et al.*, 2017; Alazi and Ram, 2018). Therefore, it can be expected that *N. crassa* expresses a specific set of genes for each carbon source it is confronted with.

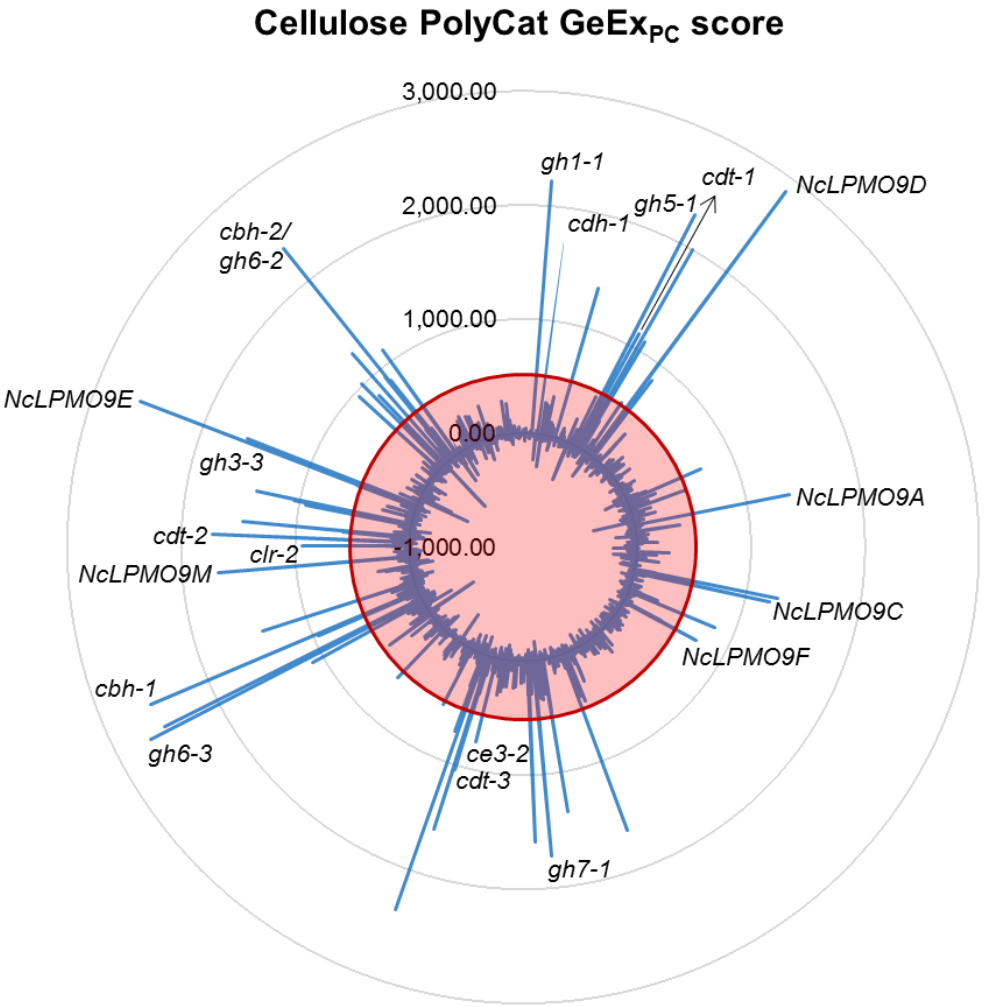

Figure 2-2: Exemplary determination of identifier genes for cellulose via cellulose PolyCat GeEx scores.
The red line represents the minimum threshold (4 x SD). All genes inside the red area were not considered specific enough to be an identifier gene. Published CAZy-encoding genes, cellodextrin transporter genes and the *clr-2* gene are indicated.

A set of **polysaccharide categories** (**PolyCats**) was defined to find genes that fulfill these prerequisites. These PolyCats should represent the main polysaccharides a fungus can encounter in a plant cell and were chosen based on the known chemical composition of plant cell walls. Therefore, PolyCats for cellulose, xylan, xyloglucan, mannan(s), pectin and starch were determined (Figure 5-2). ENCODE carbon source conditions were assigned to each PolyCat, if they were related to the respective represented polysaccharide (e.g. the PolyCat “cellulose” comprised: cellobiose as a cellulose degradation product and signaling

molecule, the commercial micro-crystalline cellulose Avicel and bacterial cellulose; Table 5-18).

A subset of 28 ENCODE carbon conditions, consisting of all mono-, di- and polysaccharides, was used to search for genes specifically up-regulated on the individual PolyCat carbon sources. A **gene expression** (**GeEx**) **score** was calculated for each gene in each PolyCat, which took into account differential expression over NoC and overall expression strength of the genes.

Genes that had an up-regulated gene expression exclusively on the conditions that formed a PolyCat achieved a higher score than genes that were also strongly expressed on other carbon sources (OTable 02). Only genes that passed an applied minimum GeEx score threshold were considered to represent valid and appropriate identifier genes. STable 6-1 contains the PolyCats and their respective identifier genes. A total of 362 identifier genes were found for all PolyCats; of these were 45 genes associated with the PolyCat cellulose, 35 genes with xylan, 62 genes with xyloglucan, 84 genes with mannan, 63 genes with pectin and 73 genes with starch.

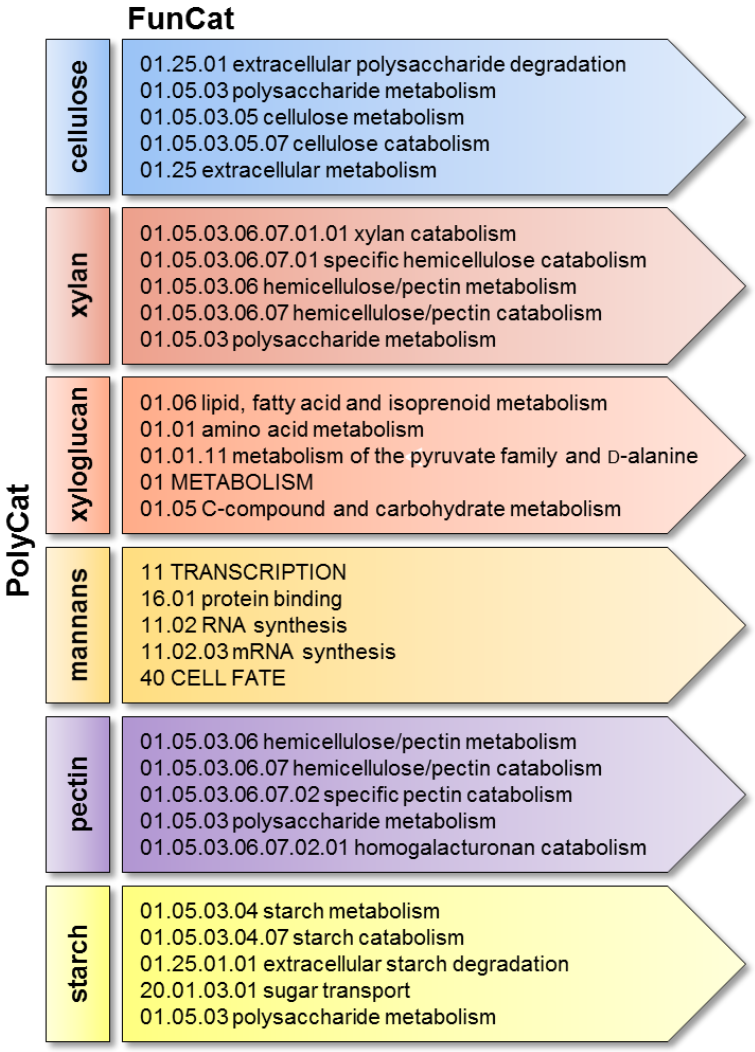

Figure 2-3: Gene enrichment analysis of PolyCat identifier genes.
Expanded FunCats were used to detect significant gene enrichments in the PolyCat identifier genes. The five most significantly enriched categories are presented in this figure for each PolyCat. The complete enrichment data can be found in OTable 03.

The identifier genes of the cellulose, xylan and pectin PolyCats were compared against the published regulons of CLR-1, CLR-2, XLR-1 and PDR-1 (Craig *et al.*, 2015; Thieme *et al.*, 2017) (Figure 2-1). The cellulose PolyCat identifier genes comprised 61.5% and 66.7% of

the genes in the CLR-1 and CLR-2 regulons, respectively. All genes of the XLR-1 regulon were found in the identifier genes of the xylan PolyCat and 72.7% of the genes comprising the PDR-1 regulon were also part of the pectin PolyCat identifier genes.

In addition, manual annotation of the cellulose PolyCat identifier genes based on previously published data (Craig *et al.*, 2015; Samal *et al.*, 2017; Wu *et al.*, 2019) showed that the majority of cellulases, cellodextrin transporters and the transcription factor gene *clr-2* were among the most specific and strongest expressed genes (Figure 2-2). Similar observations could be made for hemicellulases, pectinases and amylases in the xylan, pectin and starch PolyCats, respectively (OTable 02).

Furthermore, an enrichment analysis using expanded functional categories (FunCat; Figure 5-1; Ruepp, 2004; Thieme *et al.*, 2017) displayed that identifier genes of the cellulose, xylan, pectin and starch PolyCats were significantly enriched in the categories of extracellular polysaccharide metabolism ($p = 1.54 \times 10^{-42}$) and either cellulose metabolism ($p = 1.60 \times 10^{-42}$), xylan catabolism ($p = 1.87 \times 10^{-24}$), pectin catabolism ($p = 3.00 \times 10^{-32}$) or starch metabolism ($p = 8.10 \times 10^{-10}$), respectively. FunCats for carbon compound metabolism ($p = 3.18 \times 10^{-08}$) were significantly enriched in the xyloglucan PolyCat, though the majority of enriched FunCats were unrelated to polysaccharide degradation and catabolism (Figure 2-3; OTable 03). The significance for enrichment was low in the mannan PolyCat compared to the other PolyCats, but it also had significant enrichment in the hemicellulose/pectin metabolism category ($p = 6.25 \times 10^{-04}$; OTable 03).

Overall, the identifier genes of the cellulose, xylan, pectin and starch PolyCats were thus found to contain most of the expected genes coding for enzymes and transporters for these carbon sources, while the genes found for the mannan and xyloglucan PolyCats are less functionally associated. The response of *N. crassa* to mannans and xyloglucan thus appears to be an indirect one, indicating that the detection of *N. crassa* is not specialized towards these carbon sources.

2.1.2. Transcriptional response to complex plant biomass by *N. crassa*

Chemical plant biomass composition differs distinctively between grasses, softwoods and hardwoods (Haffner *et al.*, 2013; Mitchell *et al.*, 2014; Hassan *et al.*, 2017). These complex biomasses are comprised of several polysaccharides, lignin, proteins, as well as other chemical compounds and have varying physical properties, e.g. crystallinity and density. Together, these factors could influence how *N. crassa* perceives a complex carbon source and changes its transcriptional response based on these parameters.

A correlation study was performed to discern which polysaccharides can be detected in complex plant biomasses by *N. crassa*. To this end, the expression levels of all identifier

genes on 15 complex ENCODE plant biomass conditions was correlated to expression on the 28 PolyCat mono-, di- and polysaccharide conditions using Pearson's correlation. The resulting correlation factors were used to perform a Euclidean distance clustering of the complex carbon sources.

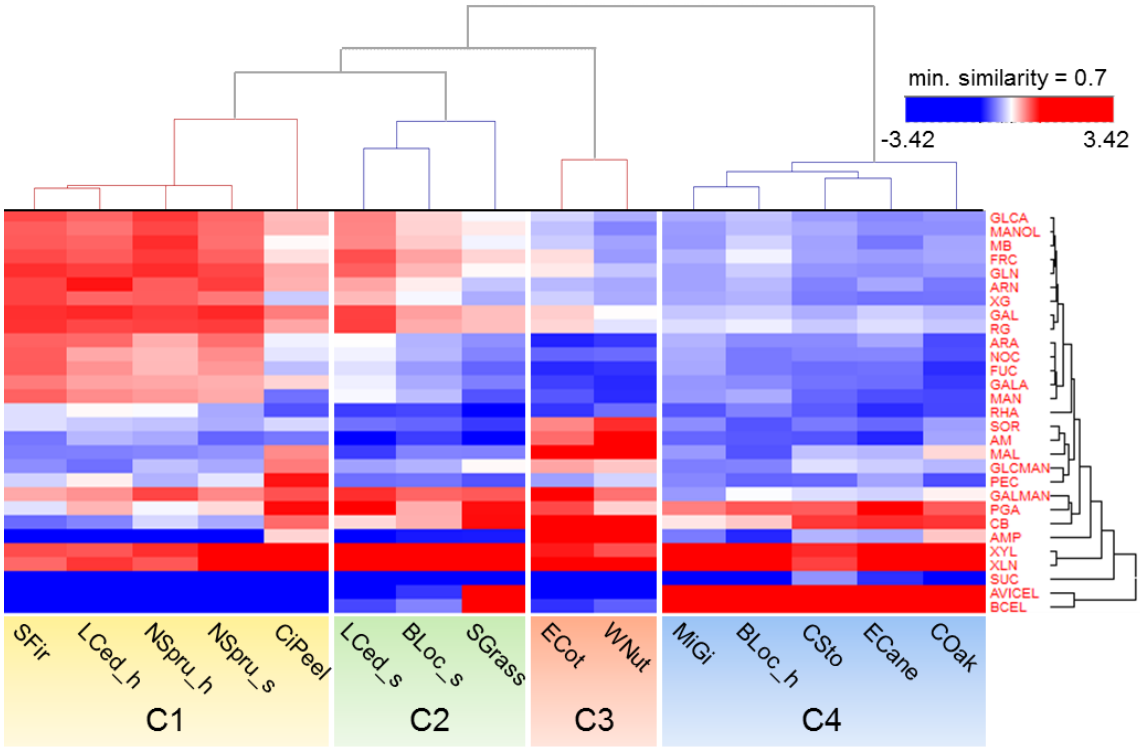

Figure 2-4: Euclidean distance clustering of correlation *p*-values between complex carbon source conditions and mono-, di- and polysaccharide conditions.
Cluster (C) 1 contains mainly softwoods and citrus peel, C2 contains one softwood, one hardwood and one grass, C3 contains two hardwoods and C4 the remaining hardwoods and grasses. SUC = sucrose, PGA = polygalacturonic acid, CB = cellobiose, MB = mannobiose, SOR = sorbose, XYL = xylose, RHA = rhamnose, MAL = maltose, MANOL = mannitol, RG = rhamnogalacturonan, GLN = galactan, ARN = arabinan, GLCA = glucuronic acid, GALA = galacturonic acid, ARA = arabinose, MAN = mannose, FRC = fructose, GAL = galactose, AM = amylose, FUC = fucose, NOC = no carbon, BCEL = bacterial cellulose, XG = xyloglucan, PEC = pectin, XLN = xylan, GLCMAN = glucomannan, GALMAN = galactomannan, AMP = amylopectin, CSto = Corn stover, MiGi = *Miscanthus* x giganteus, CiPeel = citrus peel, ECane = Energy cane, SGrass = Switchgrass, SFir = Silver fir, NSpru = Norway spruce, LCed = Lebanon cedar, BLoc = Black locust, COak = Common oak, ECot = Eastern cottonwood, WNut = Chinese wingnut. Abbreviations with *_s are referring to sapwood, while *_h refers to heartwood.

The carbon sources could be divided into four clusters (Figure 2-4). The first cluster contained most of the softwood conditions and the citrus peel condition, though the similarity between the citrus peel condition and the softwood conditions was low (Figure 2-4 C1). In the second cluster, the sapwood conditions of Lebanon cedar and Black locust clustered together with the Switchgrass condition (Figure 2-4 C2). The softwood conditions in cluster C1 and C2 showed a significant correlation to mannobiose, mannose, xylan, xylose, galactomannan, hemicellulose and pectin-related monosaccharide conditions.

Two hardwood conditions, Eastern cottonwood and Chinese wingnut, formed the third cluster, and their correlation pattern was dissimilar to softwood and the remaining hardwood conditions (Figure 2-4 C3). The fourth cluster was comprised of the remaining hardwood and grass conditions, which showed high similarity in their correlation patterns (Figure 2-4 C4). All grasses, as well as the majority of hardwoods in clusters C2 and C4, with the exception of Black locust heartwood, correlated significantly with cellulose, xylan, xylose, cellobiose and polygalacturonic acid (PGA) conditions. The remaining hardwood conditions, Eastern cottonwood and Chinese wingnut exhibited good correlation factors with xylan, xylose, PGA, cellobiose and starch related conditions, but not with cellulose.

It appears that *N. crassa* is able to detect multiple polysaccharides inside a complex lignocellulosic biomass in parallel and tailors a specific expression response to these carbon sources. While most of the time complex carbon sources that are similar in their physiochemical properties elicit a similar expression pattern in *N. crassa*, there are obvious exceptions to this rule, suggesting so far undescribed differences for example in bio-availability.

2.1.3. Transcriptional plant biomass “perception” using PolyCat scores

One goal of this study was the visualization of the carbon source “perception” of *N. crassa*. The different PolyCats were designed to reflect the polysaccharides that could be encountered by the fungus during plant cell wall degradation and the identifier genes of the PolyCats exhibited an expression profile specific for these polysaccharides. Therefore, the overall expression of the identifier genes of one PolyCat could be used as a marker to identify to what extent a respective polysaccharide is detected by *N. crassa*. Therefore, a single score was calculated for each PolyCat, the **PolyCat score**, which represented how similar the expression of the identifier genes associated to one PolyCat was to the expression of *N. crassa* induced with a complex carbon source. A PolyCat score of 100% would indicate that the overall expression of identifier genes in a complex carbon source condition was equal to the expression induced with mono-, di- and polysaccharides. Deviations above or below 100% PolyCat score would indicate increased or decreased expression of the identifier genes induced by a complex carbon source, respectively.

To calculate the PolyCat scores, an expression value in FPKMs had to be assigned to the identifier genes. The maximum expression strength of an identifier gene across the ENCODE carbon sources that were part of a PolyCat was used. For example, the FPKMs of each identifier gene in the ENCODE conditions xylan and xylose were compared for the xylan PolyCat. The highest FPKM value of these two ENCODE conditions was then used as expression strength during further analyses. Afterwards, a quotient was calculated by

dividing the determined expression strength of each identifier gene in a PolyCat by the expression strength of the same gene induced on a complex carbon source (Figure 5-2). The resulting quotients were averaged over all identifier genes of a PolyCat to determine the PolyCat score.

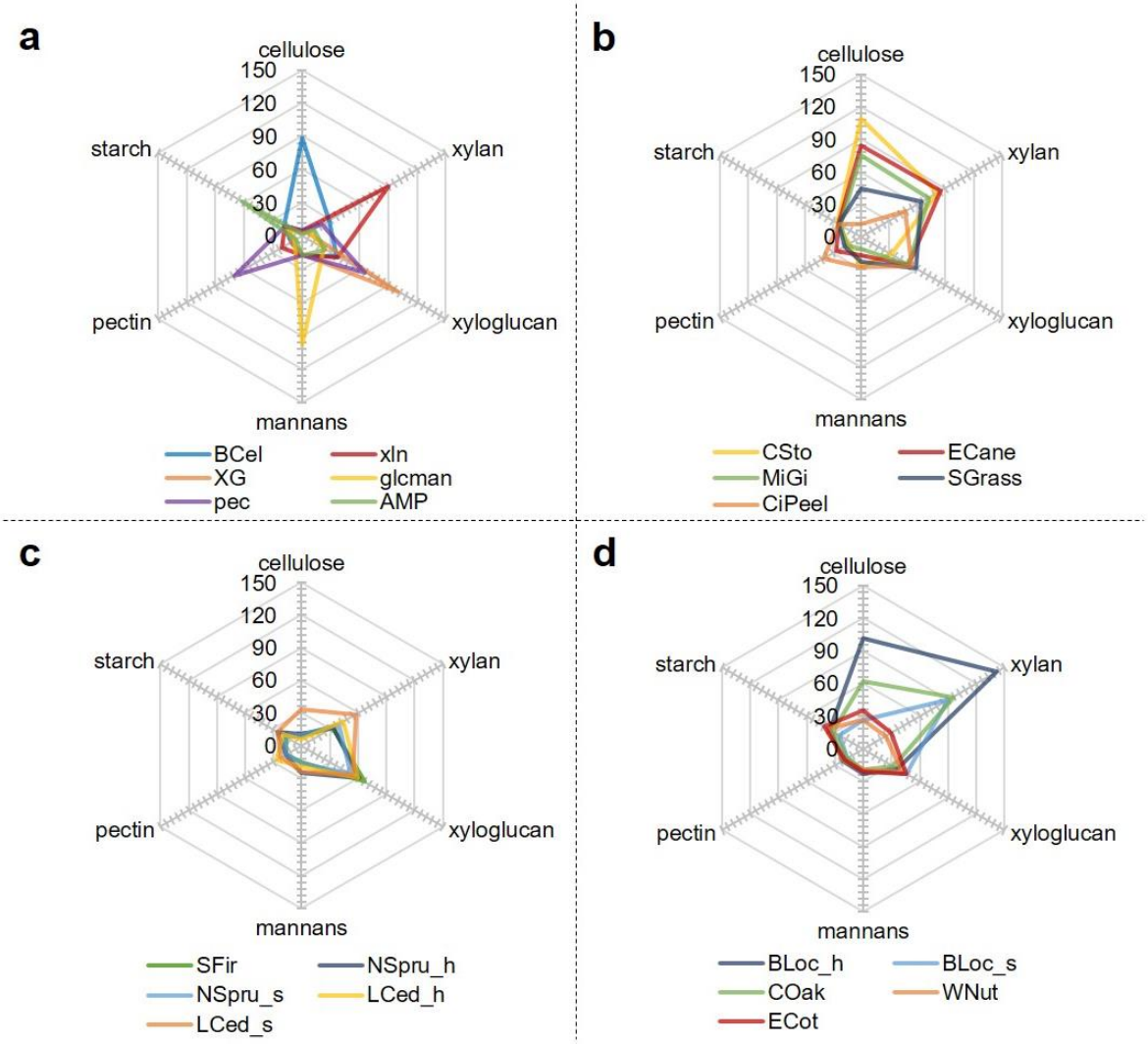

Figure 2-5: Radar plots of PolyCat scores.
PolyCat scores of **a)** polysaccharide conditions, **b)** grass and citrus peel conditions, **c)** softwood conditions and **d)** hardwood conditions. BCel = bacterial cellulose, XG = xyloglucan, pec = pectin, xln = xylan, glcman = glucomannan, AMP = amylopectin, CSto = Corn stover, MiGi = *Miscanthus x giganteus*, CiPeel = citrus peel, ECane = Energy cane, SGrass = Switchgrass, SFir = Silver fir, NSpru = Norway spruce, LCed = Lebanon cedar, BLoc = Black locust, COak = Common oak, ECot = Eastern cottonwood, WNut = Chinese wingnut. Abbreviations with *_s are referring to sapwood, while *_h refers to heartwood.

Table 2-1: PolyCat scores of ENCODE plant biomass conditions.
The PolyCat score represents the similarity between the expression of identifier genes induced with mono-, di- and polysaccharides and the same genes induced with complex carbon sources. The mean score of each PolyCat (over all identifier genes of the respective PolyCat) is shown here.

	PolyCat scores [%]					
condition:	**cellulose**	**xylan**	**xyloglucan**	**mannan**	**pectin**	**starch**
amylopectin	1.9	12.3	24.0	17.5	6.0	62.3
bacterial cellulose	88.0	28.3	36.4	17.6	11.0	18.3
Black locust heartwood	101.5	142.1	36.2	23.1	22.2	35.9
Black locust sapwood	26.2	90.0	45.9	20.2	16.7	24.9
Chinese wingnut	26.3	23.8	41.6	19.3	21.4	37.8
citrus peel	11.4	47.0	54.3	28.0	39.7	23.8
Common oak	61.6	95.3	32.3	19.4	17.5	32.5
Corn stover	109.2	81.0	31.9	26.4	13.1	25.3
Eastern cottonwood	35.8	29.3	45.9	21.1	20.1	41.5
Energy cane	84.6	85.0	50.8	17.3	26.5	23.8
glucomannan	3.2	7.8	22.9	98.1	7.0	16.5
Lebanon cedar heartwood	5.5	44.1	60.0	19.5	26.8	20.3
Lebanon cedar sapwood	33.3	57.2	54.4	23.8	21.8	25.2
Miscanthus* x *giganteus	75.9	72.3	51.0	10.7	15.3	22.3
Norway spruce heartwood	10.4	33.6	61.0	25.6	17.0	25.3
Norway spruce sapwood	9.9	39.5	52.6	16.8	16.1	17.5
pectin	4.6	20.8	64.9	17.2	70.7	17.6
Silver fir	8.6	33.1	67.1	15.6	16.4	16.8
Switchgrass	44.5	64.5	58.3	22.5	17.0	23.9
xylan	4.6	89.8	37.7	17.3	21.0	17.0
xyloglucan	2.8	5.7	100.0	16.3	11.0	11.6

To examine if the determined PolyCat scores were specific for plant cell wall polysaccharides, PolyCat scores were calculated for bacterial cellulose, xylan, xyloglucan, glucomannan, pectin and amylopectin ENCODE conditions (Figure 2-5a; Table 2-1). The tested polysaccharide ENCODE conditions, with the exception of pectin, showed one peak of ~60% to ~90% with their respective PolyCat (e.g. bacterial cellulose to cellulose PolyCat, glucomannan to mannan PolyCat, etc.).

The pectin ENCODE condition had peaks of ~71% at the pectin PolyCat and ~65% at the xyloglucan PolyCat. Only the xyloglucan condition reached a PolyCat score of 100%, while the remaining five conditions had a PolyCat score below 100%. Both observations were not unexpected, since the PolyCats, except for the xyloglucan PolyCat, had multiple ENCODE conditions assigned to them. Since the expression value of the identifier genes was based on the maximal expression value (FPKMs) between the used ENCODE conditions, single ENCODE poly-saccharide conditions could not induce all related identifier genes to 100%. This deliberation is confirmed by the xyloglucan PolyCat, which was comprised of only the xyloglucan ENCODE condition, and therefore showed a PolyCat score of 100% (Figure 2-5a; Table 2-1).

Since the overlap between the PolyCats was therefore minimal, the results of this analysis showed that the PolyCat scores can be used to determine a specific response of *N. crassa* to a given carbon source. In addition, the PolyCat scores represent how strongly *N. crassa* reacts to the tested carbon sources and could therefore be used to determine if *N. crassa* is detecting or adapting to a polysaccharide in its vicinity. In a next step, the PolyCat scores of grasses, citrus peel, softwoods and hardwoods were analyzed to visualize the transcriptional response of *N. crassa* to these complex carbon sources.

Citrus peel induced mostly identifier genes of the pectin, xylan and xyloglucan PolyCats

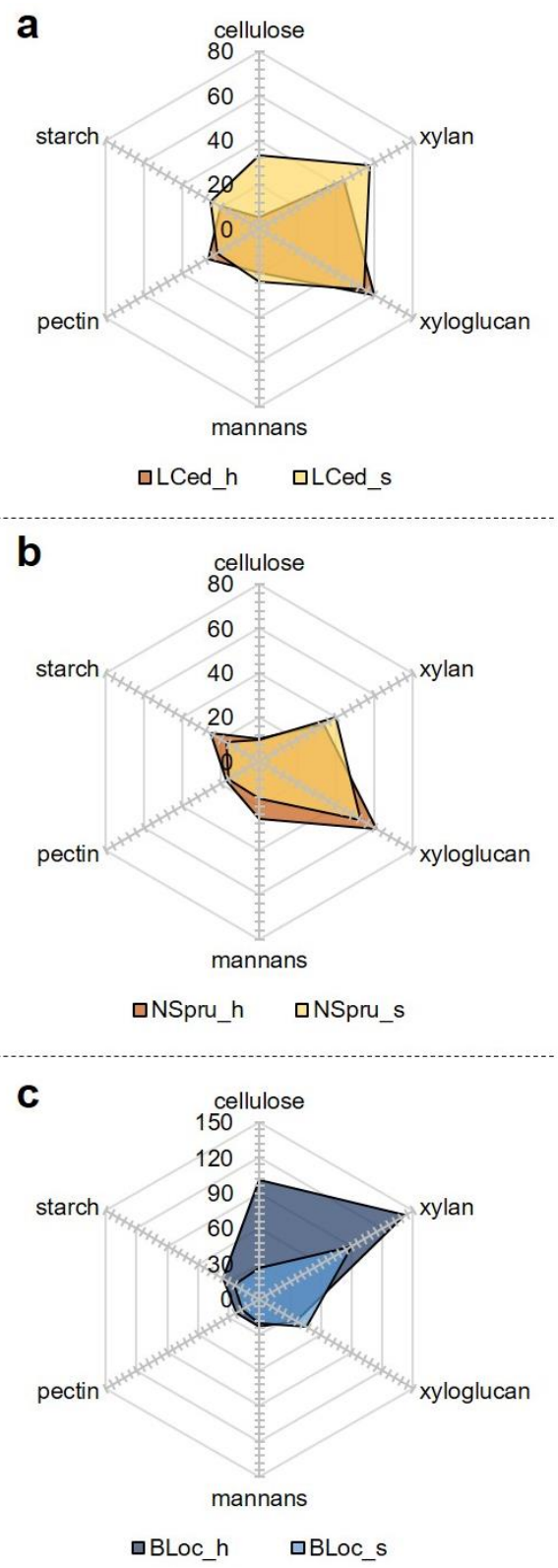

Figure 2-6: PolyCat scores comparison of sapwood and heartwood.
Sapwood and heartwood PolyCat scores of **a)** Lebanon cedar (LCed), **b)** Norway spruce (NSpru) and **c)** Black locust (BLoc) were compared. Abbreviations with *_s are referring to sapwood, while *_h refers to heartwood.

(Figure 2-5b; Table 2-1). Though citrus peel still has a cellulose content of ~17% (J. P. Benz *et al.*, 2014), the expression of *N. crassa* did not shift towards cellulose degradation. In contrast, the highest PolyCat score in *Miscanthus*, Energy cane and Corn stover was cellulose, followed by xylan and xyloglucan (Figure 2-5b; Table 2-1). Switchgrass showed similar induction of the xylan and xyloglucan PolyCat identifier genes as the remaining grasses, but the cellulose induction in this species was only at ~45%, although all tested grass species have a similar cellulose content (Mitchell *et al.*, 2014).

The softwood conditions, with exception of Lebanon cedar sapwood, showed similar inductions of xylan and xyloglucan identifier genes (Figure 2-5c; Table 2-1). However, the cellulose PolyCat score was very low for these tree species. The sapwood of Lebanon cedar exhibited similar xylan and xyloglucan PolyCat scores as the remaining softwood conditions, but surprisingly, its cellulose PolyCat score was about three to six times higher than the same scores in the other softwood conditions (Figure 2-6a).

Contrary to the softwood conditions, the hardwood conditions showed more diverse substrate perception patterns (Figure 2-5d; Table 2-1). The highest PolyCat score in Black locust heartwood and Common oak could be found for the xylan PolyCat, followed by the score of the cellulose PolyCat. The PolyCat scores of the remaining categories was much lower than the xylan and cellulose PolyCat scores. Unexpectedly, Eastern cottonwood and Chinese wingnut showed much lower PolyCat scores for the xylan and cellulose PolyCats compared to Black locust heartwood and Common oak (Figure 2-5d; Table 2-1).

Significant differences were also observed between PolyCat scores for conditions using sapwood (outer, live wood) or heartwood (core wood) as carbon source, but derived from the same species. Although the difference in their polysaccharide composition is usually minor, sapwood and heartwood can differ greatly in their physicochemical properties (e.g. toxic extractives in heartwoods) (Meerts, 2002; Taylor *et al.*, 2002; Bertaud and Holmbom, 2004; Hassan *et al.*, 2019). Particularly the sapwood and heartwood samples of Lebanon cedar and Black locust displayed major differences in their PolyCat scores. However, these appeared to be inverse between the two tree species. While Lebanon cedar sapwood exhibited increased cellulose and xylan PolyCat scores when compared to heartwood, these scores were drastically decreased in Black locust sapwood compared to heartwood (Figure 2-6a, c; Table 2-1). In contrast, Norway spruce only showed minor differences between sapwood and heartwood PolyCat scores (Figure 2-6b; Table 2-1).

These results corroborate previous observations of this work, indicating strongly that *N. crassa* can detect multiple polysaccharides inside a complex carbon source in parallel. The transcriptional response of *N. crassa* appears to be specifically tailored to the substrates at hand, although general patterns were differentiable between grasses, citrus peel, softwood and hardwood conditions. However, the transcriptional program of *N. crassa* induced with

complex carbon sources, such as heartwood and softwood samples, appears to be influenced additionally by a wide variety of physicochemical factors (e.g. presence of further plant cell wall components, such as extractives, or the bioavailability of the polysaccharides within the plant cell wall), greatly altering the resultant expression patterns in a non-uniform way.

2.1.4. Principal component analysis of ENCODE conditions

Principal component analyses (PCA) were performed on the fungal nutritional ENCODE data in an approach to identify the major driving forces throughout the individual expression patterns of the conditions. Published transcriptome data induced for 1 h or 2 h with different glucose concentrations was included in these PCA analyses (Wang *et al.*, 2017) .The first PCA compares the expression of mono-, di- and polysaccharide conditions, while polysaccharide and plant biomass conditions were analyzed in a second PCA (Figure 2-7a; Figure 2-9a). The PCAs were further analyzed by k-means clustering using five randomly scattered centers to identify conditions that group together. The first and second principal component (PC) of the PCA created using data from mono-, di- and polysaccharide conditions explained ~71% vs. ~11% of the observed variance, respectively (Figure 2-7a). Different metabolic states appear to be separated along the axis of the first and main PC, therefore possibly reflecting one of the major driving forces induced by these conditions in *N. crassa*.

The first and second k-means clusters (Figure 2-7a clusters A and B) contain conditions comprised of high glucose concentrations: either sucrose and glucose directly (cluster A) or glucose- and galactose-containing di- and polysaccharides (cluster B). High concentrations of glucose and sucrose can induce CCR in *N. crassa* and other organisms (Sun and Glass, 2011; Vinuselvi *et al.*, 2012; Brown *et al.*, 2014). However, cluster B also contains a 1 h starvation condition switched from sucrose (NoC_1h), indicating that the conditions in this cluster are at least partially released from CCR or that CCR is not fully activated by the di- and polysaccharides in cluster B, probably since they have to be depolymerized before they can be metabolized by the fungus.

Cluster D is, among other things, comprised of the 4 h starvation condition (NoC_4h), Avicel, mannobiose, arabinose and arabinan (Figure 2-7a). In contrast to clusters A and B, the substrates in this cluster therefore appear to release CCR almost completely and/or activate the starvation response of *N. crassa*. Coradetti *et al.* already showed that there is a substantial overlap between Avicel and NoC (starvation) gene expression (Coradetti *et al.*, 2013). Moreover, we realized that the growth of *N. crassa* is reduced on arabinan and

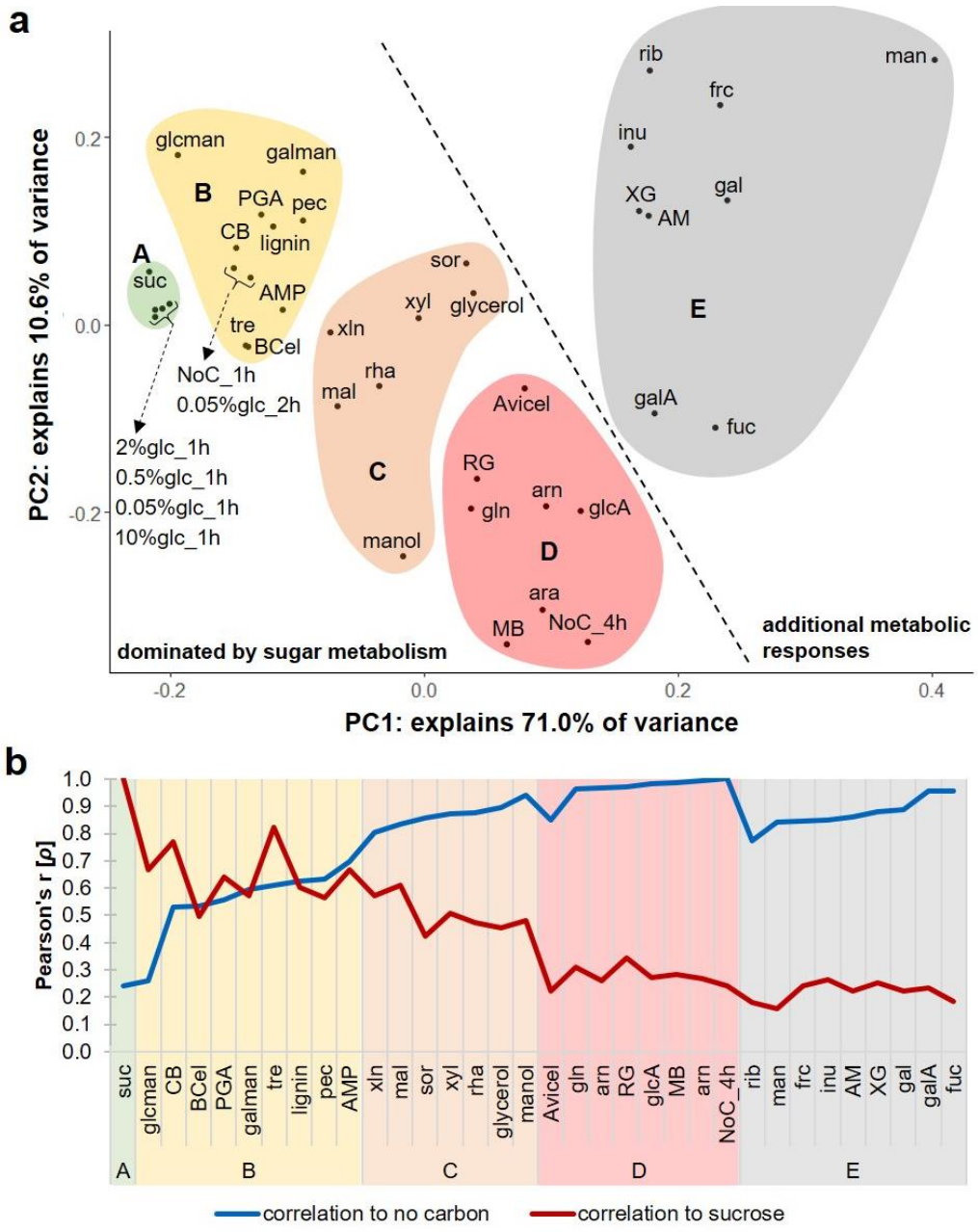

Figure 2-7: Principal component and correlation analysis of mono-, di- and polysaccharide conditions.

The fungal nutritional ENCODE transcriptome data were analyzed together with published expression data of glucose (0.05% to 10% concentration) and NoC conditions induced for either 1 h or 2 h (Wang *et al.*, 2017). **a)** PCA of lignin, glycerol, mono-, di- and polysaccharide conditions. The indicated clusters (A to E) represent conditions that were assigned to one of the five k-means clustering centers. **b)** Pearson's correlation of the conditions used in the PCA to either NoC or sucrose conditions. PC = principal component, suc = sucrose, glc = glucose, PGA = polygalacturonic acid, CB = cellobiose, MB = mannobiose, tre = trehalose, sor = sorbose, xyl = xylose, rha = rhamnose, mal = maltose, manol = mannitol, RG = rhamnogalacturonan, gln = galactan, arn = arabinan, glcA = glucuronic acid, galA = galacturonic acid, ara = arabinose, rib = ribose, man = mannose, frc = fructose, inu = inulin, gal = galactose, AM = amylose, fuc = fucose, NoC = no carbon, BCel = bacterial cellulose, XG = xyloglucan, pec = pectin, xln = xylan, glcman = glucomannan, galman = galactomannan, AMP = amylopectin

arabinose compared to other mono- and polysaccharides (data not shown), indicating that these carbon sources are not favored by the fungus.

Therefore, the correlation of all conditions used in this PCA to either the NoC or the sucrose condition was determined (Figure 2-7b). This analysis revealed that the mono-, di- and polysaccharide conditions in clusters A, C and D showed an inverse correlation to NoC and sucrose condition, while the correlation to NoC and sucrose was similar in cluster B. The correlation to sucrose was decreasing throughout these four clusters, while the correlation to NoC was increasing. These results support the hypothesis that clusters A to D are mainly dominated by responses to sugar metabolism (i.e. CCR and starvation).

The conditions forming the fifth k-means cluster (Figure 2-7a cluster E) are positioned behind cluster D which contains the starvation condition (NoC_4h). If the first PC would solely represent the CCR/starvation response of *N. crassa*, the conditions of cluster E should be positioned in between clusters A to D. Since this is not the case, other driving factors than CCR or starvation might influence the expression patterns of these conditions. The correlation analysis showed that the conditions of cluster E exhibited a weaker correlation to starvation than cluster D, while their correlation to sucrose remained low. It is therefore likely that other responses might influence the positioning of these conditions in the PCA. To test which responses these might be, the gene expression profiles of the conditions that formed PCA cluster E (plus sucrose and NoC conditions as controls) were hierarchically clustered, which revealed 24 clusters (Figure 2-8a; OTable 04). The clusters 6 and 14 contained genes that were up-regulated on the control conditions NoC or sucrose, respectively. In addition, ribose and amylose responses formed distinct and major clusters (C10 and C20, respectively). Cluster 1 encompassed genes up-regulated on all conditions except NoC, sucrose, ribose and amylose. A search for enriched functional categories in this cluster revealed that protein synthesis ($p = 1.60 \times 10^{-12}$), RNA processing ($p = 3.24 \times 10^{-09}$), fatty acid metabolism ($p = 1.67 \times 10^{-08}$), alcohol fermentation ($p = 3.67 \times 10^{-07}$) and organic acid metabolism ($p = 3.97 \times 10^{-06}$) were significantly enriched in addition to carbohydrate metabolism ($p = 1.17 \times 10^{-07}$) (OTable 04). It appears therefore that other metabolic processes besides sugar metabolism, such as fatty acid metabolism, fermentation and organic acid metabolism, were activated by these carbon sources, leading to a major shift in the PCA.

Genes specifically up-regulated on ribose and amylose formed clusters 10 and 20, respectively. An enrichment analysis of the genes in cluster 10 revealed significant enrichment in detoxification ($p = 1.66 \times 10^{-06}$), secondary metabolism ($p = 4.27 \times 10^{-05}$), carbohydrate metabolism ($p = 1.52 \times 10^{-04}$), ABC transporters ($p = 2.29 \times 10^{-04}$) and pentose-phosphate pathway ($p = 2.43 \times 10^{-04}$) categories (OTable 04).

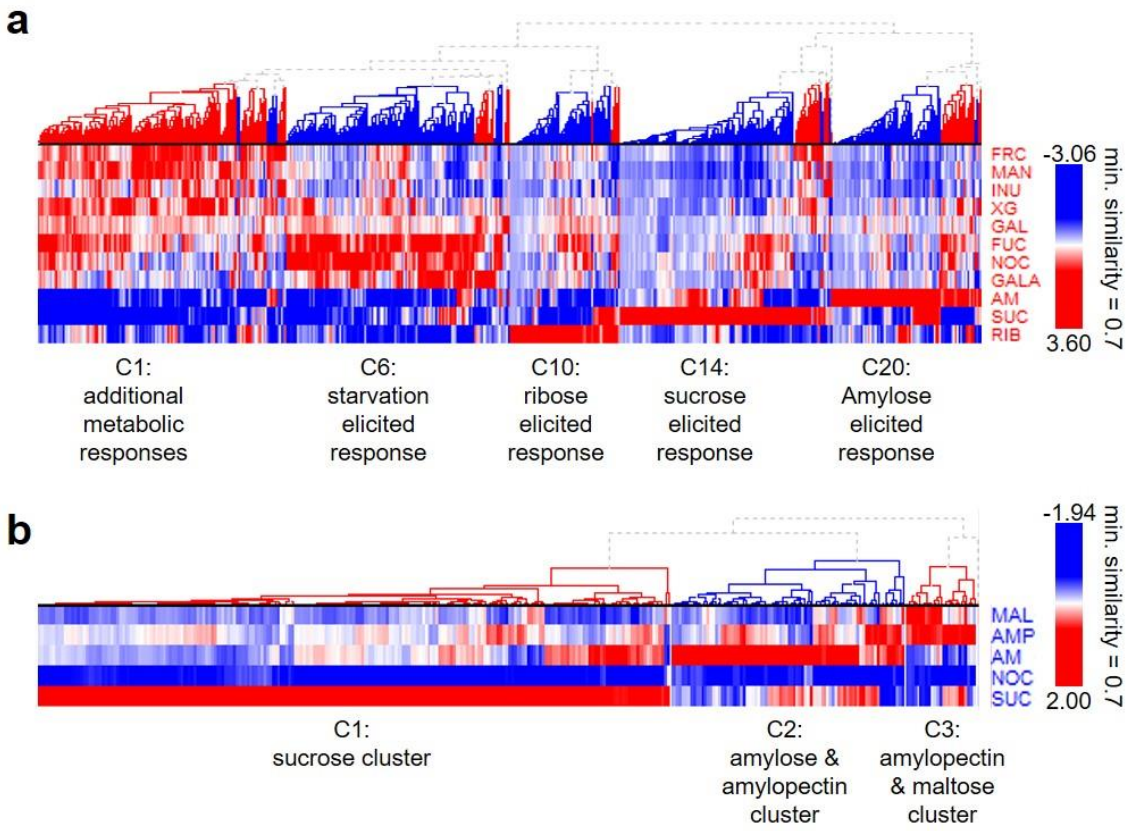

Figure 2-8: Hierarchical clusterings of conditions used in the PCA analysis.
a) Clustering of the conditions that comprised PCA cluster E. **b)** Clustering of the 363 COL-26 dependent genes (Xiong *et al.*, 2017) using the amylopectin, amylose, maltose, no carbon and sucrose conditions. C = cluster, FRC = fructose, MAN = mannose, INU = inulin, XG = xyloglucan, GAL = galactose, FUC = fucose, NOC = no carbon, GALA = galacturonic acid, AM = amylose, SUC = sucrose, RIB = ribose, MAL = maltose, AMP = amylopectin

These results indicate that ribose as a carbon source either has to be detoxified before it can be catabolized in the pentose-phosphate pathway or that degradation of ribose leads to toxic intermediates.

Surprisingly, most genes that showed an elevated expression on amylose (Cluster 20) were connected to growth, developmental processes, environmental sensing and signal transduction (cell growth/morphogenesis, $p = 6.09 \times 10^{-10}$; cell type differentiation, $p = 1.34 \times 10^{-09}$; directional cell growth, $p = 9.73 \times 10^{-07}$; cellular signaling, $p = 1.10 \times 10^{-06}$; regulation of carbohydrate metabolism, $p = 1.71 \times 10^{-05}$; OTable 04). While categories for starch metabolism were still significantly enriched (starch metabolism, $p = 1.50 \times 10^{-04}$), these processes appear to be weaker driving forces for *N. crassa* on amylose. These results were unexpected, since the other starch related conditions, amylopectin and maltose, were part of clusters B and C in the PCA and thus appear to be more strongly related to sugar metabolism.

To analyze how different amylose expression was from amylopectin and maltose elicited gene expression, the genes regulated by COL-26, a transcription factor involved in the

regulation of starch degradation in *N. crassa* (Xiong *et al.*, 2017), were clustered using amylopectin, amylose, maltose, sucrose and NoC conditions (Figure 2-8b; OTable 05). There were three major clusters revealed by this hierarchical clustering. The first cluster contained all genes significantly up-regulated on sucrose, while the second and third cluster were composed of genes with increased expression on either amylose or amylopectin and maltose, respectively. Gene enrichment analysis using functional categories showed that the amylopectin and maltose cluster was most strongly enriched in starch-related categories (starch metabolism, $p = 5.79 \times 10^{-09}$; extracellular starch degradation, $p = 2.92 \times 10^{-06}$; sugar transport, $p = 2.43 \times 10^{-}04$; OTable 05). The amylose-specific response cluster exhibited significant enrichment in categories of glutamate group metabolism ($p = 4.68 \times 10^{-04}$), sugar transport ($p = 5.88 \times 10^{-04}$) and weaker, yet significant, to starch metabolism ($p = 1.50 \times 10^{-03}$). In addition, the major amylase gene *gla-1* (NCU01517) was strongly expressed on maltose and amylopectin (3755 FPKMs and 3176 FPKMs, respectively), but weaker on amylose (535 FPKMs).

Although amylose and amylopectin are both starch polysaccharides, they exhibit differences in their structure (Green *et al.*, 1975). Amylose forms helical chains that can overlap with each other, making the polysaccharide insoluble in water and reducing its viscosity, while amylopectin is more branched and therefore more soluble, leading to higher viscosity (Green *et al.*, 1975; Zhong *et al.*, 2006; Juhász and Salgó, 2008). It is therefore feasible that amylose is harder to decompose for the fungus, which might explain a weaker induction of amylase genes compared to amylopectin. The difference in bio-availability could explain why amylose is grouped in cluster E of the PCA, close to the starvation condition, while the potentially easier degradable amylopectin and maltose are positioned in clusters B and C, closer to sucrose as CCR-inducing condition (Figure 2-7a).

The second PCA of polysaccharide and plant biomass conditions was similar to the first PCA described above (Figure 2-9a). The first PC explained ~61% of the observed variance, while the second PC explained ~11% of the observed variance. Once more, the first PC appears to be related to the different metabolic responses of *N. crassa*. The first k-means cluster (Figure 2-9b cluster A) contained sucrose, glucose and glucomannan conditions and could therefore be dominated by CCR.

Similar to the first PCA of mono-, di- and polysaccharides, the second cluster (cluster B) of this PCA encompassed the 1 h starvation condition and conditions that led to strong cellulose and hemicellulose response during the PolyCat analyses, such as hardwoods and grasses.

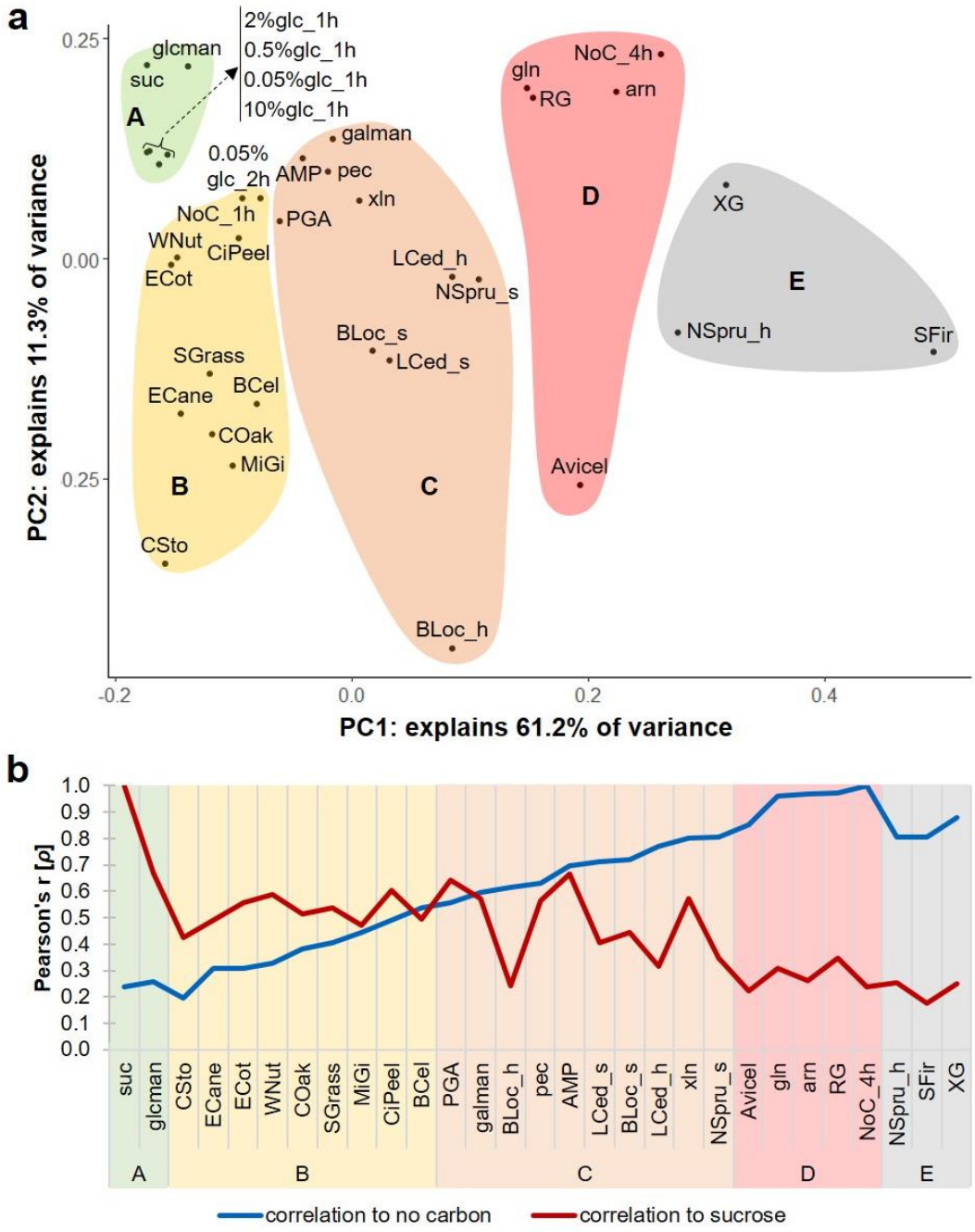

Figure 2-9: Principal component and correlation analysis of polysaccharide and plant biomass conditions.

The fungal nutritional ENCODE transcriptome data were analyzed together with published expression data of glucose (0.05% to 10% concentration) and NoC conditions induced for either 1 h or 2 h (Wang *et al.*, 2017). **a)** PCA of polysaccharide and plant biomass conditions. The indicated clusters (A to E) represent conditions that were assigned to one of the five k-means clustering centers. **b)** Pearson's correlation of the conditions used in the PCA to either NoC or sucrose conditions. PC = principal component, suc = sucrose, glc = glucose, PGA = polygalacturonic acid, RG = rhamnogalacturonan, gln = galactan, arn = arabinan, NoC = no carbon, BCel = bacterial cellulose, XG = xyloglucan, pec = pectin, xln = xylan, glcman = glucomannan, galman = galactomannan, AMP = amylopectin, CSto = Corn stover, MiGi = *Miscanthus x giganteus*, CiPeel = citrus peel, ECane = Energy cane, SGrass = Switchgrass, SFir = Silver fir, NSpru = Norway spruce, LCed = Lebanon cedar, BLoc = Black locust, COak = Common oak, ECot = Eastern cottonwood, WNut = Chinese wingnut. Abbreviations with *_s are referring to sapwood, while *_h refers to heartwood.

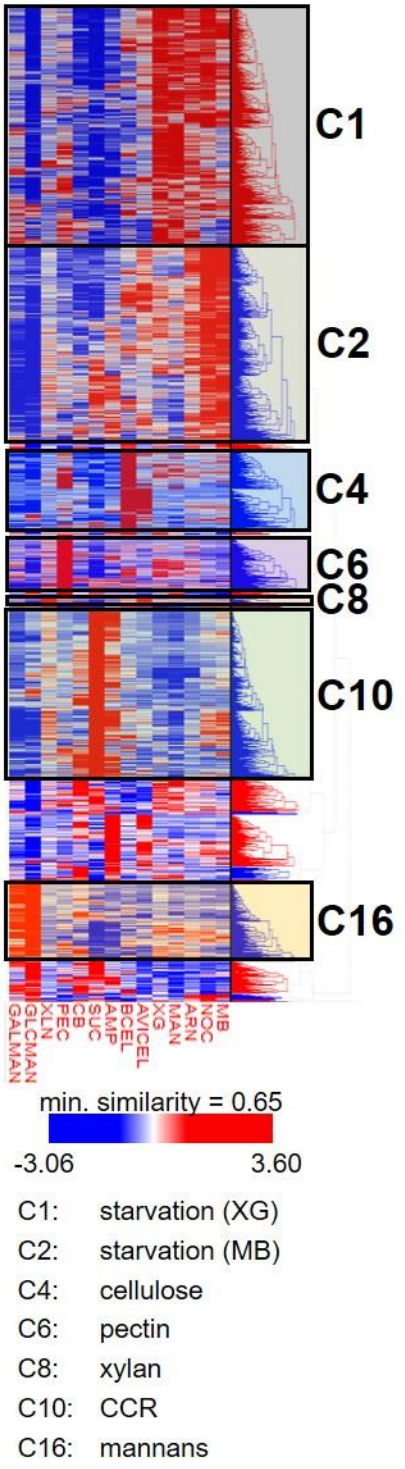

The NoC condition induced for 4 h, Avicel, arabinan, galactan and rhamnogalacturonan were part of the fourth cluster (cluster D), mirroring the results of the first PCA. In addition, the fifth k-means cluster (cluster E) contained the xyloglucan condition.

A correlation analysis of these conditions against either NoC or sucrose conditions revealed a similar result as for the first PCA (Figure 2-9b). Again, the conditions of k-means cluster A correlated strongly with sucrose, but showed only a weak correlation to NoC, while the third and fourth cluster (clusters C and D) exhibited an increasing correlation to NoC, but a decreasing correlation to sucrose. However, the decreasing trend of correlation to sucrose in thes e clusters was not as pronounced in the second PCA as it was in the first PCA. In addition, the trend of increasing correlation to NoC was steadier throughout the conditions of the PCA of polysaccharide and plant biomass conditions, as compared to the previous correlation analysis. Whereas cluster B in the first PCA showed similar correlation values to NoC and starvation, the correlation to NoC is constantly increasing in the cluster of the second PCA (Figure 2-7b, Figure 2-9b). The fifth k-means cluster (cluster E) of the PCA of polysaccharide and plant biomass conditions showed a weaker correlation to NoC than the conditions in cluster D but exhibited a similar correlation to sucrose. These results reflect the observations of the first PCA.

Figure 2-10: Hierarchical clustering to determine di- and polysaccharide induced expression patterns.

Pearson's hierarchical clustering of ENCODE expression data. 20 clusters (C) could be identified. C1 and C2 show genes up-regulated on no carbon and either xyloglucan, arabinan, mannose or mannobiose conditions, respectively. C4, C6 and C8 exhibit genes up-regulated on either cellulose, pectin or xylan conditions. Genes in C10 were up-regulated on sucrose as well as amylopectin conditions and were related to CCR. C16 contains genes that were up-regulated on gluco- and galactomannan conditions. MB = mannobiose, NOC = no carbon, ARN = arabinan, MAN = mannose, XG =xyloglucan, BCEL = bacterial cellulose, AMP = amylopectin, SUC = sucrose, CB = cellobiose, PEC = pectin, XLN = xylan, GLCMAN = glucomannan, GALMAN = galactomannan

In conclusion, the conditions in both PCAs clustered at least partly according to their correlation to NoC and sucrose conditions, although the correlation to sucrose was of lesser importance for the complex plant biomass conditions compared to the mono-, di- and polysaccharide conditions. These result indicate that the availability of sugars with high nutritional value (or a lack thereof) is a crucial driving force in the fungal response to the ENCODE conditions. Moreover, alternative metabolic responses or changes in metabolic state could also be differentiated by the PCAs. While these responses might not be directly linked to sugar metabolism, they indicate that the carbon sources eliciting them might be problematic for *N. crassa*.

2.1.5. Hierarchical clustering of polysaccharide conditions

Some conditions, like mannobiose, mannose, xyloglucan and arabinan, were positioned closely to starvation conditions in the PCA analysis and exhibited a strong correlation to the starvation condition. However, *N. crassa* is able to grow on these carbon sources and also contains genes for their degradation (Samal *et al.*, 2017; Hassan *et al.*, 2019). To analyze whether these conditions exhibit to the most part starvation-like expression patterns or show carbon source-specific ones nevertheless, a hierarchical clustering of selected carbon sources, including mannose as well as cell wall di- and polysaccharide conditions, was performed (Figure 2-10; OTable 06). Although arabinan, xyloglucan, mannose and mannobiose lead to an up-regulation of genes that were also induced by NoC, the expression patterns of these conditions only partly overlapped to NoC expression, suggesting that these carbon sources were still directly or indirectly inducing specific gene expression profiles in *N. crassa* (Figure 2-10 C1 and C2). FunCat analysis of cluster 1 showed that categories for protein synthesis ($p = 8.07 \times 10^{-16}$), sugar transport ($p = 1.07 \times 10^{-09}$), RNA processing ($p = 1.15 \times 10^{-09}$), but also oxidation of fatty acids ($p = 1.04 \times 10^{-07}$), secondary metabolism ($p = 4.07 \times 10^{-05}$) and fermentation ($p = 3.10 \times 10^{-04}$) were significantly enriched (OTable 06).

In contrast, the genes that were up-regulated similarly between mannobiose and NoC conditions in cluster 2 showed significant enrichment in cell cycle and DNA processing ($p = 1.56 \times 10^{-33}$), biogenesis of cellular components ($p = 6.17 \times 10^{-22}$), protein fate ($p = 7.23 \times 10^{-20}$), transcription ($p = 3.27 \times 10^{-19}$), cell motility ($p = 1.26 \times 10^{-14}$), cell growth/morphogenesis ($p = 2.00 \times 10^{-14}$) and regulation of metabolism ($p = 1.76 \times 10^{-13}$) categories (OTable 06). It appears that arabinan, mannose and xyloglucan are similar to the starvation response of *N. crassa*, because their presence leads to the activation of alternative metabolic processes. Intriguingly, presence of mannobiose does not lead to expression of mannanases as known from *Aspergillus oryzae* (Ogawa *et al.*, 2012), but the

disaccharide also does not fully induce the starvation response. It is feasible that *N. crassa* metabolizes mannobiose as a carbon source, but its presence is not linked to a specific degradation response in the fungus.

The clusters C4, C6 and C8 of the hierarchical clustering contained genes up-regulated on cellulose, pectin and xylan, respectively (Figure 2-10 C4, C6 and C8). These results were confirmed by gene enrichment analysis, which showed that categories for extracellular cellulose degradation ($p = 2.85 \times 10^{-27}$), specific pectin catabolism ($p = 1.27 \times 10^{-20}$) and xylan catabolism ($p = 4.04 \times 10^{-16}$) were significantly enriched in the cellulose, pectin and xylan clusters, respectively (OTable 06).

Table 2-2: Expression of mannanase genes on different ENCODE conditions.
Overview of the expression of the β-mannosidase gene *gh2-1* (NCU00890) and endo-mannanase gene *gh5-7* (NCU08412) on mannan and cellulose related conditions. glcman = glucomannan, galman = galactomannan, MB = mannobiose, CB = cellobiose, BCel = bacterial cellulose, NoC = no carbon, suc = sucrose

	Expression on ENCODE condition in FPKM							
gene	**glcman**	**galman**	**MB**	**CB**	**Avicel**	**BCel**	**NoC**	**suc**
NCU00890	2.1	5.2	7.0	15.4	40.5	26.9	4.7	1.1
NCU08412	97.6	23.1	44.8	412.2	513.0	1301.0	6.5	1.9

Unexpectedly, genes up-regulated after gluco- and galactomannan induction formed their own cluster, but this cluster did not contain mannanase genes like the β-mannosidase gene *gh2-1* (NCU00890) or endo-mannanase gene *gh5-7* (NCU08412) (Figure 2-10 C16; OTable 06). These genes were instead found in the cellulose cluster (C4) and especially the β-mannosidase gene *gh2-1* was strongly induced by cellulose and cellobiose conditions, while it showed only low expression values on gluco- and galactomannan (Table 2-2). Since functional categories for development ($p = 1.66 \times 10^{-04}$), cytokinesis ($p = 2.05 \times 10^{-04}$), protein synthesis ($p = 5.79 \times 10^{-04}$), transcription ($p = 9.34 \times 10^{-04}$), cell fate ($p = 1.58 \times 10^{-03}$) and even apoptosis ($p = 2.34 \times 10^{-03}$) were significantly enriched in cluster C16, it appears that the fungus is preparing for fundamental changes in its life cycle when confronted with mannan (OTable 06). However, these changes are apparently different to the ones made during starvation, as genes up-regulated by both gluco- and galactomannan do not cluster with genes up-regulated during NoC.

Overall, the results of the hierarchical clustering suggest that arabinan, mannose and xyloglucan induce at least partially a starvation-like response in *N. crassa*. Moreover, mannose and mannobiose are not perceived as strong inducing molecules by *N. crassa*, since both carbon sources induced gene expression similar to NoC. Finally, mannanase

genes were only slightly up-regulated in the presence of either gluco- or galactomannan and can confirmed to be co-regulated with the cellulose response (Craig *et al.*, 2015).

2.1.1. Identification of genes up-regulated specifically by complex plant biomass

It is feasible that certain signaling pathways need multiple environmental cues to become fully activated and that single polysaccharides lead to an incomplete induction of certain parts of the plant cell wall degradation machinery. Synergistic effects might play a crucial role during the regulation of fungal carbon metabolism, since plant biomass is naturally composed of several polysaccharides. To test this hypothesis, the data of the 'Fungal Nutritional ENCODE Project' were utilized to identify genes that exhibit their strongest expression on complex plant biomass conditions as opposed to simple carbon sources.

To this end, the full set of ENCODE conditions was screened for genes that had their expression maximum in at least one of the complex plant biomass conditions. Therefore, the maximum FPKM value of each gene was determined over all mono-, di- and polysaccharides. A ratio was calculated for each gene by dividing the expression value on each complex plant biomass condition by the previously determined maximum expression value on the control conditions. A minimum ratio threshold of +1.5x (or 150% over controls) was applied to filter for genes that showed their strongest expression on complex plant biomass conditions, and genes that passed this threshold were deemed significantly up-regulated.

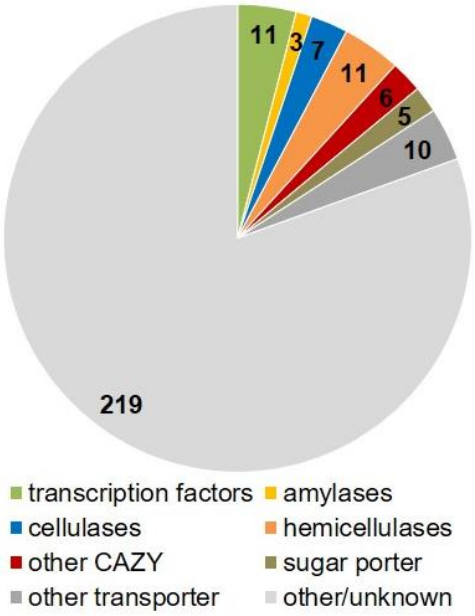

Figure 2-11: Genes specifically up-regulated on complex plant biomass conditions.

A set of 272 genes was found to fit these parameters (Figure 2-11; OTable 07). Only 27 of the up-regulated genes were CAZymes, such as amylase, cellulase, hemicellulase, and chitinase genes. Five genes were classified as sugar porters by TCDB and 10 genes encoded transporter proteins of other TCDB categories. Intriguingly, this gene set contained 11 transcription factor genes, including the transcription factors *vib-1* (NCU03725) and *clr-2* (NCU08042). The remaining 219 genes were analyzed for functional enrichment, revealing that categories for tetracyclic and pentacyclic triterpene metabolism ($p = 5.35 \times 10^{-10}$), secondary metabolism ($p = 6.76 \times 10^{-07}$), cell cycle and DNA processing ($p = 1.48 \times 10^{-06}$), detoxification ($p = 1.01 \times 10^{-04}$),

aerobic aromate catabolism (p = 1.39 x 10^{-04}), regulation of C-compound and carbohydrate metabolism (p = 3.62 x 10^{-04}) and disease, virulence and defense (p = 3.64 x 10^{-04}) were significantly enriched (OTable 07). These data indicate that a small part of the plant cell wall degradation machinery is strongly up-regulated on complex plant biomass conditions. To a greater extend however, complex C-sources seem to activate the expression of genes coding for alternative metabolic processes and pathways for detoxification.

Table 2-3: List of genes that showed a significantly up-regulated expression after induction with complex plant biomasses.
The grasses group contained the *Miscanthus x giganteus*, Corn stover, Energy cane and Switchgrass ENCODE conditions. The softwoods group encompassed the Silver fir, Norway spruce heart- and sapwood and Lebanon cedar heart- and sapwood conditions. The heartwoods group contained the Common oak, Chinese Wingnut, Eastern Cottonwood and Black locust heart- and sapwood conditions. An X indicates genes that showed a significantly up-regulated expression in the respective group.

	condition group				condition group		
gene ID	grasses	soft-woods	hard-woods	gene ID	grasses	soft-woods	hard-woods
NCU00162			x	NCU04819			x
NCU00711		x	x	NCU04953	x		x
NCU01353			x	NCU04997		x	x
NCU01653	x	x	x	NCU05317		x	x
NCU01699	x		x	NCU05319		x	x
NCU01849	x		x	NCU05376	x	x	
NCU02030	x	x		NCU05519	x		x
NCU02059			x	NCU06055			x
NCU02344			x	NCU06170			x
NCU02485			x	NCU06364	x		x
NCU02855	x		x	NCU06526		x	
NCU02856	x			NCU07088	x	x	x
NCU03294			x	NCU07353	x		x
NCU03322	x		x	NCU07581	x		x
NCU03369	x	x		NCU07582			x
NCU03421	x			NCU07760	x		x
NCU04089	x	x		NCU09024	x	x	
NCU04108	x		x	NCU09155	x		x
NCU04494			x	NCU09479	x		x
NCU04496	x		x	NCU09830			x
NCU04501		x	x	NCU10687			x

In the following, it was analyzed whether the genes responding strongest to complex plant biomass were induced specifically by one of the plant biomass groups, e.g. grasses, softwoods or hardwoods, or if their induction was more generic. The softwood group contained the Silver fir, Norway spruce and Lebanon cedar conditions (incl. heart- and sapwood where present). The hardwood group encompassed the Common oak, Chinese

Wingnut, Eastern Cottonwood and Black locust heart- and sapwood conditions, while the grasses group contained the *Miscanthus x giganteus*, Corn stover, Energy cane and Switchgrass conditions. If the expression of a gene was 1.5-fold up-regulated in more than 50% of the conditions in a group, the gene was viewed as positively induced by this plant biomass group.

A total of 42 genes showed a significant up-regulation in at least one of these groups (Table 2-3). Functional categories for extracellular metabolism ($p = 2.25 \times 10^{-08}$), nutrient perception and nutritional adaptation ($p = 3.18 \times 10^{-05}$), extracellular protein degradation ($p = 4.35 \times 10^{-05}$), disease and virulence defense ($p = 8.69 \times 10^{-05}$), but also extracellular polysaccharide degradation ($p = 1.23 \times 10^{-04}$) and nutrient starvation response ($p = 2.26 \times 10^{-04}$) were significantly enriched in this set of genes (OTable 07).

The expression of five genes was specific to soft- and hardwood conditions; among them were the chitinase gene *gh18-6* (NCU05317) and the endo-β-1,4-xylanase gene *gh10-3* (NCU04997), while only two genes showed a significantly increased expression after induction with grass conditions, including the uncharacterized zinc finger transcription factor gene *znf-23* (NCU03421), and only one hypothetical gene was significantly up-regulated on softwoods (NCU06526).

The hardwood condition led to the up-regulation of 13 genes, including the menadione-induced ABC multidrug transporter gene *mig-12* (NCU09830), the mixed-linkage glucanase gene *gh16-1* (NCU01353), the acetyl xylan esterase gene *ce1-2* (NCU04494) and a lytic polysaccharide monooxygenase (LPMO) 1 gene (NCU02344). Additional 14 genes were upregulated on hardwood and grass conditions; among them were the endoglucanase IV and putative LPMO gene *gh61-2*, endo-β-1,4-xylanase gene *gh11-1* (NCU02855) and the isoamyl alcohol oxidase gene *iao-3* (NCU04108). Five genes showed significantly increased expression on softwood and grass conditions, including the P450 monooxygenase genes *cyp450-6* (NCU04089; pisatin demethylase) and *cyp450-10* (NCU05376), as well as the menadione-induced gene *mig-8* (NCU03369). Finally, the expression of two hypothetical genes (NCU07088 and NCU01653) was upregulated in all three complex plant biomass conditions.

Overall, only few cellulase genes were more strongly induced by complex plant biomass (here: mostly hardwoods) than polysaccharides, and wood plant biomasses in general led to a better induction of some hemicellulase genes. However, the majority of found genes appear to be related to other processes, mainly disease defense and nutritional adaptation. These results support the notion that single polysaccharides are sufficient to elicit an almost complete transcriptional response towards polysaccharide degradation in *N. crassa*.

2.2. Identification and characterization of transcription factors regulating pectin degradation

The following results that describe the identification and characterization of the transcription factor PDR-1 were published in Thieme *et al.*, 2017.

The soluble sugars detected during plant polysaccharide perception lead to changes in the transcriptome and proteome of *N. crassa* (Huberman *et al.*, 2016), which results in an adaptation of the metabolic state to the present and utilizable carbon sources. Pectin, a major plant polysaccharide (Somerville, 2004; Caffall and Mohnen, 2009), induced a specific set of identifier genes in this study and leads to a distinctive transcriptional response in *N. crassa* (J. P. Benz *et al.*, 2014; Samal *et al.*, 2017). The degradation of pectin requires a wide array of different enzymatic activities to achieve full depolymerization (J. P. Benz *et al.*, 2014), since it has the highest complexity of all plant cell wall polysaccharides (Somerville, 2004; Caffall and Mohnen, 2009; Harholt *et al.*, 2010). However, no transcription factor related to pectin degradation was described in *N. crassa* at the beginning of this work.

2.2.1. Identification of the transcription factor PDR-1

To identify transcription factors involved in pectin degradation, the transcription factor deletion strain set of the Fungal Genetics Stock Center (McCluskey *et al.*, 2010) was searched for transcription factor mutants that exhibited a growth defect on pectin as sole carbon source. The wild-type (WT) strain and the Δ*gh28-1* strain, which has a deletion of the endo-polygalacturonase (endo-PGase) gene NCU02369 (J. P. Benz *et al.*, 2014), were used as controls in these growth assays. Twelve transcription factor deletion strains showed an atypical growth phenotype on pectin and these strains were used in a second screen on medium containing either 2% sucrose, 1% cellulose, or 1% xylan as sole carbon sources. Only one strain, carrying a deletion of the gene NCU09033, showed a purely pectin specific growth reduction (data not shown). Therefore, the NCU09033 locus was named pectin degradation regulator-1 (*pdr-1*).

Figure 2-12: Schematic depiction of conserved domains/signals in the transcription factor PDR-1 (NCU09033).

The amino acid sequence of *N. crassa* PDR-1 (NCU09033) was used in a conserved domain search, as well as NLS and NES prediction. GAL4 = GAL4-like $Zn(II)_2Cys_6$ (or C6 zinc) binuclear cluster DNA-binding domain, fungal TF MHR = fungal transcription factor regulatory middle homology region, green triangle = nuclear localization signal, red triangle = nuclear export signal.

The transcription factor PDR-1 is 971 amino acid long, contains one predicted nuclear localization signal (NLS), one predicted nuclear export signal (NES), a GAL4-like $Zn(II)_2Cys_6$ binuclear cluster DNA-binding domain and a fungal transcription factor regulatory middle homology region (fungal TF MHR) (Figure 2-12). The amino acid sequence of PDR-1 was compared to the sequence of RhaR, a regulator of rhamnose catabolism and RG degradation that is conserved in *A. niger* and *A. nidulans* (Gruben *et al.*, 2014; Pardo and Orejas, 2014). The sequence alignments showed an identity of 47% and 48% between the full-length sequences of *N. crassa* PDR-1 and RhaR of *A. niger* or *A. nidulans*, respectively.

The strain *pdr-1-comp* was created to confirm that the inability to grow on pectin was caused by deletion of *pdr-1*. To create this strain, the *pdr-1* gene under control of its native promoter and terminator was transformed into the *his-3* locus of a *pdr-1* deletion strain. The strain *pdr-1-comp* showed a WT-like growth phenotype and protein secretion when incubated in pectin, indicating a functional complementation of the NCU09033 deletion (Figure 2-13; SFigure 6-1).

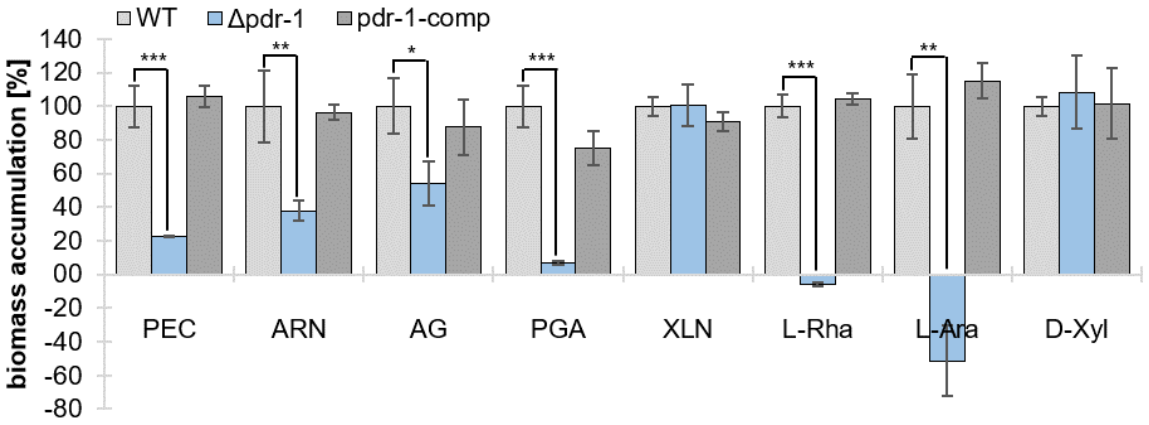

Figure 2-13: Biomass accumulation of the WT, Δ*pdr-1* and *pdr-1-comp* strains on pectin and pectin constituent sugars.

The biomass of *N. crassa* WT, Δ*pdr-1* and *pdr-1-comp* was determined. Strains were grown for 3 days in 3 ml cultures with 1% polysaccharide as carbon source. Alternatively, the strains were pre-incubated for 16 h in medium containing 2% sucrose, then washed, transferred to a 2 mM monosaccharide medium and incubated for additional 2 days with regular medium switches. After three days of incubation, the biomass was determined as dry weight. The samples were normalizec to WT biomass. Error bars represent standard deviation (n = 3). Significance was determined by an independent two-sample *t*-test of WT against Δ*pdr-1* or *pdr-1-comp* with *p < 0.05, **p < 0.01 and ***p < 0.001. PEC = pectin, ARN = arabinan, AG = arabinogalactan, PGA = polygalacturonic acid, XLN = xylan, L-Rha = rhamnose, L-Ara = arabinose, D-Xyl = xylose.

2.2.2. PDR-1 regulates pectin depolymerization and catabolism

Since the PDR-1 homologs RhaR only showed a slight growth reduction on pectin (Gruben *et al.*, 2014; Pardo and Orejas, 2014), while the Δ*pdr-1* strain on pectin showed a severe growth defect (SFigure 6-1a), it is feasible that *N. crassa* PDR-1 might regulate a broader range of genes related to pectin degradation. To test this hypothesis, the *N. crassa* WT, Δ*pdr-1* and *pdr-1-comp* strains were grown on pectin, several pectic carbon sources and xylan as a hemicellulose control and the dry weight of the strains was determined after three to seven days (depending on carbon source) (Figure 2-13). The *pdr-1* deletion strain exhibited significant growth defects on pectin backbone as well as pectin sidechain related carbon sources, while the growth of the *pdr-1-comp* strain was indistinguishable from the WT. These results confirm, that the Δ*pdr-1* mutant phenotype is the result of a lack of PDR-1. Additionally, the tested strains were incubated for 2 days in the pectin constituent monosaccharides rhamnose and arabinose along with xylose as control, after an overnight pre-incubation on 2% sucrose (Figure 2-13). The Δ*pdr-1* strain lost biomass during the incubation period on rhamnose and arabinose, while the growth of WT and *pdr-1-comp* was not affected. These results indicate that *pdr-1* is necessary for rhamnose and arabinose catabolism.

When the growth of the WT, Δ*pdr-1* and *pdr-1-comp* strains was tested on galacturonic acid as the sole carbon source, even the WT strain grew poorly (data not shown). Galacturonic acid is more oxidized than neutral monosaccharides, and an increased amount of reduction equivalents is necessary for its catabolism, making this process energetically expensive (Richard and Hilditch, 2009; Edwards and Doran-Peterson, 2012). However, the necessary reduction equivalents might be obtained from the pentose phosphate pathway (PPP), if a small amount of extra sugar was supplied in addition to galacturonic acid (Kruger and von Schaewen, 2003). It is feasible that xylose, arabinose and rhamnose alleviate the imbalance in reduction equivalents for *N. crassa* during pectin degradation, since they are part of the pectin backbone and side chains (Caffall and Mohnen, 2009).

To test this hypothesis, mycelial biomass of an overnight culture of WT, Δ*pdr-1* and *pdr-1-comp* strains incubated in 2% sucrose was transferred into a medium containing 2 mM galacturonic acid and 0.5 mM xylose. After two additional days of growth, the WT and *pdr-1-comp* strains exhibited a significantly increased dry weight on the galacturonic acid plus xylose medium as compared to growth on either galacturonic acid or xylose alone (Figure 2-14a). In contrast, the Δ*pdr-1* strain failed to accumulate additional biomass on galacturonic acid plus xylose medium. Instead, the biomass of the mixed monosaccharide incubation was similar to the biomass of the *pdr-1* deletion strain on xylose as sole carbon source. These results indicate that *N. crassa* PDR-1 is either directly or indirectly involved

in the catabolism of galacturonic acid and that the reduced growth of *N. crassa* WT strain on galacturonic acid can be alleviated by adding additional monosaccharides.

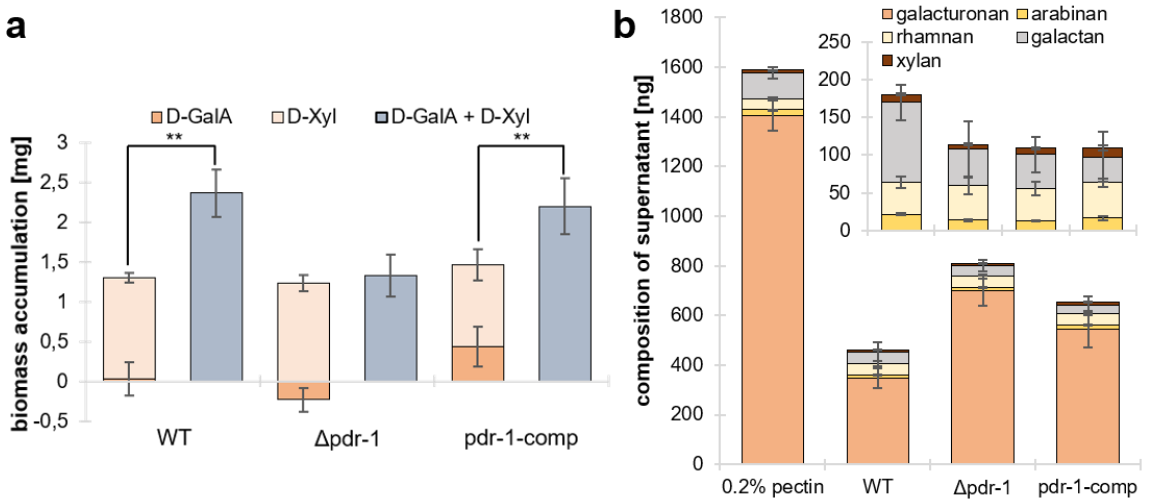

Figure 2-14: Biomass accumulation of galacturonic acid and pectin degradation profile of the WT, Δ*pdr-1* and *pdr-1-comp* strains.
a) The biomass of *N. crassa* WT, Δ*pdr-1* and *pdr-1-comp* was determined. Strains were pre-incubated for 16 hours in medium containing 2% sucrose, then washed, transferred to either 2 mM galacturonic acid, 0.5 mM xylose or 2 mM galacturonic acid and 0.5 mM xylose. The strains were incubated for additional 2 days with regular medium switches. The biomass was determined as dry weight. Significance was determined by an independent two-sample *t*-test of 0.5 mM xylose against 2 mM galacturonic acid and 0.5 mM xylose with **p < 0.01. D-GalA = galacturonic acid, D-Xyl = xylose. **b)** Residual culture supernatants of *N. crassa* WT, Δ*pdr-1* and *pdr-1-comp* strains grown for two days on 0.2% pectin as well as the pectin medium itself were broken down into monosaccharides for a compositional analysis. The sugars were quantified by HPAEC-PAD. The inlay diagram shows a magnified version of arabinan, rhamnan, galactan and xylan. Error bars represent standard deviation (n = 3)

The extent of PDR-1 mediated pectin degradation cannot be fully explained by the observed growth phenotypes, although they indicate that PDR-1 is necessary for a functional regulation of intracellular or extracellular degradation processes. Therefore, the WT, Δ*pdr-1* and *pdr-1-comp* strains were pre-incubated in sucrose and switched to 0.2% pectin for two additional days of growth. A compositional analysis of pectin before and after incubation was performed using a combined acid and enzymatic hydrolysis (Garna *et al.*, 2004, 2006). The resulting monosaccharide composition was analyzed by high-performance anion-exchange chromatography with pulsed amperometric detection (HPAEC-PAD) and showed only minor differences in the residual arabinose, xylose and galactose contents between the WT, *pdr-1-comp* and Δ*pdr-1* strains (Figure 2-14b). The concentration of galacturonic acid was greatly reduced in the supernatant of the WT strain, while the Δ*pdr-1* mutant supernatant showed the least reduction of galacturonic acid concentration. Intriguingly, rhamnose levels were unchanged in all strains compared to uninoculated pectin, indicating that either the RG-I backbone had not been exposed to degradation or that the

rhamnogalacturonan lyase ASD-1 was not active under the (slightly acidic) conditions applied. These results indicate that the HG degradation machinery was also impaired in the Δ*pdr-1* strain.

2.2.3. Determination of PDR-1 regulated genes by RNA-Seq

The deletion of *pdr-1* leads to a reduced growth of *N. crassa* on many pectic carbon sources, which implies that multiple pectin-related metabolic processes are impaired in this mutant. The transcriptional profile of *N. crassa* WT and Δ*pdr-1* strains was determined to assess the PDR-1 regulated genes using the ENCODE RNA-Seq data. The strains were induced for 4 h with either NoC, 2 mM rhamnose or 1% pectin prior to RNA-Seq and differential expression (DEseq) analysis was performed on the transcriptome data.

The DEseq analysis of WT induced with pectin or rhamnose versus NoC showed that most of the genes predicted to be involved in pectin degradation (J. P. Benz *et al.*, 2014) were significantly up-regulated on pectin (fold-change ≥ 3; Table 2-4). The genes that were at least 3-fold up-regulated in the WT or Δ*pdr-1* strain on either pectin or rhamnose were compared using Venn diagrams (Figure 2-15; OTable 08). Functional categories were determined for each group of the Venn diagram with more than 20 genes. Categories with a *p*-value ≤ 5×10^{-5} were deemed as enriched with high significance (OTable 08). Among others, the functional categories for specific pectin catabolism and/or hemicellulose/rhamnogalacturonan catabolism were significantly enriched in the following groups: genes exclusively up-regulated in WT strain on pectin and/or rhamnose (375 genes), the Δ*pdr-1* and WT strains on pectin (139 genes), as well as WT strain on both pectin and rhamnose together with the Δ*pdr-1* strain on pectin only (31 genes).

However, no significant enrichment for functional categories related to pectin degradation was found in the groups of genes solely up-regulated in the Δ*pdr-1* strain on pectin (73 genes), rhamnose (332 genes), or under both conditions (56 genes), as well as the WT strain alone or together with Δ*pdr-1* strain on rhamnose (284 genes or 27 genes, respectively). Following these analyses, genes differentially expressed in the Δ*pdr-1* strain compared to WT strain on 1% pectin were determined by DEseq analysis (Figure 2-16a). A ±3x fold-change threshold was applied to the data, which returned 80 genes as differentially expressed. An increased expression level in the Δ*pdr-1* strain was exhibited in 49 of these genes (Figure 2-16a; red dots, repressed by PDR-1). Among these genes were all three lyases encoded in the *N. crassa* genome: the pectate lyase genes *ply-1* (NCU06326) and *ply-2* (NCU08176) and the rhamnogalacturonan lyase gene *asd-1* (NCU05598). In addition, the pectin methylesterase gene *ce8-1* (NCU10045), the β-glucuronidase encoding gene *gh79-1* (NCU00937), and the putative β-1,4-xylosidase gene *gh43-3* (NCU06861) also

showed increased expression levels in the *pdr-1* deletion strain. The remaining 31 differentially expressed genes showed reduced expression levels in the Δ*pdr-1* strain compared to the WT strain (Figure 2-16a; red dots, activated by PDR-1). This set of genes included the endo-PGase gene *gh28-1* (NCU02369), the unsaturated rhamnogalacturonyl hydrolase gene *gh105-1* (NCU02654), the *lra3* homolog NCU09034, the β-galactosidase genes *gh35-1* (NCU00642) and *gh35-2* (NCU04623), and the L-arabinitol 4-dehydrogenase gene *ard-1* (NCU00643). More genes showed a stronger mis-regulation in the DEseq analysis between Δ*pdr-1* and WT strains induced with 2 mM rhamnose compared to the results on pectin (Figure 2-16b). After applying a ±3x fold-change threshold to these data, 297 genes showed an increased up- or down-regulation. Of these genes, 91 showed higher expression levels in the Δ*pdr-1* mutant, although no pectinolytic gene was present in this gene set (Figure 2-16b; red dots, repressed by PDR-1). The remaining 206 genes showed a higher expression in WT strain (Figure 2-16b; red dots, activated by PDR-1). Among these genes were *gh28-1*, the exo-PGase gene *gh28-2* (NCU06961), *gh35-2*, *gh105-1*, two putative *lra4* homologs (NCU03086, NCU05037), the putative *lra3* and *rha1* homologs (NCU09034 and NCU09035, respectively), the putative *gaaB*/*lgd1* homolog (NCU07064), *ard-1* (NCU00643) and the GCY protein-coding gene NCU01906.

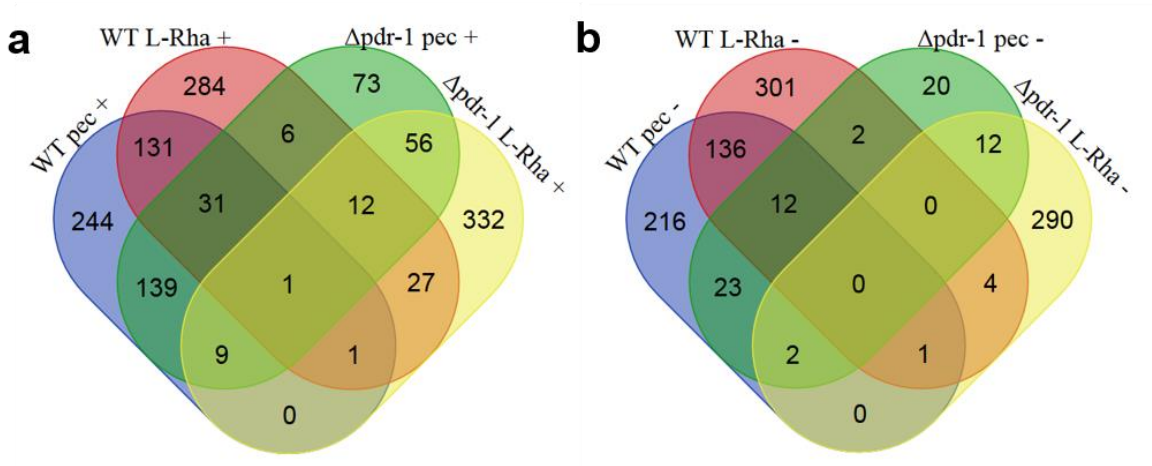

Figure 2-15: Venn diagrams of DEseq results.
WT and Δ*pdr-1* strains were pre-grown for 16 h on 2% sucrose and then switched to an induction medium of either 1% pectin (pec) or 2 mM rhamnose (L-Rha) for an additional 4 h. DEseq was performed on the RNA-seq data. a) Genes that were 3-fold upregulated. b) Genes that were 3-fold downregulated. WT on 1% pectin was used in biological duplicates; all other conditions were used in biological triplicates for the RNA-seq analysis.

Table 2-4: Pectin degradation genes of *N. crassa*.
The number of PDR-1 consensus binding sites (PB sites) with a stringency score > 0.6 are indicated. The fold change threshold for DEseq was 3 for rhamnose (L-Rha) and pectin (log_2-fold ≥ 1.58). *p*-values < 5 x 10^{-5} were considered significant. The cluster number refers to Figure 2-16.

Pectin degradation genes				DEseq (WT vs NoC on L-Rha)		DEseq (WT vs Δ*pdr-1* on L-Rha)		DEseq (WT vs NoC on pectin)		DEseq (WT vs Δ*pdr-1* on pectin)		
cat.	ID	name	# of PB sites	log2-fold change	p-value	log2-fold change	p-value	log2-fold change	p-value	log2-fold change	p-value	Cluster
TF	NCU09033	*pdr-1*	5	3.2	0.00E+00	-11.3	1.89E-272	1.6	3.48E-51	-9.7	3.82E-252	C1
backbone acting	NCU02369	*gh28-1*	2	3.7	5.68E-89	-3.3	3.70E-98	4.7	5.70E-93	-1.8	5.46E-26	C13
	NCU06961	*gh28-2*	0	1.5	8.98E-26	-2.1	4.77E-64	4.9	2.89E-162	1.2	2.74E-07	C5
	NCU10045	*ce8-1*	0	0.6	7.59E-06	-0.6	5.25E-06	2.7	2.34E-62	2.2	1.81E-07	C5
	NCU06326	*ply-1*	0	1.9	1.48E-21	-1.7	6.48E-29	5.3	4.01E-143	2.8	2.32E-21	C5
	NCU08176	*ply-2*	0	0.3	5.22E-01	-0.3	4.33E-01	7.2	1.73E-146	3.3	2.14E-56	C5
	NCU05598	*asd-1*	0	0.7	9.97E-06	-0.5	2.14E-04	3.2	3.42E-88	2.2	2.77E-29	C5
	NCU09976	*ce12-1*	0	1.1	2.97E-03	-2.1	8.51E-10	3.8	4.69E-40	-0.4	1.59E-01	
	NCU02654	*gh105-1*	3	4.4	3.57E-269	-4.5	0.00E+00	2.4	3.56E-59	-2.1	7.10E-20	C1
side chain acting	NCU09170	*gh43-4*	0	0.6	2.73E-03	-0.3	2.81E-01	4.0	3.76E-128	0.6	4.77E-03	
	NCU07326	*gh43-6*	0	0.1	5.07E-01	-0.6	2.90E-09	3.6	8.31E-207	-1.4	9.22E-08	
	NCU05965	*gh43-7*	0	-0.2	1.09E-01	0.3	1.17E-02	4.0	2.13E-232	1.0	3.55E-16	
	NCU02343	*gh51-1*	0	0.0	8.18E-01	0.0	7.50E-01	4.5	0.00E+00	-0.6	3.99E-06	
	NCU09775	*gh54-1*	0	0.2	6.70E-01	0.9	5.46E-02	7.5	2.59E-29	0.7	1.34E-03	
	NCU00972	*gh53-1*	0	0.7	1.15E-07	-1.5	1.82E-31	2.8	5.48E-114	0.9	1.61E-06	
	NCU00642	*gh35-1*	0	1.1	7.03E-24	-1.1	1.26E-18	4.5	0.00E+00	-2.1	3.58E-46	C13
	NCU04623	*gh35-2*	1	3.0	1.74E-202	-2.7	5.00E-175	4.7	0.00E+00	-2.8	4.84E-65	C13

Table 2-4: Pectin degradation genes of *N. crassa* (continued).

Pectin degradation genes (continued)				DEseq (WT vs NoC on L-Rha)		DEseq (WT vs Δ*pdr-1* on L-Rha)		DEseq (WT vs NoC on pectin)		DEseq (WT vs Δ*pdr-1* on pectin)		
cat.	ID	name	# of PB sites	log2 fold change	p-value	log2 fold change	p-value	log2 fold change	p-value	log2 foldchange	p-value	Cluster
side chain acting	NCU00810	*gh2-3*	0	1.3	2.61E-25	-1.3	8.41E-35	2.5	5.00E-66	-1.2	4.03E-12	
	NCU05882	*gh5-5*	0	-0.2	1.45E-02	-0.2	1.30E-01	1.0	3.68E-23	0.9	2.54E-04	
	NCU09923	*gh3-7*	0	-0.3	3.70E-01	0.0	8.79E-01	7.1	7.53E-263	-1.0	1.77E-03	
	NCU06861	*gh43-3*	0	-0.4	2.28E-02	0.3	1.29E-01	1.5	6.26E-15	1.8	3.18E-13	C5
	NCU00937	*gh79-1*	0	-0.2	2.80E-01	0.5	4.79E-07	0.2	2.21E-01	1.8	4.32E-12	C5
	NCU09491	*fae-1*	0	1.5	4.10E-20	-2.7	1.98E-63	5.2	4.24E-284	0.2	1.15E-01	
transporters	NCU02188	*lat-1*	0	-0.1	5.64E-01	-0.3	5.82E-03	4.0	8.40E-245	-0.7	3.82E-05	
	NCU00988	*gat-1*	0	-0.5	4.27E-08	-0.1	2.95E-01	3.1	2.32E-103	1.0	2.37E-06	
catabolism genes	NCU09035	put. *rha1*	3	5.8	0.00E+00	-4.7	0.00E+00	2.9	7.21E-72	-1.6	3.31E-19	C1
	NCU03605	put. *lra2*	0	2.2	7.96E-152	-1.6	8.26E-77	0.3	4.44E-04	0.1	6.66E-01	
	NCU09034	put. *lra3*	2	8.9	0.00E+00	-6.2	0.00E+00	5.0	0.00E+00	-1.9	2.34E-26	C1
	NCU05037	put. *lra4*	4	6.9	0.00E+00	-4.7	1.04E-238	2.2	1.44E-42	-1.3	7.85E-08	C1
	NCU03086	put. *lra4*	1	4.5	0.00E+00	-3.3	3.53E-243	0.9	5.78E-10	0.0	9.16E-01	C1
	NCU09533	*gaaA/gar2-homolog*	0	-0.2	1.91E-01	-0.5	2.93E-04	6.0	2.15E-179	0.1	5.11E-01	
	NCU07064	*gaaB/lgd1-homolog*	0	2.9	5.27E-73	-3.0	4.45E-114	4.1	1.31E-133	0.4	2.80E-02	C5
	NCU09532	*gaaC/lga1-homolog*	0	0.2	3.12E-01	-0.8	6.06E-07	4.7	8.46E-169	-0.3	1.78E-01	
	NCU00643	*ard-1*	2	1.9	1.79E-86	-1.8	4.30E-72	5.9	0.00E+00	-2.2	1.97E-48	C13
	NCU01906	*GCY protein*	0	1.7	7.53E-54	-2.0	4.64E-65	3.2	1.17E-191	0.3	1.81E-01	C5

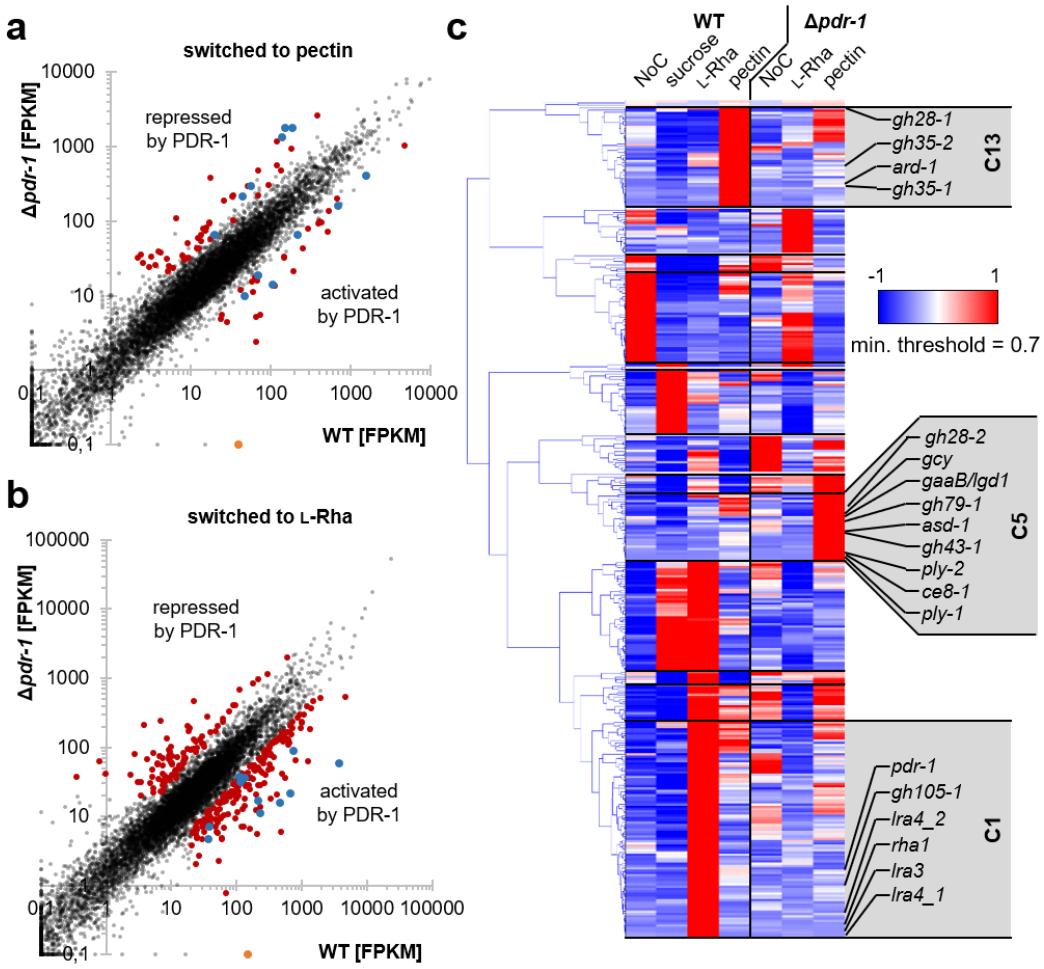

Figure 2-16: Scatterplots and clustering of RNA-Seq data from WT and Δ*pdr-1* strains. Scatterplot diagram (a, b) axes are log_{10}-scaled. **a)** Full-genome expression profile of WT induced for 4 h on 1% pectin was plotted against the transcriptional response of the Δ*pdr-1* mutant induced on the same medium (black dots). Genes of Δ*pdr-1* strain that were 3-fold up- or down-regulated to WT are marked with red dots. Genes that code for pectin degrading enzymes (according to Table 2-4) are represented by blue colored dots. The position of *pdr-1* is denoted with an orange dot. **b)** As in **(a)**, but 2 mM rhamnose was used for induction. **c)** 367 genes were either repressed or activated by PDR-1 and this subset was analyzed by hierarchical clustering. RNA-Seq data of WT or Δ*pdr-1* strain after 4 h on either 2 mM rhamnose, 1% pectin, 2% sucrose (only WT) or no carbon source (NoC) was used. The position of pectinases and rhamnose/galacturonic acid catabolism genes are indicated next to their respective clusters (C1, C5 or C13). lra4_1 = NCU05037, lra4_2 = NCU03086.

In particular the failed induction of the endo-PGase gene *gh28-1* and NCU07064, which might be encoding the L-galactonate dehydratase of the galacturonic acid catabolism, might explain the observed growth phenotypes of the Δ*pdr-1* strain on HG as well as on galacturonic acid.

Genes that showed either a 3-fold up- or down-regulation in the DEseq analysis of the WT strain versus the Δ*pdr-1* strains on pectin or rhamnose, respectively, were combined for hierarchical clustering. The FPKMs of these 367 genes in both strains on NoC, 2% sucrose (WT only), 2 mM rhamnose and 1% pectin were used for the clustering (Figure 2-16c;

OTable 08). The genes were distributed over 13 clusters with and the clusters 1, 5, 12 and 13 contained genes with increased expression levels on only one carbon source (cluster 1 and 13: on rhamnose or pectin in WT strain; cluster 5 and 12: on pectin or rhamnose in Δ*pdr-1* strain). Only in cluster 1, 5 and 13 were genes found which are involved in pectin degradation and catabolism (Table 2-4; Figure 2-16c; OTable 08). Most genes that showed increased expression in the Δ*pdr-1* strain on pectin grouped together in cluster 5 (*ply-1*, *ply-2*, *asd-1*, *ce8-1*, *ce79-1*, *gaaB*/*lgd1* homolog, *gh28-2*, *gh43-1*, NCU01906). Cluster 1 contained most genes predicted to be involved in the rhamnose catabolism (putative *rha1*, *lra3* and *lra4* homologs), *gh105-1*, and the *pdr-1* gene itself, while cluster 13 was comprised of genes that exhibited increased expression level in the WT strain on pectin (*gh28-1*, *gh35-1*, *gh35-2*, and *ard-1*).

The reliability of the pectin specific RNA-Seq data was confirmed by comparing it to quantitative real-time PCR (RT-qPCR) expression data. The expression of *gh28-1*, *gh28-2*, *gh105-1*, *ce12-1*, *ce8-1*, *ply-1*, *ply-2* and *asd-1* in WT and Δ*pdr-1* strains was analyzed after induction on pectin versus NoC (SFigure 6-2) and a correlation analysis was performed between the RT-qPCR and RNA-Seq data. The Pearson's correlation coefficient (ρ) for the WT and Δ*pdr-1* strains was 0.886 and 0.999, respectively, indicating a strong correlation of these data sets and thus supporting the reliability of the RNA-Seq results.

2.2.4. PDR-1 mediated regulation of pectin backbone acting enzymes

The RNA-Seq data showed a significantly weaker expression of the endo-PGase gene *gh28-1* in the Δ*pdr-1* strain on pectin, while the expression level of pectate lyases was increased (Figure 2-16a, Table 2-4). To confirm whether the observed changes in transcription for these genes encoding HG backbone acting enzymes is translated to the protein level, the *N. crassa* WT, Δ*pdr-1* and *pdr-1-comp* strains were grown on 1% pectin and 1% xylan as control carbon source. The mycelial biomass and culture supernatants were taken after three days of growth for dry weight measurements and enzymatic activity assays, respectively.

The pectate lyase activity in culture supernatants from WT, Δ*pdr-1* and *pdr-1-comp* strains exhibited that the pectate lyase activity was significantly increased in Δ*pdr-1* strain compared to the other strain (Figure 2-17a), which corroborates the RNA-Seq results. For the analysis of endo-PGase activity, additionally the control strain Δ*gh28-1* was used. As expected, the *gh28-1* deletion strain showed no detectable enzymatic activity, while the activity of the WT and *pdr-1-comp* strains was similar (Figure 2-17b). However, the Δ*pdr-1* strain exhibited significantly reduced endo-PGase activity, which is consistent with the RNA-Seq results that also showed a strongly reduced *gh28-1* expression in this strain.

GH28-1 is the only endo-PGase in *N. crassa* and is important for growth on pectin (J. P. Benz *et al.*, 2014). However, the *gh28-1* gene was not properly induced in the Δ*pdr-1* strain (Figure 2-16c; Figure 2-17b), therefore the pectin-deficient phenotype might be caused by the lack of endo-PGase. To test this hypothesis, a *gh28-1* overexpression strain (strain *gh28-1-oex*) was created in the Δ*pdr-1* background, which was used to assess if overexpression of gh28-1 might complement the lack of *pdr-1*. In addition, a control strain that overexpresses *gh28-1* in the Δ*gh28-1* background (strain *gh28-1-comp*) was also constructed. Overexpression of *gh28-1* was confirmed by comparing both *gh28-1* overexpression strains to WT on pectin by RT-qPCR (SFigure 6-3a). Both strains showed ~3.5-fold elevated *gh28-1* expression compared to the WT strain.

The extent of complementation was determined by dry weight measurements and endo-PGase activity in culture supernatants of the overexpression strains compared to the WT

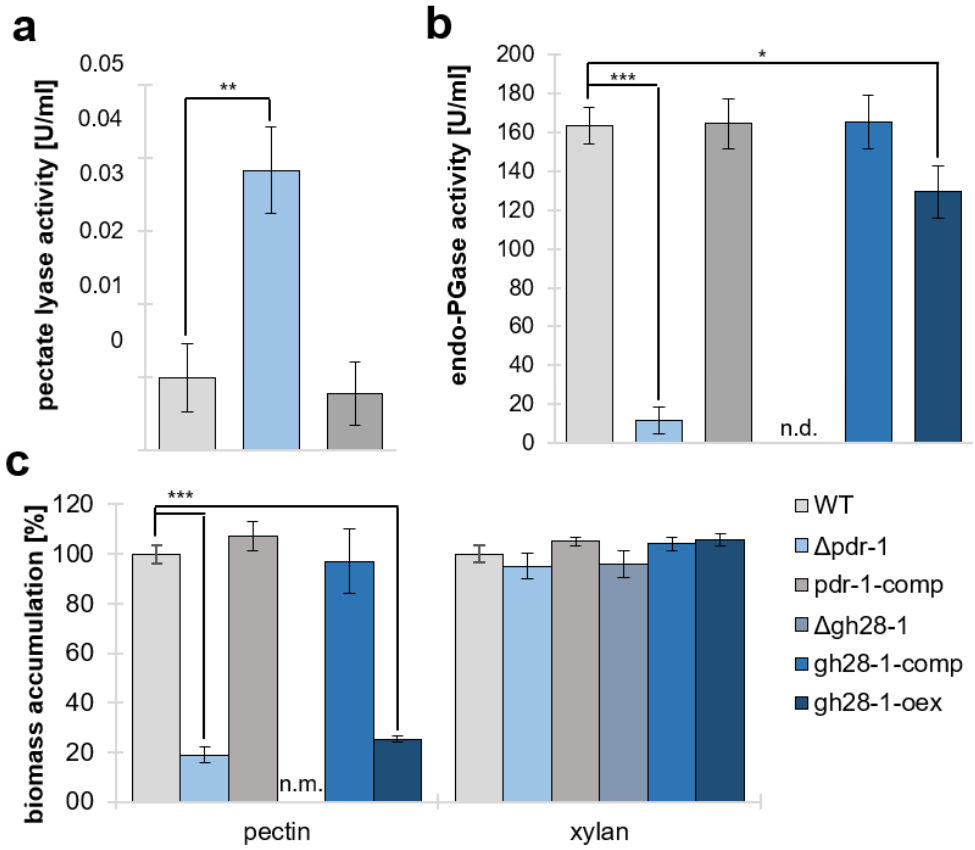

Figure 2-17: Enzymatic activity assays and biomass determination of WT, Δ*pdr-1*, Δ*gh28-1* and complementation strains.

Strains were grown for three days on either 1% pectin or 1% xylan. **a)** Supernatants from the WT, Δ*pdr-1* and *pdr-1-comp* strains were used to analyze pectate lyase activity. **b)** endo-PGase activity of culture supernatants from the WT, Δ*pdr-1* and *pdr-1-comp* strains (n.d.: none detected). **c)** Biomass of the strains by dry weight. Biomass of Δgh28-1 on 1% pectin was not measurable (n.m.), since supernatant was highly viscous and could not be separated from mycelium. Error bars represent standard deviation (n = 3). Significance was determined by an independent two-sample *t*-test of WT against all other strains with *p < 0.05, **p < 0.01 and ***p < 0.001.

strain and Δ*pdr-1* mutant grown on 1% pectin (Figure 2-17b, c). The *gh28-1-comp* strain showed WT-like biomass accumulation and enzymatic activity, verifying that overexpression of *gh28-1* complemented the loss of the endo-PGase. However, although the endo-PGase activity was partially restored in the *gh28-1-oex* strain (Figure 2-17b), it still exhibited a Δ*pdr-1* strain-like growth on pectin (Figure 2-17c). These results indicate that the observed growth phenotype of the Δ*pdr-1* strain on pectin was not solely caused by reduced expression of *gh28-1*. Instead, they suggest that intracellular catabolic pathways might be affected in addition to the expression of HG backbone degrading enzymes.

2.2.5. PDR-1 regulatory activity is associated with rhamnose

The RNA-Seq expression profile of *pdr-1* on NoC, 2% sucrose, 2 mM rhamnose and 1% pectin showed that rhamnose induced the strongest *pdr-1* expression, while the *pdr-1* expression levels were the lowest on sucrose (SFigure 6-4a). In addition, *pdr-1* expression was increased on NoC compared to sucrose, suggesting that *pdr-1* may be influenced by CCR and derepressed in the absence of a carbon source. This derepressed state could be achieved by autoinduction of PDR-1. However, it is known that some transcription factors are post-transcriptionally or -translationally modified before they can become fully active (Mehra *et al.*, 2009; Noguchi *et al.*, 2011).

To test the hypothesis that PDR-1 needs post-transcriptional activation to achieve full functionality, a strain was created that constitutively expresses *pdr-1* in the Δ*pdr-1* background (strain *pdr-1-oex*). The overexpression phenotype of *pdr-1-oex* was confirmed by comparing *pdr-1* expression of this strain to the WT strain through RT-qPCR (SFigure 6-3a). The *pdr-1-oex* strain showed a ~33-fold increase in *pdr-1* expression compared to the WT. In a next step, the WT, Δ*pdr-1* and *pdr-1-oex* strains were incubated for three days on xylan, as non-pectic control, or xylan with a regular supplementation of either 0.5 mM rhamnose or galacturonic acid. The biomass accumulation of these strains was determined by dry weight and their culture supernatants were used for endo-PGase activity assays. The biomass accumulation for all strains and conditions was similar (SFigure 6-4b), indicating that the low concentrations of inducing sugars (rhamnose or galacturonic acid) added to the medium did not suffice to generate additional biomass.

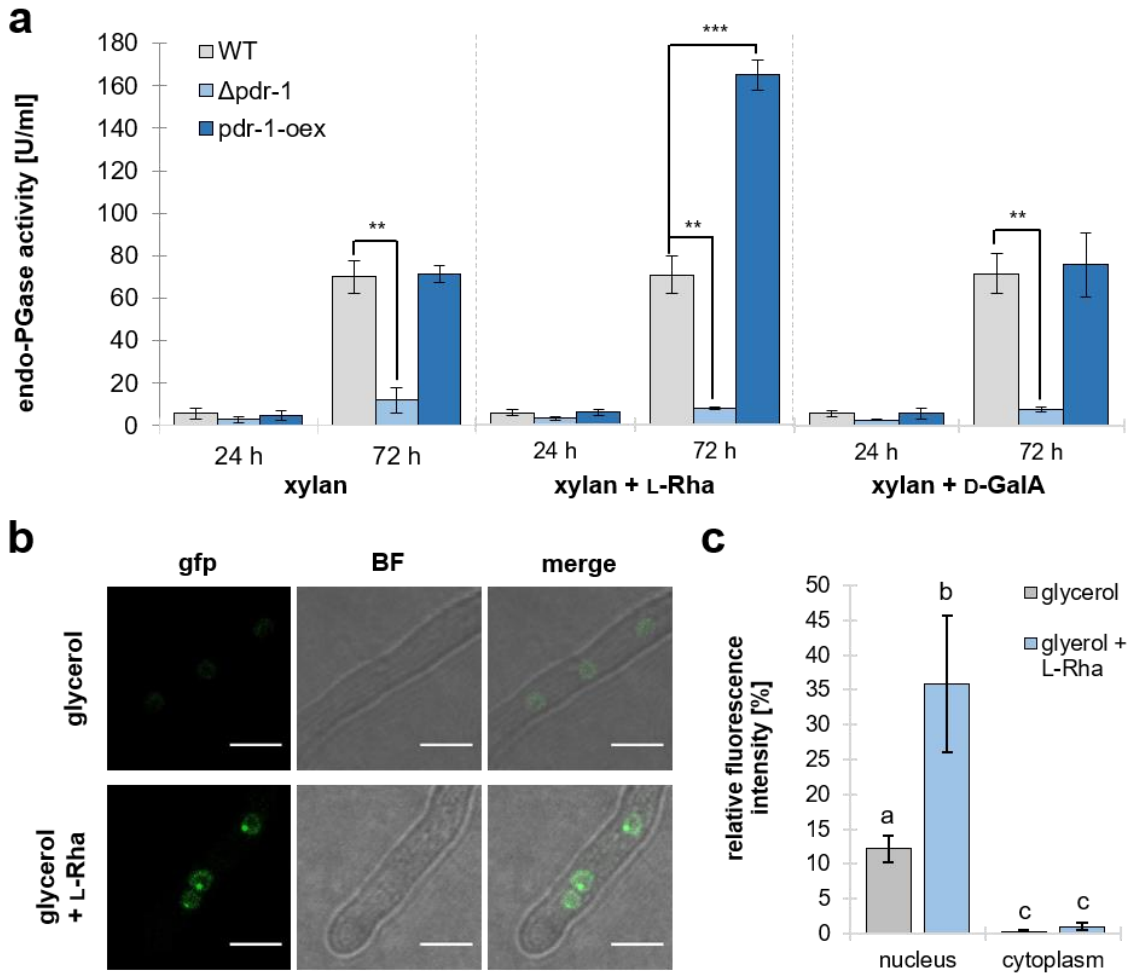

Figure 2-18: Endo-PGase activity of *pdr-1-oex* and subcellular localization of *pdr-1-gfp* in the presence of inducer molecules.

a) Strains were grown on 1% xylan plus 0.5 mM rhamnose or galacturonic acid or 1% xylan without any additives for 3 days. Endo-PGase activity was determined from culture supernatants taken after 24 or 72 hours, respectively. Error bars represent standard deviation (n = 3). Significance was determined by an independent two-sample *t*-test of WT against all other strains with **p < 0.01 and ***p < 0.001. **b)** The *pdr-1-gfp* strain was grown for 3 h on either 2% glycerol plus 2 rhamnose or 2% glycerol without any additives and fluorescence (gfp) as well as brightfield (BF) images were taken to determine the subcellular localization of PDR-1-GFP. Scale bars equal 5 µm. **c)** Fluorescence intensity was measured for both culture conditions described in (b). Error bars represent standard deviation (glycerol: n = 65; glycerol + rhamnose: n = 74). Significance was determined by Analysis of variance (ANOVA) followed by a post-hoc Tukey's test. The letters above each bar indicate statistical significance; bars sharing the same letter show no significant difference, while different letters represent a significant mean difference of p < 0.001.

Endo-PGase activity was measured in culture supernatants taken 24 h (before the addition of any monosaccharide) and 72 h (after 48 h of incubation on xylan plus either rhamnose or galacturonic acid) after inoculation. Only weak endo-PGase activity was measurable in all strains and growth conditions after 24 h of incubation (Figure 2-18a). After 72 h incubation, the WT and *pdr-1-oex* strains showed increased enzymatic activity on xylan media, while the endo-PGase activity of the Δ*pdr-1* strain remained unchanged. Since the

supernatants of the WT and *pdr-1-oex* strains showed an elevated endo-PGase activity on xylan alone, the composition of xylan was determined through acidic hydrolysis and measured by HPAEC-PAD (SFigure 6-5). Indeed, minor rhamnose concentrations of below 1% were presented in the xylan used in this study, which might explain the increased endo-PGase activity on xylan for the WT and *pdr-1-oex* strains. However, significantly increased enzymatic activity was observable for the *pdr-1-oex* strain compared to WT strain on xylan supplemented with additional rhamnose (Figure 2-18a), indicating that rhamnose is a specific inducer of endo-PGase activity through PDR-1.

To further corroborate these findings, the expression of *pdr-1* and a putative PDR-1 target gene, the *lra3* homolog NCU09034, was determined in the presence or absence of rhamnose by RT-qPCR. The WT and *pdr-1-oex* strains were incubated for 48 h on xylan and the medium was supplemented with 2 mM rhamnose after this incubation period. The expression of both target genes was compared to a non-induced (xylan only) control after 30 min of induction (SFigure 6-3b). While the WT strain showed an ~12-fold increase in *pdr-1* expression, the expression of *pdr-1* in the *pdr-1-oex* strain was independent of rhamnose. Nevertheless, both strains showed a strongly up-regulated expression of the target gene NCU09034 in the presence rhamnose (WT: ~27-fold, *pdr-1-oex*: ~90-fold). Since *pdr-1* expression in the *pdr-1-oex* strain did not change (SFigure 6-3b), the drastically increased NCU09034 expression was most likely caused through post-transcriptional activation of PDR-1. Together with the results of the endo-PGase assays, the RT-qPCR data indicate that PDR-1 activity is directly or indirectly dependent on the presence of rhamnose.

A GFP-tagged pdr-1-fusion construct driven by a constitutive promoter was transformed into *N. crassa* (*pdr-1-gfp*) to determine whether PDR-1 might be regulated through nuclear exclusion, as demonstrated for the transcription factor GaaR in *B. cinerea* (Zhang *et al.*, 2016). This strain was incubated for 3 h in medium containing either 2% glycerol or 2% glycerol plus 2 mM rhamnose. Although a weak fluorescence signal was detectable in the nuclei under non-inducing conditions (glycerol) (Figure 2-18b), the signal was found to be several times stronger in medium containing rhamnose (Figure 2-18c). In addition, a small but strongly fluorescing dot was visible inside most nuclei under inducing conditions (Figure 2-18b). Since the expression of GFP-tagged PDR-1 should be induction independent due to the utilization of a constitutive promoter, these results indicate that PDR-1 is not induced inside the nucleus, but instead recruited to the nucleus when rhamnose is present.

2.2.6. *In silico* determination of the PDR-1 DNA-binding motif

Electrophoretic Mobility Shift Assays (EMSA) of Pardo and Orejas showed that the DNA binding motif of the PDR-1 homolog RhaR has a palindromic core motif of an 11 nucleotide

long spacer region flanked by a CGG triplet on each side (CGG-X11-CCG) (Pardo and Orejas, 2014). Such a DNA binding site is typical for Gal4p-like transcription factors, which bind their recognition site as homodimers (Vashee *et al.*, 1993; MacPherson *et al.*, 2006). A large-scale analysis of protein-DNA binding microarrays by Weirauch *et al.* identified the corresponding DNA binding consensus sequence for *N. crassa* PDR-1 (Weirauch *et al.*, 2014). This motif, available at http://cisbp.ccbr.utoronto.ca, contained a highly conserved TCGG motif, but was not palindromic (Weirauch *et al.*, 2014).

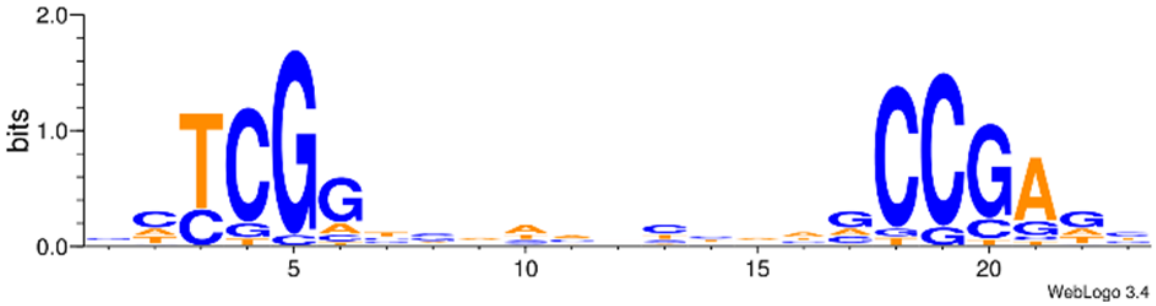

Figure 2-19: Putative consensus binding site of genes in the PDR-1 regulon.
A palindromic core motif of TCGG with an 11 nucleotide long spacer region was identified as described in chapter 5.6.3.

Based on these results, an *in silico* search for the full PDR-1 DNA binding motif was performed in this study. To increase the specificity of the query for a putative PDR-1 DNA binding site, a conserved DNA motif search was performed in the promoter regions of five major pectinase genes regulated by PDR-1 (NCU09034, NCU09035, *gh28-1*, *gh105-1*, and *pdr-1* itself). The search parameters were set to identify Gal4p-like inverted repeats with a TCGG motif in these promoter sequences, but also allowed for imperfect matches. This effort resulted in the consensus sequence as shown in Figure 2-19. A search of the whole *N. crassa* genome with this PDR-1 binding site returned 194 genes with at least one binding site on the sense or anti-sense strand in a 1000 bp upstream region of the gene and a stringency score of 0.6 or greater (OTable 08; chapter 5.6.3). Enrichment in functional categories was determined for these genes and the categories hemicellulose/pectin metabolism and hemicellulose/pectin catabolism were highly significant enriched (p-value below 5×10^{-5}) (OTable 08). Of these 194 genes, nine genes were encoding pectinolytic enzymes that were regulated transcriptionally by PDR-1 (Table 2-4): *gh28-1*, *gh35-2*, most genes of the rhamnose catabolism (*rha1*, *lra3* and *lra4* homologs) and the transcription factor *pdr-1* itself.

Table 2-5: Genes of the putative PDR-1 core regulon.
PDR-1 DNA binding sites (PB sites) with a stringency score of more than 0.6 were used. The clusters refer to Figure 2-16.

ID	name/annotation	# of PB sites	Cluster
NCU00643	*ard-1*	2	C13
NCU01700	hypothetical protein	2	C1
NCU01701	*rok-1*	2	C1
NCU01871	hypothetical protein	3	C1
NCU02369	*gh28-1*	2	C13
NCU02653	*mfs-20*	3	C1
NCU02654	*gh105-1*	3	C1
NCU03086	put. *lra4*	1	C1
NCU04130	*acy-1*	2	C1
NCU04623	*gh35-2*	1	C13
NCU05037	put. *lra4*	4	C1
NCU05985	*chol-6*	1	C1
NCU06138	*mfs-19*	1	C13
NCU07225	*gh11-2*	1	C13
NCU07506	*fah-2*	3	C1
NCU08475	hypothetical protein	2	C1
NCU09033	*pdr-1*	5	C1
NCU09034	put. *lra3*	2	C1
NCU09035	put. *rha1*	3	C1
NCU10106	*emp-19*	2	C1
NCU11253	glyoxalase	2	C1
NCU11278	hypothetical protein	2	C1

Matching all genes that contained a putative PDR-1 DNA binding motif to the genes in the PDR-1-affected clusters 1, 5, 12 and 13 resulted in a small set of 22 genes (Table 2-5). However, only genes in clusters 1 and 13 contained genes with a PDR-1 binding site including the nine pectinolytic ones mentioned above. Therefore, most of the putative rhamnose catabolism genes were present in this set (*rha1*, *lra3* and *lra4* homologs), as well as the endo-PGase gene *gh28-1*, the β-galactosidase gene *gh35-2*, the L-arabinitol 4-dehydrogenase *ard-1*, the glycosyl hydrolase gene *gh105-1* and *pdr-1*. The remaining 13 genes encode the ribitol kinase *rok-1* (NCU01701), the allantoate permease *mfs-20* (NCU02653), the acylase (or putative γ-glutamyltransferase) *acy-1* (NCU04130), the glycerol-3-phosphate O-acyltransferase *chol-6* (NCU05985), the quinate permease *mfs-19* (NCU06138), the endo-1,4-β-xylanase *gh11-2* (NCU07225), the fumarylacetoacetate hydrolase *fah-2* (NCU07506), the mitochondrial triosephosphate isomerase *emp-19* (NCU10106), a glyoxalase (NCU11253) and four hypothetical proteins (NCU01700, NCU01871, NCU08475 and NCU11278). These genes form the PDR-1 core regulon, because they contain a putative PDR-1 DNA binding site and exhibited a significantly reduced expression in the *pdr-1* deletion strain.

2.2.7. Identification of the transcription factor PDR-2

Although *N. crassa* PDR-1 is involved in the regulation of most rhamnose catabolism genes as well as genes encoding HG depolymerization enzymes, the *pdr-1* deletion strains still showed ~20% of WT biomass when grown on pectin (Figure 2-13). This indicates that the loss of *pdr-1* is not sufficient to prevent *N. crassa* from utilizing pectin as carbon source. In addition, *Aspergillus* RhaR only showed a slight growth defect on pectin (Gruben *et al.*, 2014; Pardo and Orejas, 2014), which implies that there might be additional transcription factors that are regulators of pectin degradation.

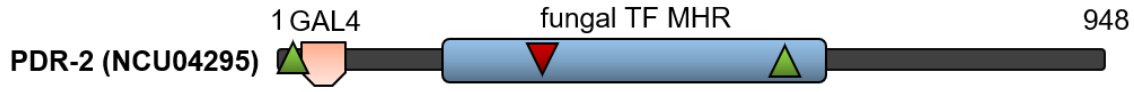

Figure 2-20: Schematic depiction of conserved domains/signals in the transcription factor PDR-2 (NCU04295).
The amino acid sequence of *N. crassa* PDR-2 (NCU04295) was used in a conserved domain search, as well as NLS and NES prediction. GAL4 = GAL4-like $Zn(II)_2Cys_6$ (or C6 zinc) binuclear cluster DNA-binding domain, fungal TF MHR = fungal transcription factor regulatory middle homology region, green triangle = nuclear localization signal, red triangle = nuclear export signal.

Therefore, the transcriptome data of the 'Fungal Nutritional ENCODE Project' was used to search for additional regulators of pectin degradation (Glass *et al.*, 2013a). A hierarchical clustering using Pearson's correlation was performed on RNA-Seq expression data of genes induced for 4 h with polysaccharides (Figure 2-10). The sixth cluster (C6) contained most of the previously published pectinase genes (J. P. Benz *et al.*, 2014) and also exhibited a significant functional gene enrichment for specific pectin catabolism ($p = 1.27 \times 10^{-20}$; OTable 06). This cluster contained the putative $Zn(II)_2Cys_6$ transcription factor NCU04295 (OTable 06), suggesting that the expression pattern of NCU04295 was similar to pectinase expressing genes on the tested carbon sources.

The transcription factor NCU04295 is 948 amino acid long, contains two predicted nuclear localization signal (NLS), one predicted nuclear export signal (NES), a GAL4-like $Zn(II)_2Cys_6$ binuclear cluster DNA-binding domain and a fungal transcription factor regulatory middle homology region (fungal TF MHR) (Figure 2-20). To test if NCU04295 could be involved in the regulation of pectin depolymerization, the WT and ΔNCU04295 strains were incubated for 3 days in 1% pectin and their biomass was determined by dry weight. Indeed, the deletion of NCU04295 reduced the biomass of the ΔNCU04295 strain to ~50% of WT biomass (Figure 2-21a). In addition, the amino acid sequence of NCU04295 was compared to the sequences of the published galacturonic acid degradation regulators GaaR of *B. cinerea* and *A. niger* (Alazi *et al.*, 2016; Zhang *et al.*, 2016). The sequence alignments showed an identity of 53% and 47% between the full-length sequences of *N.*

crassa NCU04295 and GaaR of *B. cinerea* or *A. niger*, respectively. The NCU04295 locus was therefore named pectin degradation regulator-2 (*pdr-2*).

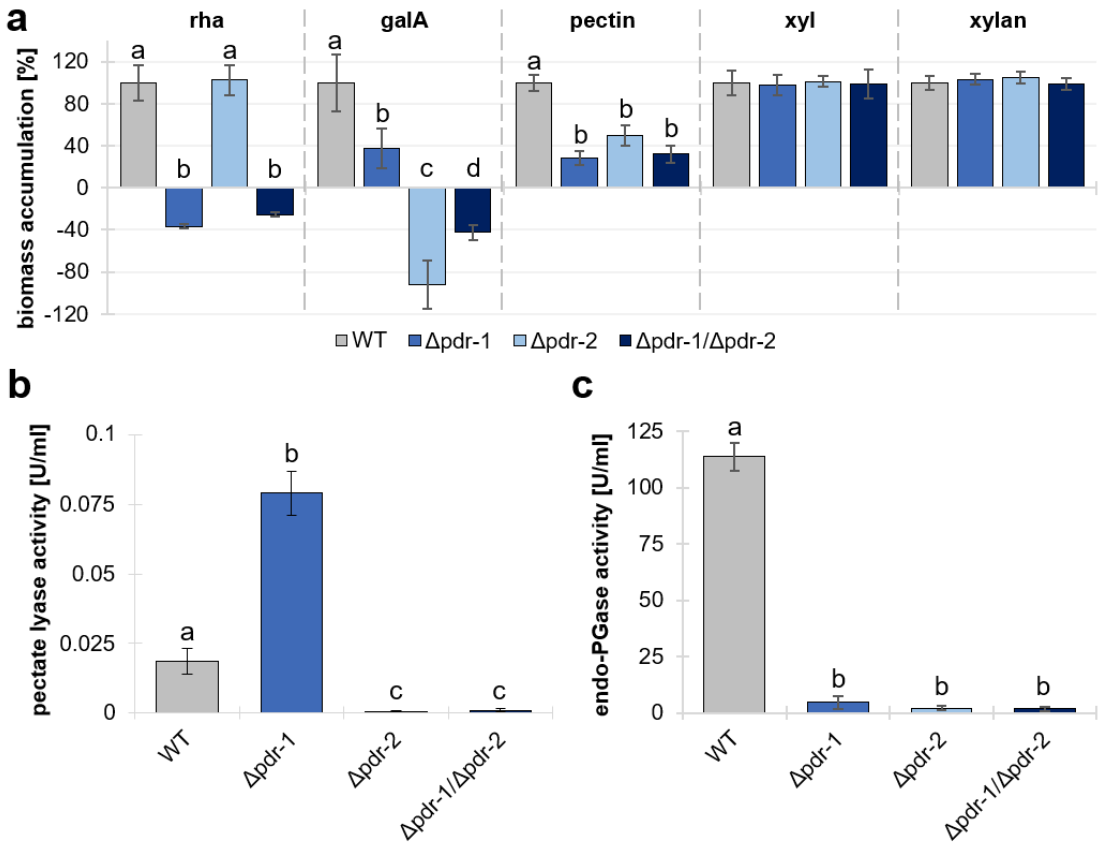

Figure 2-21: Biomass accumulation and pectinase activity of the WT, Δ*pdr-1*, Δ*pdr-2* and Δ*pdr-1*/Δ*pdr-2* strains.
a) The biomass of *N. crassa* WT, Δ*pdr-1*, Δ*pdr-2* and Δ*pdr-1*/Δ*pdr-2* strains was determined. Strains were grown for 3 days in 3 ml cultures with 1% polysaccharide as carbon source. Alternatively, the strains were pre-incubated for 16 h in medium containing 2% sucrose, then washed, transferred to a 2 mM monosaccharide medium and incubated for additional 2 days with regular medium switches. After three days of incubation, the biomass was determined as dry weight. The samples were normalized to WT biomass. rha = rhamnose, galA =galacturonic acid, xyl = xylose. **b)** Supernatants from the strains were used to analyze pectate lyase activity or **c)** endo-PGase activity. Error bars represent standard deviation (n = 3). Significance was determined by ANOVA followed by a post-hoc Tukey's test. The letters above each bar indicate statistical significance; bars sharing the same letter show no significant difference, while different letters represent a significant mean difference of $p < 0.05$.

2.2.8. PDR-2 mediates HG depolymerization and galacturonic acid catabolism

To assess the hierarchy between PDR-1 and PDR-2 during pectin degradation, the Δ*pdr-1* and Δ*pdr-2* strains were crossed to create a double deletion strain (Δ*pdr-1*/Δ*pdr-2*). The double deletion strain, both single deletion mutants and the WT strain were incubated in either 1% pectin, 2 mM rhamnose or 2 mM galacturonic acid, while 2 mM xylose and 1%

xylan were used as control conditions. The biomass of the strains was determined as dry weight and the supernatants of the strains incubated in pectin was used to determine pectate lyase and endo-PGase activity (Figure 2-21). While the Δ*pdr-1* strain could not accumulate any biomass on rhamnose and showed a severe growth defect on pectin as well as galacturonic acid, the growth of the Δ*pdr-2* strain was WT-like on rhamnose, significantly reduced on pectin and completely abolished on galacturonic acid (Figure 2-21a). These results indicate, that PDR-2 could be the main regulator of galacturonic acid catabolism, but PDR-1 may also be necessary for the full functionality of this catabolic process. In contrast, the rhamnose catabolism is not affected by loss of *pdr-2*, which suggests that PDR-1 might be the sole regulator of rhamnose degradation in *N. crassa*, similar to its homologs RhaR in *Aspergilli* (Gruben *et al.*, 2014; Pardo and Orejas, 2014). Intriguingly, the *pdr-1* and *pdr-2* double deletion strain always mimicked the phenotype of either Δ*pdr-1* or Δ*pdr-2* but did not lead to a more severe growth defect on pectin (Figure 2-21a). This indicates that PDR-1 and PDR-2 are both necessary for a fully functional pectin degradation machinery. Moreover, the results of the growth assay suggest that PDR-1 is not regulated by PDR-2 and vice versa.

Since the pectate lyase genes and the endo-PGase gene *gh28-1* were mis-expressed in the *pdr-1* deletion strain, the activity of these enzymes was determined in the Δ*pdr-2* and Δ*pdr-1*/Δ*pdr-2* strains to examine potential overlaps in regulation between PDR-1 and PDR-2. Both enzymatic assays were performed with supernatants of the WT, Δ*pdr-1*, Δ*pdr-2* and the Δ*pdr-1*/Δ*pdr-2* strains incubated in pectin (Figure 2-21b, c). The pectate lyase assay showed that loss of *pdr-2* completely abolished pectate lyase activity in both the Δ*pdr-2* and the Δ*pdr-1*/Δ*pdr-2* strains (Figure 2-21b). Additionally, the Δ*pdr-2* and the Δ*pdr-1*/Δ*pdr-2* strains exhibited significantly reduced endo-PGase activity, similar to the Δ*pdr-1* strain (Figure 2-21c). Based on these results, it appears that PDR-2 is the main activator of pectate lyase expression in *N. crassa* and that the presence of both transcription factors is necessary for a WT-like endo-PGase activity. Moreover, since the Δ*pdr-1* strain exhibited significantly increased pectate lyase activity compared to the WT strain (Figure 2-21b), PDR-2 might be up-regulating pectate lyase expression to compensate the loss of HG backbone acting enzymes in the Δ*pdr-1* strain. This hypothesis was corroborated by additional experiments in the Δ*gh28-1* strain, which showed that the absence of GH28-1 leads to increased pectate lyase activity (data not shown).

2.2.9. Transcriptome analysis of PDR-1 and PDR-2 regulated genes

The transcriptome data of the ‘Fungal Nutritional ENCODE Project’ was used to determine which genes are regulated by either PDR-1, PDR-2 or both transcription factors (Glass *et*

al., 2013a). A hierarchical clustering based on Pearson's correlation was performed using RNA-Seq expression data of the WT, Δ*pdr-1* and Δ*pdr-2* strains induced for 4 h with 1% citrus peel.

A total of six clusters were revealed by this method and the previously annotated pectinase genes (J. P. Benz *et al.*, 2014) were located in the clusters 1, 3 and 4 (Figure 2-22; OTable 09). The first cluster (C1) contained genes that were down-regulated in the Δ*pdr-2* strain compared to the Δ*pdr-1* as well as WT strain and most pectinase genes in this cluster were at least 2-fold down-regulated in the absence of *pdr-2*. Therefore, this cluster contained genes that are considered PDR-2 dependent and PDR-1 modulated, including, among others, the pectate lyase genes *ply-1* and *ply-2*, the rhamnogalacturonan lyase gene *asd-1*, the exo-PGase gene gh28-2, the methylesterase gene *ce8-1*, as well as genes encoding galacturonic acid catabolic enzymes (the *gar2* homolog NCU09533 and *lga1* homolog NCU09532) and the galacturonic acid transporter gene *gat-1*. The mis-expression of the pecate lyase genes supports the results of the pectate lyase assays (Figure 2-21b).

Most genes in the the third cluster (C3) were deemed as dependent of PDR-1 and PDR-2 as they were significantly down-regulated (at least 2-fold) in both deletion strains compared to the WT strain (Figure 2-22; OTable 09). This cluster contained many gene encoding enzymes involved in pectin backbone and side-chain degradation, such as the rhamnogalacturonyl hydrolase gene *gh105-1*, rhamnogalacturonan acetylesterase gene *ce12-1*, the β-galactosidase genes *gh35-1* and *gh35-2*. Intriguingly, the endo-PGase gene *gh28-1* was also in this cluster, corroborating the results of the endo-PGase assay that loss of either *pdr-1* or *pdr-2* almost completely abolishes endo-PGase activity in *N. crassa* (Figure 2-21c).

Lastly, only two pectinase genes were in the fourth cluster (C4), the transcription factor *pdr-1* and the L-arabinitol 4-dehydrogenase gene *ard-1*, and both genes were significantly down-regulated (at least 2-fold; Figure 2-22; OTable 09). This cluster was considered to contain PDR-1 dependent genes, since all genes in this cluster were down-regulated in the Δ*pdr-1* strain compared to the Δ*pdr-2* strain and WT strain.

Taken together, the RNA-Seq data supports the previous experimental results for PDR-1 and PDR-2. Moreover, these data show that there is an extensive overlap in regulation between both transcription factors, although PDR-2 appears to regulate more genes than PDR-1 on citrus peel. It is important to notice that citrus peel still contains significant concentrations of other polysaccharides (J. P. Benz *et al.*, 2014), which might influence the observed expression patterns.

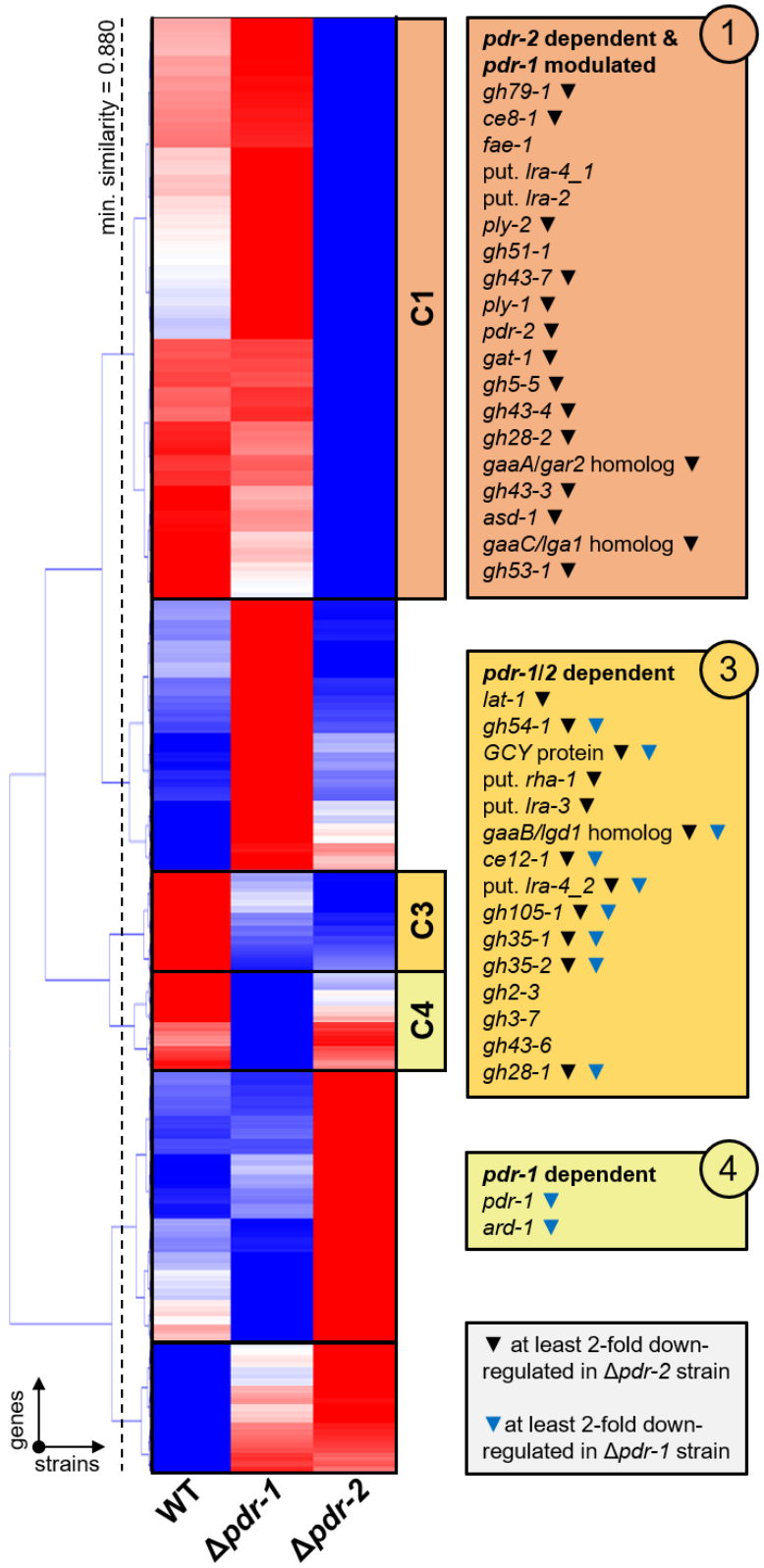

Figure 2-22: Hierarchical clustering of RNA-Seq data from WT, Δ*pdr-1*, Δ*pdr-2* and Δ*pdr-1*/Δ*pdr-2* strains.

RNA-Seq data of WT, Δ*pdr-1*, Δ*pdr-2* and Δ*pdr-1*/Δ*pdr-2* strains induced for 4 h on 1% citrus peel was used. The position of pectinases and rhamnose/galacturonic acid catabolism genes are indicated next to their respective clusters (C1, C3 or C4). lra4_1 = NCU03086, lra4_2 = NCU05037.

2.2.10. Identification of an Ara1 homolog in *N. crassa*

A part of the pectin backbone is decorated with side-chains composed of different monosaccharides, mostly arabinose and galactose (Caffall and Mohnen, 2009; Harholt *et al.*, 2010). Although PDR-1 and PDR-2 were involved in the regulation of some arabinanase genes and the Δ*pdr-1* strain exhibited a growth defect on arabinose as well as arabinan, the arabinose and galactose metabolisms are regulated by specialized transcription factors in several ascomycetes (Benocci *et al.*, 2017). While the transcription factors AraR and

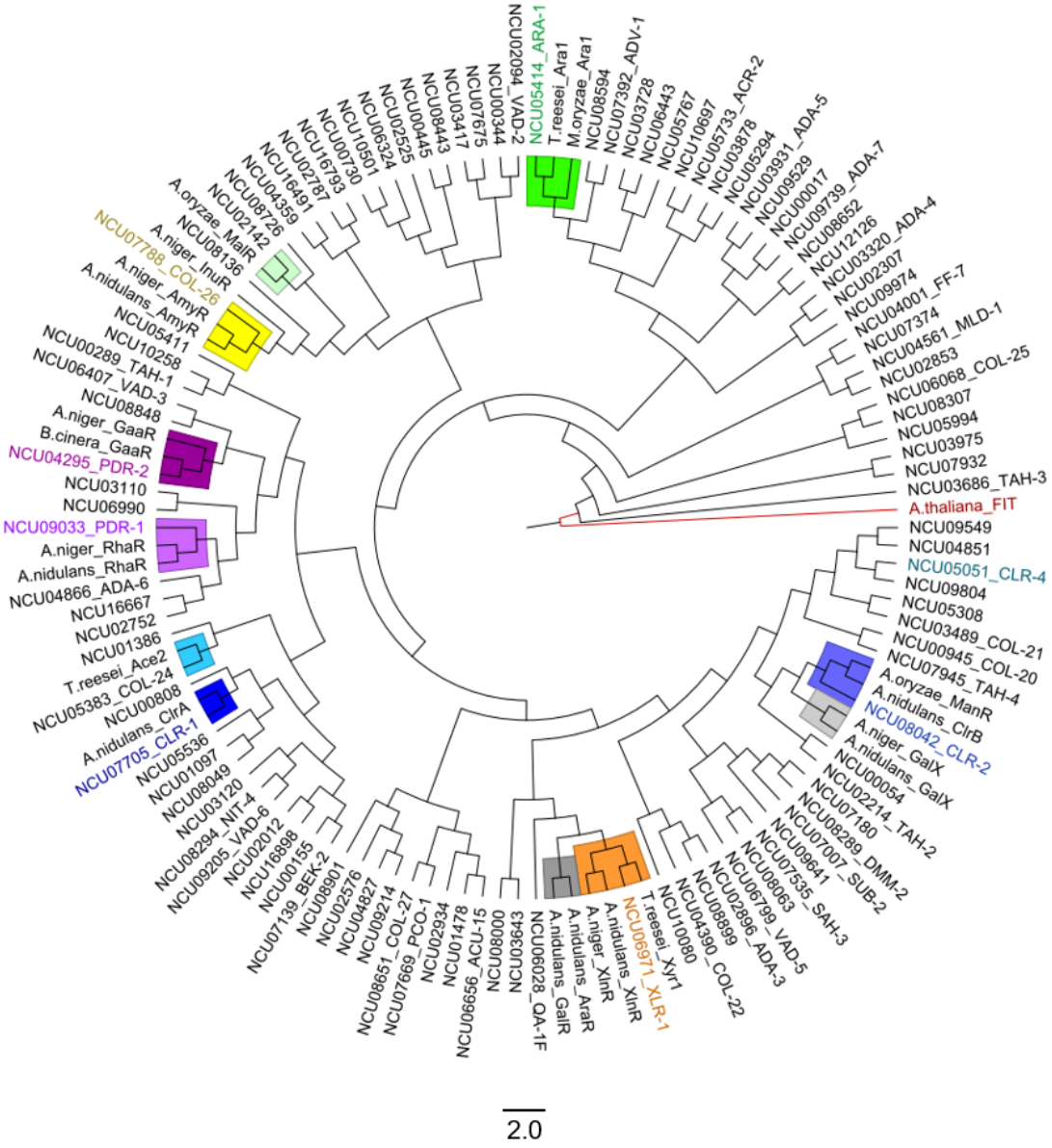

Figure 2-23: Phylogenetic tree of all known Zn(II)$_2$Cys$_6$ transcription factors of *N. crassa* and published regulators of polysaccharide degradation from other ascomycetes.
Names of *N. crassa* transcription factors described in this work or already published are highlighted in color. Close phylogenetic relations between known transcription factors are marked by color on the respective clades. The transcription factor FIT from *Arabidopsis thaliana* was used as outgroup (marked in red).

GalX/GalR are described for the regulation of either arabinose or galactose catabolism in *Aspergilli*, respectively (Battaglia *et al.*, 2011b; Christensen *et al.*, 2011; Gruben *et al.*, 2012), only Ara1 is described as regulator of arabinose catabolism in Sordariomycetes (Klaubauf *et al.*, 2016; Benocci *et al.*, 2018).

Figure 2-24: Schematic depiction of conserved domains/signals in the transcription factor ARA-1 (NCU05414).
The amino acid sequence of *N. crassa* ARA-1 (NCU05414) was used in a conserved domain search, as well as NLS and NES prediction. GAL4 = GAL4-like $Zn(II)_2Cys_6$ (or C6 zinc) binuclear cluster DNA-binding domain, fungal TF MHR = fungal transcription factor regulatory middle homology region, green triangle = nuclear localization signal.

To identify whether *N. crassa* has one or more specialized regulators of the arabinose or galactose catabolism, a phylogenetic tree was created which was comprised of all known $Zn(II)_2Cys_6$ transcription factors protein sequences of *N. crassa*, as well as published sequences for most polysaccharide degradation related transcription factors from other ascomycetes (Figure 2-23). The phylogenetic tree showed that no undescribed $Zn(II)_2Cys_6$ transcription factor of *N. crassa* is closely related to *Aspergilli* AraR or GalR/GalX and only NCU05414 clustered close to Ara1 of *T. reesei* and *M. oryzae*.

NCU05414 encodes a 663 amino acid long transcription factor that contains a GAL4-like $Zn(II)_2Cys_6$ binuclear cluster DNA-binding domain, a fungal transcription factor regulatory middle homology region (fungal TF MHR) and one predicted nuclear localization signal (NLS), but no predicted nuclear export signal (NES) (Figure 2-24). Furthermore, the amino acid sequence of NCU05414 was compared to the sequences of the published arabinose catabolism regulator Ara1 of *T. reesei* and *M. oryzae* (Klaubauf *et al.*, 2016; Benocci *et al.*, 2018). The sequence alignments showed an identity of 53% and 51% between the full-length sequences of *N. crassa* NCU05414 and Ara1 of *T. reesei* or *M. oryzae*, respectively. Therefore, the locus of NCU05414 was tentatively named *ara-1*.

To further corroborate that ARA-1 is a regulator of arabinose as well as galactose catabolism (Benocci *et al.*, 2018), a growth assay of the WT and Δ*ara-1* strains was performed on 1% arabinan, 1% arabinogalactan, 1% pectin and 1% xylan as control. In addition, the strains were also incubated on either 2 mM arabinose, 2 mM galactose or 2 mM xylose as control (Figure 2-25). The Δ*ara-1* strain exhibited a severe growth defect on arabinan, and its growth was still significantly reduced on arabinogalactan. Furthermore, the *ara-1* deletion strain was unable to accumulate any biomass on galactose and arabinose.

These results support that *N. crassa* ARA-1 is indeed a regulator of arabinose and galactose catabolism.

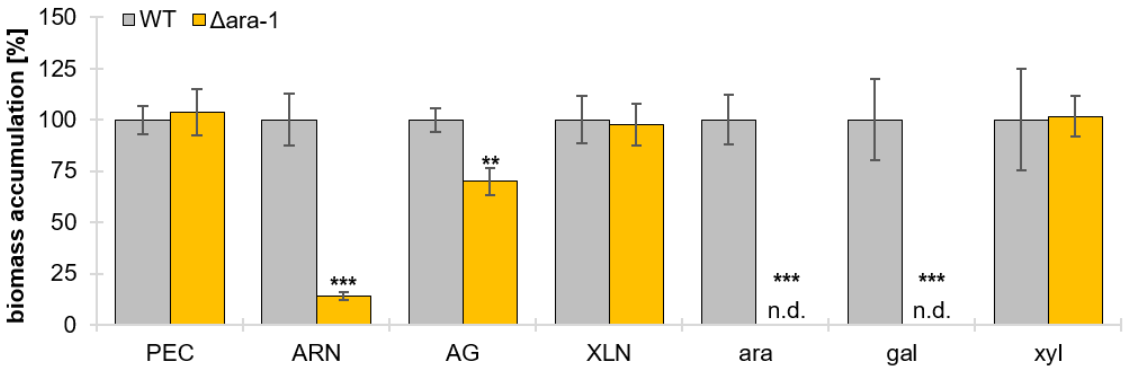

Figure 2-25: Growth assay of WT and Δ*ara-1* strains.
Strains were grown for three days on 1% polysaccharide. Alternatively, the strains were pre-incubated for 16 h in medium containing 2% sucrose, then washed, transferred to a 2 mM monosaccharide medium and incubated for additional 2 days with regular medium switches. After three days of incubation (5 days for arabinogalactan), the biomass was determined as dry weight. The samples were normalized to WT biomass. Error bars represent standard deviation (n = 3). Significance was determined by an independent two-sample *t*-test of WT against Δ*ara-1* with **p < 0.01 and ***p < 0.001. n.d. = no growth detected, PEC = pectin, ARN = arabinan, AG = arabinogalactan, XLN = xylan, ara = arabinose, gal = galactose, xyl = xylose.

2.3. Analysis of additional regulatory elements influencing pectin degradation

2.3.1. Identification and characterization of a rhamnose transporter in *N. crassa*

Although transcription factors are important regulators of the metabolic state in *N. crassa*, since they activate or repress the utilization of certain carbon sources (Huberman *et al.*, 2016; Seibert *et al.*, 2016; Benocci *et al.*, 2017; Schmitz *et al.*, 2019), fungal metabolism is also directly or indirectly regulated by other proteins. Transport proteins determine through their substrate affinity and uptake capacity, which and in what concentration soluble molecules are present in *N. crassa* (Cai *et al.*, 2014; J. Benz *et al.*, 2014; Kim *et al.*, 2014; Wang *et al.*, 2017; Hassan *et al.*, 2019). Moreover, transport proteins might act as transceptors (Znameroski *et al.*, 2014) and the regulation of genes encoding transport proteins is modulating fungal metabolism (Portnoy *et al.*, 2011; Sloothaak *et al.*, 2016; Wang *et al.*, 2017). Therefore, a better knowledge of fungal sugar transporters is necessary to fully understand the perception and regulation of plant polysaccharides in fungi.
While two transport proteins are described in *N. crassa* that take up monosaccharides which are released during pectin depolymerization, the galacturonic acid transporter GAT-1 and the arabinose transporter LAT-1 (J. Benz *et al.*, 2014; J. P. Benz *et al.*, 2014), no rhamnose

transporter is published for *N. crassa*. However, rhamnose is an important building block of pectin (Caffall and Mohnen, 2009; Harholt *et al.*, 2010) and *N. crassa* is able to metabolize rhamnose (Figure 2-13; Figure 2-21), which implies that it should be able to transport this monosaccharide into the cytosol.

The transcriptome of the 'Fungal Nutritional ENCODE Project' was utilized to identify a rhamnose transporter in *N. crassa*. An expression screen of the ENCODE data by Dietschmann found three potential rhamnose transporter candidates with good expression on either rhamnose or pectin (Dietschmann, 2015). By further analyzing these transporter genes using TCDB annotation, the gene sugar transporter 28 (*sut-28*, NCU05897) was classified as part of the Fucose:H^+ symporter (FHS) family (2.A.1.7). Since fucose, as 6-deoxy-L-galactose, and rhamnose, as 6-deoxy-L-mannose, are both structurally very similar, it is feasible that a fucose transporter could be able to take up rhamnose. In addition, the expression profile of *sut-28* showed elevated gene expression on rhamnose as well as pectin (Figure 2-26a), and the deletion strain of *sut-28* exhibited significantly reduced growth on pectin, rhamnose and PGA compared to the WT strain (Figure 2-26b).

To analyze if the deletion of *sut-28* leads to a reduced uptake of rhamnose, the WT and Δ*sut-28* strains were pre-grown on sucrose and then transferred to an induction medium of pectin, since *sut-28* exhibited a high expression on pectin in the RNA-Seq. After a 4 h induction period, the strains were transferred to a rhamnose medium and several supernatant samples were taken over time. The residual rhamnose concentration in these supernatants was determined by HPAEC-PAD (Figure 2-26c). While the WT strain almost depleted the rhamnose in the medium over the course of 60 minutes, the Δ*sut-28*strain showed no uptake of rhamnose. To determine the SUT-28 uptake specificity, additional uptake assays of both strains were performed. WT and Δ*sut-28* were induced with xylan and their uptake of fucose, galactose or xylose was determined over time (SFigure 6-6). Unsurprisingly, the deletion of the putative fucose:H+ symporter gene *sut-28* completely abolished the uptake of fucose, while xylose and galactose uptake were WT-like in the Δ*sut-28* strain.

Since the transcription factor PDR-1 only becomes fully active in the presence of rhamnose, a loss of the putative rhamnose transporter gene *sut-28* should prevent the expression of the PDR-1 target gene NCU09034 (Table 2-5). To test this hypothesis, the NCU09034 expression was determined in the WT, Δ*pdr-1* and Δ*sut-28* strains by RT-qPCR. An 4 h induction period with rhamnose failed to induce NCU09034 expression in the Δ*pdr-1* and Δ*sut-28* strains compared to the WT strain (Figure 2-26d). Based on these results, *sut-28* encodes the sole rhamnose transporter in *N. crassa*. Therefore, the author proposes to rename the NCU05897 locus to fucose rhamnose transporter 1 (*frt-1*).

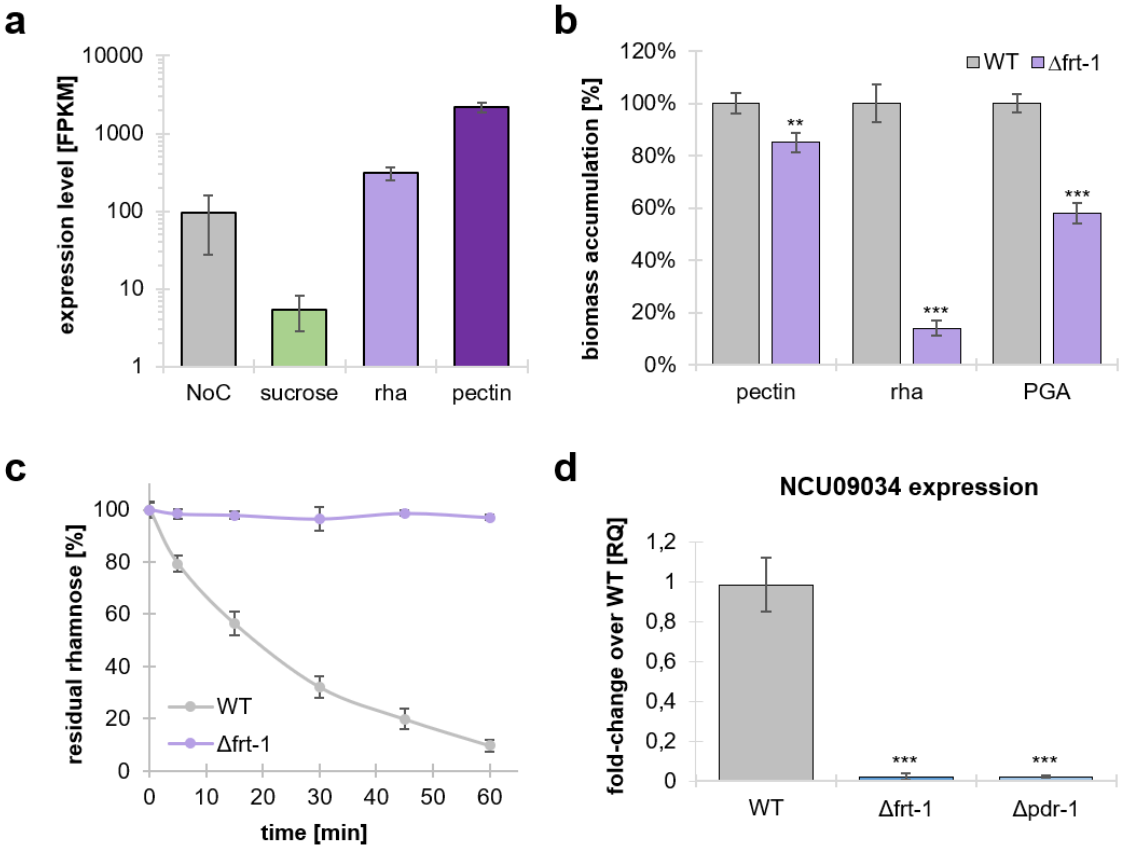

Figure 2-26: Characterization of the fucose rhamnose transporter 1 (FRT-1; NCU05897) by expression, growth and rhamnose uptake.

a) Expression profile of *frt-1* using RNA-Seq data of WT induced for 4 h on NoC, 2% sucrose, 2 mM rhamnose or 1% pectin. Diagram axes are log_{10}-scaled. **b)** The biomass of *N. crassa* WT and Δ*frt-1* strains was determined. Strains were grown for 3 days in 3 ml cultures with 1% polysaccharide as carbon source. Alternatively, the strains were pre-incubated for 16 h in medium containing 2% sucrose, then washed, transferred to a 2 mM monosaccharide medium and incubated for additional 2 days with regular medium switches. After three days of incubation, the biomass was determined as dry weight. The samples were normalized to WT biomass. **c)** Uptake of rhamnose in the WT and Δ*frt-1* strains. Both strains were pre-incubated for 16 h in 2% sucrose, washed and transferred to 0.5% pectin medium to induce gene expression. After 4 h of induction, the biomass was transferred to 100 µM of rhamnose and sample supernatant was taken at defined time points. The monosaccharide content of the supernatants was measured using HPAEC-PAD. **d)** The WT, Δ*frt-1* and Δ*pdr-1* strains were incubated for 16 h in 2% sucrose, washed and then transferred to 2 mM rhamnose. The expression level of NCU09034 was determined after a 4 h induction period by RT-qPCR. The WT strain was used as reference. Error bars represent standard deviation (n = 3). Significance was determined by an independent two-sample *t*-test of WT against all other strains with **p < 0.01 and ***p < 0.001. rha = rhamnose

2.3.2. Expression of *frt-1* is repressed by CRE-1 during CCR

The deletion of *frt-1* significantly changed the substrate "perception" of *N. crassa*, because the loss of rhamnose uptake most likely prevented the activation of PDR-1, which in turn would affect all PDR-1 mediated genes. This implies that the regulation of genes encoding transporter proteins can lead to far reaching changes in the metabolic state of *N. crassa*. Therefore, it was determined which effect CRE-1 mediated CCR has on *frt-1* expression.

The expression level of *frt-1* was determined in WT and Δ*cre-1* strains induced with either rhamnose or rhamnose plus glucose by RT-qPCR (Figure 2-27a). While rhamnose alone elicited a WT-like expression of *frt-1* in the Δ*cre-1* strain, the induction with rhamnose and glucose drastically reduced *frt-1* expression in the WT strain. Moreover, the co-induction with rhamnose plus glucose led to a 6-fold greater *frt-1* expression in the Δ*cre-1* strain compared to the WT strain induced with only rhamnose.

Additional uptake assays were performed, since the effects of CRE-1 mediated CCR could occur during induction of *frt-1* expression or directly during substrate uptake, e.g. by post-translational modification of FRT-1 in the presence of glucose. Expression of *frt-1* was induced in the WT and Δ*cre-1* strains with pectin and the uptake medium contained either rhamnose (control) or rhamnose plus glucose. In addition, both strains were induced with

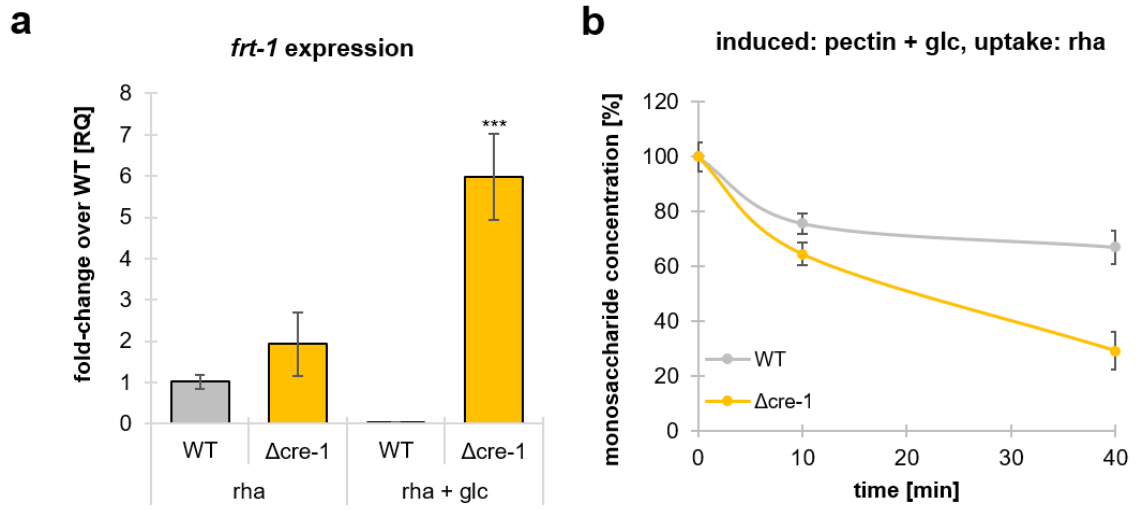

Figure 2-27: Expression of *frt-1* is repressed by CRE-1

a) The WT and Δ*cre-1* strains were incubated for 16 h in 2% sucrose, washed and then transferred to either 2 mM rhamnose or 2 mM rhamnose plus 2% glucose. The expression level of *frt-1* was determined after a 4 h induction period by RT-qPCR. The WT strain was used as reference. **b)** Uptake of rhamnose in the WT and Δ*cre-1* strains. Both strains were pre-incubated for 16 h in 2% sucrose, washed and transferred to 0.5% pectin plus 2% glucose medium to induce gene expression. After 4 h of induction, the biomass was transferred to 100 µM of rhamnose and sample supernatant was taken at defined time points. The monosaccharide content of the supernatants was measured using HPAEC-PAD. Error bars represent standard deviation (n = 3). Significance was determined by an independent two-sample *t*-test of WT against all other strains with ***p < 0.001. rha = rhamnose, glc = glucose

pectin plus glucose and the uptake medium contained only rhamnose. The induction with pectin plus glucose reduced the rhamnose uptake in the WT strain, but not in the Δ*cre-1* strain (Figure 2-27b). However, induction with only pectin and uptake of rhamnose did not alter the uptake of the WT or Δ*cre-1* strain. In addition, the uptake curves of this experimental setup were similar to the control setup, i.e. induction with pectin and uptake of rhamnose (SFigure 6-7).These results indicate that *frt-1* is a target of CRE-1 and that glucose induced CCR influences the transcription of *frt-1*, but not the uptake of the transport protein.

2.3.3. Analysis of the Δ*frp-1* transcriptome

The *N. crassa exo-1* strain was generated by UV-mutagenesis and exhibits a pleiotropic phenotype of α-amylase, glucoamylase, invertase, pectinase, cellobiase and trehalase hypersecretion (Gratzner and Sheehan, 1969; Gratzner, 1972; Sternberg and Sussman, 1974; Polizeli *et al.*, 1991; Spinelli *et al.*, 1996). A recent DNA-sequencing of the strain revealed that an insertion mutation in the F-box protein required for pathogenicity 1 (*frp-1*) gene was causative for the observed phenotype (Gabriel *et al.*, 2019). F-box proteins convey substrate specificity through protein-protein interaction domains to the SKP1 (suppressor of kinetochore protein 1) -CUL1 (cullin 1)-F-box (SCF) complex, which is a multi-protein complex of the E3 ligase family (Skowyra *et al.*, 1997; Lechner *et al.*, 2006). Most commonly, ubiquitin E3 ligases attach polyubiquitin chains to target proteins, which mark these proteins for degradation in the 26S proteasome (Lechner *et al.*, 2006). The controlled and targeted degradation of proteins is an important mechanism during many biological processes in Eukaryotes and it appears that the adaptation of the metabolism to altered substrate conditions is at least partly regulated by FRP-1 in *N. crassa*. Therefore, the *frp-1* deletion strain was used in this study to determine how the loss of FRP-1 causes a significant increase in enzyme secretion.

Early studies using the Δ*frp-1* strain showed that the hypersecretion of enzymes occurs after the strain is released from CCR (Gratzner and Sheehan, 1969; Gratzner, 1972; Sternberg and Sussman, 1974). An RNA-Seq analysis was conducted to discern which genes are mis-expressed after carbon source depletion in the Δ*frp-1* strain compared to the WT strain. Both strains were pre-incubated in sucrose and then transferred to induction media containing either glucose, Avicel or NoC. Gene expression was induced for 16 h before the transcriptome of the strains was determined. The extended induction period was chosen, because the hypersecretion phenotype of the Δ*frp-1* strain usually occurred several hours after the strain had depleted its carbon source (Gratzner and Sheehan, 1969; Gabriel *et al.*, 2019). Surprisingly, comparison of gene expression between WT and the

Δ*frp-1* strain showed that more genes were significantly down- than up-regulated in the Δ*frp-1* strain on all conditions (SFigure 6-8). However, the glucose condition induced the least mis-expression of genes in the *frp-1* deletion strain (150 gene up- and 392 genes down-regulated; SFigure 6-8a), while the NoC condition led to a mis-expression of almost twice as much genes in the Δ*frp-1* strain (299 gene up- and 701 genes down-regulated; SFigure 6-8b). These results support the previously published results that the hypersecretion phenotype occurs after carbon source depletion (Gratzner and Sheehan, 1969; Gratzner, 1972; Sternberg and Sussman, 1974).

Venn diagrams were created using the genes that were either significantly up- or down-regulated in the Δ*frp-1* strain compared to the WT strain (Figure 2-28; OTable 10) and the resulting gene groups were analyzed using FunCat (OTable 10). Genes up-regulated in the Δ*frp-1* strain on Avicel and NoC (89 genes) showed a significant enrichment ($p < 0.0005$) for starch metabolism, sugar transport and hemicellulose/pectin metabolism (Figure 2-28a).

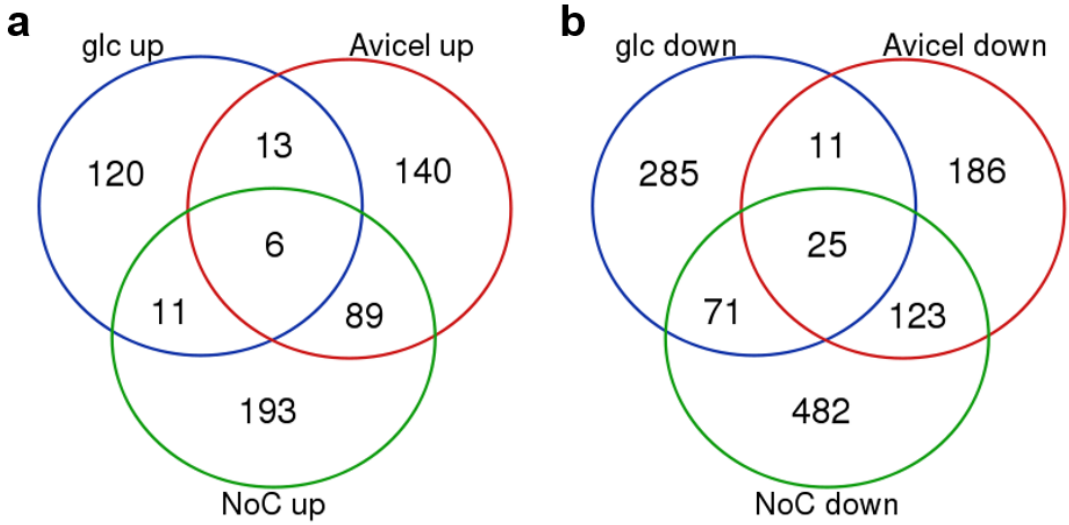

Figure 2-28: Expression comparison of genes induced with glucose, Avicel or NoC in the Δ*frp-1* strain versus the WT strain.
RNA-Seq data of the WT and Δ*frp-1* strains induced for 16 h with either glucose (glc), Avicel or NoC were compared for significantly mis-regulated genes by CuffDiff. Only genes that exhibited at least a 2-fold expression change in the mutant compared to the WT and had at least 10 FPKMs in either strain were used in this analysis. **a)** Genes that were significantly up-regulated in the Δ*frp-1* strain compared to the WT strain. **b)** Genes that were significantly down-regulated in the Δ*frp-1* strain compared to the WT strain.

The transcriptional response of the Δ*frp-1* strain to NoC (193 genes) exhibited significant enrichment for extracellular polysaccharide degradation and most of its respective sub-categories. However, no category was significantly enriched in the *frp-1* deletion strain on Avicel alone (140 genes). In contrast, most down-regulated genes of the Δ*frp-1* strain on Avicel (186 genes) were related to extracellular polysaccharide degradation, hemicellulose/pectin metabolism and cellulose metabolism (Figure 2-28b), indicating that

polysaccharide metabolism is also negatively affected by loss of *frp-1*. When induced with glucose, the Δ*frp-1* strain exhibited no significant enrichment in up-regulated (120 genes) or down-regulated genes (285 genes) for categories that are related to polysaccharide degradation and metabolism.

The RNA-Seq data of 236 genes encoding CAZymes or 102 genes encoding transport proteins were hierarchical clustered to further discern which genes could be relevant for the observed secretion phenotypes (Figure 2-29; OTable 10). The clustering of CAZy genes revealed 21 clusters, of which the majority contained genes that exhibited a down-regulated expression in the Δ*frp-1* strain compared to the WT strain (Figure 2-29a; OTable 10). Only

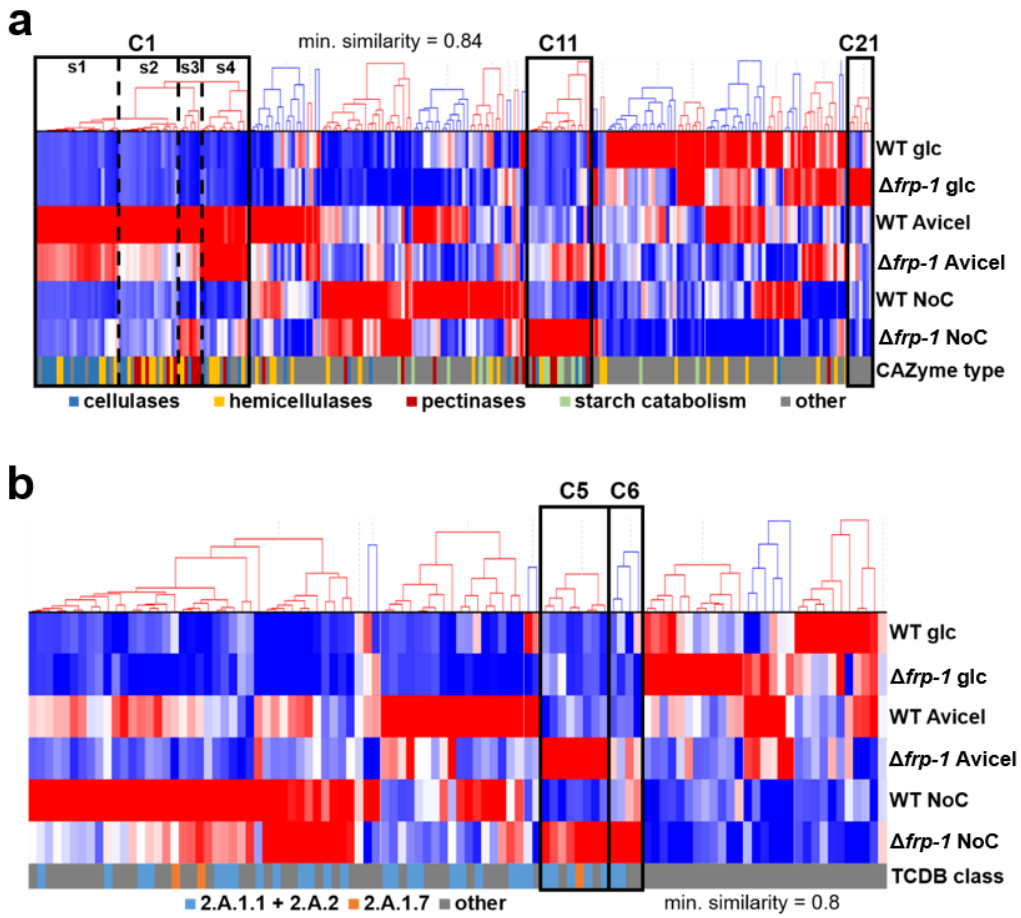

Figure 2-29: Hierarchical clustering of genes encoding CAZymes and transport proteins. RNA-Seq data of the Δ*frp-1* and WT strains induced for 16 h with glucose (glc), Avicel or NoC. A minimum FPKM threshold of 10 was applied to the expression data. **a)** Clustering of genes encoding CAZymes. Clusters (C) that contained genes up-regulated specifically in the Δ*frp-1* strain are highlighted in the diagram. Cluster 1 was divided into four sub-clusters (s1 to s4). A broad categorization of the CAZy genes is presented color-coded below the clustering. **b)** Clustering of genes encoding transport proteins. Clusters that contained genes up-regulated specifically in the Δ*frp-1* strain are highlighted in the diagram. A categorization of the transporter genes based on TCDB annotation is presented color-coded below the clustering. 2.A.1.1: sugar porters, 2.A.2: sucrose transporter, 2.A.1.7: fucose-proton symporter.

cluster 1, 11 and 21 contained genes significantly up-regulated in the Δ*frp-1* strain. Most of genes in cluster 1 (C1) were at least 2-fold up-regulated in the Δ*frp-1* strain induced with NoC, but these genes exhibited a reduced expression in the *frp-1* deletion strain induced with Avicel and were repressed by CCR under glucose. Furthermore, this cluster exhibited four distinct sub-clusters. The first one (s1) contained mostly cellulase genes, the second sub-cluster (s2) was composed of hemicellulase genes, the third sub-cluster (s3) encompassed mostly pectinases, while the fourth sub-cluster (s4) contained cellulase, hemicellulase and pectinase genes. The eleventh cluster (C11) exhibited genes with at least 2-fold up-regulation in the Δ*frp-1* strain on Avicel and NoC compared to the WT strain. This cluster contained mostly genes for starch degradation, but also some genes encoding cellulases and pectinases. The last cluster (C21) encompassed genes that had a higher expression in the Δ*frp-1* strain on glucose. However, most these genes were either hypothetical or not related to plant cell wall degradation.

The hierarchical clustering of the transporter genes exhibited nine distinct clusters and the genes were further classified using TCDB categories (Figure 2-29b; OTable 10). The majority of the cluster showed genes that were down-regulated in the *frp-1* deletion strain compared to the WT strain. Only the cluster 5 and 6 (C5 and C6) contained genes that were up-regulated in the mutant strain on Avicel and NoC, including, among others, the major low-affinity glucose transporter gene *glt-1* (NCU01633), the high-affinity glucose transporter genes *hgt-1* (NCU10021) and *hgt-2* (NCU04963), the xylose transporter gene *xyt-1* (NCU05627) and the rhamnose transporter gene *frt-1* (OTable 10).

Taken together, these results show that the loss of *frp-1* in the Δ*frp-1* strain led to a significantly increased expression of a small and defined set of genes during starvation or starvation like conditions. Most of these genes were related to the degradation of starch, cellulose, hemicellulose or pectin. However, the majority of mis-regulated genes in the Δ*frp-1* strain were down-regulated, including some genes necessary for plant cell wall depolymerization.

2.3.4. Enzyme hypersecretion occurs after CCR is relieved in the Δ*frp-1* mutant

The RNA-Seq analyses showed, that the expression of genes is induced in the absence of a carbon source in the *frp-1* deletion strain. However, pectinase secretion of the Δ*frp-1* strain was described as being inducible with galactose (Polizeli *et al.*, 1991; Crotti *et al.*, 1998b, 1998a). To determine whether pectinase hypersecretion is induced by galactose or carbon source depletion, a growth assay of the WT and Δ*frp-1* strains was conducted. Both strains were pre-grown on sucrose and then transferred to galactose medium. Sample

supernatants were taken during an incubation period of two days. The residual galactose concentration, as well as endo-PGase, α-amylase and arabinanase activities were determined in these supernatants (Figure 2-30; SFigure 6-9).

The galactose was depleted in the WT and Δ*frp-1* strain after 27 h and the enzyme assays revealed that endo-PGase, α-amylase, as well as arabinanase activities increased after carbon source depletion in the mutant strain, but not the WT strain. While the α-amylase and endo-PGase activities increased 5 to 7-fold, respectively, the arabinanase activity only increased 2-fold. These results indicate, that the Δ*frp-1* secretion phenotype, including hypersecretion of pectinases, is only prevalent in the absence of an easy to metabolize carbon source. Furthermore, while arabinanase genes were mis-expressed in the Δ*frp-1* strain, the effect of *frp-1* deletion only leads to a slightly increased arabinanase secretion.

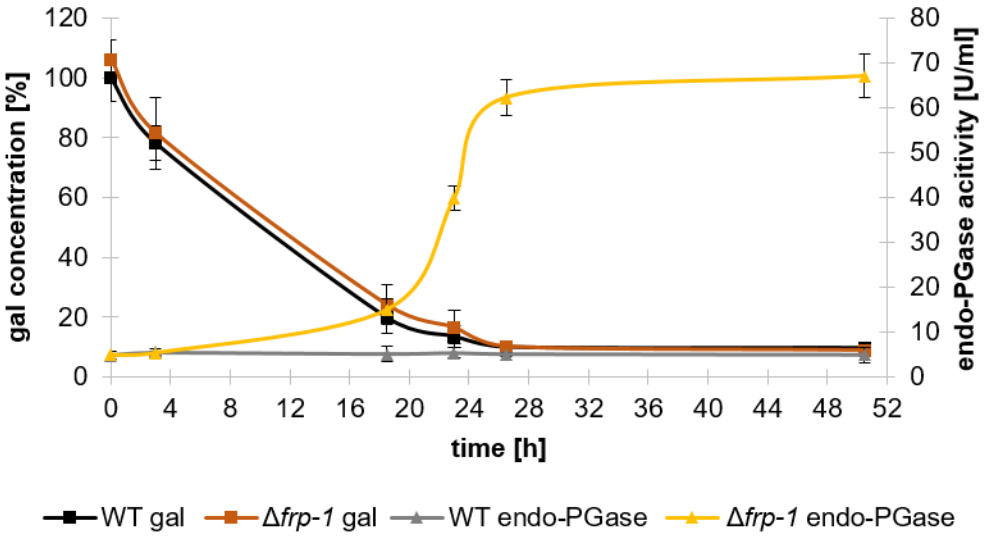

Figure 2-30: Galactose depletion induces secretion of endo-PGase in the Δ*frp-1* strain.
The WT and Δ*frp-1* strains were pre-grown for 16 h in 2% sucrose and then transferred to 25 mM galactose (gal) medium for an additional 2 days of incubation. Sample supernatants were taken ir regular intervals. The supernatants were used to determine the galactose concentration and endo-PGase activity in the sample supernatants. Error bars represent standard deviation (n = 3).

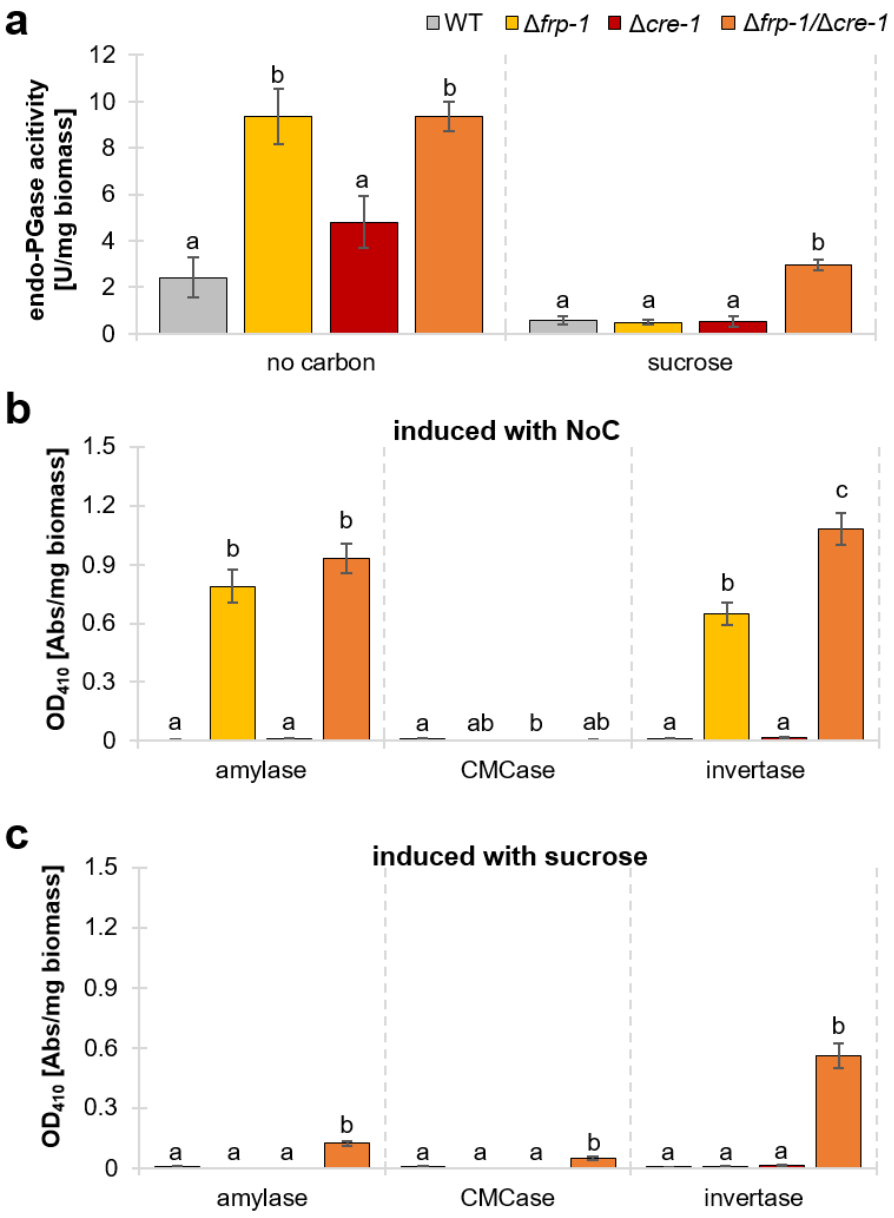

Figure 2-31: Enzyme activities of the WT, Δ*frp-1*, Δ*cre-1* and Δ*frp-1*/Δ*cre-1* strains.
The strains were incubated for 48 h in 2% glycerol and then transferred to either NoC or 2% sucrose, followed by an additional incubation period of 24 h. Biomass and sample supernatants were taken after 72 h. The supernatants were used to determine enzyme activities in the sample supernatants. The biomass was determined as dry-weight and used to normalize the enzyme activities. **a)** endo-PGase activity of the strains. **b)** α-amylase, cellulase activity on carboxymethyl cellulose (CMC) and invertase activity of the strains incubated with NoC. **c)** As in described in (b), but the strains were incubated for 24 h in sucrose. Error bars represent standard deviation (n = 3). Significance was determined by ANOVA followed by a post-hoc Tukey's test. The letters above each bar indicate statistical significance; bars sharing the same letter show no significant difference, while different letters represent a significant mean difference of $p < 0.05$.

The hypersecretion phenotype of the Δ*frp-1* strain occurs after carbon source depletion, i.e. after release from CCR, which suggests that CRE-1 might be involved in the suppression of the *frp-1* deletion phenotype when galactose and glucose is present. To test this hypothesis, the Δ*frp-1* and Δ*cre-1* strains were crossed to create a strain carrying a deletion of the *frp-1* and *cre-1* genes (Δ*frp-1*/Δ*cre-1* strain). The WT, Δ*frp-1*, Δ*cre-1* and double deletion strains were then incubated for 48 on glycerol, since sucrose leads to a stunted growth of the Δ*cre-1* strain (Sun and Glass, 2011). Afterwards, the mycelial biomass was transferred to either NoC or sucrose medium and supernatants were taken after an additional incubation period of 24 h. These supernatants were used to determine endo-PGase, α-amylase, cellulase (CMCase) and invertase activity of the strains (Figure 2-31). As observed previously, the tested enzyme activities, with the exception of CMCase activity, were significantly increased after growth on NoC in the Δ*frp-1* strain, but also the Δ*frp-1*/Δ*cre-1* strain (Figure 2-31a, b). The Δ*cre-1* strain exhibited WT-like enzyme activities on NoC. In contrast, only the Δ*frp-1*/Δ*cre-1* strain showed significantly elevated enzyme activities after growth on sucrose, while the enzyme activities of the remaining strains were almost not detectable (Figure 2-31a, c). These results support the hypothesis, that the suppression of the Δ*frp-1* phenotype is at least partially regulated by CRE-1 during CCR inducing conditions.

2.3.5. The Δ*frp-1* secretion phenotype is partially caused by COL-26

Starch degradation is dependent on the transcription factor COL-26 in *N. crassa* (Xiong *et al.*, 2017). The deletion of the *col-26* gene leads to a significant reduction in the expression of α-amylase and invertase genes. In contrast, the deletion of the *frp-1* gene in the Δ*frp-1* strain leads to hypersecretion of these enzymes. To examine the link between COL-26 and FRP-1, the list of COL-26 dependent genes (genes down-regulated in the Δ*col-26* strain) was compared to the genes that were up-regulated in the Δ*frp-1* strain induced with NoC (Figure 2-32a; OTable 11). While the majority of genes were not shared between these strains, 36 genes were mis-regulated in both strains. Gene enrichment analysis using FunCat showed that the categories for starch metabolism ($p = 4.76 \times 10^{-10}$), starch catabolism ($p = 4.76 \times 10^{-10}$) and extracellular starch degradation ($p = 8.97 \times 10^{-06}$) were significantly enriched in these 36 genes (OTable 11).

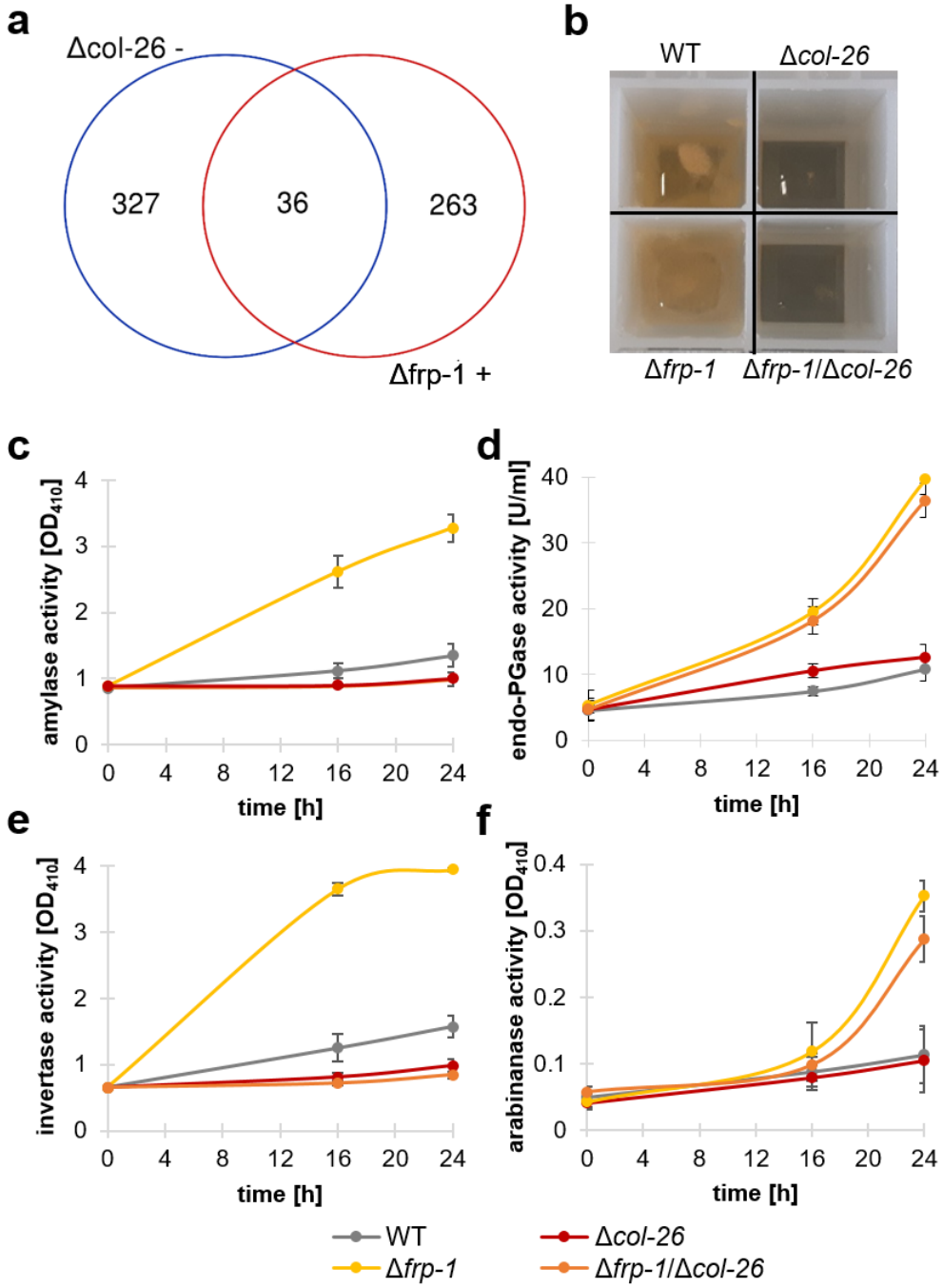

Figure 2-32: Loss of *col-26* prevents the α-amylase and invertase secretion phenotype of the Δ*frp-1* strain.

a) Venn diagram comparing the COL-26 dependent genes (Δ*col-26* –) and genes that were up-regulated in the Δ*frp-1* strain on NoC (Δ*frp-1* +). **b)** Growth phenotype of the WT, Δ*col-26*, Δ*frp-1* and Δ*frp-1*/Δ*col-26* strains on 2% maltose. **c - f)** The strains were pre-incubated for 48 h in 2% acetate and afterwards transferred to NoC for an additional incubation period of 24 h. Sample supernatants were taken 0, 16 and 24 h after medium switch and **c)** α-amylase, **d)** endo-PGase, **e)** invertase or **f)** arabinanase activity was determined in the supernatants. Error bars represent standard deviation (n = 3).

To further determine whether the presence of COL-26 is necessary in the *frp-1* deletion strain to induce hypersecretion, the Δ*frp-1* and Δ*col-26* strains were crossed to generate a double deletion strain (Δ*frp-1*/Δ*col-26*). The Δ*frp-1*/Δ*col-26* strain was unable to grow on maltose, similar to the Δ*col-26* strain, while the Δ*frp-1* strain showed WT-like growth on this carbon source (Figure 2-32b). Following this growth assay, the α-amylase, endo-PGase, invertase and arabinanase secretion of the WT, Δ*frp-1*, Δ*col-26* and Δ*frp-1*/Δ*col-26* strains were analyzed by enzymatic activity assays. The strains were pre-incubated on acetate medium and transferred after 48 h of growth to a NoC medium for an additional incubation period of 24 h. During this time, sample supernatants were taken after 0 h, 16 h and 24 h to determine enzymatic activity (Figure 2-32c to f). The Δ*col-26* strain exhibited low WT-like activities in all assays, while the Δ*frp-1* strain showed significantly increased α-amylase, endo-PGase, invertase and arabinanase activities. In contrast, the α-amylase and invertase activity were reduced to WT levels in the Δ*frp-1*/Δ*col-26* strain, while the endo-PGase and arabinanase activities of this strain remained similar to the Δ*frp-1* strain.

These results support the notion that the hypersecretion of α-amylases and invertases by the Δ*frp-1* strain is dependent on the presence of COL-26. Whether there is a direct or an indirect interaction of FRP-1 with COL-26 cannot be discerned based on the performed experiments. However, the observed results also suggest that FRP-1 is involved in the regulation of the pectin degradation machinery, since the pectinase secretion of the Δ*frp-1*/Δ*col-26* strain was not altered.

3. Discussion

3.1. Plant biomass perception of *N. crassa*: Transcriptional response profiling

3.1.1. CCR and carbon starvation stress response are major driving forces of transcription in *N. crassa*

Studies of lignocellulosic substrate degradation in ascomycete fungi commonly utilize plant biomass with potential use in biorefinery applications, purified polysaccharides or their constituent monosaccharides. These carbon sources elicit a specific transcriptional response in fungi that was first analyzed in *N. crassa*, *A. niger* and *T. reesei* using microarray and RNA-Seq experiments (Tian *et al.*, 2009; Delmas *et al.*, 2012; Ries *et al.*, 2013). Collectively, these studies showed that three phases can be distinguished during the process of polysaccharide perception, which follow the same pattern in all tested species (Delmas *et al.*, 2012; Glass *et al.*, 2013b):

Firstly, CCR is released during carbon starvation, which leads to de-repression (1) of genes encoding lignocellulolytic enzymes and sugar transporters. In the scouting phase (2), the de-repressed enzymes will be expressed in low quantities and secreted in the extracellular space, where they may detect carbon sources. After coming into contact with a polysaccharide, the enzymes release soluble sugars which act as inducing molecules. These inducers inform the fungus about the carbon sources in its proximity and induce the transcription of corresponding degradation pathways. During this initiation phase (3), the fungus adapts its metabolic response towards the detected polysaccharides.

We found CCR and the carbon starvation stress response (CSSR) to be two competing metabolic states that significantly influence fungal transcription throughout substrate perception; a notion that has been eluted to already in earlier studies (Bailey and Arst, 1975; Gancedo, 1998; Stülke and Hillen, 1999; Sun and Glass, 2011; Szilagyi *et al.*, 2013). While CCR is induced by easily metabolized carbon sources like glucose and leads to the repression of genes that encode lignocellulolytic enzymes (Bailey and Arst, 1975; Ronne, 1995; Gancedo, 1998; Stülke and Hillen, 1999; de Vries *et al.*, 2002; Glass *et al.*, 2013b; Huberman *et al.*, 2016), CSSR becomes active in the absence of a carbon source and leads to far reaching changes in the transcriptome, since the fungus has to maintain enough energy to sustain its survival in addition to searching for new carbon sources (Winderickx *et al.*, 2003; Szilagyi *et al.*, 2013).

In this study, PCAs and correlation analyses were performed to determine major driving forces of transcription in *N. crassa* by analyzing the transcriptional responses induced by

the large set of conditions employed in the 'Fungal Nutritional ENCODE Project' (Glass *et al.*, 2013a). Although only ~6% of the ENCODE conditions correlated with a ρ of at least ~0.7 to sucrose, indicating a robust similarity at the whole-genome level and thus likely an active CCR, a strictly inverse correlation of ENCODE conditions to sucrose and starvation could be observed over the vast majority of conditions (Figure 2-7; Figure 2-8). This correlation pattern supports the competing nature of CCR and CSSR. Moreover, swift release from CCR was observed, since only the conditions in the first k-means cluster of the PCAs correlated well with sucrose and showed enrichment in categories of hyphal growth and protein synthesis, while the second and fourth k-means clusters contained NoC conditions induced for either 1 h or 4 h, respectively, and showed an increasing correlation to the NoC condition, which is necessary for the fungus to exploit new carbon sources (Sun and Glass, 2011; Glass *et al.*, 2013b; Hunter *et al.*, 2013).

One of the major regulators of CCR in *N. crassa*, *T. reesei*, *A. niger* and *A. nidulans* is the transcription factor CRE-1/Cre1/CreA (Dowzer and Kelly, 1989, 1991; Ilmén *et al.*, 1996; Ebbole, 1998; Sun and Glass, 2011), though other, CRE-independent, modes of CCR regulation have been described (Ruijter and Visser, 1997; Denton and Kelly, 2011; Tamayo-Ramos *et al.*, 2012; Hunter *et al.*, 2013; Huberman *et al.*, 2016; Alam *et al.*, 2017; Benocci *et al.*, 2017). Cre1/CreA-mediated CCR is regulated post-translationally in *T. reesei* and *A. niger* by protein phosphorylation in the presence of glucose, which leads to increased DNA binding affinity of the transcription factor (Strauss *et al.*, 1999; Cziferszky *et al.*, 2002). Since protein phosphorylation is a fast acting and reversible process (Krebs and Beavo, 1979), a swift activation of (or release from) CCR is possible, which could explain why only few carbon sources induced significant CCR in the 'Fungal Nutritional ENCODE Project'. Moreover, the swift release from CCR was observable in the PCA, as already 1 h of NoC induced only a weak CCR-like response in *N. crassa* (Figure 2-7; Figure 2-8). However, at least 4 h of NoC were necessary to almost completely abolish the CCR response of *N. crassa*, which indicates that CCR remains slightly active throughout most of the ENCODE conditions.

The analysis of the 'Fungal Nutritional ENCODE Project' data showed that around 60% of the used conditions correlated with a ρ of at least ~0.7 to the NoC condition in *N. crassa*, indicating that there is also a sizeable overlap in gene expression between most plant cell wall-related saccharides and pure starvation (Figure 2-7; Figure 2-8). The correlation to starvation was increasing throughout the k-means clusters of the PCAs, showing that starvation is a major driving force in *N. crassa*. It appears that the presence of most mono-, di- and polysaccharides, as well as complex plant biomasses is not sufficient to fully release CSSR in *N. crassa*.

CSSR in *A. nidulans* influenced a wide array of processes, e.g. cell wall homeostasis, activation of programmed cell death, secondary metabolite production, enhanced conidiation and increased synthesis of proteins with functions in transcription and secretion, in addition to adaptations of the carbon and nitrogen metabolisms (Dragovic *et al.*, 2002; Keller *et al.*, 2005; Emri *et al.*, 2009; Kim *et al.*, 2011; Szilagyi *et al.*, 2013). Similarly, the starvation response of *N. crassa* influenced many processes besides carbon metabolism, such as protein synthesis, secondary metabolism and apoptosis, as shown by gene enrichment analysis (Figure 2-10; OTable 06). Szilagyi *et al.* proposed that induced macroautophagy and autolytic cell wall degradation of older colony parts are necessary during carbon starvation to maintain conidiation and hyphal tip growth of the fungus, which are necessary to discover and exploit new carbon sources. In addition, secondary metabolites and other biologically active compounds may help the fungus to survive the lack of carbon source. They could be used to defend the fungus against other organisms or securing new carbon sources against potential rivals (Szilagyi *et al.*, 2013). Some of these processes may remain necessary during the degradation of plant biomass. For example, fast areal growth could enable *N. crassa* to contest carbon sources more efficiently, and production of secondary metabolites may be necessary to protect released mono- and disaccharides from scavenging organisms or the fungus from its natural enemies.

Taken together, these analyses confirmed that CCR and CSSR are competing transcriptional states in *N. crassa* that affect large parts of the genome and play a crucial role during substrate perception and activation of the lignocellulosic degradation machinery. CCR seems to be regulated more tightly and is only strongly active in a few tested carbon sources (sucrose, glucose and glucomannan), but traces can be found in most conditions. On the other hand, CSSR increases gradually throughout the ENCODE conditions, indicating a complex and specifically coordinated regulation. While these findings allow for the first time to rate carbon sources for their specific nutritional value for *N. crassa* by a kind of transcriptional “fingerprint”, it remains to be explored which the causative factors are that lead to CSSR despite the presence of certain polysaccharides and complex plant biomasses. Certainly, the speed of internal catabolism of a carbon source – and therefore the possible accumulation of intermediates - will affect CSSR, but also extractives and other metabolites that could potentially harm fungi (Wink, 1988). Alternatively, *N. crassa* might not be able to perceive all polysaccharides or their constituent sugars, which would lead to a starvation-like response even though a carbon source is present (see below).

3.1.2. Evaluation of PolyCat identifier gene reliability

Transcriptome data of the 'Fungal Nutritional ENCODE Project' were used to visualize the transcriptional response of *N. crassa* to plant biomass and to determine to what extent the fungus will be able to perceive the presence of each constituent polysaccharides within the plant cell walls. This was only possible, because the ENCODE project encompassed expression data of *N. crassa* induced with 46 plant cell wall related carbon sources. For the first time, the expression patterns of mono-, di- and polysaccharides as well as plant biomasses were available all at once for detailed comparison. The wealth of information provided by the ENCODE data was used to determine which polysaccharides *N. crassa* can detect in complex plant biomasses. PolyCats and PolyCat scores were used as a novel approach to analyze ENCODE data (Figure 5-2). The transcriptional response of polysaccharide-specific identifier genes was profiled to determine PolyCat specific expression patterns. The identifier genes were determined in a *top-down* approach, by searching for genes with strong expression induced by carbon sources that represent one specific polysaccharide. In contrast, previous studies generally used a *bottom-up* approach for transcriptome analysis, relating the expression of pre-selected enzyme, transporter or transcription factor genes to the degradation of one or more polysaccharides (van den Brink and de Vries, 2011; Culleton *et al.*, 2013; Gruben *et al.*, 2017; Thieme *et al.*, 2017; Wu *et al.*, 2019).

As only genes that showed a significantly up-regulated and PolyCat-specific expression profile were accepted as identifier genes, the cellulose, xylan, pectin and starch PolyCat-specific gene sets overlapped extensively with previously published cellulase, hemicellulase, pectinase and amylase genes of *N. crassa*, respectively (Figure 2-1) (J. P. Benz *et al.*, 2014; Craig *et al.*, 2015; Samal *et al.*, 2017; Thieme *et al.*, 2017; Wu *et al.*, 2019). However, these sets also contained many uncharacterized genes, which might express proteins that have auxiliary functions during polysaccharide degradation, but they could also be involved in associated activities like protein secretion, signal transduction or stress response. Overall, expression profiling of the identifier genes of the cellulose, xylan, pectin and starch PolyCats appears to be a reliable way to determine and visualize the polysaccharide perception of *N. crassa*, indicating that these carbon sources elicit a rather specific response.

In contrast, the identifier genes specific for the mannan and xyloglucan PolyCats did not contain clear mannanase or xyloglucanase genes, respectively. Most of the genes found for these two PolyCats were either uncharacterized or related to other processes, as shown by the respective functional gene enrichment analyses (Figure 2-3). The identifier genes specific for the xyloglucan PolyCat showed a similar expression pattern to starvation, and

xyloglucan was clustered in the PCA next to other conditions that appear to be related to starvation (Figure 2-7; Figure 2-10). In addition, the identifier genes of the xyloglucan PolyCat showed significant enrichment in functional categories related to amino acid catabolism and secondary metabolism. These results imply that *N. crassa* has no specific transcriptional response induced by xyloglucan for degradation of this polysaccharide, even though the organism is able to grow on xyloglucan and has xyloglucanase genes (Craig *et al.*, 2015; Damasio *et al.*, 2017; Samal *et al.*, 2017). Instead, the xyloglucanase gene *cel74a* (NCU05955) exhibited elevated expression on cellulose conditions (OTable 06) and is a direct target of the transcription factors CLR-1 and CLR-2 in *N. crassa* (Craig *et al.*, 2015). In *A. niger*, the expression of xyloglucanases is at least partially under the control of the transcription factor XlnR, a regulator of hemicellulase degradation (van Peij *et al.*, 1998; de Vries *et al.*, 1999; Gielkens *et al.*, 1999). In contrast, Samal *et al.* could show that overexpression of *xlr-1*, the *xlnR* homolog in *N. crassa* (Sun *et al.*, 2012; Craig *et al.*, 2015), did not lead to better growth on xyloglucan (Samal *et al.*, 2017). However, growth of *N. crassa* on xyloglucan was drastically increased when the transcription factor CLR-2 was overexpressed, supporting the ChIP-seq results of Craig *et al.* that xyloglucanase expression is regulated by CLR-1 and CLR-2 (Craig *et al.*, 2015; Samal *et al.*, 2017).

Hierarchical clustering and PCA showed that also the mannose and mannobiose conditions showed expression patterns similar to starvation (Figure 2-7; Figure 2-10), while the glucomannan and galactomannan conditions clustered closely to CCR-related conditions in the PCA and had a unique expression pattern in the hierarchical clustering. None of the known mannanase genes of *N. crassa* (Samal *et al.*, 2017) were part of the mannose, mannobiose, glucomannan or galactomannan clusters in the hierarchical clustering. Instead, these genes were part of the cellulose cluster, and a significant enrichment of mannan catabolism genes was determined in the identifier genes of the cellulose PolyCat through FunCat analysis. These findings were corroborated by chromatin immunoprecipitation sequencing (ChIP-seq) of the major cellulose degradation regulators CLR-1 and CLR-2, which revealed that the endo-mannanase gene *gh5-7* is one target of these transcription factors (Coradetti *et al.*, 2012; Craig *et al.*, 2015). In addition, Tian *et al.* published that the expression of the β-mannosidase gene *gh2-1* was significantly up-regulated on Avicel (Tian *et al.*, 2009). Moreover, growth assays of Δ*clr-1* and Δ*clr-2* deletion strains, as well as overexpression strains of the same transcription factors revealed that glucomannan degradation is regulated by CLR-2 (Samal *et al.*, 2017).

The regulation of mannan degradation by CLR-2 is not unexpected, since the CLR-2 homolog in *Aspergillus oryzae*, ManR, is the major regulator for mannan and cellulose degradation in that fungus (Ogawa *et al.*, 2012, 2013; Tani *et al.*, 2014). However, while mannan degradation was induced by β-1,4-D-mannobiose in *A. oryzae* (Ogawa *et al.*, 2012),

mannan degradation appears not to be induced significantly by mannobiose in *N. crassa*, as indicated by the transcriptome data and mannanase gene expression under cellulose conditions. Nonetheless, other inducers, for example intermediate degradation products of mannobiose, might act as inducers for mannan degradation in *N. crassa*. The *A. niger* transcription factor GaaR, which regulates homogalacturonan degradation and galacturonic acid catabolism, is induced by 2-keto-3-deoxy-L-galactonate, an intermediate product of the galacturonic acid catabolism (Alazi *et al.*, 2016, 2017) and the *T. reesei* transcription factor Xyr1 is induced by sophorose, the transglycosylation product of cellobiose (Vaheri *et al.*, 1979; Stricker *et al.*, 2006; Kubicek *et al.*, 2009; Herold *et al.*, 2013). It is therefore feasible that other inducers or modes of induction activate the degradation of mannan in *N. crassa*. This could nevertheless also be independent of CLR-2, since gluco- and galactomannan induction were found to lead to drastic changes in the transcriptome towards a new, albeit unspecific and not CLR-2-like, state in this study. What's more, a recent publication by Hassan *et al.* demonstrates that even small amounts of mannobiose lead to reduced cellulase induction in *N. crassa*, implying a competition between mannobiose and cellobiose on the signaling level (Hassan *et al.*, 2019).

Based on these results, the identifier genes of the xyloglucan and mannan PolyCat are not reliable enough to determine the detection of these carbon sources by *N. crassa*. The identifier genes of the xyloglucan PolyCat are mostly representing the transcriptional response of *N. crassa* to starvation. Since most of the ENCODE softwood conditions, as well as pectin and Avicel conditions (data not shown) showed a high xyloglucan PolyCat score, these results indicate that *N. crassa* has partly activated its starvation response on these carbon sources. These observations were further corroborated by the PCA, where these carbon sources were placed in the starvation response-related clusters (Figure 2-7). In contrast, the observed transcriptional response of *N. crassa* to gluco- and galactomannan is unique and indicates a significant change in metabolic state (Figure 2-10), but the identifier genes of the mannan PolyCat do not reflect these observations. Instead, the mannan PolyCat score for grasses, softwoods and hardwoods was ~30%, even though a significant mannan content is only present in the softwood conditions (Fengel and Grosser, 1975; Mitchell *et al.*, 2014; Hassan *et al.*, 2019). The mannan PolyCat identifier genes might instead represent a state of metabolic and developmental adaptation of *N. crassa*, when the fungus is confronted with a carbon source that can potentially lead to CCR but at the same time is not clearly identifiable by the fungus. Since genes for both xyloglucan and mannan degradation are at least partly controlled by CLR-2 (Samal *et al.*, 2017) and induced under cellulose conditions, it is feasible that *N. crassa* is not able to differentiate these carbon sources. Using the transcriptional profile of *N. crassa* induced with mannan or xyloglucan to visualize the specific detection of these carbon sources might therefore not

be possible. Furthermore, since at least cellobiose and mannobiose appear to be competing during the signaling phase of carbon source detection (Hassan *et al.*, 2019), it is possible that *N. crassa* is not able to differentiate between mannan and cellulose degradation on a transcriptional level.

3.1.3. The plant biomass perception of *N. crassa* is influenced by substrate availability, fungal regulatory networks and the physicochemical properties of plant biomasses

The polysaccharides of plant cell walls are suitable carbon sources for lignocellulose-degrading ascomycete fungi, although depolymerization of the intricate mesh formed by cellulose, hemicelluloses and pectin is a complex and difficult task. The plant cell wall is a three-dimensional structure, where cellulose, the most recalcitrant polysaccharide, forms a scaffold, which is interconnected by hemicelluloses. Pectin, a complex polymer composed of a wide variety of different monosaccharides, acts like an adhesive between polysaccharides and also between adjacent cells (McCann *et al.*, 1990; Fujino *et al.*, 2000; Somerville, 2004; Mohnen, 2008; Caffall and Mohnen, 2009). These polysaccharides have varying physicochemical properties, e.g. crystallinity or viscosity, that influence how fast and efficient they can be dissolved by enzymatic reactions (Fan *et al.*, 1981; Nishitani and Masuda, 1981; Mansfield *et al.*, 1999; Harris and Smith, 2006; Hassan *et al.*, 2017). Moreover, the macro structures formed by plant cells may also influence how well fungi can perceive the plant biomass. Different chemical composition as well as altered physical properties of stem, leaves, fruits, different plant species or even developmental stages of plants could play a crucial role during fungal substrate detection (Morre, 1968; Fengel and Grosser, 1975; Albersheim *et al.*, 1996; Bertaud and Holmbom, 2004; Pinto *et al.*, 2004; Hassan *et al.*, 2019). All of these factors influence which parts of the plant cell wall a fungus can detect at any given time and how they are adapting their response based on the perceived information.

The analysis of the PolyCat scores and Euclidean distance clustering showed that *N. crassa* is able to detect multiple polysaccharides inside complex plant biomass at the same time (Figure 2-4; Figure 2-5). However, the strength of the polysaccharide-specific responses differed between plant biomass conditions and could not always be related to the chemical composition of the plant biomass alone. For example, the cellulose content of the softwood, hardwood and grass species used in the analyses was between 30% and 40% (Mitchell *et al.*, 2014; Hassan *et al.*, 2019), and it was therefore feasible that these plant biomasses elicit a similar transcriptional response towards cellulose degradation in *N. crassa*. However, the PolyCat scores as well as the Euclidean distance clustering (that used correlation values

between mono-, di- and polysaccharide and plant biomass conditions), showed that the cellulose-specific transcriptional response of *N. crassa* was distinct between the different groups of plant species. Moreover, the transcriptional response related to cellulose even differed within these groups in some cases, e.g. between the heart- and sapwood regions of the wood biomasses or between different hardwood species (Figure 2-6). Similar observations were made for xylan, pectin and starch PolyCat scores. The xylan PolyCat scores were sometimes even greater than the cellulose PolyCat scores in some hardwood species, although the chemical xylan content of these plant biomasses was lower - between 12% and 20% (Mitchell *et al.*, 2014; Hassan *et al.*, 2019). Together, these results strongly suggest that besides chemical composition additional factors affect the perception of plant cell wall components. While this creates a bias (or off-set) to the expected values based on a simple compositional analysis, the combination these factors for the most part seems to elicit an overall similar transcriptional response, allowing *Neurospora* to differentiate between grass, softwood and hardwood substrates.

The results of this study regarding simultaneous perception of plant cell wall polysaccharides in *N. crassa* are supported by previous transcriptome analyses of Wang *et al.*, where genes up-regulated in *N. crassa* induced with five major crop residues were compared to the genes of the Avicel, xylan and pectin regulons (Coradetti *et al.*, 2012; Sun *et al.*, 2012; J. P. Benz *et al.*, 2014; Wang *et al.*, 2015). This study showed that crop residue-induced genes overlapped significantly with the polysaccharide regulons, which implies that *N. crassa* is able to detect cellulose, xylan and pectin at the same time (Wang *et al.*, 2015). The expression of these genes was also inducible by low concentrations of polysaccharide, as genes of the pectin regulon were activated by the crop residues, even though their pectin content is below 10% (Jarvis *et al.*, 1988; Caffall and Mohnen, 2009; Wang *et al.*, 2015). Moreover, the gene expression of *N. crassa* on the crop residues was distinctly different between monocot and dicot crop residues, although their chemical composition was very similar, which indicates that additional factors besides the chemical composition of the plant cell wall influence the transcription of *N. crassa* growing on complex plant biomasses (Wang *et al.*, 2015). Overall therefore, the chemical composition of plant biomass is not the exclusive determinant of polysaccharide perception of *N. crassa*.

One possible explanation for the observed differences in polysaccharide perception through PolyCat scores could be different preferences in mono- and disaccharide utilization. These small soluble sugars act as inducers to activate the degradation machinery for the related polysaccharides (Glass *et al.*, 2013b; Seibert *et al.*, 2016; Schmitz *et al.*, 2019). A reduced preference for certain mono- and disaccharides, e.g. through low uptake rates or because these sugars have to be further modified (Vaheri *et al.*, 1979; Lagunas, 1993; Stricker *et al.*, 2007; Dos Reis *et al.*, 2013; Alazi *et al.*, 2017; Wang *et al.*, 2017), might influence the

temporal dynamics of a transcriptional activity elicited by different plant biomasses. Diauxie is researched extensively in bacteria and describes the preferred utilization of one carbon source over another when a microorganism is confronted with two monosaccharides at the same time (Englesberg, 1959; Loomis and Magasanik, 1967; Grimmler *et al.*, 2010). A similar behavior regarding mono- and disaccharide utilization was observed for fungi (Hsiao *et al.*, 1982; Mountfort and Asher, 1983; Lameiras *et al.*, 2018; Mäkelä *et al.*, 2018). While glucose was preferred in bacteria over all other supplied carbon sources (Englesberg, 1959; Loomis and Magasanik, 1967; Grimmler *et al.*, 2010), fructose, mannose and galactose were utilized before glucose in *A. niger* (Mäkelä *et al.*, 2018). Arabinose, galacturonic acid and rhamnose were utilized after most other monosaccharides in *A. niger* (Lameiras *et al.*, 2018; Mäkelä *et al.*, 2018). In contrast, the anaerobic fungus *Neocallimastix frontalis* preferentially utilized glucose over other monosaccharides, but disaccharides like sucrose and cellobiose were preferred over glucose (Mountfort and Asher, 1983). In addition, the basidiomycete yeast *Rhodosporidium toruloides* was recently described as being able to utilize galacturonic acid in parallel to glucose (Protzko *et al.*, 2019).

Another explanation for differences between PolyCat scores and the chemical composition of the plant cell walls could be related to the regulatory pathways that control the expression of genes involved in lignocellulose degradation. Although PolyCats and the expression of their related identifier genes were specific for one polysaccharide, the regulation of the identifier genes might not be stringent enough to be specific for one polysaccharide. An overlap in regulation could therefore lead to PolyCat scores that do not fully represent the abundance of polysaccharides in a complex carbon source. For example, the evaluation of the identifier genes showed that the expression of CAZyme-encoding genes is not necessarily induced by the carbon source on which the enzymes later act on. As it was shown for mannan and xyloglucan degradation in this and prior works, these two catabolic pathways are primarily induced by cellulose in *N. crassa*, whereas xyloglucan and mannan themselves induce a starvation-like response (Figure 2-10) (Samal *et al.*, 2017). Recent studies by Hassan *et al.* described a decrease in cellulolytic activity of *N. crassa* and *T. reesei* when cellulose was mixed with small amounts of glucomannan or mannobiose. The authors hypothesize that mannobiose may compete with cellobiose for the induction of the cellulolytic pathway because both disaccharides are structurally very similar (Hassan *et al.*, 2019). This “crosstalk” indicates that the complex regulation machinery involved during plant cell wall degradation may distort the transcriptional response of *N. crassa* towards certain polysaccharides. Indeed, transcriptional analyses of CAZyme-encoding genes induced with Avicel, xylan and pectin showed an extensive overlap in induced genes (J. P. Benz *et al.*, 2014). These results were further corroborated by a meta-analysis of

physiological, genomic, transcriptomic and proteomic data of *N. crassa*, which revealed a significant overlap in activation of cellulolytic and hemicellulolytic genes, as well as hemicellulolytic and pectinolytic genes (Samal *et al.*, 2017). Similarly, an expression-based clustering of CAZyme-encoding genes and comparison of these data to published transcription factor studies displayed that most genes encoding CAZymes were regulated by at least two transcription factors in *A. niger* (Gruben *et al.*, 2017).

Taken together, the observed PolyCat scores cannot be entirely explained by the chemical composition of the plant biomasses that were used to induce transcription in *N. crassa*. Other factors, besides overlap in fungal regulatory pathways or carbon source preferences, might also critically influence fungal substrate perception. Likely, the accessibility of the plant cell wall polysaccharides will have a major influence on the release of inducer molecules, which in turn would alter the transcriptional response of *N. crassa*. The plant cell wall is a physical barrier which achieves the tensile strength and rigidity necessary to fulfill its function through the interconnectivity of the plant cell wall polysaccharides (Keegstra, 2010; Cosgrove and Jarvis, 2012). Hemicellulose fibrils are anchored inside the cellulose microfibrils and interconnect them, while pectin covers large portions of both the cellulosic and hemicellulosic part of the plant cell walls (Dick-Pérez *et al.*, 2011). These interactions may reduce the accessibility of the polysaccharides for fungal lignocellulolytic enzymes or mask present carbon sources, which would lead to an altered transcriptional response of the fungus specific to each substrate.

The lignin content of the plant cell wall also influences the activity of cellulases drastically, as delignified plant cell walls lead to significantly higher cellulase activity compared to untreated cell walls. It was hypothesized that lignin might block access for fungal cellulases to the deeper layers of the plant cell wall (Ding *et al.*, 2012). The lignin content differed quite significantly between the softwood, hardwood and grass biomasses used in the Fungal Nutritional ENCODE Project. The softwood samples used in this work had a lignin content of ~30%, while the hardwood and grass samples had a lignin content of only ~20% (Mitchell *et al.*, 2014; Hassan *et al.*, 2019). In addition, two P450 monooxygenases were significantly up-regulated in softwood species compared to all other ENCODE conditions in this study (Table 2-3). P450 monooxygenases are involved in the bioconversion of lignin in basidiomycetes (Syed *et al.*, 2014; Aranda, 2016; Mallinson *et al.*, 2018), but it is not published if they play a similar role in ascomycetes. It is feasible that the generally low PolyCat scores observed for softwood conditions were caused by the increased lignin content, which may have reduced lignocellulolytic enzyme activities on these substrates. In addition, the mannan content of the used softwood species was between ~7% to ~14%, while mannan contributed to less than 3% or below 1% of the biomass in the hardwood and grass species, respectively (Mitchell *et al.*, 2014; Hassan *et al.*, 2019). As previously noted,

presence of mannan leads to a reduced expression of genes involved in polysaccharide degradation (Hassan *et al.*, 2019), which might delay the activation of cellulolytic and xylanolytic pathways in softwoods.

Furthermore, the release of inducer molecules is also affected by the crystallinity of the substrate; especially cellulase activity is influenced by the recalcitrance of cellulose (Mansfield *et al.*, 1999; Peciulyte *et al.*, 2014; Hassan *et al.*, 2017). Cellulases exhibit high activity on the amorphous regions of cellulose, because the cellulose microfibrils are more accessible for the enzymes in these regions (Ding *et al.*, 2012; Bubner *et al.*, 2013; Orłowski *et al.*, 2015). Indeed, Agarwal *et al.* could show that the cellulose crystallinity of different wood samples differed dramatically between tested species (Agarwal *et al.*, 2011). Since already small changes in the crystallinity index (CrI) significantly altered cellulase expression in *N. crassa* (Hassan *et al.*, 2017), it is feasible that the highly variable crystallinity of cell wall cellulose influences cellulose detection.

The complex plant biomasses utilized for the transcriptome studies of this work also differed in their morphological properties, which may have influenced how efficient *N. crassa* was able to liberate soluble sugars from these plant cell walls. Softwoods in general have a lower average density of ~0.4 g/cm³ and hardness of ~2000 N compared to most of the tested hardwoods, which have published densities of at least ~0.6 g/cm³ and hardness values of at least ~5000 N (Jiang *et al.*, 2013). As an exception to the rule, the hardwoods Eastern cottonwood and Chinese wingnut exhibit densities and hardness values similar to softwoods (Jiang *et al.*, 2013), although the chemical composition of their cell walls is similar to the remaining hardwood species (Mitchell *et al.*, 2014; Hassan *et al.*, 2019). However, the used plant biomasses were ball-milled before their utilization in the ENCODE RNA-Seq experiments, which should reduce the influence of these factors, because they are mostly derived from the superstructure of the plant. Moreover, the hardwood conditions with a higher density showed a better induction of cellulose and xylan-related PolyCat identifier genes, compared to the species with a reduced density. While the morphological features of the used plant biomasses might thus influence the expression of genes involved in the degradation of intact lignocellulolytic material in *N. crassa*, ball-milling of plant materials should reduce the influence of density and hardness on plant cell wall perception of *N. crassa.*

Intriguingly, the correlation analysis of Eastern cottonwood and Chinese wingnut to the mono-, di- and polysaccharide conditions of the ENCODE project showed that the expression patterns of both hardwood species are similar to the ones induced by starch-related sugars (Figure 2-5). In addition, both species show a higher PolyCat score of the starch PolyCat than any other plant biomass tested. Poplar species, for example Eastern cottonwood, accumulate starch in their ray storage tissue (Sauter and van Cleve, 1994),

which might explain this expression pattern. Starch may induce CCR in these organisms, leading to a reduced expression of genes encoding lignocellulolytic enzymes (Ebbole, 1998; Gancedo, 1998; Sun and Glass, 2011).

Some wood samples of the Fungal Nutritional ENCODE Project were taken from either the

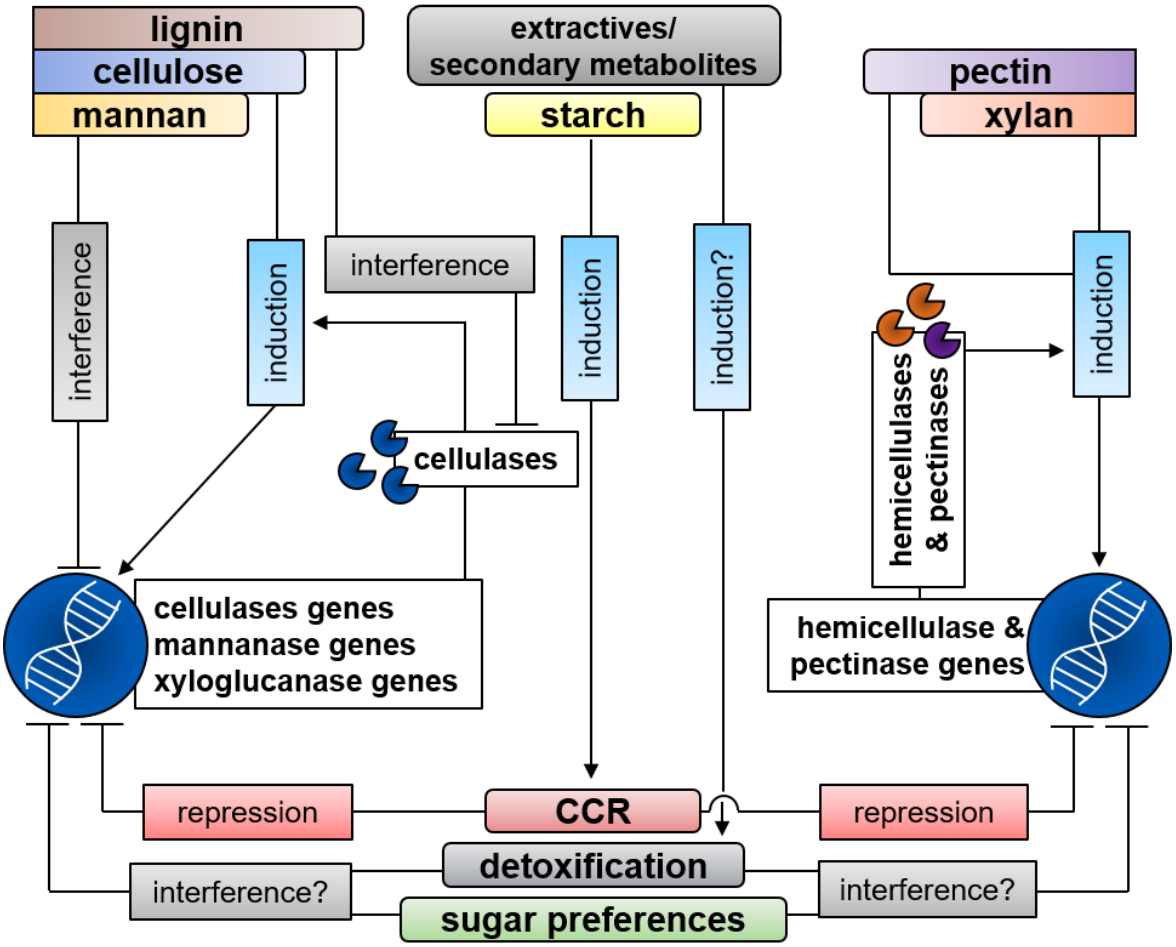

Figure 3-1: Model of extrinsic and intrinsic factors that influence the polysaccharide perception of *N. crassa*.

The mannan content of plant cell walls interferes with cellulase expression, leading to a diminished perception of cellulose. In addition, high concentrations of lignin and cellulose crystallinity reduce the accessibility of cellulose, resulting in a decreased release of inducer molecules. The presence of starch in the plant cell might activate CCR in *N. crassa* through fast liberation of glucose from this polysaccharide. CCR down-regulates the lignocellulolytic response of *N. crassa*. The presence of secondary metabolites/extractives, which include anti-fungal agents, and the process of their detoxification might influence the strength of lignocellulolytic responses. Finally, the intrinsic substrate preferences of *N. crassa* might influence the formation of a degradation response.

heart- or sapwood region of the tree. Heart- and sapwood are two different developmental stages of wood, with heartwood being formed in the inner layers of wood by cells that ceased to live, while sapwood represents the living part of the wood (Taylor *et al.*, 2002). Both wood tissues exhibit specific characteristics. For example, heartwood does not contain any storage polysaccharides, has reduced moisture and can contain secondary metabolites,

commonly referred to as extractives. In contrast, sapwood usually has a higher moisture content but fewer extractives and still contains reserve materials like starch (Fengel and Grosser, 1975; Taylor *et al.*, 2002; Bertaud and Holmbom, 2004). Plant secondary metabolites, including wood extractives, are used as pigments and for plant defense (Taylor *et al.*, 2002; Lattanzio *et al.*, 2006). A wide variety of anti-fungal agents can be stored in the heartwood, considerably increasing the durability of the wood against attacks from lignocellulose-degrading fungi (Fengel and Grosser, 1975; Taylor *et al.*, 2002; Lattanzio *et al.*, 2006). The high extractive content of heartwood may also influence the substrate perception of *N. crassa*, since the fungus would have to detoxify the extractives in parallel to lignocellulose degradation. The results of the 'Fungal Nutritional ENCODE Project' showed that Black locust sapwood had drastically reduced PolyCat scores in all categories compared to the heartwood sample of the same tree species (Figure 2-6). A similar trend was observable for Lebanon cedar, albeit on a much smaller scale. The cellulose PolyCat score of Lebanon cedar heartwood only reached 30% and was less than 10% in sapwood, while the same score was reduced from 100% in Black locust heartwood to around 25% in sapwood. Since the extractive content of Black locust as well as Lebanon cedar heart- and sapwood were not determined in this study and the sample sizes of heart- as well as sapwood conditions was low, it is not possible to correlate reduced fungal perception to extractives at this point.

Taken together, the results of the analyses performed on the ENCODE data showed that many extrinsic and intrinsic factors influence the polysaccharide perception of *N. crassa* (Figure 3-1). The plant cell wall is a complex structure of the crosslinked polysaccharides cellulose and hemicellulose that are embedded in a matrix of pectin and the polyphenolic substance lignin. To detect these carbon sources, fungi secrete lignocellulolytic enzymes in their environment that cleave di- and monosaccharides from polysaccharides. The bioavailability of plant cell wall polysaccharides is therefore a major factor influencing the perception of fungi. If a polysaccharide is coated by another part of the plant cell wall or cannot be reached otherwise by the fungal enzymes, it is masked for fungal detection. Lignin appears to significantly limit the accessibility of cellulose to fungal enzymes (Ding *et al.*, 2012) and the crystallinity of cellulose influences cellulase activity, presumably because the less amorphous regions of cellulose might be more hydrophobic and cannot be physically reached by cellulases (Matthews *et al.*, 2006; Hassan *et al.*, 2017). Thus, both lignin content and cellulose crystallinity influence the liberation of inducer molecules, which results in a reduced 'visibility' of cellulose. Furthermore, anti-fungal secondary metabolites/extractives are used by plants as host defense (Wink, 1988; Taylor *et al.*, 2002; Lattanzio *et al.*, 2006). Since these substances might decrease the viability of *N. crassa*, a

reduced transcriptional response towards plant cell wall polysaccharides is feasible during degradation of biomass that contains anti-fungal compounds.

CCR and starvation were identified as two opposing states in *N. crassa*. If plant cells contain carbon sources that induce CCR, like glucose-rich and easy to hydrolyze starch, the depolymerization of the plant cell wall will be delayed until the CCR inducing carbon sources are depleted (Vinuselvi *et al.*, 2012; Glass *et al.*, 2013b). After the CCR response is reduced significantly, the CSSR gets activated. This process serves at least two functions: 1) to conserve enough energy for the organism to continue growth and self-protection, which are crucial to find new carbon sources (Szilagyi *et al.*, 2013) and 2) initiate the search for new carbon sources by de-repressing enzyme and transporter genes that are necessary for scouting of new carbon sources (Tian *et al.*, 2009; J. P. Benz *et al.*, 2014).

Mono- and disaccharides released by scouting enzymes play a crucial role for the induction of polysaccharide degradation machineries. They induce complex metabolic changes in the fungal cell after their perception. However, structural similarity between two or more inducing molecules might interfere with the correct perception of substrates, as it was shown for the structurally very similar cello- and mannobiose in *N. crassa* (Hassan *et al.*, 2019). It is feasible that both disaccharides are competing for binding with a so far unknown receptor protein, which is part of the signaling pathway inducing cellulose degradation.

Lastly, the polysaccharide perception of fungi is also dependent on the intrinsic regulatory networks of fungi. Different preferences for the utilization of liberated soluble sugars might influence the order in which polysaccharides are perceived. In addition, the degradation of certain polysaccharides might not have a unique signaling/regulatory pathway. For example, genes that encode mannanases and xyloglucanases are activated as part of the cellulose degradation machinery in *N. crassa* (Tian *et al.*, 2009; Craig *et al.*, 2015; Samal *et al.*, 2017), while mannan and xyloglucan cannot induce them. It is tempting to assume, that these unified degradation machineries indicate that *N. crassa* always ‘expects’ to find mannan, xyloglucan and cellulose present at the same time in its target biomass. However, there is no concrete evidence to support this hypothesis as of now.

3.2. Regulation of pectin degradation in *N. crassa*

3.2.1. Three conserved transcription factors regulate the depolymerization of pectin and the catabolism of released monosaccharides

Pectin is composed of a wide variety of sugar moieties and modifications, which together form the most complex of the plant cell wall polysaccharides (Caffall and Mohnen, 2009; Harholt *et al.*, 2010). Conceivably, a similarly complex regulatory system is necessary to orchestrate the expression of the numerous genes that are necessary to efficiently break

down such a complex carbon source. When this study was initiated, no transcription factor with a major growth defect mutant phenotype on pectin had been described in fungi. By utilizing the genetic resources of *N. crassa*, three transcription factors were now successfully identified as regulators of pectin degradation and subsequent catabolic pathways in this fungus. The three transcription factors PDR-1, PDR-2 and ARA-1 all belong to the $Zn(II)_2Cys_6$ binuclear cluster family and have orthologues in other ascomycetes, such as RhaR from the *Aspergilli* (Gruben *et al.*, 2014; Pardo and Orejas, 2014), GaaR in *B. cinerea* and *A. niger* (Alazi *et al.*, 2016; Zhang *et al.*, 2016) or Ara1 in *M. oryzae* and *T. reesei* (Klaubauf *et al.*, 2016; Benocci *et al.*, 2018), respectively.

N. crassa PDR-1 was found to affect the regulation of genes involved in the degradation of the HG backbone, the RG-I backbone, RG-I arabinogalactan side chains as well as rhamnose catabolism. The lack of induction of the *gh28-1* endo-PGase gene as well as the L-galactonate dehydratase and *lgd1* homolog NCU07064 (the second step in galacturonic acid catabolism) most likely caused the observed strong growth defect of the *pdr-1* deletion strain on PGA and galacturonic acid (Figure 2-17; Table 2-4). RG-I backbone degradation appears to be regulated by PDR-1 through the unsaturated rhamnogalacturonan hydrolase gene *gh105-1*, which was part of the PDR-1 core regulon, as the gene was uninduced in the *pdr-1* mutant strain and its promoter contained three PDR-1 binding motifs. The inability of the Δ*pdr-1* strain to utilize rhamnose was most likely caused by the down-regulation of the *rha1* homolog NCU09035, the putative *lra2* homolog NCU03605, the *lra3* homolog NCU09034 and the two possible *lra4* homologs NCU05037 and NCU03086 in the Δ*pdr-1* strain compared to the WT. These genes, with the exception of NCU03605, were also part of the PDR-1 core regulon and contain at least one PDR-1 binding motif in their promoter regions. In addition, the L-arabinitol dehydrogenase gene *ard-1* is part of the PDR-1 regulon (Table 2-5), which explains the additional significant growth defect of the Δ*pdr-1* mutant on both arabinan and arabinose.

In contrast to *N. crassa* PDR-1, its homolog RhaR in *Aspergilli* is an exclusive regulator of RG-I degradation or rhamnose catabolism (Gruben *et al.*, 2014; Pardo and Orejas, 2014). However, a limited influence on arabinogalactan side-chain degradation is described for *A. niger* RhaR (Gruben *et al.*, 2014), which was also observable for *N. crassa* PDR-1, since two β-galactosidase genes (*gh35-1* and *gh35-2*), a putative β-1,4-xylosidase gene (*gh43-3*) and a β-glucuronidase gene (*gh79-1*) failed to be induced in the Δ*pdr-1* strain. The Eurotiomycetes (and most prominently the *Aspergilli*) have developed a highly-expanded set of pectin catabolic genes as well as a number of additional transcription factors, such as GalX, GalR (only in *A. nidulans*) and AraR (Battaglia *et al.*, 2011b; Gruben *et al.*, 2012). Because of this increased division of labor, it is feasible that RhaR might have developed a more focused regulatory function compared to *N. crassa* PDR-1.

The results of this work suggest that activated PDR-1 probably binds its responsive elements as a homodimer, since its DNA binding site is arranged as an inverted repeat, typical for Gal4p-like transcription factors (Figure 2-19) (Vashee *et al.*, 1993; MacPherson *et al.*, 2006). However, it is unlikely that the originally described Gal4p responsive element CGG-X_{11}-CCG is specific enough to act as recognition element for PDR-1 (Pardo and Orejas, 2014). EMSA constructs used by Pardo and Orejas found an extra T nucleotide in at least one half-site of the TCGG-X_{11}-CCG motif (Pardo and Orejas, 2014), which was also found in the shorter binding motif identified by Weirauch *et al.* (Weirauch *et al.*, 2014) and is important for strong rhamnose-dependent induction of *lra3* in *Pichia pastoris* (Liu *et al.*, 2016). Therefore, it is likely that the PDR-1 binding site is represented by the *in silico* expanded TCGG-X_{11}-CCGA motif.

Although *N. crassa* PDR-1 regulates the expression of a wide variety of pectinolytic enzymes, it is not the sole regulator of HG-backbone degradation or the catabolism of the monosaccharides derived from pectin depolymerization. The transcription factor PDR-2 is an equally important regulator of enzyme functions that are necessary for pectin degradation, as shown by the growth defect of the Δ*pdr-2* strain on pectin (Figure 2-21). Moreover, genes encoding pectin backbone-acting enzymes, such as the exo-PGase gene *gh28-2*, the pectate lyase genes *ply-1* and *ply-2*, the rhamnogalacturonan lyase gene *asd-1* and the pectin methylesterase gene *ce8-1*, were mis-expressed in the absence of PDR-2. Particularly the lyase genes appear to be exclusively regulated by this transcription factor, since the deletion of *pdr-2* led to a failed induction of these genes and also completely abolished pectate lyase activity in the sample supernatants of the Δ*pdr-2* strain (Figure 2-22). Furthermore, two genes of the galacturonic acid metabolism, the *gar2* homolog NCU09533 and *lga1* homolog NCU09532, as well as the galacturonic acid transporter gene *gat-1* failed to be induced in the *pdr-2* mutant strain. These results explain why the Δ*pdr-2* strain was unable to accumulate any biomass on galacturonic acid, as an efficient utilization of this monosaccharide should not be possible when two genes of its catabolism pathway are not sufficiently expressed. Moreover, mis-expression of the *gat-1* gene would prevent the uptake of galacturonic acid, since GAT-1 is the only galacturonic acid transporter in *N. crassa* (J. Benz *et al.*, 2014).

The function of PDR-2 as regulator of HG-backbone degradation and galacturonic acid catabolism appears to be conserved in *A. niger* (Alazi *et al.*, 2016). The loss of the PDR-2 orthologue GaaR caused a severe growth defect on PGA also in that fungus. Moreover, growth on galacturonic acid was completely abolished in the *gaaR* deletion strain. In contrast, deletion of *gaaR* in the necrotrophic fungal plant pathogen *B. cinerea* caused a significant but much less severe growth defect on pectin and galacturonic acid (Zhang *et al.*, 2016). Zhang *et al.* showed that GaaR specifically induces the expression of genes

related to galacturonic acid utilization. However, the comparatively mild mutant phenotype of the *gaaR* deletion strain suggests that additional factors besides GaaR are involved in the regulation of this process in *B. cinerea*. It has been reported that pectinases are important for the virulence of *B. cinerea* (Have *et al.*, 1998; Kars *et al.*, 2005; Nafisi *et al.*, 2014), which could have resulted in an expanded and potentially multi-layered regulatory network controlling pectin degradation in this organism.

Intriguingly, PDR-1 and PDR-2 were both involved in the regulation of a number of pectinases, such as the rhamnogalacturonyl hydrolase gene *gh105-1*, rhamnogalacturonan acetylesterase gene *ce12-1*, the β-galactosidase genes *gh35-1* and *gh35-2*, as well as the endo-PGase gene *gh28-1* (Figure 2-22). The *pdr-2* deletion strain did not show any endo-PGase activity similar to the Δ*pdr-1* strain, which indicates that both transcription factors are necessary for the expression of this gene. Based on these results, it appears that PDR-1 and PDR-2 have to be present together for a fully functional expression of many pectinase genes. Whether both transcription factors exert the same regulatory influence on these genes cannot be answered at this point. It is feasible, however, that the expression of certain genes is dependent on the presence of one transcription factor, while the other one only modulates the expression. However, no clear regulatory hierarchy could be determined between PDR-1 and PDR-2, because the Δ*pdr-1*/Δ*pdr-2* double deletion strain only exhibited the phenotype of either the Δ*pdr-1* or the Δ*pdr-2* strain, but never an increased severity in defects.

Although pectin is mostly composed of galacturonic acid and (to a lesser extent) rhamnose, galactose and arabinose decorate the pectin backbone as side-chain sugars (Caffall and Mohnen, 2009). These monosaccharides are therefore suitable carbon sources for *N. crassa*. The transcription factors PDR-1 and PDR-2 are involved in the regulation of arabinan degradation, since key genes like the L-arabinitol dehydrogenase *ard-1* and the arabinose transporter *lat-1* exhibit a reduced expression level in the Δ*pdr-1* or Δ*pdr-2* strains, respectively. However, the *pdr-1* deletion strain was still able to grow on arabinan and arabinose, albeit at a significantly reduced rate. It is therefore feasible that other regulatory elements might influence arabinan degradation or arabinose catabolism.

In this study, the phylogenetic analysis of $Zn(II)_2Cys_6$ binuclear transcription factors showed that Ara1 is conserved in *N. crassa*, while no orthologs of AraR or GalX/GalR could be found (Figure 2-23). The ENCODE data were analyzed by Vincent Wu (UC Berkeley) to determine the mis-expressed genes of the Δ*ara-1* strain vs. the WT grown on *Miscanthus* dried grass powder (Wu, 2017; Wu *et al.*, 2019). These analyses showed that the expression of the *lat-1* transporter gene and the *ard-1* gene were significantly down-regulated in the mutant strain compared to the WT. LAT-1 is the only arabinose transporter present in *N. crassa*, and deletion of *lat-1* almost completely prevents *N. crassa* from taking up arabinose (J. P.

Benz *et al.*, 2014). The gene *ard-1* encodes the L-arabinitol 4-dehydrogenase, which catalyzes the second reaction of arabinose catabolism by converting L-arabinitol into L-xylulose (Seiboth and Metz, 2011). Moreover, this enzyme also plays a role as galactitol dehydrogenase during the third step of the oxidoreductive galactose catabolism in *T. reesei* and *A. niger*, where it converts galactitol to L-xylo-3-hexulose (Mojzita *et al.*, 2012). The growth assays of the Δ*ara-1* strain corroborated the RNA-Seq data, as deletion of *ara-1* resulted in the inability of *N. crassa* to grow on arabinose and galactose, while growth on arabinan and arabinogalactan was significantly reduced (Figure 2-25). The orthologues of *N. crassa* ARA-1 in *M. oryzae* and *T. reesei* exhibited similar growth phenotypes. Deletion of *M. oryzae ara1* resulted in reduced growth on arabinan and completely abolished any biomass accumulation on arabinose (Klaubauf *et al.*, 2016). Furthermore, a deletion of *ara1* resulted in the inability of *T. reesei* to grow on galactose in addition to being not able to accumulate any biomass on arabinose (Benocci *et al.*, 2018). It is feasible that the residual growth of the Δ*ara-1* strain on arabinan and arabinogalactan could be explained through additional sugars in these carbon sources, since the manufacturer of both tested polysaccharides declares that they only have a purity of ~95%.

Intriguingly, the *ard-1* gene was significantly mis-expressed in the Δ*pdr-1* strain and contained two PDR-1 binding motifs, while *lat-1* expression was significantly reduced in the Δ*pdr-2* strain. It appears that ARA-1 thus is not the sole regulator of arabinose/galactose catabolism in *N. crassa*, but that it rather co-regulates the degradation of pectic side chains together with PDR-1 and/or PDR-2. Further experiments are necessary to determine the direct or indirect regulatory overlap of ARA-1 and PDR-1/PDR-2 during the mediation of arabinose and galactose catabolism.

3.2.2. Pectin degradation is modulated through subcellular localization of regulators, inducer availability and proteolysis

Pardo and Orejas reported that the *pdr-1* homolog *rhaR* of *A. nidulans* was neither auto-regulated nor carbon catabolite repressed; instead the authors suggested that RhaR is activated post-translationally in the presence of rhamnose (Pardo and Orejas, 2014). In contrast, *A. niger rhaR* clearly responded to repressing and inducing conditions (Gruben *et al.*, 2014), which is in agreement with the observations of this study in *N. crassa* that expression of *pdr-1* is down-regulated under CCR-inducing conditions and enhanced on rhamnose and pectin (SFigure 6-4a). These contrasting results might be explained by the overall low expression values of *pdr-1*/*rhaR* that cannot be accurately measured by semi-quantitative methods like the RT-PCR employed by Pardo and Orejas (Pardo and Orejas,

2014). To differentiate between transcriptional (auto-)induction and post-transcriptional activation of *pdr-1*, the *pdr-1-oex* strain was created in this study to constitutively express the *pdr-1* gene (Figure 2-18a). The results of these experiments showed that (1) a fraction of the PDR-1 pool is always active (or de-repressed), since endo-PGase activity was detectable in the non-induced state, and that (2) PDR-1 is post-transcriptionally or post-translationally regulated by rhamnose, as substantially higher endo-PGase activity was measured after addition of rhamnose, but not galacturonic acid, in the *pdr-1-oex* strain. Moreover, the expression of the *pdr-1* target gene NCU09034 was also significantly enhanced in the *pdr-1-oex* strain induced by rhamnose compared to a non-induced control (Figure 2-18).

Some zinc binuclear cluster transcription factors, such as for example *N. crassa* CLR-2, are constitutively active and only transcriptionally regulated through other transcription factors (e.g. CLR-1 up-regulates CLR-2 expression) (Coradetti *et al.*, 2012, 2013). Nonetheless, activation by binding of an inducing molecule or interaction with a metabolic intermediate is equally common in the $Zn(II)_2Cys_6$ binuclear transcription factor family (MacPherson *et al.*, 2006). For example, xylose and arabinose or their respective catabolic intermediates have been implicated as inducers for hemicellulolytic pathways in filamentous fungi. Reversible hyper-phosphorylation of *Aspergillus* XlnR was observed as an effect of induction (Noguchi *et al.*, 2011). A similar effect has long been known for Gal4p in yeast (Mylin *et al.*, 1990). Moreover, *A. niger* GaaR, *T. reesei* XYR1 and *N. crassa* XLR-1 have been engineered for constitutive activation, which could be a next logical step also for PDR-1 (Derntl *et al.*, 2013; Craig *et al.*, 2015; Alazi *et al.*, 2018).

The interaction of transcription factors with their target genes can also be effectively controlled by subcellular re-localization such as by transport into or out of the nucleus. The transcription factor XlnR, which regulates the expression of genes encoding xylanolytic and cellulolytic enzymes in *A. niger*, loses its regulatory function if it has mutations that interfere with the nuclear import of this transcription factor (Hasper, 2004). Xyr1, the homolog of XlnR in *T. reesei*, is also translocated into the nucleus when xylose is present (Lichius *et al.*, 2014). In this study, sequence analyses predicted one NLS and NES region in the protein sequence of *N. crassa* PDR-1 (Figure 2-12), which implies that this transcription factor could also be regulated by nuclear exclusion. Indeed, the presence of rhamnose led to a translocation of PDR-1 into the nucleus, and this translocation event was independent of transcriptional induction, since the PDR-1-GFP fusion construct used in this experiment was constitutively expressed. Intriguingly, a spot of increased fluorescence was visible inside most nuclei after induction with rhamnose, which might represent PDR-1 bound to its promoter target sites (Figure 2-18). However, it is equally possible that these spots indicate the formation of regulatory protein complexes that include PDR-1 (Lamond and Spector,

2003; Matera *et al.*, 2009). Together with previous observations about rhamnose-dependent activation of PDR-1, these results suggest that (inactive) PDR-1 might be present in the cytoplasm while rhamnose leads to a post-translational activation and/or translocation of this transcription factor into the nuclei of *N. crassa*. Similar translocation events were observed in *B. cinerea* for the PDR-2 homolog GaaR when galacturonic acid was used as carbon source (Zhang *et al.*, 2016). Since *N. crassa* PDR-2 contains 2 predictable NLS and 1 predicted NES region (Figure 2-20), it is thus possible that the activity of PDR-2 is also regulated through nuclear localization or exclusion events.

The transcriptional response of fungi to nutrient availability is modulated by numerous signals from varying sources, which integrate the current nutritional and physiological state of the organism with the information received from its extracellular environment. In *N. crassa*, the cellulolytic response of the fungus is regulated by the two transcription factors CLR-1 and CLR-2 (Coradetti *et al.*, 2012, 2013). Recent studies by Huberman *et al.* demonstrated that the activity of CLR-1 is actually repressed by the protein CLR-3 and that this repression is relieved in the presence of cellulose (Huberman *et al.*, 2017). A similar regulatory mechanism is described in *A. niger*, where the GaaR repressor protein GaaX suppresses GaaR activity in the absence of galacturonic acid (Niu *et al.*, 2017). An orthologue of *gaaX* was also found in *N. crassa* (Niu *et al.*, 2017), which opens up the possibility that the activity of PDR-2, the GaaR homolog in *N. crassa*, might similarly be repressed in the absence of an inducing molecule like galacturonic acid.

The activity of transcription factors can also be regulated through the availability of inducing molecules. By regulating the expression of genes encoding transporter proteins, all inducer-dependent activities are also influenced. So far, two transporters of pectic monosaccharides are described for *N. crassa*, the galacturonic acid transporter GAT-1 (J. Benz *et al.*, 2014) and the arabinose transporter LAT-1 (J. P. Benz *et al.*, 2014). In this study, the first rhamnose transporter was identified in *N. crassa*. The transport protein FRT-1 is the sole transporter of rhamnose (and fucose) in *N. crassa*, as a deletion of the *frt-1* gene completely abolished any uptake of these monosaccharides (Figure 2-26). Moreover, the Δ*frt-1* strain showed a severe growth defect on rhamnose. While rhamnose-specific transporters were published for *Escherichia coli* and *Salmonella typhimurium* in the early 1990s (Tate *et al.*, 1992), these proteins have no homolog in Eukaryotes and no MFS-type transporter has been associated with rhamnose transport in fungi until recently (Sloothaak *et al.*, 2016).

Since the activity of the transcription factor PDR-1 is dependent on the presence of rhamnose, the regulation of *frt-1* expression could be a tool to regulate pectin degradation in *N. crassa*. Indeed, a strain carrying a *frt-1* deletion failed to induce the expression of the PDR-1 target gene NCU09034 in the presence of rhamnose, similar to the Δ*pdr-1* strain (Figure 2-26). Furthermore, the FRT-1 orthologue in *A. niger*, RhtA, was regulated by CreA-

mediated CCR, as *rhtA* expression was drastically reduced on rhamnose plus glucose in the WT strain, while deletion of *creA* allowed the induction of *rhtA* in these conditions (Sloothaak *et al.*, 2016). The experiments performed in this work corroborate the CreA/Cre-1-mediated regulation of RhtA/FRT-1, since co-incubation of rhamnose and glucose also significantly reduced *frt-1* expression in the WT strain, while the *frt-1* expression levels were increased in the Δ*cre-1* strain (Figure 2-27). These results were further supported by uptake assays of the WT and Δ*cre-1* strain induced with pectin and glucose, which showed that presence of glucose prevents rhamnose uptake in the WT strain, but not in the Δ*cre-1* mutant. Additionally, DNA affinity purification sequencing (DAPseq) of CRE-1 was performed by Wu *et al.* to determine potential targets of this transcription factor through DNA binding studies with the promoter regions of annotated genes in *N. crassa* (Wu, 2017; Wu *et al.*, 2019). These experiments showed that CRE-1 bound at least once to the promoters of 329 genes, including *frt-1*.

CRE-1 and its homologs in other ascomycetes regulate the expression of genes in a double-lock manner by repressing both the expression of genes encoding lignocellulolytic enzymes and also the genes encoding the respective transcriptional activators (Kulmburg *et al.*, 1993; Mathieu and Felenbok, 1994; Orejas *et al.*, 1999; Tamayo *et al.*, 2008; Sun and Glass, 2011). Based on the results of this study and the data from Wu *et al.* (Wu, 2017; Wu *et al.*, 2019), it is more likely that CRE-1 repression acts in a “triple-lock” manner by preventing the uptake of inducing molecules through the repression of transporter gene expression in addition to the previously described regulatory mechanisms. Taken together, regulation of FRT-1 through CRE-1 induced CCR is another efficient way to regulate pectin metabolism in *N. crassa*, since it directly influences the presence of inducer molecules in the cytosol.

The majority of regulatory mechanisms described in this work so far affect polysaccharide degradation on the level of transcription, by either directly or indirectly altering gene expression. However, the transition between different metabolic states, because of changed substrate availability, also necessitates an adaptation of the fungus on the protein level. Proteolysis is one possible way to remove existing regulatory proteins upon perception of altered metabolic conditions. Protein degradation through the 26S proteasome is regulated by multi-protein E3 ligase complexes in Eukaryotes (Skowyra *et al.*, 1997; Lechner *et al.*, 2006). The SCF complex is part of the E3 ligase family and attaches polyubiquitin chains to target proteins. The ubiquitination marks these proteins for subsequent degradation in the proteasome. F-box proteins are an important part of the SCF complex, since they determine which proteins will be modified by it. F-box proteins convey substrate-specificity through their protein-protein interaction domains (Lechner *et al.*, 2006).

It was determined through a recent DNA-sequencing study that the *frp-1* gene, which encodes an F-box protein, is causative for the hypersecretion phenotype of the classical *N.*

crassa exo-1 mutant strain (Gabriel *et al.*, 2019). The *exo-1* strain was generated by UV-mutagenesis and secretes α-amylase, glucoamylase, invertase, cellobiase and trehalase in large quantities after depletion of its carbon source (Gratzner and Sheehan, 1969; Gratzner, 1972; Sternberg and Sussman, 1974; Spinelli *et al.*, 1996). Additionally, it was published that the *exo-1* strain secretes pectinases after induction with galactose (Polizeli *et al.*, 1991; Crotti *et al.*, 1996, 1998b). In contrast to the described pectinase secretion phenotypes of Polizeli *et al.*, the endo-PGase and arabinanase assays of this study showed that the activity of pectinases, and consequently their expression and secretion, was increased not after addition, but after depletion of galactose (Figure 2-30). The RNA-Seq analysis of the WT and Δ*frp-1* strain confirmed this observation, as most genes encoding lignocellulolytic enzymes, including pectinases, were only up-regulated in the *frp-1* deletion strain under starvation (Figure 2-28) (NoC). In contrast, the expression of most genes was low and WT-like in the Δ*frp-1* strain induced with glucose. Moreover, α-amylase, invertase and endo-PGase activity were increased in the Δ*frp-1*/Δ*cre-1* strain incubated in sucrose, while the same enzymatic activities were repressed in the Δ*frp-1* strain on sucrose (Figure 2-31). These results indicate that CRE-1-mediated CCR is still active in the Δ*frp-1* strain.

Intriguingly, more CAZy and transporter genes were down-regulated in the Δ*frp-1* strain than up-regulated (Figure 2-29). Based on these results, it was concluded that deletion of *frp-1* may prevent the proteolysis of certain regulators that might be direct or indirect targets of FRP-1. The resulting mis-regulation of the metabolism might have caused a) the increased target gene expression of these falsely present regulators and b) a dramatic down-regulation of the remaining metabolic genes as a compensatory mechanism.

The transcription factor COL-26 was described as being essential for starch degradation, the integration of carbon and nitrogen metabolism as well as for glucose sensing in *N. crassa* (Xiong *et al.*, 2014, 2017). Deletion of this transcription factor significantly reduced the expression of the α-amylase gene *gla-1*, as well as other α-amylase genes, and the invertase gene NCU04265. Therefore, the overlap between the COL-26-dependent genes and genes that were up-regulated in the absence of FRP-1 was determined (Figure 2-32). This analysis showed that most α-amylase and invertase genes were in the overlap between COL-26 and FRP-1. Enzymatic assays in the Δ*frp-1*/Δ*col-26* double deletion strain confirmed that the loss of *col-26* completely abolishes the hypersecretion of α-amylases and invertases in the *frp-1* deletion background. These results suggest that COL-26 is either directly or indirectly targeted by FRP-1. However, the hypersecretion of endo-PGases and arabinanase was not altered in Δ*frp-1*/Δ*col-26*, indicating that FRP-1 might influence additional transcription factors which are involved in pectin degradation.

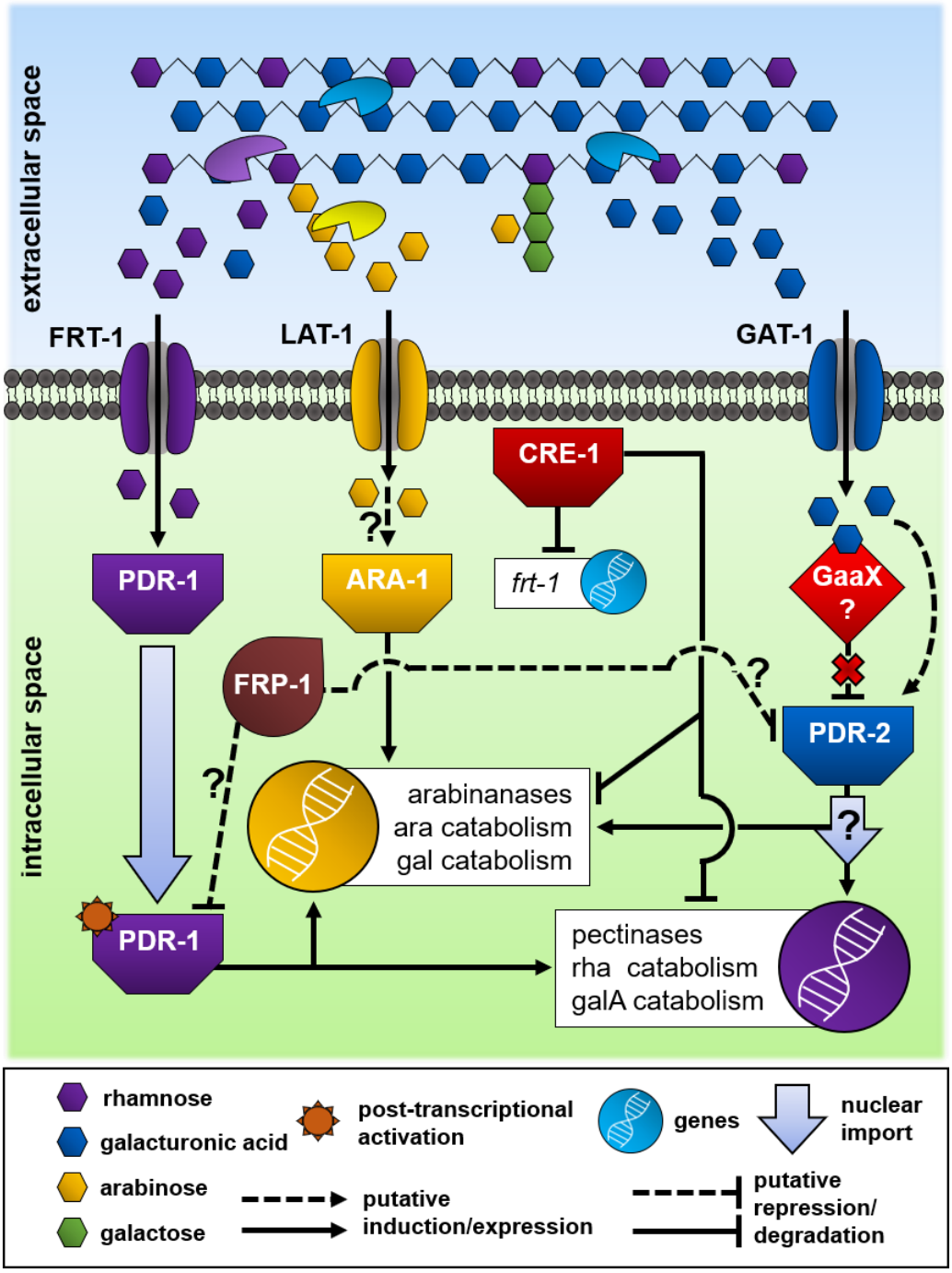

Figure 3-2: Model of regulatory elements affecting pectin degradation.
The transporters FRT-1, GAT-1 and LAT-1 take up rhamnose (rha), galacturonic acid (galA) or arabinose (ara), respectively. The expression of *frt-1* and all other genes encoding lignocellulolytic enzymes is repressed by CRE-1 during CCR-inducing conditions. PDR-1 gets post-transcriptionally activated when rhamnose is in the cytosol and also translocates into the nucleus. PDR-2 might be repressed by a so far undescribed GaaX homolog in absence of galacturonic acid. Alternatively, galacturonic acid (or one of its degradation products) might directly induce PDR-2 activity, which may result in translocation into the nucleus. PDR-1 and PDR-2 regulate the expression of most pectinase genes, as well as rhamnose and galacturonic acid catabolism genes. ARA-1 might be induced by arabinose. ARA-1 induces the expression of arabinanase genes, as well as arabinose and galactose (gal) catabolism genes. PDR-1 and PDR-2 also partly modulate the expression of these genes. FRP-1 may be involved in the proteolysis of PDR-1 and/or PDR-2.

Based on the results reported in this and previous studies, activation and maintenance of pectin degradation involves the following regulatory elements in *N. crassa* (Figure 3-2): In the absence of a CCR-inducing carbon source, the genes encoding the transport proteins *frt-1*, *gat-1* and *lat-1* may be de-repressed together with some pectinase genes. The de-repressed pectinases release soluble pectic monosaccharides, i.e. rhamnose, arabinose and galacturonic acid, which are transported into the cytosol by the aforementioned transport proteins. The presence of rhamnose in the cytosol activates the transcription factor PDR-1 post-transcriptionally and also leads to a translocation of PDR-1 into the nucleus. At the same time, the transcription factor PDR-2 might be released from repression from a so far undescribed GaaX homolog in the presence of galacturonic acid. Alternatively, PDR-2 might be directly activated by galacturonic acid or one of its degradation products. The activation of PDR-2 might result in a translocation of this transcription factor into the nucleus, similar to PDR-1. PDR-1 and PDR-2 activate the expression of the majority of pectinase genes as well as genes encoding enzymes of the rhamnose or galacturonic acid catabolism. Although PDR-1 and PDR-2 have their own target genes, the presence of both transcription factors is necessary for a full activation of the majority of their genes. However, ENCODE expression data suggest that neither PDR-1 nor PDR-2 regulate the expression of *frt-1*. In parallel to the activation of PDR-1 and PDR-2, the transcription factor ARA-1 might either be activated by the presence of arabinose or is regulated otherwise. ARA-1 induces the expression of arabinanase genes as well as genes encoding enzymes of the arabinose and galactose catabolism. PDR-1 and PDR-2 are involved directly or indirectly in the mediation of some of these genes. Finally, the F-box protein FRP-1 is involved in the correct shutdown of pectin degradation, as FRP-1 might mark PDR-1 or PDR-2 as targets for the SCF complex and subsequent proteolysis.

4. Concluding remarks and outlook

Fungal perception and degradation of plant cell wall polysaccharides are complex processes that are influenced by numerous extrinsic and intrinsic factors. This study showed, that the complete and efficient depolymerization of lignocellulosic biomass is dependent on the interplay between fungi and their biomass. Bioavailability, cell wall components and the physicochemical properties of plant cell walls significantly affect fungal substrate perception and as a result lignocellulolytic enzyme secretion. On the other hand, one has to consider overlapping regulatory networks in fungi or their inability to perceive certain substrates when choosing a strain for plant biomass degradation.

The PolyCat scores described in this work are a novel method to visualize which polysaccharides can be detected by *N. crassa*. Moreover, PolyCat scores also give an

indication if a carbon source is perceived well or poorly by the fungus. They have been proven to be a suitable tool to analyze fungal plant cell wall perception in *N. crassa* and provided new insights into this topic. However, the used ENCODE data only contained expression patterns of genes induced for 4 h with a respective carbon source. As substrate "confusion" and CCR delay the perception of plant cell wall polysaccharides, the full response of *N. crassa* on substrates rich in mannan, lignin and starch has yet to be determined. Moreover, whether the perception of different plant cell wall polysaccharides shifts in strength over time or remains constant cannot be answered based on the currently available data. A time-course RNA-Seq experiment using *N. crassa* induced with one or two complex biomasses could provide more insights into temporal changes occurring during fungal polysaccharide perception.

The second part of this thesis analyzed the regulation of pectin degradation. Pectin is the most complex plant polysaccharide and its degradation is regulated by at least three transcription factors in *N. crassa*. Furthermore, the uptake of monosaccharides, post-translational activation of transcription factors, their subcellular localization as well as CCR determine the response of *N. crassa* to pectin (and polysaccharides in general).To better understand the regulatory processes that mediate pectin degradation, early signaling events, for example through phosphorylation, have to be analyzed. Moreover, the signaling pathways that transmit the signals from the membrane to transcription factors and other regulators are still unknown. The proteins that might form these signaling cascades, for example mitogen-activated protein kinase (MAPK) or G-coupled receptors, would be suitable targets for genetic engineering. In addition, fungi need to swiftly adapt their metabolism to altered carbon conditions, which necessitates the removal of counteracting regulators. Based on the results of this work, it appears that F-box proteins mediate the proteolysis of several transcription factors and therefore indirectly regulate polysaccharide degradation.

Overall, the identified regulatory elements of pectin degradation provide new angles of strain engineering for biorefinery purposes. While the deletion or constitutive expression of transcription factors like PDR-1, PDR-2 or ARA-1 could be used to globally up- or down-regulate pectinase expression, the deletion of F-box proteins may enable a substrate independent secretion of target enzymes.

5. Materials and methods

5.1. Used instruments, materials and strains

5.1.1. Instruments and software

Table 5-1: List of used instruments.

name	model	manufacturer
autoclave	Varioklav 135 S	Thermo Fisher Scientific (Waltham, USA)
ball mill	MM 200	Retsch (Haan, Germany)
confocal laser scanning microscope	TCS SP5	Leica Microsystems (Wetzlar, Germany)
electroporator	Eporator	Eppendorf (Hamburg, Germany)
gel imaging system	Fusion solo S	Vilber Lourmat (Eberhardzell, Germany)
heating block	TSC ThermoShaker	Analytik Jena (Jena, Germany)
heating block with cover	ThermoMixer C	Eppendorf (Hamburg, Germany)
high-performance anion-exchange chromatography with pulsed amperometric detection (HPAEC-PAD)	Dioncex ICS-3000	Thermo Fisher Scientific (Waltham, USA)
Incubator 30 °C	Heratherm IGS100	Thermo Fisher Scientific (Waltham, USA)
Incubator 37 °C	IR 1500	Flow Laboratories (Inglewood, USA)
incubator shaking	Excella 24	New Brunswick Scientific (Edison, USA)
laboratory bead mill	BeadBug 24 D1030	Süd-Laborbedarf Gauting (Gauting, Germany)
large scale centrifuge	Megafuge 40R	Heraeus (Hanau, Germany)
light Incubator 25 °C	BK 5060 EL	Heraeus (Hanau, Germany)
light incubator shaking	Innova 42	New Brunswick Scientific (Edison, USA)
sequencing system	MiSeq	Illumina (San Diego, USA)
oven	Jouan	Thermo Fisher Scientific (Waltham, USA)
pH-meter	SevenEasy	Mettler Toledo (Columbus, USA)
plate incubator	INCU-Mixer MP	Benchmark Scientific (Edison, USA)
plate reader	Infinite 200 PRO NanoQuant reader	Tecan (Männedorf, Switzerland)
rocking machine	RT 26	Analytik Jena (Jena, Germany)
tabletop centrifuge	Centrifuge 5424	Eppendorf (Hamburg, Germany)
tabletop centrifuge (cooled)	Centrifuge 5427 R	Eppendorf (Hamburg, Germany)
thermocycler	ProfessionalTRIO	Analytik Jena (Jena, Germany)
thermocycler gradient	peqStar 2x Gradient	VWR (Radnor, USA)
tube revolver	Rotator	Analytik Jena (Jena, Germany)
stereo microscope	S8AP0	Leica Microsystems (Wetzlar, Germany)
sterile bench	BDK-S	BDK Luft- und Reinraumtechnik (Sonnenbühl-Genkingen, Germany)
water purifier	mini-UP+	Berrytec (Grünwald, Germany)

Table 5-2: List of software and online tools used for data analysis.

name & version	usage	manufacturer
Adobe Photoshop CS2, V9.0	figure preparation	Adobe Systems (Mountain View, USA)
AnnHyb V4.946	determination of primer melting temperatures	Olivier Friard (Torino, Italy)
Basic Local Alignment Search Tool (BLAST)	search for and comparison of nucleotide and amino acid sequences, determination of sequence identity	National Center for Biotechnology Information (NCBI) (Bethesda MD, USA)
Carbohydrate-Active enZYmes (CAZY) Database	classification of catalytic and carbohydrate-binding modules of enzymes that degrade glycosidic bonds	Université d'Aix-Marseille, architecture et function des macromolecules biologiques (Marseille, France)
Chromeleon Chromatography Data System V7.2 SR3	recording and analysis of HPAEC-PAD data	Thermo Fisher Scientific (Waltham, USA)
Catalog of Inferred Sequence Binding Preferences database (CIS-BP)	retrieval of direct or inferred transcription factor DNA binding consensus sequences	University of Toronto, Molecular Genetics (Toronto, Canada)
Clustal Omega	Sequence alignment and creation of phylogenetic trees	The European Bioinformatics Institute (EMBL-EBI) (Cambridgeshire, United Kingdom)
Draw Venn diagrams	preparation of Venn diagrams	Ghent University, Bioinformatics Institute Ghent (Ghent, Belgium)
FigTree v1.4.3	creation of phylogenetic trees and phylogenetic analysis	Institute of Evolutionary Biology University of Edinburgh (Edinburgh, United Kingdom)
Fungal Genetics Stock Center (FGSC)	collection of *N. crassa* strain information, navigation for the *N. crassa* deletion strain stock collection	Kansas State University, Department of Plant Pathology (Manhattan KS, USA)
fungal and oomycete genomics resources (FungiDB)	nucleotide and protein sequence retrieval, homology searches	National Institute of Allergy and Infectious Diseases (NIAID) (Maryland, USA) and University of California, Riverside (Riverside, USA)
Galaxy Server	creating a pipeline to analyze RNA-Seq data	Pennsylvania State University, Center for Computational Biology and Bioinformatics (CCBB) (Pennsylvania, USA), John Hopkins University (Baltimore, USA) and Oregon Health & Science University, Computational Biology (Portland OR, USA)
Hierarchical Clustering Explorer V3.5	hierarchical clustering of gene expression data	University of Michigan (Ann Arbor, USA)

Table 5-2: List of software and online tools used for data analysis (continued).

name & version	usage	manufacturer
ImageJ 1.47t	fluorescence intensity measurements, microscopy figure preparation	National Institutes of Health (Maryland, USA)
LAS AF	microscopy figure preparation	Leica Microsystems (Wetzlar, Germany)
Molecular Evolutionary Genetics Analysis (MEGA) Software V7.0.21	alignment of nucleotide sequences	Temple University (Philadelphia, USA) and Tokyo Metropolitan University (Tokyo, Japan)
Microsoft Office 2013	statistical analysis, manuscript preparation	Microsoft (Redmond, USA)
NCBI Conserved Domains	prediction of conserved domains on nucleotide/amino acid sequences	National Center for Biotechnology Information (NCBI) (Bethesda MD, USA)
NetNES 1.1 Server	prediction of nuclear export signals (NES) in amino acid sequences	Technical University of Denmark Bioinformatics (Lyngby, Denmark)
Nine Amino Acids Transactivation Domain 9aaTAD Prediction Tool	prediction tool for transactivation domains	Centre for Information Technologies - Management of the University Campus at Bohunice (Slovakia)
NucPred - Predicting Nuclear Localization of Proteins	prediction of nuclear localization signals (NLS) in amino acid sequences	Stockholm University Bioinformatics Center (Stockholm, Sweden)
Pfam	gene product type/class annotation	The European Bioinformatics Institute (EMBL-EBI) (Cambridgeshire, United Kingdom)
Phylogeny.fr	creation of phylogenetic trees and phylogenetic analysis	Laboratoire d'Informatique, de Robotique et de Microélectronique de Montpellier (France)
Rstudio 1.1.453 (2016)	statistical analysis, figure preparation	RStudio: Integrated Development for R. RStudio, Inc.
SnapGene Viewer V3.2.1	primer design, *in silico* plasmid assembly	GSL Biotech LLC (Chicago, USA)
Transporter Classification Database (TCDB)	sub-classification of (putative) transporter protein sequences	University of California San Diego, Division of Biological Sciences (San Diego, USA)
UniProt Database	amino acid sequence retrieval, prediction of cellular protein localization	The European Bioinformatics Institute (EMBL-EBI) (Cambridgeshire, United Kingdom), Swiss Institute of Bioinformatics (SIB) (Lausanne, Switzerland) and Protein

	Information Resource (Delaware, USA)

5.1.2. Chemicals and other consumables

Table 5-3: List of used carbon sources.

name	purity	order number	manufacturer
arabinan from sugar beet	~95.0%	P-ARAB	Megazyme (Bray, Ireland)
arabinogalactan from larch wood	≥95.0%	P-ARGAL	Megazyme (Bray, Ireland)
L-arabinose	≥99.5%	10839	Merck (Darmstadt, Germany)
cellulose (Avicel PH-101)	-	11365	Merck (Darmstadt, Germany)
L-fucose	≥99.0%	A16789	VWR (Radnor, USA)
D-galactose	≥99.0%	G0750	Merck (Darmstadt, Germany)
D-galacturonic acid monohydrate	≥97.0%	48280	Merck (Darmstadt, Germany)
D-glucose anhydrous	≥99.5%	X997	Carl Roth (Karlsruhe, Germany)
D-glucuronic acid	≥98.0%	4124.1	Carl Roth (Karlsruhe, Germany)
pectin from citrus peel	≥74.0%	P9135	Merck (Darmstadt, Germany)
polygalacturonic acid (PGA)	≥90.0%	81325	Merck (Darmstadt, Germany)
L-rhamnose monohydrate	≥99.0%	R3875	Merck (Darmstadt, Germany)
soluble starch	-	S9765	Merck (Darmstadt, Germany)
sucrose	≥99.5%	S7903	Merck (Darmstadt, Germany)
xylan from beechwood	≥90.0%	X4252	Merck (Darmstadt, Germany)
D-xylose	≥99.0%	X3877	Merck (Darmstadt, Germany)

Table 5-4: List of carbon sources used for the fungal transcriptional ENCODE project (modified from Wu, 2017).

name	CAS number	source and specifications
Abies alba	-	HFM[a]
amylopectin	9037-22-3	Sigma from corn A-7780
amylose	9005-82-7	Sigma from corn A-7043
arabinan	11078-27-6	Megazyme (sugar beet)
L-arabinose	5328-37-0	Sigma L (+) min 99% a3256
bacterial cellulose	-	EBI[b]
Cedrus libani heartwood	-	HFM[a]
Cedrus libani sapwood	-	HFM[a]
cellobiose	528-50-7	Fluka D (+) >99%
cellulose (Avicel)	9004-34-6	Fluka
citrus peel (CiPeel)	-	EBI[b]
Corn stover	-	EBI[b]
eastern cottonwood	-	EBI[b]
energy cane	-	EBI[b]
D-fructose	0609-06-03	Research organics
L-fucose	2438-80-4	Sigma
galactan	39300-87-3	Megazyme (lupin)
galactomannan	-	Megazyme (carob low viscosity)
D-galactose	59-23-4	Acros D (+) 99+%
D-galacturonic acid	91510-62-2	Fluka 48280

glucomannan	37220-7-0	Konjac Foods

[a] Holzforschung München, Munich, Germany; [b] Energy Biosciences Institute, Berkeley, USA

Table 5-4: List of carbon sources used for the fungal transcriptional ENCODE project (modified from Wu, 2017) (continued).

name	CAS number	source and specifications
D-glucuronic acid	6556-12-3	Sigma 98%
glycerol	56-81-5	Thermo Fisher Scientific
inulin	9005-80-5	Sigma
lactose	5989-81-1	Sigma β lactose >99%
lignin	9005-53-2	EBI[b]
maltose	6363-53-7	Sigma D (+) min 98% <0.3% glucose <1.0% maltotriose
mannan	-	Megazyme (ivory nut)
mannitol	69-65-8	Thermo Fisher Scientific
mannobiose	O-MBI	Megazyme
D-mannose	3458-38-4	Acros D (+) 99+%
Miscanthus x giganteus	-	EBI[b]
pectin	9000-69-5	Sigma from orange peel
Picea abies heartwood	-	HFM[a]
Picea abies sapwood	-	HFM[a]
polygalacturonic acid	25990-10-7	Sigma
Quercus robur	-	HFM[a]
rhamnogalacturonan	-	Megazyme (potato)
L-rhamnose	10030-85-0	TCI R0013
ribose	50-69-1	TCI R0025
Robinia pseudoacacia heartwood	-	HFM[a]
Robinia pseudoacacia sapwood	-	HFM[a]
sorbose	87-79-6	Calbiochem L(-) 99.6%
sucrose	57-50-1	Sigma
switchgrass	-	EBI[b]
trehalose	6138-23-4	Acros D 99%
wing nut	-	in house (EBI,
xylan	9014-63-5	Sigma from beechwood
xyloglucan	37294-28-3	Megazyme (from tamarind)
D-xylose	58-86-6	Acros Organics 225990050

[a] Holzforschung München, Munich, Germany; [b] Energy Biosciences Institute, Berkeley, USA

Table 5-5: List of used chemicals.

name	order number	manufacturer
acetic acid 100%	3738	Carl Roth (Karlsruhe, Germany)
agar-agar, Kobe I	5210	Carl Roth (Karlsruhe, Germany)
agar-agar, bacteriological	2266	Carl Roth (Karlsruhe, Germany)
agarose	AG02	Nippon Genetics Europe (Dueren, Germany)
ammonium chloride	5470	Carl Roth (Karlsruhe, Germany)
ammonium iron(II) sulfate hexahydrate	P728	Carl Roth (Karlsruhe, Germany)

ammonium nitrate	K299	Carl Roth (Karlsruhe, Germany)
ammonium sulfate	5606	Carl Roth (Karlsruhe, Germany)
Ampicillin sodium salt	HP62	Carl Roth (Karlsruhe, Germany)

Table 5-5: List of used chemicals (continued).

name	order number	manufacturer
D-biotin	3822	Carl Roth (Karlsruhe, Germany)
boric acid	6943	Carl Roth (Karlsruhe, Germany)
bovine serum albumin (BSA) fraction V	8076	Carl Roth (Karlsruhe, Germany)
Bromophenol Blue	B0126	Merck (Darmstadt, Germany)
calcium chloride dihydrate	5239	Carl Roth (Karlsruhe, Germany)
citric acid monohydrate	20276	VWR (Radnor, USA)
copper (II) sulfate pentahydrate	23174	VWR (Radnor, USA)
Cyclosporin A	100507	VWR (Radnor, USA)
di-potassium phosphate	P749	Carl Roth (Karlsruhe, Germany)
di-sodium phosphate	4984	Carl Roth (Karlsruhe, Germany)
ethylenediaminetetraacetic acid (EDTA) disodium salt dihydrate	X986	Carl Roth (Karlsruhe, Germany)
ethanol >96%	T171	Carl Roth (Karlsruhe, Germany)
ethanol >99%	9065	Carl Roth (Karlsruhe, Germany)
Ficoll 400	F2637	Merck (Darmstadt, Germany)
D-fructose	4981	Carl Roth (Karlsruhe, Germany)
glycerol	3783	Carl Roth (Karlsruhe, Germany)
L-histidine	H5659	Merck (Darmstadt, Germany)
hydrochloric acid	4625	Carl Roth (Karlsruhe, Germany)
4-hydroxybenzhydrazide	H-9882	Megazyme (Bray, Ireland)
Hygromycin B Gold	ant-hg-1	Thermo Fisher Scientific (Waltham, USA)
Kanamycin sulfate	T832	Carl Roth (Karlsruhe, Germany)
magnesium chloride hexahydrate	M2670	Merck (Darmstadt, Germany)
magnesium sulfate heptahydrate	P027	Carl Roth (Karlsruhe, Germany)
manganese (II) sulfate monohydrate	25303	VWR (Radnor, USA)
potassium acetate	T874	Carl Roth (Karlsruhe, Germany)
potassium chloride	P9333	Merck (Darmstadt, Germany)
potassium dihydrogen phosphate	3904	Carl Roth (Karlsruhe, Germany)
potassium nitrate	P021.1	Carl Roth (Karlsruhe, Germany)
2-propanol	6752	Carl Roth (Karlsruhe, Germany)
Roti-phenol/chloroform/isoamyl-mix	A156	Carl Roth (Karlsruhe, Germany)
Roti-Quant 5x	K015	Carl Roth (Karlsruhe, Germany)
ruthenium red	R2751	Merck (Darmstadt, Germany)
sodium acetate anhydrous	6773	Carl Roth (Karlsruhe, Germany)
sodium chloride	3957	Carl Roth (Karlsruhe, Germany)
sodium phosphate dibasic	T879	Carl Roth (Karlsruhe, Germany)
sodium hydroxide solution 50%	87938290	VWR (Radnor, USA)
sodium molybdate dihydrate	0274	Carl Roth (Karlsruhe, Germany)
sodium nitrate	A136	Carl Roth (Karlsruhe, Germany)
sodium sulfate decahydrate	T108	Carl Roth (Karlsruhe, Germany)
sodium thiosulfate anhydrous	APPCA6830	VWR (Radnor, USA)
D-sorbitol	S6021	Merck (Darmstadt, Germany)
L-sorbose	4028	Carl Roth (Karlsruhe, Germany)

sulfuric acid 96%	4623	Carl Roth (Karlsruhe, Germany)
trifluoroacetic acid (TFA)	T6508	Merck (Darmstadt, Germany)
Tris(hydroxymethyl)-aminomethane	AE15	Carl Roth (Karlsruhe, Germany)

Table 5-5: List of used chemicals (continued).

name	order number	manufacturer
trisodium citrate dihydrate	3580	Carl Roth (Karlsruhe, Germany)
Triton X-100	T8787	Merck (Darmstadt, Germany)
tryptone/peptone from casein	8952	Carl Roth (Karlsruhe, Germany)
Tween 20	P9416	Merck (Darmstadt, Germany)
Xylene Cyanol FF	X4126	Merck (Darmstadt, Germany)
yeast extract	2363	Carl Roth (Karlsruhe, Germany)
Zeocin	ant-zn-1	Thermo Fisher Scientific (Waltham, USA)
zinc sulfate heptahydrate	29253236	VWR (Radnor, USA)

Table 5-6: List of used consumables and kits.

name	order number	manufacturer
100 bp Quick-Load DNA ladder	N0467	New England Biolabs (Ipswich, USA)
24 deep well plate	742926	Biozym (Hessisch Oldendorf, Germany)
CarboPac PA20 analytical column for HPAEC-PAD	60142	Thermo Fisher Scientific (Waltham, USA)
CarboPac PA200 column for HPAEC-PAD	62895	Thermo Fisher Scientific (Waltham, USA)
Deoxynucleotide solution set	N0447	New England Biolabs (Ipswich, USA)
DNA ladder 1 kb	N3232	New England Biolabs (Ipswich, USA)
DNase I (RNase-Free)	M0303	New England Biolabs (Ipswich, USA)
DpnI restriction enzyme	R0176	New England Biolabs (Ipswich, USA)
ELISA 96 well micro test plate, F	82.1581	Sarstedt (Nümbrecht, Germany)
Filtropur BT 50, 0.2 µm filter	83.1823.101	Sarstedt (Nümbrecht, Germany)
GeneJet RNA Purification Kit	K0731	Thermo Fisher Scientific (Waltham, USA)
glass fiber filter 1	5056823	Schubert & Weiss Omnilab (Marktoberdorf, Germany)
High Capacity cDNA Reverse Transcription Kit	10400745	Thermo Fisher Scientific (Waltham, USA)
Hi-Yield Plasmid Mini Prep DNA Isolierungskit	30 HYDF100	Süd-Laborbedarf Gauting (Gauting, Germany)
Midori Green Advance	MG04	Nippon Genetics Europe (Dueren, Germany)
MiSeq Reagent Kit v3	MS-102-3001	Illumina (San Diego, USA)
NotI restriction enzyme	R3189	New England Biolabs (Ipswich, USA)

One Taq DNA polymerase	M0480	New England Biolabs (Ipswich, USA)
PacI restriction enzyme	R0547	New England Biolabs (Ipswich, USA)

Table 5-6: List of used consumables and kits (continued).

name	order number	manufacturer
PeqGOLD Trifast DNA/RNA/protein-purification kit	30-2010DE	VWR (Radnor, USA)
Phusion High-Fidelity PCR Kit	E0553	New England Biolabs (Ipswich, USA)
qPCRBIO SyGreen Mix Separate-ROX	PB20. 14	Nippon Genetics Europe (Dueren, Germany)
quartz cuvette, 10 mm layer thickness	Z276650	Merck (Darmstadt, Germany)
Qubit dsDNA BR Assay Kit	Q32850	Thermo Fisher Scientific (Waltham, USA)
SbfI restriction enzyme	R3642	New England Biolabs (Ipswich, USA)
Sealing Film, for 96 and 384 Well Microplates	CORNBF400S	Schubert & Weiss Omnilab (Marktoberdorf, Germany)
syringe filter 0.2 µm Filtropur S	83.1826.001	Sarstedt (Nümbrecht, Germany)
syringe filter Millex 5 µM	10054850	Thermo Fisher Scientific (Waltham, USA)
T4 DNA Ligase	M0202	New England Biolabs (Ipswich, USA)
TruSeq RNA Single Indexes Set A and B	20020492 and 20020493	Illumina (San Diego, USA)
TruSeq Stranded Total RNA Prep kit	20020596	Illumina (San Diego, USA)
Viscozyme L	V2010	Merck (Darmstadt, Germany)
Vivaspin 20 centrifugal concentrators, 10 kDa	Z614602	Merck (Darmstadt, Germany)
Wizard SV Gel and PCR Clean-up System	A9281	Promega (Fitchburg, USA)
Zero Blunt cloning Kit	440302	Thermo Fisher Scientific (Waltham, USA)
Zirkonium beads (Ø = 0.5 mm)	24 D1132-05	Süd-Laborbedarf Gauting (Gauting, Germany)

5.1.3. Media and solutions

Substances used in media and solutions were dissolved in double distilled water (ddH_2O) and *N. crassa* was incubated in 1x Vogel's solution plus either 2 mM monosaccharides or 1% polysaccharides, if not stated otherwise. Uptake solutions were a mixture of 1x Vogel's solution plus 100 µM monosaccharide, modifications of this composition are described in the respective experiments.

Table 5-7: List of used media and solutions.

name	substances	concentration
D-biotin stock solution	D-biotin	0.1 mg/ml
	filter sterilize	
trace elements stock solution	citric acid monohydrate	60.0 mM
	zinc sulfate heptahydrate	42.0 mM
	ammonium iron(II) sulfate hexahydrate	6.5 mM
	copper (II) sulfate pentahydrate	2.5 mM
	manganese (II) sulfate monohydrate	0.75 mM
	boric acid	2.0 mM
	sodium molybdate dihydrate	0.52 mM
	filter sterilize	
50x Vogel's solution (Vogel, 1956)	trisodium citrate dihydrate	0.43 M
	potassium dihydrogen phosphate	1.84 M
	ammonium nitrate	1.25 M
	magnesium sulfate heptahydrate	40.0 mM
	calcium chloride dihydrate (pre-dissolve in water)	34.0 mM
	D-biotin stock solution (0.1 mg/ml)	0.25% (v/v)
	trace elements stock solution	0.50% (v/v)
Vogel's Minimal Medium (MM)	sucrose	2.0% (w/v)
	50x Vogel's solution	2.0% (v/v)
	agar-agar (only solid medium)	1.5% (w/v)
10x FIGS solution	L-sorbose	20.0% (w/v)
	D-fructose	0.5% (w/v)
	D-glucose	0.5% (w/v)
	filter sterilize	
bottom agar (BA)	50x Vogel's solution	2.0% (v/v)
	agar-agar (only solid medium)	1.5% (w/v)
	autoclave, then add 10x FIGS solution	10.0% (v/v)
top agar (TA)	50x Vogel's solution	2.0% (v/v)
	agar-agar (only solid medium)	1.0% (w/v)
	autoclave, then add 10x FIGS solution	10.0% (v/v)

Table 5-7: List of used media and solutions (continued).

name	substances	concentration
modified 50x Vogel's solution (for RNA-Seq samples)	trisodium citrate dihydrate pH 6.0 (pre-dissolve in water)	2.43 M
	potassium dihydrogen phosphate	1.84 M
	ammonium sulfate (pre-dissolve in water)	1.25 M
	magnesium sulfate heptahydrate	40.0 mM
	calcium chloride dihydrate (pre-dissolve in water)	34.0 mM
	D-biotin stock solution (0.1 mg/ml)	0.25% (v/v)
	trace elements stock solution	0.50% (v/v)
2x Westergaard's solution (Westergaard and Mitchell, 1947)	potassium nitrate	0.2% (w/v)
	di-potassium phosphate	0.14% (w/v)
	potassium dihydrogen phosphate	0.1% (w/v)
	magnesium sulfate heptahydrate	0.1% (w/v)
	sodium chloride	0.02% (w/v)
	calcium chloride dihydrate (pre-dissolve in water)	0.02% (w/v)
	D-biotin stock solution (0.1 mg/ml)	0.01% (v/v)
	trace elements stock solution	0.02% (v/v)
	filter sterilize	
Westergaard's medium (WGM)	2x Westergaard's solution	50.0% (v/v)
	sucrose	1.5% (w/v)
	agar-agar	2.0% (w/v)
Lysogeny Broth (LB) Medium (Bertani, 1951)	yeast extract	0.5% (w/v)
	tryptone/peptone	1.0% (w/v)
	sodium chloride	1.0% (w/v)
	agar-agar (only solid medium)	1.5% (w/v)
LB low salt medium (Bertani, 1951)	yeast extract	0.5% (w/v)
	tryptone/peptone	1.0% (w/v)
	sodium chloride	0.5% (w/v)
	agar-agar (only solid medium)	1.5% (w/v)
super optimal broth with catabolite repression (SOC) medium (Hanahan, 1983)	yeast extract	0.5% (w/v)
	tryptone/peptone	2.0% (w/v)
	sodium chloride	10.0 mM
	potassium chloride	2.5 mM
	magnesium chloride	10.0 mM
	magnesium sulfate monohydrate	10.0 mM
	set pH to 7.0 and autoclave	
	D-glucose	20.0 mM
plasmid DNA medium (PDM) (Danquah and Forde, 2007)	yeast extract	0.44% (w/v)
	tryptone/peptone	0.79% (w/v)
	ammonium chloride	0.05% (w/v)
	magnesium sulfate heptahydrate	0.05% (w/v)
	di-sodium phosphate	0.68% (w/v)
	potassium dihydrogen phosphate	0.3% (w/v)
	autoclave	
	D-glucose	5.0% (wV)

Table 5-7: List of used media and solutions (continued).

name	substances	concentration
5x Taq buffer	Tris HCl pH 8.5	0.25 M
	sodium chloride	0.1 M
	magnesium chloride hexahydrate	10.0 mM
	Ficoll 400	12.5% (w/v)
	BSA	0.25% (w/v)
	Xylene Cyanol FF	0.1% (w/v)
50x Tris Acetate EDTA (TAE) stock solution	Tris	2.0 M
	acetic acid 100%	1.0 M
	EDTA disodium salt dihydrate	50.0 mM
buffer citrate phosphate (BCP)	citric acid monohydrate	50.0 mM
	set pH to 5.0 with sodium phosphate dibasic	
	PGA (only endo-polygalacturonase substrate)	5.0 mg/ml
pectate lyase (PL) substrate buffer	Tris HCL pH 8.0	42.0 mM
	calcium chloride dihydrate	1.0 mM
	PGA	1.0 mg/ml
PAHBAH reagent A	4-hydroxybenzhydrazide	32.9 mM
	hydrochloric acid	72.3 mM
PAHBAH reagent B	trisodium citrate dihydrate	42.3 mM
	calcium chloride dihydrate	7.5 mM
	sodium hydroxide	0.5 M
gDNA extraction lysis buffer	sodium hydroxide	50.0 mM
	EDTA disodium salt dihydrate	1.0 mM
	Triton X-100	1.0% (v/v)

Table 5-8: List of used additives and supplements.
All additives and supplements were sterile filtered.

name	substances	concentration
1000x Ampicillin stock solution	Ampicillin sodium salt	100 mg/ml
1000x Cyclosporin A stock solution	Cyclosporin A	5 mg/ml
100x histidine stock solution	L-histidine	20 mg/ml
500x Hygromycin B stock solution	Hygromycin B Gold	200 mg/ml
1000x Kanamycin stock solution	Kanamycin sulfate	30 mg/ml
1000x Zeocin stock solution	Zeocin	25 mg/ml

5.1.4. Primers and plasmids

Table 5-9: List of used cloning and quantitative real-time PCR (RT-qPCR) primers.
Restriction sites are marked in red and with boldface letters. Primers used for advanced quick assembly (AQUA) cloning have a 16 bp overlap to the neighboring DNA fragments. These overlaps are written in lower case letters. The oligonucleotides were bought from Eurofins Genomics (Ebersberg, Germany).

amplified fragment	name	sequence	Tm
pdr-1 promoter (Ppdr1), full-length *pdr-1* (from gDNA) and *pdr-1* terminator Tpdr1	p9033-fwd-NotI	AT**GCGGCCGC**AGGCCGACGTGCCCTTCC	72.0 °C
	t9033-rev-NotI	AT**GCGGCCGC**ATGCTTATGCCTATGCCTGCC	70.9 °C
full-length *pdr-1* (from gDNA)	NCU09033-fwd-NotI	AT**GCGGCCGC**ATGGCTGCTGCTGCTTCCG	72.0 °C
	NCU09033-rev-PacI	GC**TTAATTAA**ATCGGATGCAAACCACCCTC	60.5 °C
full-length *gh28-1* (from gDNA)	2369_CSR-GPD_F	ATTA**CCTGCAGG**ATGAAAATCACCGCCTCTCTTTTGC	66.1 °C
	2369_CSR-GPD_R	ATCA**TTAATTAA**CTAACACCACGCGCCCGA	62.2 °C
full-length *pdr-1* (from gDNA) with overlap to pCCG-C-Gly-GFP	pdr1gfp_AQUA_fragment_F	catcaaccaaatctagATGGCTGCTGCTGCTTCCGG	67.9 °C
	pdr1gfp_AQUA_fragment_R	ccttaattaacccgggAAGAGTCGCCCCAGCGCCTTC	70.8 °C
full-length pCCG-C-Gly-GFP with overlap to *pdr-1*	pdr1gfp_AQUA_vector_F	cgctggggcgactcttCCCGGGTTAATTAAGGGCGGA	72.0 °C
	pdr1gfp_AQUA_vector_R	aagcagcagcagccatCTAGATTTGGTTGATGTGAGGGG	69.0 °C
pdr-1 DNA binding domain (BD) and dimerization domain (DD) from gDNA with 5' overlap to pCCG-C-Gly-HAT-FLAG and 3' overlap to *clr-2* activation domain (AD)	pdr1-BD_F	catcaaccaaatctagATGGCTGCTGCTGCTTCCGG	67.9 °C
	pdr1-BD-DD_R	cgagtgtcttgcgcgaGCCTGCTCTGAGGCCGGGC	72.0 °C
clr-2 activation domain (AD) from gDNA with 5' overlap to *pdr-1* DD and 3' overlap to pCCG-C-Gly-HAT-FLAG	clr2-TF_F	cggcctcagagcaggcTCGCGCAAGACACTCGAAGC	72.0 °C
	clr2-TF_R	tagaagtggcgcctacTCAGTAGGTGTACCCATCCATACCTC	68.7 °C
full-length pCCG-C-Gly-HAT-FLAG with 5' overlap to *pdr-1* BD and 3' overlap to *clr-2* AD	pCCG-pdr1+clr2_F	tgggtacacctactgaGTAGGCGCCACTTCTAAATAAGC	66.7 °C
	pCCG-pdr1+clr2_R	aagcagcagcagccatCTAGATTTGGTTGATGTGAGGG	68.1 °C

Table 5-9: List of used cloning and quantitative real-time PCR (RT-qPCR) primers (continued).

amplified fragment	name	sequence	Tm
short fragment of NCU04173 near the 3' end of the gene	qPCR_actin_fwd2	CATCGACAATGGTTCGGGTATGTG	58.0 °C
	qPCR_actin_rev2	CCCATACCGATCATGATACCATGATG	56.9 °C
short fragment of *pdr-1* near the 3' end of the gene	qPCR9033_F1	CCAAGTGTGGAGAGCAAGTTGTA	56.8 °C
	qPCR9033_R1	ACAGTCGTGTGCGAGTACAAAGA	58.4 °C
short fragment of *gh28-1* near the 3' end of the gene	qPCR2369_F	TCGTCCTCCTGCACCTTCAG	57.9 °C
	qPCR2369_R	GATCTCTTGGCAGGAGCTGTGT	58.4 °C
short fragment of NCU09034 near the 3' end of the gene	qPCR9034_F	CGACAGCGGACCTTAATAAGCC	56.7 °C
	qPCR9034_R	TAAGCACTAGGAATCAACTTTGCCC	57.1 °C
short fragment of NCU05897 near the 3' end of the gene	fucP_qPCR_F	CCTGTGATGCCTTTACTACGG	54.8 °C
	fucP_qPCR_R	GACCGACTTGGAAACAACAC	53.8 °C

Table 5-10: List of used plasmids.

name	features	plasmid map ref.
pCCG-C-Gly-GFP	5' and 3' flank of *his-3* gene, *ccg-1* promoter, MCS, GFP, *adh-1* terminator and Ampicillin resistance	SFigure 6-10, page 166
pCCG-C-Gly-HAT-FLAG	5' and 3' flank of *his-3* gene, *ccg-1* promoter, MCS, histidine affinity tag (HAT) and FLAG tag, *adh-1* terminator and Ampicillin resistance	SFigure 6-11, page 167
pCSR-knock-in	5' and 3' flank of *csr-1* gene, MCS and Ampicillin resistance	SFigure 6-12, page 168
pTSL126B	5' and 3' flank of *csr-1* gene, *gpd-3* promoter, MCS, *trpC* terminator and Ampicillin resistance	SFigure 6-13, page 169

5.1.5. *N. crassa* and *E. coli* strains

Table 5-11: List of used *N. crassa* and *E. coli* strains.

The *N. crassa* wild-type (WT) reference strain was OR74A (Colot *et al.*, 2006). The *N. crassa* deletion strains used in this work were obtained from the Fungal Genetics Stock Center (FGSC; http://www.fgsc.net/) (McCluskey *et al.*, 2010).

#[a]	name	genotype	origin
1	WT	oak ridge (OR) 74, *mat A*	FGSC #2489
3	PC2	*his-3::Pccg-1-clr-2 rid-1* Δ*sad-1*; Δ*clr-2*, *mat A*	EBI[b], Glass lab (Coradetti *et al.*, 2013)
16	Δ*pdr-1*, his-	Δ*NCU09033::hph, his3*$^{-}$, *mat a*	EBI[b], Glass lab

[a] Wood Bioprocesses *N. crassa* glycerol stock number; [b] Energy Biosciences Institute, Berkeley, USA; [c] Technical University Munich

Table 5-11: List of used *N. crassa* and *E. coli* strains (continued).

#[a]	name	genotype	origin
17	Δ*pdr-1*	ΔNCU09033*::hph*, *mat A*	FGSC #11390
18	Δ*pdr-2*	ΔNCU04295*::hph*, *mat a*	FGSC #18855
22	WT, *his*$^{-}$	*his-3*$^{-}$, *mat A*	FGSC #6103
23	*pdr-1-comp*	Δ*pdr-1::hph*, *csr-1-::Ppdr1-pdr-1*, *mat a*	this study
25	Δ*frt-1*	ΔNCU05897*::hph*, *mat A*	FGSC #13717
53	*pdr-1-oex*	Δ*pdr-1::hph*, *csr-1::Pgpd1-pdr-1*, *mat a*	this study
65	Δ*gh28-1*	ΔNCU02369*::hph*, *mat a*	FGSC #10763
68	Δ*cre-1*	ΔNCU08807::hph, *mat a*	FGSC #18633
69	*gh28-1-comp*	Δ*gh28-1::hph*, *csr1::Pgpd1-gh28-1*, *mat A*	this study
90	*gh28-1-oex*	Δ*pdr-1::hph*, *csr1::Pgpd1-gh28-1*, *mat a*	this study
92	Δ*ara-1*	ΔNCU05414*::hph*, *mat A*	FGSC #21219
124	*pdr-1-gfp*	*his3::Pccg1-pdr-1-gfp*, *mat A*	this study
125	Δ*frp-1*	ΔNCU09899*::hph*, *mat a*	FGSC #19860
174	Δ*pdr-1*/Δ*pdr-2*	Δ*pdr-1::hph*, Δ*pdr-2::hph*	this study
181	Δ*col-26*	ΔNCU07788*::hph*, *mat A*	FGSC #11031
194	Δ*frp-1*/Δcol-26	Δ*frp-1::hph*, Δ*col-26::hph*	this study
201	Δ*frp-1*/Δ*cre-1*	Δ*frp-1::hph*, Δ*cre-1::hph*	this study
-	*E. coli* DH5α	F– Φ80l*acZ*ΔM15 Δ(*lacZYA-argF*) U169 *recA1 endA1 hsdR17* (rK–, mK+) *phoA supE44* λ– *thi-1gyrA96 relA1*	Thermo Fisher Scientific (Waltham, USA)

[a] Wood Bioprocesses *N. crassa* glycerol stock number; [b] Energy Biosciences Institute, Berkeley, USA; [c] Technical University Munich

5.2. Physiological methods

All experiments including *N. crassa* strains or culture supernatants were performed in biological triplicates, if not stated otherwise.

5.2.1. Pectin sterilization

Pectin could not be autoclaved and was sterilized with the following method. Three to five grams of pectin were suspended in 10 ml of 70% (v/v) ethanol in an autoclaved beaker and stirred for 16 h at 400 rpm and 65 °C. The sterilized pectin was ball-milled after the ethanol had evaporated.

5.2.2. *N. crassa* propagation

N. crassa conidia were transferred with a wood applicator from glycerol stocks or from previously growing *N. crassa* strains to slanted tubes containing 2 ml solid Vogel's Minimal Medium (MM) (Vogel, 1956). They were incubated for 2 d at 30 C and without light. Afterwards, the tubes were placed in the 25 °C light incubator, where they were incubated for additional 5 to 8 d. The 7 to 10 d old conidia of these cultures were harvested by adding 1 ml ddH_2O to the slant, vortexing it vigorously and transferring the conidia suspension to a 1.5 ml reaction tube. The tubes were centrifuged at 1000 rpm for 1 min and the supernatant was removed. The conidia were then re-suspended in 0.5 ml ddH_2O and could be used to create new glycerol stocks, start assays or extract gDNA.

5.2.3. Glycerol stocks

N. crassa glycerol stocks were created by mixing 700 µl of a conidia suspension with 300 µl of a sterile filtered 70% (v/v) glycerol solution. The glycerol-conidia mixture was quickly vortexed and then frozen in liquid nitrogen. The glycerol suspension was stored at -80 °C.

5.2.4. Growth assays

Direct incubation of conidia

Ten day old *N. crassa* conidia were inoculated in a concentration of 1 x 10^6 conidia/ml in 1x Vogel's solution plus 1% (w/v) polysaccharide, if not stated otherwise. The conidia concentration was determined with the Tecan plate reader by measuring the OD_{600} of the conidia suspension. The equation $V_{conidia\ suspension} = \frac{0.0123}{OD_{600} \times dilution} \times V_{total}$ was used to determine the volume of conidia suspension that is necessary to achieve the desired concentration. The constant 0.0123

was determined by cell counting with a hemocytometer and correlating a standard series of cell counts with measured OD_{600}. The following volumes were used as V_{total}: 200 µl medium in 96 well plates, 3 ml medium in 24 deep well plates, 20 ml medium in 100 ml flasks and 50 ml in 250 ml flasks.

The *N. crassa* strains were incubated for 7 d (Avicel, PGA and AG) or 4 d (other carbon sources) at 25 °C, 200 rpm and constant light. Biomass and culture supernatants were harvested afterwards for further analysis.

Medium switch cultures

Cultures of *N. crassa* used for enzymatic activity assays, uptake assays, compositional analysis, RT-qPCR or RNA-Seq experiments were pre-incubated in MM before their incubation/induction in the final carbon source. Similar to the directly incubated strains, 1 x 10^6 10 d old conidia/ml were inoculated and incubated for 16 h at 25 °C, 200 rpm and constant light. Changes to the experimental setup are described in the results sections where they apply. The *N. crassa* strains were washed three times in 1x Vogel's NoC for 10 min after the initial incubation period and then transferred to the target carbon sources.

Strains used for enzymatic activity assays or compositional analysis were grown for another 2 d to 4 d in 0.2% to 1% (w/v) of carbon source, if not stated otherwise, and their biomass and culture supernatants were collected afterwards.

To obtain the mycelial biomass or culture supernatant for uptake assays, RT-qPCR samples and RNA-Seq experiments, the *N. crassa* strains were induced for 4 h or 16 h in the target carbon sources (see pages 134, 138 and 140 for more details).

Feeding cultures

When monosaccharides were used as carbon source for *N. crassa*, the strains were pre-incubated on MM, washed and transferred to a new carbon source as described in the previous section. The transferred mycelium was incubated at 25 °C, 200 rpm and constant light in 24 deep well plates containing 3 ml 1x Vogel's solution plus 2 mM monosaccharide(s). The medium was replaced two times per day with new 1x Vogel's plus 2 mM monosaccharide(s) and the strains were incubated for additional 2 to 3 days. Afterwards, culture supernatants and biomass were collected for further analysis.

5.2.5. Mycelial dry weight

Biomass from *N. crassa* strains grown in 24 deep well plates was harvested after incubation, washed once with ddH_2O and excess liquid was removed by shortly dipping the mycelium on tissue. Following this step, the biomass was transferred to pre-weighted aluminum pans

and dried for 16 h at 105 °C. The dried biomass was weighted again and the difference between both measurements was calculated.

5.2.6. Microconidia isolation

N. crassa macroconidia were transformed, as described in 5.3.8 (page 132), to create some of the strains used in this work. The transformed strains were heterokaryotic after the transformation process, if histidine prototrophy was used as selection marker.

To create homokaryotic strains carrying the altered genome, the respective strains were grown on 1x Vogel's solution with 2% agar-agar for 3 d in a humidity chamber at 30 °C without light. After the incubation period, the plates were removed from the humidity chamber and incubated additional 5 d to 7 d at RT and daylight. A volume of 2 ml ddH_2O was added unto the mycelium on the plates and carefully scraped with a pipette tip to remove most of the formed (micro-)conidia. The conidia suspension was transferred into a 1.5 ml reaction tube and filtered through a 5 µm filter. The suspension was centrifuged for 5 min at 13,000 rpm and the supernatant was removed. 100 µl ddH_2O was added to the microconidia, the pellet was resuspended, and a new plate was inoculated with the spore suspension. The suspension was spread evenly on the plate and incubated for 16 h at 30 °C without light. Afterwards, germinating hyphae were picked under the stereo microscope and transferred into tubes containing 2 ml slanted MM. They were incubated as described in 5.2.2 (page 124) and their genotype was confirmed by selection or genotyping PCR (page 128) of gDNA extracted from conidia (page 133).

5.2.7. Crossing of *N. crassa* strains

To create *N. crassa* strains carrying a double gene deletion, strains with a single gene deletion were crossed. One of the crossing partners was used as female crossing partner and inoculated on a WGM plate. The strain was incubated for 2 d at 30 °C without light and then transferred to 25 °C with daylight. After additional incubation over 9 d to 14 d, protoperithecia formation was confirmed with the stereo microscope. The male crossing partner, carrying another gene deletion and the opposite mating type allele, was incubated as described in 5.2.2 (page 124). After 7 d to 10 d incubation, the conidia of the male crossing partner were harvested by adding 1 ml ddH_2O to the slanted tube and vortexing it vigorously. Then, 200 µl of the conidia suspension was pipetted on the WGM plate with the protoperithecia showing female crossing partner and dispersed equally by moving the liquid gentle with a pipette tip.

The crossed strains were incubated for additional 10 d to 20 d, until the perithecia had formed and the ascospores were disseminated. The ascospores were harvested by

dropping 2 ml ddH_2O on the petri dish cover and transferring the ascospore suspension into a 1.5 ml reaction tube. The spores were stored at 4 °C.

An amount of 250 to 500 ascospores were plated on a MM plate (with fitting selection supplements, e.g. Hygromycin) and incubated 16 h at RT. Germinated ascospores were picked under the stereo microscope, transferred to a tube containing 2 ml of slanted MM plus selection supplements and incubated as described in 5.2.2 (page 124). The genotype of the crossed strains was confirmed by selection, and genotyping PCR (page 128) of gDNA extracted from conidia (page 133).

5.2.8. Protein localization by cLSM and intensity measurements

The cellular localization of the *PDR-1* TF was determined using a GFP tagged *PDR-1* variant. Glass slides with a ~1 mm thick layer of 2% (w/v) agar–agar in ddH_2O were inoculated with conidia of the *N. crassa pdr-1-gfp* strain and 1x Vogel's solution plus either 2% glycerol or 2% glycerol and 2 mM rha was added on these slides before they were incubated for 3 h. After the incubation period, the slides were covered with cover slips and GFP fluorescence images were made using a Leica TCS SP5 System. The laser excitation was set to 488 nm and emission was detected at 510 nm. Brightfield and fluorescence images were made using the LAS AF software and the fluorescence intensity of several nuclei per image and their surrounding cytoplasm was measured with the ImageJ software. Six to ten images of each condition were randomly picked for analysis. A background correction was performed by measuring hyphae free spaces on each image and subtracting the measured mean intensity of these areas from all other results.

5.3. Molecular biological methods

5.3.1. Phusion PCR

Phusion DNA polymerase was used for fragment amplification of cloning experiments. The PCR mixtures and thermocycler runs were prepared and performed as described by the manufacturer. Table 5-12 list the components and concentrations of the PCR reaction buffer and Table 5-13 shows the used thermocycler program.

Table 5-12: Phusion DNA polymerase PCR reaction buffer.

component	volume	final concentration
ddH_2O	33.0 µl	-
5x Phusion HF buffer	10.0 µl	1x
10 mM dNTPs	1.0 µl	200.0 µM
10 µM forward primer	2.5 µl	0.5 µM
10 µM reverse primer	2.5 µl	0.5 µM
template DNA	1.0 µl	500 ng gDNA or 0.5 ng plasmid DNA
Phusion DNA polymerase	0.5 µl	1.0 unit

Table 5-13: Phusion DAN polymerase PCR thermocycler program.

step	temperature	time	cylces
initial denaturation	98.0 °C	30 s	-
denaturation	98.0 °C	10 s	35x
annealing	lowest Tm of primer pair + 2 °C	30 s	
elongation	72.0 °C	30 s per kb	
final elongation	72.0 °C	7 min	-
hold	16.0 °C	unlimited	-

5.3.2. Taq PCR

Genotyping and colony PCRs were performed with Taq DNA Polymerase. The PCR reaction buffer and respective thermocycler program are described in Table 5-14 and Table 5-15.

Table 5-14: Taq DNA polymerase PCR reaction buffer.

component	volume	final concentration
ddH_2O	8.5 µl	-
5x Phusion HF buffer	3.0 µl	1x
10 mM dNTPs	0.3 µl	200.0 µM
10 µM forward primer	1.0 µl	0.7 µM
10 µM reverse primer	1.0 µl	0.7 µM
template DNA	1.0 µl	500 ng gDNA or 0.5 ng plasmid DNA
Taq DNA polymerase	0.2 µl	1.0 unit

Table 5-15: Taq DAN polymerase PCR thermocycler program.

step	temperature	time	cylces
initial denaturation	95.0 °C	5 min	-
denaturation	95.0 °C	30 s	35x
annealing	lowest Tm of primer pair in °C	30 s	
elongation	72.0 °C	1 min per kb	
final elongation	72.0 °C	7 min	-
hold	16.0 °C	unlimited	-

5.3.3. Agarose gels

PCR products and plasmid digests were analyzed by size exclusion chromatography using agarose gels. 1x TAE buffer was mixed with 1% agarose to differentiate DNA with lengths between 300 and 10,000 bp, while 1x TAE plus 2% agarose was used to run DNA fragments with sizes below 500 bp. The gel was placed in a running chamber filled with 1x TAE and the run was performed at 140 V and ~50 mA for 36 min.

5.3.4. DNA gel extraction and purification

DNA fragments used for cloning experiments were differentiated by size through agarose gels. After the gel run was performed, the bands were excised with a sterile scalpel and moved into a pre-weighted 1.5 ml reaction tube. These tubes were weighted again, and the mass difference was calculated. Based on the mass of the extracted gel slice, the DNA purification was performed. The Promega Wizard SV Gel and PCR Clean-up System was used for this step and the process was performed according to the manufacturer's instructions.

5.3.5. *N. crassa* expression cassette cloning

N. crassa expression cassettes were assembled either *in vitro* by restriction-ligation experiments or *in vivo* by using AQUA cloning (Beyer *et al.*, 2015). The *in vitro* assembled cassettes were cloned into *E. coli* plasmids and transformed into *E. coli* DH5α strains, as described in 5.3.6 (page 131) for plasmid propagation. Fragments of *in vivo* assembled expression cassettes were directly transformed into *E. coli* DH5α. Both cloning methods are briefly described below.

Restriction-ligation cloning

The expression cassettes used in the *N. crassa* strains *pdr-1-comp*, *pdr-1-oex*, *gh28-1-comp* and *gh28-1-oex* were created using restriction-ligation cloning. The *pdr-1* gene was amplified from gDNA using the primers NCU09033-fwd-NotI and NCU09033-Rev-PacI (Table 5-9) and the resulting fragment as well as the vector pTSL126B (SFigure 6-13) were digested for 16 h at 37 °C with the restriction enzymes NotI and PacI. The restriction digest reaction mix is described in Table 5-16: Restriction digest reaction mix.. Afterwards, both digested fragment and vector were purified according to 5.3.4 and ligated with T4 DNA ligase with the reaction mix described in Table 5-17 for 30 min to 1 h at RT.

Table 5-16: Restriction digest reaction mix.

component	volume or concentration
10x Cutsmart reaction buffer	5 µl
restriction enzyme 1	2 units
restriction enzyme 2	2 units
template DNA	up to 2 µg
ddH_2O	fill up to 50 µl

Table 5-17: T4 DNA ligase reaction mix.

component	volume or concentration
10x T4 DNA ligase buffer	1 µl
digested DNA fragment (insert)	3-5x the equimolar mass of used plasmid
digested plasmid (vector)	50 ng
T4 DNA ligase	5 units
ddH_2O	fill up to 10 µl

The insert:vector ratio and the resulting mass used for the DNA fragment (m_{insert}) was calculated as follows:

$$m_{insert} = \frac{m_{vector} \times l_{insert} \times Y}{l_{vector}}$$

Whereas l_{insert} and l_{vector} refer to the length of the fragment and vector in bp, respectively, and Y is a constant that stands for the concentration factor of the insert to vector ration (usually 3 to 5). m_{vector} describes the mass used in the ligation reaction (50 ng). The ligated and transformed plasmid vector was used to create the strain *pdr-1-oex*.

The *pdr-1* promoter, gene and terminator were amplified with the primers p9033-fwd-NotI and t9033-rev-NotI (Table 5-9) from gDNA. The PCR product and the plasmid pCSR-knock-in (SFigure 6-12) were restriction digested with NotI and ligated as described above. After ligation and transformation, the resulting plasmid vector was used to create the strain *pdr-1-comp*.

Similarly, the *gh28-1* gene was amplified from gDNA using the primers 2369_CSR-GPD_F and 2369_CSR-GPD_R (Table 5-9). The amplified DNA fragment and the plasmid pTSL126B (SFigure 6-13) were digested with SfbI and PacI and a ligation with T4 DNA ligase was performed, as described in the previous section. The ligated and transformed plasmid vector was used in the creation of the *N. crassa gh28-1-comp* and *gh28-1-oex* strains.

AQUA cloning

The expression cassettes used in the *N. crassa* strains *pdr-1-gfp* and p1BDc2AD were created using the AQUA cloning method published by Beyer *et al.* (Beyer *et al.*, 2015).

The *pdr-1* gene was amplified from gDNA with the primers pdr1gfp_AQUA_fragment_F and pdr1gfp_AQUA_fragment_R (Table 5-9). The plasmid pCCG-C-Gly-GFP (SFigure 6-10) was amplified with the primers pdr1gfp_AQUA_vector_F and pdr1gfp_AQUA_vector_R (Table 5-9). The primer pair of the *pdr-1* gene has a 16 bp overlap to the plasmid and vice versa. Both, DNA and plasmid PCR product, were restriction digested with DpnI to remove residual plasmid DNA and purified as described in 5.3.4. The fragment and plasmid PCR product were incubated for 1 h at RT. The fragment masses used in this reaction were calculated with the following formulas:

$m_{vector} = 12\ ng \times l_{vector}$ (with l_{vector} being the length of the plasmid in bp)

$m_{insert} = \frac{m_{vector} \times l_{fragment} \times 5}{l_{vector}}$ (with $l_{fragment}$ being the length of the fragment in bp)

A total volume of 10 µl was used for the mixture. Following this incubation, 50% of the reaction mix was transformed into *E. coli* DH5α. The resulting expression cassette was used to create the strain *pdr-1-gfp*.

The p1BDc2AD expression cassette was created amplifying the *pdr-1* DNA binding domain (BD) and dimerization domain (DD), a fragment of ~950 bp length, with the primers pdr1-BD_F and pdr1-BD-DD_R, the *clr-2* activation domain (AD) with the primers clr2-TF_F and clr2-TF_R (fragment length ~1980 bp) and the vector backbone from the pCCG-C-Gly-HAT-FLAG plasmid (SFigure 6-11) with the primers pCCG-pdr1+clr2_F and pCCG-pdr1+clr2_R (Table 5-9). All primers contain 16 bp overlaps to their respective flanking fragments: *pdr-1* BD-DD has an overlap to the plasmid and *clr-2* AD; *clr-2* AD has an overlap to *pdr-1* BD-DD and plasmid, while the plasmid shares an overlap with both the *pdr-1* and *clr-2* fragments. The fragments were then treated as described in the previous section, resulting in the expression cassette for the p1BDc2AD strain.

5.3.6. *E. coli* transformation

The expression cassettes created with restriction-ligation cloning or AQUA cloning were transformed into *E. coli* DH5α via heat shock.

A DNA aliquot of 5 µl (either ligation or AQUA mix) was mixed with 45 µl of chemical competent *E. coli* DH5α and incubated for 30 min on ice. The cell suspension was moved to a heating block and the heat shock was performed for 30 s at 42 °C. Afterwards, the cells were cooled down for 3 min on ice, followed by the addition of 450 µl of SOC medium at RT. The cells were further incubated for 60 min at 37 °C and 250 rpm. During this time, LB plates containing the right selection supplement were pre-heated to 37 °C. After the incubation period, 50 µl of the cell suspension were plated on the LB plates and incubated for 16 h at 37 °C. Then, colonies of transformed cells were picked and transferred to new LB plates and genotyping was performed by colony PCR (page 128).

5.3.7. Plasmid DNA miniprep, sequencing and storage

Plasmid DNA was extracted from transformed *E. coli* strains with the SLG Hi-Yield Plasmid Mini Prep DNA Isolierungskit according to the manufacturer's instructions. Following the specifications given out by Eurofins Genomics (Ebersberg, Germany), the purified plasmids were prepared and sequenced at a Eurofins facility. *E. coli* strains carrying a plasmid that was confirmed by sequencing were mixed with 25% glycerol, snap frozen and stored at -80 °C. Plasmids carrying an expression cassette were used for *N. crassa* transformations (see below).

5.3.8. *N. crassa* transformation by electro-transfection

The *N. crassa* strain WT, *his*$^-$ was used for transformation of expression cassettes on the plasmids pCCG-C-Gly-GFP and pCCG-C-Gly-HAT-FLAG. The expression cassettes on the plasmids pTSL1126B and pCSR-knock-in were transformed into *N. crassa* WT strain (Table 5-10). The used strains were incubated for 2 d at 30 °C without light in 250 ml flasks with 50 ml solid MM plus supplements and then transferred to 25 °C and daylight for 8 d to 18 d. The conidia were harvested after the incubation period by pouring 40 ml 1 M sorbitol into the 250 ml flask and vortexing it. The conidia suspension was filtered through sterilized gauze into a 50 ml reaction tube and the volume was filled up to 50 ml with 1 M sorbitol. The following experimental steps were performed on ice or in a centrifuge cooled to 4 °C. The conidia suspension was centrifuged at 2000 rpm for 5 min and the supernatant was removed. The conidia were washed by adding 50 ml 1 M sorbitol, spinning the cells down at 1500 rpm for 5 min, removing the supernatant and adding 50 ml fresh 1 M sorbitol. This process was repeated twice. Afterwards, the cell density was measured at OD_{600}, the suspension was centrifuged at 1500 rpm for 3 min and the supernatant was discarded. The volume to adjust the concentration to 2.5 x 10^9 conidia/ml was calculated with the following formula:

$$V_{final} = V_{suspension} \div \left(\frac{OD_{measured} \times dilution}{0{,}0123 \times 1000}\right)$$

V_{final} is the volume of 1 M sorbitol that had to be pipetted on the conidia pellet after centrifugation. $V_{suspension}$ is the volume of conidia suspension previous to the final centrifugation step.

40 µl of the conidia suspension, equaling 1 x 10^8 cells, were mixed with a solution of 10 µl ddH_2O containing 1 µg to 2 µg of purified expression cassette carrying plasmid DNA. The mixture was incubated for 30 min on ice and then transferred into an ice cold electroporation cuvette with a gap size of 1 mm. The cells were electro-transfected at 1500 V with the

Eppendorf eporator, directly mixed with 950 µl ice cold 1 M sorbitol and stored on ice until all DNA-conidia mixtures were electro-transfected.

Following this procedure, the transformed cells were transferred into 15 ml reaction tubes and mixed with 2 ml MM. The conidia were incubated for 60 min at 30 °C and centrifuged afterwards at 1500 rpm for 3 min. 2 ml of the supernatant was discarded and the conidia were re-suspended in the remaining MM. The suspension was split up into 750 µl and 250 µl aliquots that were pipetted into new 15 ml reaction tubes. A volume of 10 ml TA was added to the cells, quickly mixed and poured on prepared BA plates. Cyclosporin A was added to BA and TA as selection marker when expression cassettes on the plasmids pTSL216B or pCSR-knock-in were used. The WT, *his*$^{-}$ strain became histidine prototroph after transformation, so no additional selection marker had to be added to BA and TA (Table 5-10).

The BA plates were incubated for 2 d to 3 d at 30 °C without light. Afterwards, growing *N. crassa* colonies were picked and transferred to new tubes with 2 ml of slanted MM. The cells were handled as described in 5.2.2 (page 124). Afterwards, the transformed strains were analyzed by genotyping PCR (page 128) on gDNA extracted from conidia (see below). Microconidia isolation (page 126) was performed when the *N. crassa* WT, *his*$^{-}$ strain was the recipient of the expression cassette.

5.3.9. gDNA extraction from *N. crassa* conidia

N. crassa gDNA was extracted from 7 d to 10 d old conidia. The conidia were re-suspended in 400 µl gDNA extraction lysis buffer in a 2 ml screw cap reaction tube and 250 mg 0.5 mm silica beads were added to the tube. Cell lysis was performed with a laboratory bead mill at maximum rpm for 60 s.

The mechanically disrupted cells were incubated for 30 min at 65 °C and vortexed two to three times during this period. Afterwards, the lysis reaction was stopped by adding 80 µl of 1 M Tris HCl pH 7.5 and inverting the reaction tubes. The lysed conidia suspension was centrifuged for 1 min at 13,000 x g and RT. The supernatant was transferred to a new 1.5 ml reaction tube. A volume of phenol:chloroform:isoamylalcohol (25:24:1) equal to the sample volume was added to the supernatant and mixed by vortexing. Following this step, the reaction tubes were centrifuged for 10 min at 13,000 x g and RT. The aqueous phase was transferred to a new 1.5 ml reaction tube afterwards. Two to three sample volumes of ice cold 95% (v/v) ethanol was added to precipitate the DNA and immediately mixed by inversion. The mixture was incubated for 10 min at RT and then centrifuged for 15 min at 13,000 rpm and RT. The supernatant was decanted, followed by the addition of 600 µl 70% (v/v) ethanol to wash the DNA pellet. The reaction tubes were centrifuged for 5 min at

13,000 rpm and RT. The supernatant was removed and the pellet was air dried under the laminar flow sterile bench until the residual ethanol had evaporated. The DNA pellet was re-suspended in 50 µl ddH_2O and used in PCR reactions or stored at 4 °C.

5.3.10. RNA extraction from *N. crassa* biomass

Biomass of *N. crassa* strains used for RT-qPCR (page 134) and RNA-Seq experiments (page 140) was harvested after the incubation and induction periods described in the respective experiments. Samples were taken in biological triplicates, if not stated otherwise. The following experimental steps were performed on ice or in centrifuges cooled to 4 °C.
About 250 mg of wet-weight biomass was transferred into a 2 ml screw cap tube together with 250 mg 0.5 mm silica beads and 1 ml PeqGOLD Trifast DNA/RNA/protein-purification solution. Cell lysis was performed with a laboratory bead mill at maximum rpm for two times 30 s with a resting period of 15 s in between. Afterwards, the reaction tubes were gently shaken for 10 min. Following this step, 200 µl chloroform was added to the cell lysate and mixed by vortexing. The mixture was incubated for 3 min at RT and then centrifuged for 15 min at 12,000 x g. The supernatant was transferred to a new 1.5 ml reaction tube and 0.5 ml 2-propanol was added, as well as mixed by inversion. The solution was incubated for 10 min at RT to allow precipitation of RNA, followed by 10 min centrifugation at 12,000 x g. The supernatant was decanted and the RNA pellet washed with 1 ml 75% (v/v) ethanol by vortexing briefly. The reaction tubes were then centrifuged for 5 min at 7,500 x g and the ethanol was removed completely by pipetting. The RNA pellets were left to air dry, until the residual ethanol had evaporated, and were afterwards re-suspended in 45 µl RNAse-free ddH_2O. The RNA was stored at -80 °C until used in RT-qPCR or RNA-Seq experiments.

5.3.11. cDNA synthesis and RT-qPCR

RNA used for RT-qPCR experiments was digested with DNAse I according to the manufacturer's instructions and purified using the GeneJet RNA Purification Kit. The cDNA synthesis was performed using 1 µg of purified RNA and the High Capacity cDNA Reverse Transcription Kit. 100 ng of cDNA was used in the RT-qPCR reaction mix of the qPCRBIO SyGreen Mix Separate-ROX kit.
RT-qPCR was performed as described in Benz *et al.* (J. P. Benz *et al.*, 2014). The *act* gene (NCU04173, actin variant) was used as endogenous control to normalize the expression values of the target genes.

The *N. crassa* WT, *pdr-1-oex*, *gh28-1-comp* and *gh28-1-oex* strain were 48 h incubated on 1x Vogel's solution plus 1% pectin to determine the gene expression of *pdr-1* and *gh28-1*. The WT strain was used as control to determine relative expression levels.

The *N. crassa* WT and *pdr-1-oex* strains were incubated on 1x Vogel's solution plus 1% xylan. After this time, they were induced for 30 min by adding 2 mM rha to the medium. The expression of *pdr-1* and NCU09034 was compared in the induced strains to non-induced ones to determine relative expression levels.

To determine the expression of *frt-1* in *N. crassa* WT and Δ*pdr-1* strains, the strains were pre-grown for 24 h in MM, washed three times for 10 min in 1x Vogel's NoC and then transferred to an induction solution of 1x Vogel's solution plus either 2 mM rha or 2 mM rha with 2% glucose. The induction was performed for 4 h and relative *frt-1* expression of all strains in all conditions was compared to WT strain induced with 2 mM rha. Additionally, the expression of NCU09034 was determined in the *N. crassa* WT, Δ*pdr-1* and Δ*frt-1* strains by pre-incubating those strains for 24 h in MM, washing them three times in 1x Vogel's NoC and transferring them to 1x Vogel's solution plus 2 mM rha. The strains were induced for 4 h on rha and the relative NCU09034 expression of the Δ*pdr-1* and Δ*frt-1* strains was calculated after the induction period by comparing it to WT strain expression.

In a correlation analysis of RT-qPCR and ENCODE RNA-Seq data, the gene expression of *asd-1*, *ce12-1*, *ce8-1*, *gh28-1*, *gh28-2*, *gh105-1*, *ply-1*, and *ply-2* was determined in *N .crassa* WT and Δ*pdr-1* strains. The strains were pre-incubated in MM, washed three times for 10 min and then induced for 4 h on 1x Vogel's solution plus 1% pectin. The expression of the genes on 1x Vogel's NoC was used as reference to determine relative expression levels.

5.4. Biochemical methods

All experiments including *N. crassa* strains or culture supernatants were performed in biological triplicates, if not stated otherwise.

5.4.1. Bradford assay

The total protein content of culture supernatants was determined with the Bradford assay using BSA as standard (Bradford, 1976). Briefly, 10 µl sample supernatant was mixed with 200 µl 1x Roti-Quant and incubated for 5 min at RT. The absorbance of the samples at 535 nm was determined after the incubation period. The linear regression of the BSA standards was determined to calculate the protein concentration in the samples.

5.4.2. Endo-polygalacturonase activity assay

The endo-polygalacturonase (endoPGase) activity of *N. crassa* culture supernatants was determined using a microplate assay published by Ortiz *et al.* (Ortiz *et al.*, 2014).

A PGA in BCP standard series was used for the quantification of endoPGase activity. 8 µl of culture supernatant was added to 8 µl of a 5 mg/ml PGA in BCP solution and incubated for 20 min at 40 °C. The microplate was placed on ice for 5 min and mock samples of each culture supernatant with PGA in BCP were prepared. These mock samples were not incubated at 40 °C but were treated identically to the incubated samples hereinafter. A volume of 40 µl aqueous ruthenium red (RR, 1.125 mg/ml RR in ddH_2O) was added to all samples, followed by a 30 s orbital shaking step at maximum rpm in the Tecan plate reader and 1 min centrifugation at 3200 x g.

Afterwards, 100 µl of an 8 mM sodium hydroxide solution were added to the samples and they were again orbital shaked at maximum rpm and centrifuged for 10 min at 3200 x g. A volume of 25 µl sample supernatant was transferred into a new well containing 175 µl ddH_2O and the absorbance (*A*) was measured at 535 nm.

The endoPGase activity was calculated with the following equation:

$$U/_{ml} = \frac{A_{mock} - A_{culture\ supernatant}}{t \times V_{supernatant} \times b}$$

The endoPGase activity is expressed in U/ml, *t* equals the incubation time in min (20 min), $V_{supernatant}$ the volume of culture supernatant in ml (0.008 ml) and *b* is the slope of the linear regression that was applied to the PGA standard series.

5.4.3. Pectate lyase activity assay

Pectate lyase activity of *N. crassa* supernatants was determined with a modified version of the pectate lyase activity assay from Megazyme (Megazyme, Ireland). Briefly, 200 µl of a 2.5 mg/ml PGA in 50 mM Tris HCl pH 8 solution was combined with a 300 µl 50 mM Tris HCl pH 8 solution plus 1 mM $CaCl_2$. This enzyme reaction mixture was vortexed briefly, before 100 µl of *N. crassa* culture supernatant was added to the reaction buffer and mixed by quickly pipetting up and down, followed by Absorbance (*A*) measurement at 235 nm over 5 min at RT.

The pectate lyase activity was determined with the following equation:

$$U/_{ml} = \left(\frac{\Delta A}{\Delta T}\right) \times \frac{V_{total} \times dilution}{4.6 \times V_{supernatant}}$$

The pectate lyase activity is expressed in U/ml, $\frac{\Delta A}{\Delta T}$ equals the absorbance increase per min during the earliest linear activity phase, V_{total} is the total volume of the reaction mixture in

ml (0.6 ml), $V_{supernatant}$ is the supernatant volume in ml (0.1 ml) and 4.6 is the absorption coefficient of the unsaturated bond at 4 - 5 position of the uronic acid residue.

5.4.4. PAHBAH carbohydrate reducing ends assay

A modified version of the Megazyme carbohydrate reducing ends assay (Megazyme, Ireland) using 4-hydroxybenzhydrazide (PAHBAH) was used to determine enzyme activities that have carbohydrates with reducing ends as their product.

The PAHBAH assay was used to determine the reducing ends in enzymatic digests or residual D-galactose concentrations of culture supernatants. Enzymatic digests were performed using culture supernatants of *N. crassa* WT, Δ*frp-1*, Δ*cre-1*, Δ*col-26,* Δ*frp-1*/Δ*col-26* and Δ*frp-1*/Δ*cre-1* strains grown for up to 72 h. A volume of 10 µl culture supernatant was mixed with 90 µl 50 mM acetate buffer pH 5 containing either 1% soluble starch, 1% arabinan, 1%CMC or 1% sucrose. The samples were incubated at 40 °C for 15 min and then stored on ice.

One part PAHBAH reagent A and nine parts PAHBAH reagent B were mixed to create the working reagent. A volume of 125 µl working reagent was added to 25 µl culture supernatant or enzymatic digest. The samples were incubated for 6 min at 95 °C, then cooled on ice for 5 min and the absorbance was measured at 410 nm.

5.4.5. Compositional analysis of complex carbon sources

The constituent sugars of complex carbon sources, e.g. polysaccharides, grasses and wood species, were determined using chemical hydrolysis and, if necessary, enzymatic digestion. The different hydrolysis methods are described in the sections below.

The hydrolyzed samples were diluted to concentrations below 10 µg/ml and analyzed by HPAEC-PAD. Samples containing neutral monosaccharides were injected into a 3 x 150 mm CarboPac PA20 column with a 3 x 30 mm guard column of the same material. Uronic acids were injected in a 3 x 250 mm CarboPac PA200 column with a 3 x 50 mm guard column of the same material. The samples were eluted from the CarboPac PA20 column at 30 °C using an isocratic mobile phase of 5 mM NaOH at 0.4 ml/min for 15 min. The elution of the samples from the CarboPac PA200 was performed at 30 °C over 15 min at 0.4 ml/min, but a gradient from 50 mM to 170 mM sodium acetate in 0.1 M NaOH was used.

Chemical hydrolysis with H_2SO_4

The majority of complex carbon sources were treated with H_2SO_4 to release monosaccharides through chemical hydrolysis (Haffner *et al.*, 2013; J. P. Benz *et al.*, 2014; Hassan *et al.*, 2017).

The used carbon samples were dried for 16 h at 60 °C and 5 mg of dried carbon sample were completely dissolved in 50 µl of 72% (v/v) H_2SO_4. Samples containing cellulose were incubated for 1 h to 4 h to facilitate complete degradation of the recalcitrant cellulose fibers. The H_2SO_4 treated samples were then mixed with 1.45 ml ddH_2O and incubated for 1 h at 121 °C. Afterwards, the samples were centrifuged for 5 min at 13,000 x g and the supernatant was transferred to a new 1.5 ml reaction tube to remove residual solids. The composition of the released monosaccharides was determined as described in the previous section.

Chemical hydrolysis with TFA and pectinolytic digest of pectin

The composition of pectin cannot be fully determined by chemical hydrolysis alone, since the multitude of sidechain sugars and the relative high acidity of the HG backbone prevent complete degradation into monosaccharides by H_2SO_4. Therefore, a combined approach of acidic hydrolysis using TFA and enzymatic digest was used (Garna *et al.*, 2004, 2006).

A solution containing 500 µl 1x Vogel's solution plus 0.2% pectin was combined with 500 µl of a 0.4 M TFA solution and incubated for 72 h at 80 °C. After the incubation period, the pH of the solution was adjusted to 5 and the sample volume increased to 25 ml. 5 ml of the sample were mixed with 5 ml of 500-fold diluted Viscozyme L solution, followed by an incubation period of 24 h at 50 °C. The released monosaccharide composition was determined as described on page 137.

5.4.6. Monosaccharide uptake assay

The uptake of monosaccharides by *N. crassa* was determined as published previously (Galazka *et al.*, 2010; J. Benz *et al.*, 2014; J. P. Benz *et al.*, 2014).

Briefly, *N. crassa* conidia were harvested as described on page 124. The conidia were incubated for 16 h in 3 ml of MM containing 24 deep-well plates at 25 °C, 200 rpm and constant light. The mycelial biomass was washed three times for 10 min in 1x Vogel's NoC and transferred to an induction solution containing 1x Vogel's solution plus either 0.5 % (w/v) pectin or different concentrations of monosaccharides, as indicated in the respective result section. The strains were induced for 4 h, if not stated otherwise, then washed again three times in 1x Vogel's NoC and transferred to the uptake medium containing 1x Vogel's solution plus 100 µM monosaccharide. The strains were incubated for an additional hour while 100 µl samples of the supernatant were taken in pre-determined intervals. These samples were centrifuged for 1 min at 4 °C and 16,000 x g. A volume of 80 µl of the sample was transferred to a new 1.5 ml reaction tube. The samples were stored at -20 °C until

further use. The monosaccharide content of the samples was determined using the HPAEC-PAD method described in 5.4.5 (page 137).

5.5. Transcriptome analysis

All experiments including *N. crassa* strains or culture supernatants were performed in biological triplicates, if not stated otherwise.

5.5.1. RNA-Seq of ENCODE samples

The strains used in the 'Fungal Nutritional ENCODE Project', as well as used induction conditions and the RNA-Seq sample preparation are described in detail in Wu, 2017. To give a brief overview, *N. crassa* WT or TF deletion strains were pre-grown for 16 h on MM, washed three times with 1x Vogel's NoC for 10 min and then transferred to an induction solution containing either 1x Vogel's plus 2 mM monosaccharide, 1% plant biomatter, 1% oligo- and polysaccharide, 2% sucrose or NoC.

The RNA was extracted as described previously (Wu, 2017) and the RNA-Seq library prep Stranded cDNA libraries were generated using the Illumina TruSeq Stranded RNA LT kit. 1 µg of total RNA was purified using magnetic beads containing poly-T oligos to extract mRNA. The purified mRNA was fragmented and reverse transcribed using random hexamers and Superscript II followed by second strand synthesis. The cDNA was modified using end-pair A-tailing adapters and ten cycles of PCR. The prepared library was then quantified using KAPA Biosystem's next-generation sequencing library RT-qPCR kit and run on a Roche LightCycler 480 real-time quantitative PCR instrument. The libraries were multiplexed utilizing the TruSeq paired-end cluster kit v3 and sequenced on the Illumina HiSeq 2000 sequencer using a TruSeq SBS sequencing kit v3, following a 2 x 100 indexed run recipe.

Illumina CASAVA v1.8.4 package was used for library base calling and the raw reads were then evaluated for quality using both Geneious BBDuk and Hannonlab fastx toolkit. Following this procedure, the filtered reads were mapped against the *N. crassa* OR74A genome (v12) using Tophat 2.0.4 (Kim *et al.*, 2013) and Cufflinks 2.0.2 (Trapnell *et al.*, 2012) was used to estimate transcript abundance in fragments per kilobase of transcript per millionavicel mapped reads (FPKMs) using upper quartile normalization and mapping against reference isoforms from the Broad Institute. The mapped reads were counted by HTSeq 0.6.0 (Anders *et al.*, 2015) to obtain raw counts, followed by differential expression analysis with DEseq 2 version 3.3 (Love *et al.*, 2014).

5.5.2. RNA-Seq of WT and Δ*frp-1* strains

N. crassa WT and Δ*frp-1* conidia from 10-day-old cultures were harvested and 3 x 10^6 conidia were pre-incubated in 3 ml of 1x modified Vogel's solution plus 2% (w/v) glc for 48 h at 30 °C, 200 rpm and constant light. After the incubation phase, the strains were washed three times with 1x modified Vogel's NoC, transferred to medium containing 1x modified Vogel's solution plus either 2% (w/v) glc, 0.5% (w/v) cellulose or NoC and incubated for additional 16 h. This step was followed by snap-freezing of the mycelial biomass in liquid nitrogen. The total RNA content of the biomass was extracted as described in 5.3.10 (page 134).

The cDNA libraries were generated from 1 µg of total RNA using the TruSeq Stranded Total RNA Prep kit. The mRNA was purified with magnetic beads containing poly-T oligos, fragmented and reverse transcribed using random hexamers and Superscript II. Afterwards, the fragmented cDNA was adenylated and end-pair, A-tailing adapter ligation was performed using the TruSeq RNA Single Indexes Set A and B followed by ten cycles of PCR amplification. The prepared library was then quantified using the Qubit™ dsDNA BR Assay Kit. The 18 generated libraries were multiplexed and paired-end sequenced on a MiSeq System with the MiSeq Reagent Kit v3.

The raw reads were processed using the web-based, open source Galaxy webserver platform (https://usegalaxy.org/). Raw reads were converted to Illumina 1.8+ FASTQ quality scores by using FASTQ groomer (Galaxy Version 1.1.1) (Blankenberg *et al.*, 2010). Following this, quality scores of the groomed FASTQ files were determined using FastQC (Galaxy Version 0.69) (Andrews, 2016) and MultiQC (Galaxy Version 1.0.0.0) (Ewels *et al.*, 2016). Reads were mapped using TopHat (Galaxy Version 2.1.0) (Kim *et al.*, 2013) with paired-end reads and the *N. crassa* OR74A genome from fungidb.org as reference. Cufflinks (Galaxy Version 2.2.1.0) (Trapnell *et al.*, 2010, 2012) was used to estimate transcript abundance in fragments per kilobase of transcript per million mapped reads (FPKMs) with a *N. crassa* OR74A reference annotation from fungidb.org. A bias correction against the *N. crassa* OR74A genome, multi-read correction, length correction and upper quartile normalization were performed on the Cufflinks output. The Cufflink assemblies were merged with Cuffmerge (Galaxy Version 2.2.1.0) (Trapnell *et al.*, 2010).

Significant changes in transcript expression were determined using CuffDiff (Galaxy Version 2.2.1.3) (Trapnell *et al.*, 2010) by comparing Cufflinks outputs against each other and referencing them with the previously generated Cuffmerge transcript file. The NoC condition of *N. crassa* WT and Δ*frp-1* strains was compared to the respective strains induced on 2% glc and 0.5% cellulose. Additionally, a comparison between WT and Δ*frp-1* strains induced on the same carbon source (either NoC, 2% glc or 0.5% cellulose) was performed.

Geometric normalization, condition-based estimation, multi-read correction, as well as bias correction against the *N. crassa* OR74A genome were applied to these analyses.

5.5.3. Hierarchical clustering of transcriptome data

Hierarchical clustering of RNA-Seq data was performed as published previously (J. P. Benz *et al.*, 2014; Thieme *et al.*, 2017). The averaged FPKMs of RNA-Seq library replicates were hierarchical clustered with the Hierarchical Clustering Explorer v3.5 software. Prior to this, a minimum threshold of 10 FPKMs and row-by-row normalization $\left(\frac{X-m}{\sigma}\right)$ was applied to the data. Rows and columns were clustered using the average linkage (unweighted pair group method with arithmetic mean) method with small node arrangement to the right and similarity distribution according Pearson's correlation or Euclidian distance. A minimum similarity threshold of at least 0.65 was applied to the clustered data and the formed clusters, including outliers, were used for further analysis

5.5.4. Extended Functional Categories

Functional Categories (FunCat) were used to determine gene enrichment in RNA-Seq analyses (Ruepp, 2004). The Categories 01.05.03 polysaccharide metabolism and 01.25.01 extracellular polysaccharide degradation were updated to contain subcategories with higher specificity and more representative genes (Figure 5-1; Thieme *et al.*, 2017). These additions were made based on the following published regulons and data sets: Sun and Glass, 2011; Coradetti *et al.*, 2012; Sun *et al.*, 2012; J. P. Benz *et al.*, 2014.
The category 20.01.03.01 sugar transport was expanded with gene IDs that were categorized by TCDB (Saier *et al.*, 2016) as 2.A.1.1 sugar porter family, 2.A.1.7 The Fucose: H+ Symporter Family and 2.A.2 The Glycoside-Pentoside-Hexuronide:Cation Symporter Family (Kumar *et al.*, 2015).

5.5.5. Principal component analysis and k-means clustering

The conditions of the 'Fungal Nutritional ENCODE Project' were analyzed by principal component analysis (PCA) followed by k-means clustering. The k-means clustering was performed using five randomly seeded centers and was repeated for 10 iterations. The iteration with the best R^2 was used as final result. The R script used to create the PCA and calculate the k-means clusters is described in 6.2.1 (page 153).

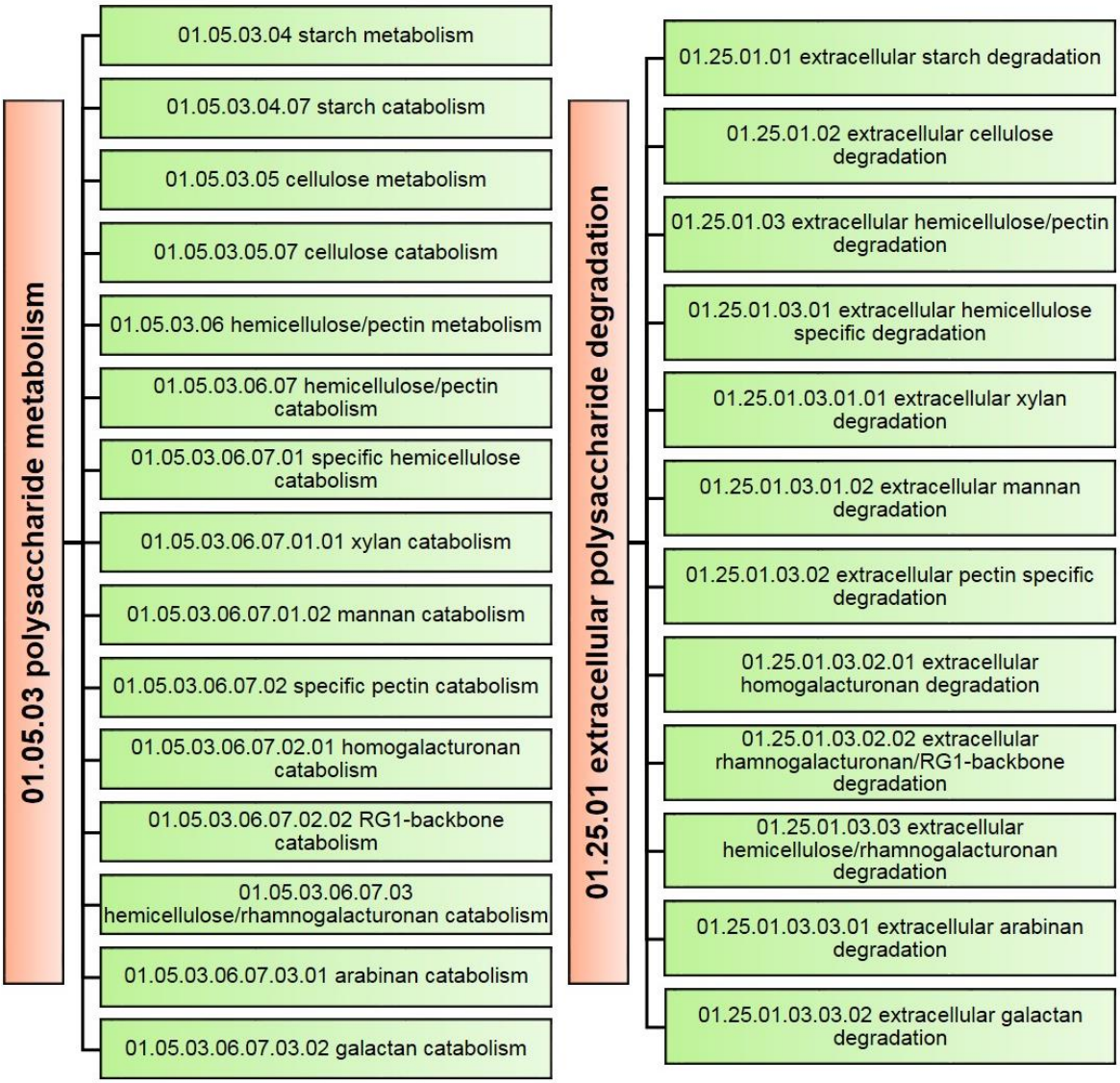

Figure 5-1: Overview of subcategories added and/or expanded in FunCat 01.05.03 and 01.25.01.

5.5.6. Polysaccharide categories

Polysaccharide Categories (PolyCat) were defined as the major polysaccharide building blocks of the plant cell wall, as well as starch as a major storage component. They contain grouped carbon source conditions of the 'Fungal Nutritional ENCODE Project' that are either related polysaccharides or constituents of these polysaccharides (Figure 5-2). The corresponding ENCODE conditions were chosen according to published results describing the chemical composition of the plant cell wall or our own experimental data (Table 5-18). These conditions were manually curated by using Pearson's correlation analysis between the used conditions of each PolyCat and PCA analysis of all ENCODE conditions.

Table 5-18: Polysaccharide categories (PolyCat).
The ENCODE carbon source conditions that were used to create the PolyCats are based on compositional analyses of published studies/reviews or experimental data (sources & explanations). The PolyCat conditions were manually curated based on PCA analysis and Pearson's correlation between conditions. ENCODE conditions or PolyCats that were ultimately not used in our analysis are marked in red.

PolyCat	ENCODE conditions	sources & explanations
cellulose	Avicel	Pettersen, 1984; Varner and Lin, 1989; Carpita and Gibeaut, 1993; Kačuráková *et al.*, 2000; Somerville, 2004; Coradetti *et al.*, 2012; Znameroski *et al.*, 2012; Glass *et al.*, 2013b; Hassan *et al.*, 2017, 2019; Samal *et al.*, 2017
	bacterial cellulose	
	cellobiose	
xylan	xylan	Thornber and Northcote, 1961; Timell, 1967; Pettersen, 1984; Varner and Lin, 1989; Carpita and Gibeaut, 1993; Kačuráková *et al.*, 2000; Somerville, 2004; Sun *et al.*, 2012; Glass *et al.*, 2013b; Samal *et al.*, 2017 and the composition of xylan was determined in this work.
	xylose	
xyloglucan	xyloglucan	Thornber and Northcote, 1961; Timell, 1967; Pettersen, 1984; Varner and Lin, 1989; Carpita and Gibeaut, 1993; Kačuráková *et al.*, 2000; Somerville, 2004; Glass *et al.*, 2013b; Samal *et al.*, 2017
mannan	galactomannan	Thornber and Northcote, 1961; Timell, 1967; Pettersen, 1984; Varner and Lin, 1989; Carpita and Gibeaut, 1993; Kačuráková *et al.*, 2000; Somerville, 2004; Samal *et al.*, 2017
	glucomannan	
	mannobiose	
pectin	arabinose	Morre, 1968; Varner and Lin, 1989; Carpita and Gibeaut, 1993; Kačuráková *et al.*, 2000; Somerville, 2004; Cosgrove, 2005; Caffall and Mohnen, 2009; J. P. Benz *et al.*, 2014; Daher and Braybrook, 2015; Anderson, 2016; Thieme *et al.*, 2017 Arabinose and galactose expression patterns do not correlate to pectin or other pectin related sugars (PCA, hierarchical clustering). Pearson's correlation between arabinose or galactose and pectin also showed only low correlation scores ($\rho < 0.5$).
	galactose	
	galacturonic acid	
	pectin	
	PGA	
	rhamnogalacturonan	
	rhamnose	

Table 5-18: Polysaccharide categories (continued).

PolyCat	ENCODE conditions	sources & explanations
arabinogalactan	Arabinan	Thornber and Northcote, 1961; Timell, 1967; Pettersen, 1984; Varner and Lin, 1989; Carpita and Gibeaut, 1993; Kačuráková *et al.*, 2000; Somerville, 2004; Cosgrove, 2005; Glass *et al.*, 2013b; J. P. Benz *et al.*, 2014; Samal *et al.*, 2017; Benocci *et al.*, 2018 Though arabinogalactan is not a primary component of the plant cell wall, arabinans and galactans, as well as arabinose and galactose, are part of the plant cell wall. In addition, experiments by Benocci *et al.* (2018) show that arabinose and galactose catabolism are regulated together by Ara1 in *T. reesei*. Therefore, we decided to create a PolyCat that includes these carbon sources. However, the arabinogalactan PolyCat had less than 10 identifier genes, which was deemed insufficient for this analysis method.
	arabinose	
	galactan	
	galactose	
starch	amylopectin	Thornber and Northcote, 1961; Timell, 1967; Pettersen, 1984; Smith *et al.*, 1995; Yoshimura *et al.*, 1998; Kavakli *et al.*, 2000; Oribe *et al.*, 2003; Samal *et al.*, 2017; Xiong *et al.*, 2017
	amylose	
	maltose	

Based on the ENCODE conditions used in each PolyCat, gene expression (GeEx) scores were calculated, as described in 5.5.7 (page 144), and used to determine identifier genes specific for each polysaccharide category. The identifier genes were necessary to calculate the PolyCat scores that are used for the analysis of the *N. crassa* polysaccharide perception. (5.5.8, page 147).

5.5.7. Gene expression scores

Gene expression (GeEx) scores were determined to discover genes that are strongly and specifically expressed on only one polysaccharide (Figure 5-2). Therefore, the $\log_2$ fold-change of genes induced on 28 ENCODE carbon sources over their expression on NoC (starvation control) was calculated. The following conditions were used: amylopectin, amylose, arabinan, arabinose, Avicel, bacterial cellulose, cellobiose, fructose, fucose, galactan, galactomannan, galactose, galacturonic acid, glucomannan, glucuronic acid, maltose, mannitol, mannobiose, mannose, pectin, polygalacturonic acid, rhamnogalacturonan, rhamnose, sorbose, sucrose, xylan, xyloglucan and xylose. In addition, the FPKMs of the genes in the 28 conditions were $\log_2$ transformed and used as

a gauge for expression strength. The following equation was used to determine the GeEx score of each gene:

$$GeEx_{gene} = log_2\left(\frac{X}{C}\right) \times log_2 X$$

Whereas X represents the expression of the gene on one of the 28 carbon conditions in FPKM and C is the expression of the same gene on the control condition (NoC, also in FPKM).

To find genes that are specific for on only one PolyCat, the used ENCODE conditions were classified as one of two groups. Group A are the ENCODE conditions that are part of the respective PolyCat (e.g. Avicel, bacterial cellulose and cellobiose in the case of the cellulose PolyCat). Group B consisted of the remaining conditions. A weighting value (Q_X) was determined for each condition with the following equation:

$$Q_X = \frac{n_{total}}{n_{group}}$$

The weighting value of group A was applied to the conditions that form this group, while the remaining conditions got the weighting value of group B. The Q_x quotient of each condition was then multiplied with the GeEx scores of all genes in the same condition:

$$GeEx_w = Q_X \times GeEx_{gene}$$

Through this calculation, GeEx scores in ENCODE conditions related to a PolyCat received a higher score than GeEx scores in unrelated conditions. The following equation was used to determine the total PolyCat based GeEx score of each gene:

$$GeEx_{PC} = \left(\sum_{i=1}^{n_A} GeEx_w\right) - \left(\sum_{i=1}^{n_B} GeEx_w\right)$$

For each gene, the weighted GeEx scores of all conditions unrelated to a specific PolyCat (n_B) were added together and subtracted from the sum of all weighted GeEx scores of all conditions related to a specific PolyCat (n_A).

Each gene now has one total $GeEx_{PC}$ score, which represents its expression strength and its specificity regarding the ENCODE conditions that form the respective PolyCat. A high $GeEx_{PC}$ score equals a strong gene expression and a highly specific expression, while a low score means that the gene is either not highly expressed and/or not very specific. To find identifier genes that are specific for a PolyCat, the standard deviation (SD) of all $GeEx_{PC}$ scores was determined over all genes. Four times SD was applied as minimum threshold on the $GeEx_{PC}$ scores and genes with a score above this threshold were used as identifier genes (Figure 5-2).

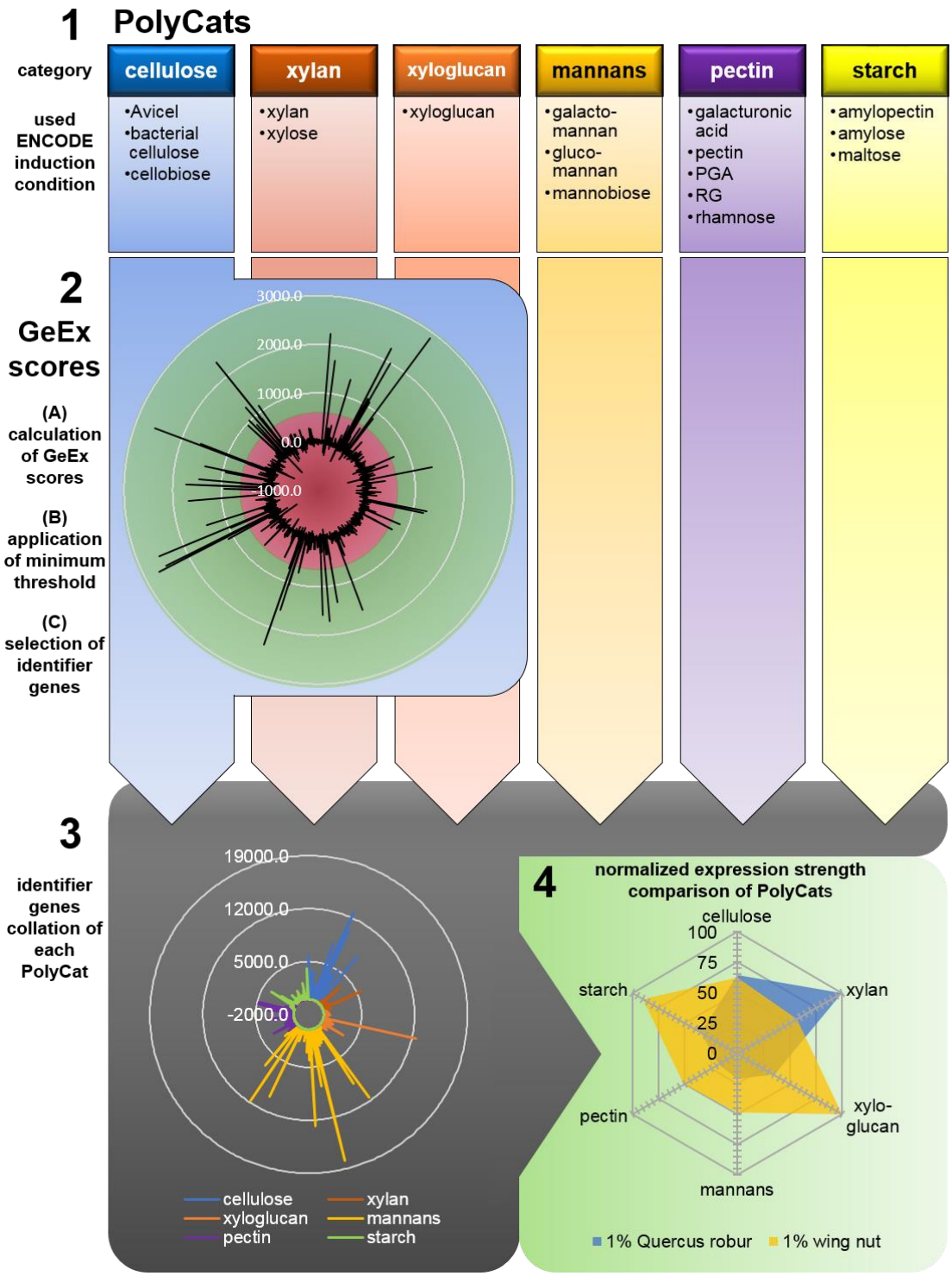

Figure 5-2: Schematic model of the pipeline used to perform the PolyCat based polysaccharide perception analysis.
(1) Polysaccharide Categories (PolyCats) were defined as the major plant cell wall or storage polysaccharides. Related transcriptome conditions (conditions where relevant polysaccharides or constituents thereof were used to induce gene expression) of the fungal nutritional ENCODE project were assigned to each PolyCat based on published results, chemical composition and experimental data. **(2)** Gene expression (GeEx) scores were calculated, assigning each gene a score that contains its relative expression compared to no carbon and its expression strength. Based on the GeEx score of 28 PolyCat related and unrelated conditions, genes could be determined which were specific for and highly expressed on only one PolyCat condition.

Figure 5-2 (continued): A minimum score threshold was applied (red circle) and all genes above this threshold were used as identifier genes (green circle). **(3)** The identifier genes were screened for uniqueness and an expression value in FPKM was assigned to each of them. This expression value was the maximum FPKM of the respective identifier genes in the ENCODE conditions assigned to a PolyCat. **(4)** The expression quotient of the identifier genes, which were induced on complex carbon sources (e.g. grasses and trees), was determined. The mean value of these quotients was calculated for each PolyCat, the PolyCat score, resulting in a single number representing the relative expression of the PolyCat. These PolyCat sores were used to visualize the carbon perception (through gene expression) of *N. crassa*.

Identifier genes should be unique for each PolyCat. However, some identifier genes were found in two or even three PolyCats. In these cases, the identifier genes were manually assigned to one PolyCat, based on their annotation, experimental data or their GeEx score. If no distinction was possible between PolyCats, the identifier gene in question was removed from the respective PolyCats.

5.5.8. Determination of PolyCat scores

The expression values (FPKMs) of an identifier gene on the ENCODE conditions that form a PolyCat were compared against each other (Figure 5-2). The maximum FPKM value in these conditions was assigned to each PolyCat identifier gene as its respective expression value (E_i). To assess the relative expression of the identifier genes induced with complex carbon sources (e.g. grasses and trees), the expression value of the identifier genes induced on these conditions (E_X) was compared to the maximum FPKM value of the PolyCat. The quotient of these expression values was calculated for each individual identifier gene:

$$Q_i = \frac{E_X}{E_i}$$

The value of Q_i shows, if an identifier gene is equally, higher or lower expressed on a complex carbon source than on the PolyCat ENCODE conditions. The mean value of these quotients was determined for each PolyCat and every complex condition analyzed to derive the respective PolyCat scores:

$$PolyCat\ score = \left(\sum_{i=1}^{n_{PC}} Qi\right) \div n_{PC}$$

n_{PC} represents the total number of PolyCat identifier genes.

These scores were then plotted in a radar plot to perform the polysaccharide perception analysis. In addition, the expression values (FPKM) of all identifier genes over all 28 ENCODE carbon conditions used during the GeEx score calculation were correlated to the expression values of complex biomasses (e.g. grasses and woods) using Pearson's correlation. The resulting ρ-values of the 28 carbon conditions were compared between all complex carbon sources by Euclidean distance clustering.

5.6. Statistical and computational methods

5.6.1. Statistical methods

Statistical significance was determined by either independent two-sample student's *t*-tests using Microsoft Excel or analysis of variance (ANOVA) followed by a post-hoc Tukey's test using R (Team RC, 2013). The R script used to calculate ANOVA is described in 6.2.2 (page 154).

5.6.2. Sequence retrieval, analysis and domain predictions

N. crassa amino acid and DNA sequences were retrieved from FungiDB (http://fungidb.org/fungidb/) as FASTA files. Protein sequences of other fungi were retrieved from UniProt database (https://www.uniprot.org/) in FASTA file format.

Phylogenetic trees were either created using phylogen.fr (Dereeper *et al.*, 2008, 2010) or Clustal Omega (https://www.ebi.ac.uk/Tools/msa/clustalo/; Sievers *et al.*, 2011; McWilliam *et al.*, 2013; Li *et al.*, 2015) and the FigTree software (http://tree.bio.ed.ac.uk/software/figtree/). The following settings were used to generate phylogenetic trees with phylogeny.fr: alignment by MUSCLE, excluding alignment curation by Gblocks and tree generation by PhyML.

The protein sequences of transcription factors or transport proteins were analyzed using the conserved domain search tool provided by the NCBI (https://www.ncbi.nlm.nih.gov/Structure/cdd/wrpsb.cgi; Marchler-Bauer and Bryant, 2004; Marchler-Bauer *et al.*, 2011, 2015, 2017). Predicted Nuclear localization signals (NLS) in the amino acid sequences were determined using the NucPred software (http://www.sbc.su.se/~maccallr/nucpred/; Brameier, Krings and MacCallum, 2007) and predicted nuclear export signals (NES) were detected with the NetNES 1.1 Server (http://www.cbs.dtu.dk/services/NetNES/; la Cour *et al.*, 2004). Protein sequence identity was determined by using the BLASTp software (https://blast.ncbi.nlm.nih.gov/Blast.cgi#alnHdr_1003746496; Altschul *et al.*, 1990; Camacho *et al.*, 2009; Boratyn *et al.*, 2012).

5.6.3. Promoter sequence study

The published PDR-1 consensus sequence by Weirauch *et al.* (Weirauch *et al.*, 2014) was retrieved (http://cisbp.ccbr.utoronto.ca/) and modified according to previously published EMSA studies of *A. nidulans* RhaR (Pardo and Orejas, 2014). The sequence was extended by a palindromic core-binding motif of a TCGG quadruple on both sides of an 11 nucleotide long spacer region (TCGG-X11-CCGA). In addition, the site was manually curated by analyzing the putative promoter-binding sites 1000 bp upstream of five major pectinase

genes regulated by PDR-1 (NCU09034, NCU09035, *gh28-1*, *gh105-1*, and *pdr-1* itself) and a position weight matrix (PWM) was created based on these results. The PWM was used to search for potential binding sites in the promoter regions 1000 bp upstream of *N. crassa* genes. The PWM contained only frequencies of each base at each position in the motif, so it was transformed into normalized log-likelihood form (Stormo, 2000):

$$P_{k,j} = log_2\left(\frac{M_{k,j}}{b_k}\right)$$

$M_{k,j}$ is the frequency of base *k* at motif position *j* and b_k is the background frequency of *k* bases in the *N. crassa* genome. Potential binding sites with a stringency value >0.6 were deemed reliable and the stringency value was defined as the ratio of motif score to the maximum possible score for the given PWM.

5.6.4. Online data storage

Online supplementary tables (OTables) are stored in the LRZ Sync+Share cloud. Please contact Prof. Dr. J. Philipp Benz or Nils Thieme using the following email addresses to get an accession link:

benz@hfm.tum.de

thieme@hfm.tum.de

6. Appendix

6.1. Abbreviations

abbreviations	description
aa	amino acid
AA	auxiliary activities (CAZY class)
AD	activation domain
act	actin variant
adh-1	alcohol dehydrogenase 1
AG	arabinogalactan
AM	amylose
AMP	amylopectin
AQUA cloning	advanced quick assembly cloning
ara	L-arabinose
arn	arabinan
BA	bottom agar
BCel	bacterial cellulose
BCP	buffer citrate phosphate
BD	DNA binding domain
BLAST	Basic Local Alignment Search Tool
BLoc_h	Black locust heartwood (*Robinia pseudoacacia*)
BLoc_s	Black locust sapwood (*Robinia pseudoacacia*)
bp	base pair
BSA	bovine serum albumin
CAZY	carbohydrate-active enzyme
CB	cellobiose
CBM	carbohydrate-binding modules (CAZY associated module class)
ccg-1	clock controlled gene 1
cDNA	complementary DNA
CE	carbohydrate esterases (CAZY class)
CIS-BP	Catalog of Inferred Sequence Binding Preferences database
CiPeel	citrus peel
clr-1/2	cellulose regulator 1 or 2
CMC	carboxymethyl cellulose
COak	Common oak (*Quercus robur*)
cre-1	carbon catabolite repressor protein 1
c-source	carbon source
csr-1	peptidyl-prolyl cis-trans isomerase 1
CSSR	carbon starvation stress response
CSto	Corn stover (*Zea mays* ssp. *mays*)
d	day(s)
DD	dimerization domain
ddH_2O	double distilled water
DNA	deoxyribonucleic acid
dNTP	deoxynucleotide triphosphates
dpi	days post inoculation

abbreviations	description
e.g.	*exempli gratia* (latin; translated to: for example)
EBI	Energy Biosciences Institute
ECane	Energy cane (*Saccharum sponteneum*)
ECot	Eastern cottonwood (*Populus deltoides*)
EDTA	ethylenediaminetetraacetic acid
ENCODE	Encyclopedia of DNA elements
endoPGase	endo-polygalacturonase
FGSC	Fungal Genetics Stock Center
frc	D-fructose
frp-1	F-box protein related to pathogenicity 1
frt-1	fucose rhamnose transporter 1
fuc	L-fucose
FunCat	functional categories
fungal MHR	fungal middle homology region
FungiDB	fungal and oomycete genomics resources
FunRich	Functional Enrichment Analysis Tool
gal	D-galactose
galA	D-galacturonic acid
galman	galactomannan
gDNA	genomic DNA
GeEx score	gene expression score
GFP	green fluorescent protein
GH	glycoside hydrolases (CAZY class)
glc	D-glucose
glcA	D-glucuronic acid
glcman	glucomannan
gln	galactan
gpd-3	glyceraldehyde-3-phosphate dehydrogenase
h	hour(s)
H_2SO_4	sulfuric acid
HAT	histidine affinity tag
HFM	Holzforschung München (german; translated to: Wood Research Munich)
HG	homogalacturonan
his-3	histidine biosynthesis trifunctional protein coding gene
i.e.	*id est* (latin; translated to: in other words)
inu	inulin
LB	lysogeny broth
LCed_h	Lebanon cedar heartwood (*Cedrus libani*)
LCed_s	Lebanon cedar sapwood (*Cedrus libani*)
lex	low-expression
mal	D-maltose
manol	D-mannitol
man	D-mannose
MB	mannobiose
MCS	multiple cloning site
MEGA	Molecular Evolutionary Genetics Analysis Software
MiGi	*Miscanthus x giganteus*

abbreviations	description
min	minute(s)
MM	Vogel's Minimal Medium
mnl	D-mannitol
mRNA	messenger RNA
NES	nuclear export signal
NLS	nuclear localization signal
NoC	no carbon source
NSpru_h	Norway spruce heartwood (*Picea abies*)
NSpru_s	Norway spruce sapwood (*Picea abies*)
OD	optical density (used wavelengths in nm are added in subscript, e.g. OD_{600})
oex	overexpression
ori	origin of replication
OTable	supplementary online table
PAHBAH	4-hydroxybenzhydrazide
PCA	principal component analysis
PCWDE	plant cell wall degradation enzyme(s)
PCWDN	plant cell wall degradation network
PCR	polymerase chain reaction
pec	pectin
PDM	plasmid DNA medium
pdr-1/-2	pectin degradation regulator 1 or 2
PGA	polygalacturonic acid
PL	polysaccharide lyases (CAZY class)
PolyCat	polysaccharide categories
RG-I/II	rhamnogalacturonan I or II
rha	L-rhamnose
rib	D-ribose
RNA	ribonucleic acid
RNA-Seq	mRNA sequencing (used to create transcriptomics data)
rpm	revolutions per minute
RR	ruthenium red
RT	room temperature
RT-qPCR	quantitative real-time PCR
SD	standard deviation
SFigure	supplementary figure
SFir	Silver fir (*Abies alba*)
SGrass	Switchgrass (*Panicum virgatum*)
SOC	super optimal broth with catabolite repression
sor	L-sorbose
STable	supplementary table
suc	surcrose
TA	top agar
TAE	Tris acetate EDTA buffer
TCDB	Transporter Classification Database
TF	transcription factor
TFA	trifluoroacetic acid
tre	trehalose

abbreviations	description
trpC	multifunctional tryptophan biosynthesis protein
TUM	Technical University Munich
WGM	Westergaard's Medium
WNut	Chinese wingnut (*Pterocarya stenoptera*)
x g	times gravity/gravitational acceleration
XG	xyloglucan
XGA	xylogalacturonan
xln	xylan
xlr-1	xylan regulator 1
xyl	D-xylose

6.2. R scripts

The R scripts used in this thesis are stored in the directory "U:\bioprozesse\projekte\2014 PhD-Student Nils Thieme\Scripts\R" and their commented code is presented in the following sections. Comments in the code are marked in lime green and start with a '#' in each line. Variables and constants that have to be changed (e.g. file names) are colored dark red.

6.2.1. Principle component analysis and k-means clustering

```
# set working directory (Sessions rider) to the folder containing your files.
library(ggfortify)

# enter the file-name of the prepared PCA file in the place of FILENAME (make sure that the file is
# placed in your working directory).
# files have to be in tabstopp delimited file format.
ALL = read.table("FILENAME.txt", sep = "\t", header = TRUE)
tALL = ALL[,-1]
tEX = as.matrix(tALL)

# variable 'A' contains the multidimensional output of the data. This can be used for PCA and
# k-means clustering.
A = t(tEX)

# start PCA calculations, create PCA plot and summarize PCA results (variance of each Principal
# component [PC] will be shown here --> can be used to determine how much of the variance PC1
# & PC2 explain).
pcaALL = prcomp(A, cor = TRUE, scores = TRUE)
autoplot(pcaALL, label=TRUE, label.size =4, label.colour = "Red", label.alpha=3/4, label.vjust=-0.7)
+ xlab("First Component") + ylab("Second Component") + theme_bw()  + theme(axis.title.x =
element_text(size=16, face="bold"), axis.title.y = element_text(size=16, face="bold"), panel.border =
```

```
element_blank(), axis.line = element_line(), axis.text.x=element_text(size=12), axis.text.y=element_text(size=12), panel.grid.major.x = element_blank(), panel.grid.major.y = element_blank(), panel.grid.minor.x = element_blank(), panel.grid.minor.y = element_blank() )
summary(pcaALL)

# calculating k-means clustering (using Euclidian distance) for all components.
# the X in brackets represents the amount of clustering centers (= number of clusters)
# applied to the data (minimum 2).
kmeans(A, X)
```

6.2.2. ANOVA and post-hoc Tukey test

```
# import the correct formatted file into R.
# files have to be in file format: two rows with the headers ‘condition’ and ‘value’.
# enter the file-name of the prepared file in the place of FILENAME.
# attach the file (use the file name, but disregard the file extension [*.txt]).
attach(FILENAME)

#generate a stripchart
stripchart(value ~ as.factor(condition), vertical = T, pch = 19, method = "jitter", jitter = 0.04, las=0)

#run ANOVA & post-hoc Tukey test
analysis <- lm(value ~ as.factor(condition))
anova(analysis)
TukeyHSD(aov(analysis))

detach(FILENAME)
```

6.2.3. Boxplots

```
# import the correct formatted file into R
# enter the file-name of the prepared file in the place of FILENAME.
# attach the file (use the file name, but disregard the file extension [*.txt])
attach(FILENAME)

# create the box plot.
boxplot(FILENAME,
    # label of Y-axis.
    ylab =" y-axis label",
    las = 1,
    # color of boxes. add as many as you have conditions.
```

```
    col = c("color_1"," color_2"," color_3"),
    par(mar = c(5,10,2,2) + 0.1),
    par(mgp=c(6,1,0)),
    par(cex.lab=2.5),
    par(cex.axis=2.2),
    # names of conditions. add as many as you have conditions.
    names = c("condition_1"," condition_2"," condition_3"))

detach(FILENAME)
```

6.3. Supplementary tables

STable 6-1: PolyCat identifier genes.

cellulose	xylan	xyloglucan	mannan	pectin	starch
NCU00130	NCU00292	NCU00236	NCU00144	NCU00259	NCU00248
NCU00206	NCU00709	NCU00263	NCU00265	NCU00260	NCU00289
NCU00449	NCU00891	NCU00304	NCU00451	NCU00642	NCU00430
NCU00762	NCU01195	NCU00552	NCU00878	NCU00643	NCU00521
NCU00801	NCU01866	NCU00591	NCU00915	NCU00810	NCU00575
NCU00836	NCU01900	NCU00721	NCU01425	NCU00988	NCU00684
NCU00870	NCU02343	NCU01744	NCU01528	NCU00990	NCU00899
NCU01050	NCU03322	NCU01816	NCU01546	NCU01061	NCU00943
NCU01076	NCU03608	NCU01829	NCU01633	NCU01132	NCU00972
NCU02240	NCU04400	NCU01830	NCU01754	NCU01904	NCU01271
NCU02855	NCU04401	NCU02126	NCU01873	NCU01905	NCU01400
NCU02916	NCU04720	NCU02127	NCU02099	NCU01906	NCU01504
NCU03181	NCU04870	NCU02238	NCU02157	NCU02097	NCU01517
NCU03328	NCU05159	NCU02361	NCU02193	NCU02188	NCU01640
NCU04522	NCU05350	NCU02397	NCU02252	NCU02291	NCU01680
NCU05057	NCU06138	NCU02526	NCU02481	NCU02369	NCU01748
NCU05846	NCU06143	NCU02704	NCU02798	NCU02653	NCU01808
NCU05853	NCU06364	NCU02948	NCU03208	NCU02654	NCU01871
NCU05863	NCU06490	NCU03421	NCU03404	NCU03086	NCU01886
NCU05864	NCU06597	NCU03913	NCU03634	NCU03283	NCU01924
NCU05924	NCU07232	NCU04169	NCU03684	NCU03651	NCU02090
NCU05955	NCU07510	NCU04430	NCU03755	NCU04130	NCU02175
NCU06607	NCU07982	NCU04475	NCU03791	NCU04298	NCU02244
NCU07143	NCU08095	NCU04605	NCU04249	NCU04591	NCU02390
NCU07190	NCU08189	NCU04797	NCU04265	NCU04623	NCU02623
NCU07225	NCU08384	NCU04908	NCU04268	NCU04675	NCU02904
NCU07326	NCU08976	NCU05137	NCU04314	NCU05037	NCU03117
NCU07340	NCU09652	NCU05498	NCU04639	NCU05089	NCU03257
NCU07487	NCU09705	NCU05499	NCU04644	NCU05585	NCU03293
NCU07898	NCU09923	NCU05537	NCU04880	NCU05598	NCU03497
NCU08042	NCU09926	NCU05805	NCU04963	NCU05751	NCU03501
NCU08114	NCU10106	NCU06448	NCU04998	NCU05908	NCU03509
NCU08398	NCU10107	NCU06616	NCU05134	NCU05965	NCU03728

STable 6-1: PolyCat identifier genes.

cellulose	xylan	xyloglucan	mannan	pectin	starch
NCU08412	NCU10110	NCU06682	NCU05291	NCU06326	NCU03730
NCU08755	NCU11353	NCU06881	NCU05338	NCU06960	NCU04307
NCU08760		NCU06895	NCU05448	NCU06961	NCU04421
NCU08785		NCU07027	NCU05561	NCU07064	NCU04537
NCU09416		NCU07153	NCU05572	NCU07465	NCU04554
NCU09491		NCU07311	NCU05627	NCU07506	NCU04603
NCU09524		NCU07737	NCU05897	NCU07569	NCU04674
NCU09582		NCU08356	NCU05995	NCU07787	NCU04847
NCU09664		NCU08418	NCU06042	NCU08176	NCU05131
NCU09680		NCU08715	NCU06076	NCU08177	NCU05133
NCU09689		NCU08771	NCU06120	NCU08648	NCU05168
NCU09764		NCU08791	NCU06137	NCU08738	NCU05309
		NCU08949	NCU06209	NCU08739	NCU05526
		NCU09041	NCU06465	NCU08882	NCU05638
		NCU09043	NCU06524	NCU08907	NCU05755
		NCU09057	NCU06532	NCU08943	NCU06315
		NCU09266	NCU06940	NCU09034	NCU06912
		NCU09285	NCU07049	NCU09035	NCU06970
		NCU09287	NCU07108	NCU09169	NCU06991
		NCU09732	NCU07222	NCU09170	NCU07016
		NCU09823	NCU07351	NCU09305	NCU07075
		NCU09864	NCU07352	NCU09532	NCU07088
		NCU09992	NCU07405	NCU09533	NCU07257
		NCU10007	NCU07442	NCU09775	NCU07375
		NCU10008	NCU07817	NCU09873	NCU07491
		NCU10276	NCU07853	NCU09924	NCU07675
		NCU10546	NCU07869	NCU09976	NCU07788
		NCU10732	NCU07914	NCU10045	NCU08229
		NCU16742	NCU07949	NCU11253	NCU08621
			NCU08167	NCU11417	NCU08746
			NCU08269		NCU08805
			NCU08330		NCU08807
			NCU08495		NCU08988
			NCU08695		NCU09355
			NCU08736		NCU09395
			NCU08859		NCU09567
			NCU09174		NCU09663
			NCU09182		NCU09805
			NCU09559		NCU10021
			NCU09683		NCU16323
			NCU09798		
			NCU09810		
			NCU09958		
			NCU10042		
			NCU10051		
			NCU11088		
			NCU11291		
			NCU11323		

STable 6-1: PolyCat identifier genes.

cellulose	xylan	xyloglucan	mannan	pectin	starch
			NCU15834		
			NCU16673		
			NCU16738		

6.4. Supplementary figures

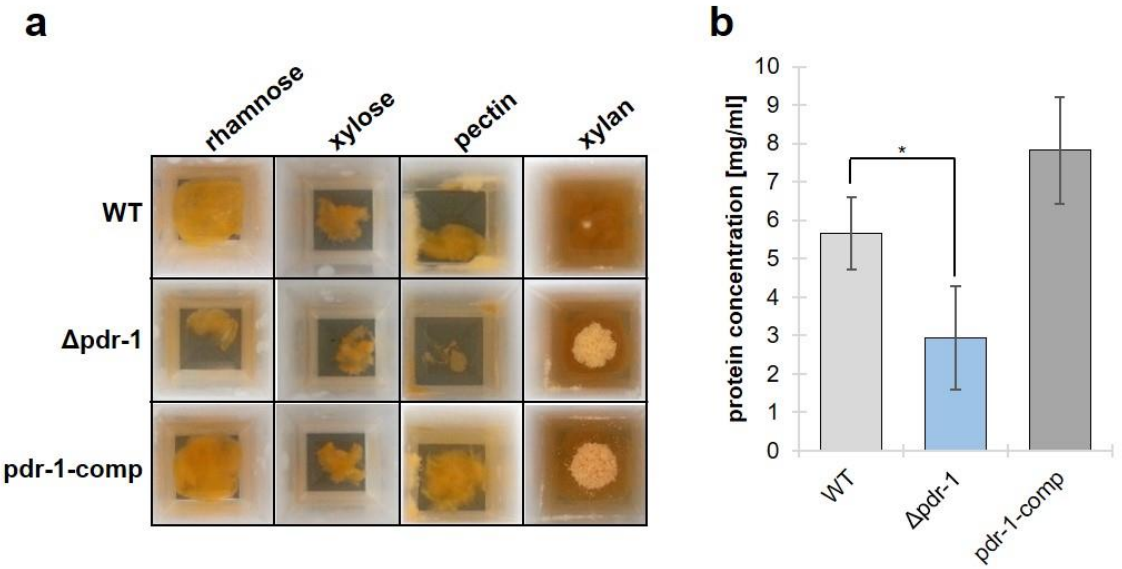

SFigure 6-1: Growth phenotypes and protein secretion of *N. crassa* WT, Δ*pdr-1* and *pdr-1-comp* strains.
(a) Observed growth phenotypes. Strains were incubated for 3 days in either 2 mM rha, 2 mM xyl, 1% pectin or 1% xylan. **(b)** MM pre-grown cultures were switched to pectin medium and the concentration of secreted protein was determined. Error bars represent standard deviation (n = 3). Significance was determined by an independent two-sample *t*-test of WT against Δ*pdr-1* or *pdr-1-comp* with $*p < 0.05$.

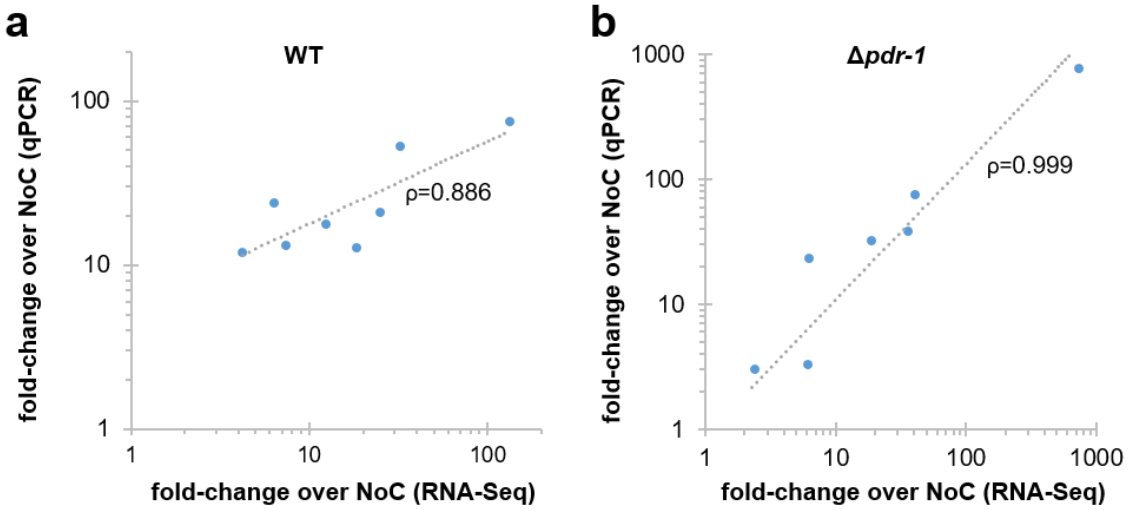

SFigure 6-2: Correlation studies of RNA-Seq to RT-qPCR data.
Correlation analysis of RT-qPCR data to RNA-Seq data. Axes are $\log_{10}$-scaled. The fold-change expression of several key pectinase genes was determined by RT-qPCR in **a)** the WT strain and **b)** the Δ*pdr-1* strain. Gene expression of both strains were induced with 1% pectin and plotted against their respective RNA-seq data. The Pearson's correlation coefficient (ρ) was determined. Two biological replicates were used for RT-qPCR except for *ply-2*, where only one was used. All biological replicates were analyzed as three technical replicates.

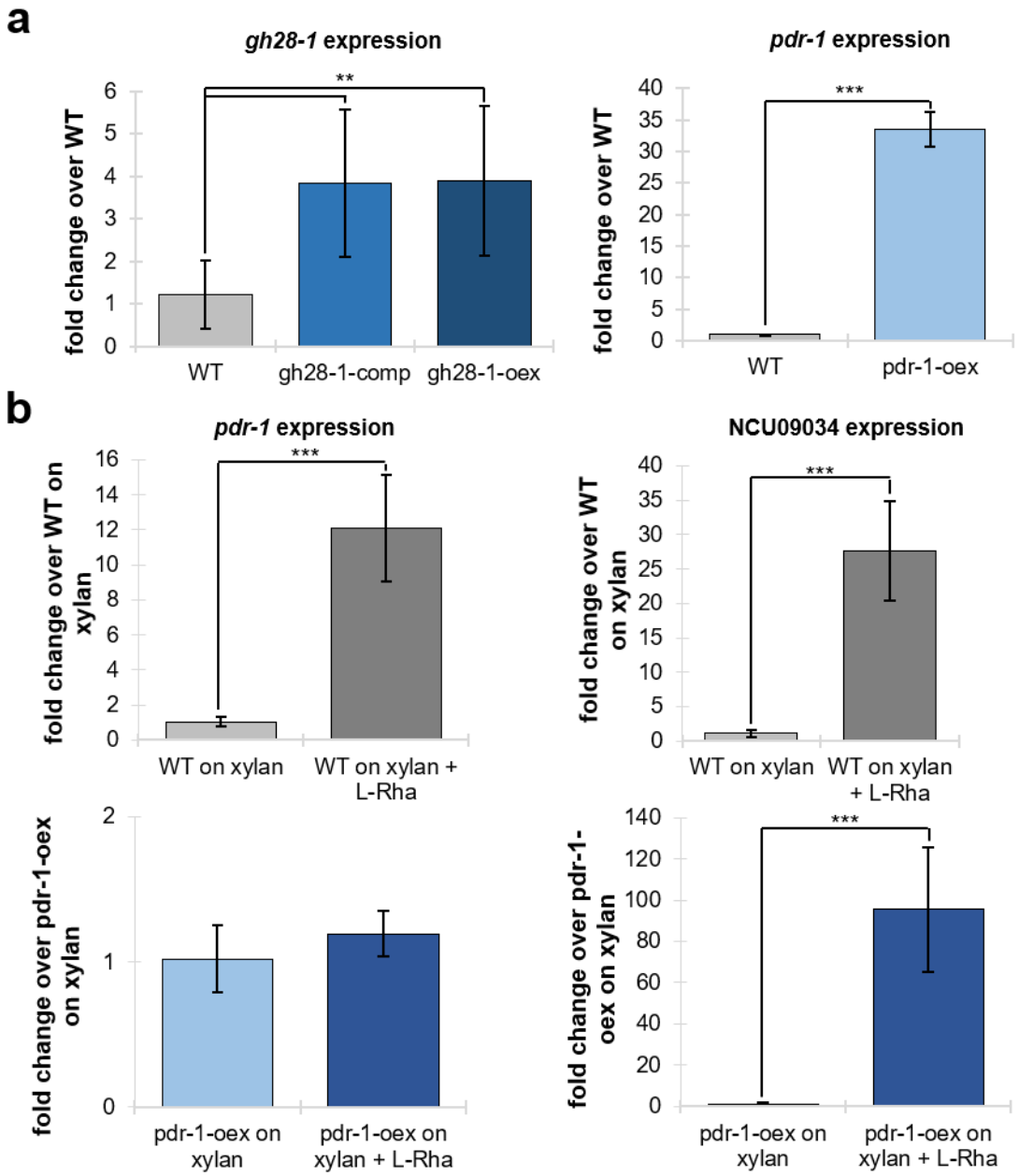

SFigure 6-3: Expression levels of *pdr-1*, *gh28-1* and NCU09034 determined by RT-qPCR. **a)** The strains were grown for 2 days on 1% pectin and the expression level of *pdr-1* in the *pdr-1-oex* strain or *gh28-1* in the *gh28-1-oex* and *gh28-1-comp* strain was determined. The WT strain was used as reference. **b)** The WT and *pdr-1-oex* strain were incubated for 48 hours on 1% xylan. 2 mM rhamnose was added and the strains were incubated for an additional 30 minutes before harvesting the RNA for RT-qPCR. Strains incubated for the same time but without rhamnose were used as controls. The expression of *pdr-1* and NCU09034 was determined for both strains. Three biological replicates were used, except for *pdr-1* in WT on pectin and NCU09034 in WT on xylan plus rhamnose, where only two were used. All biological replicates were analyzed as three technical replicates. Error bars represent standard deviation. Significance was determined by an independent two-sample *t*-test with **p < 0.01, ***p < 0.001. L-Rha = rhamnose

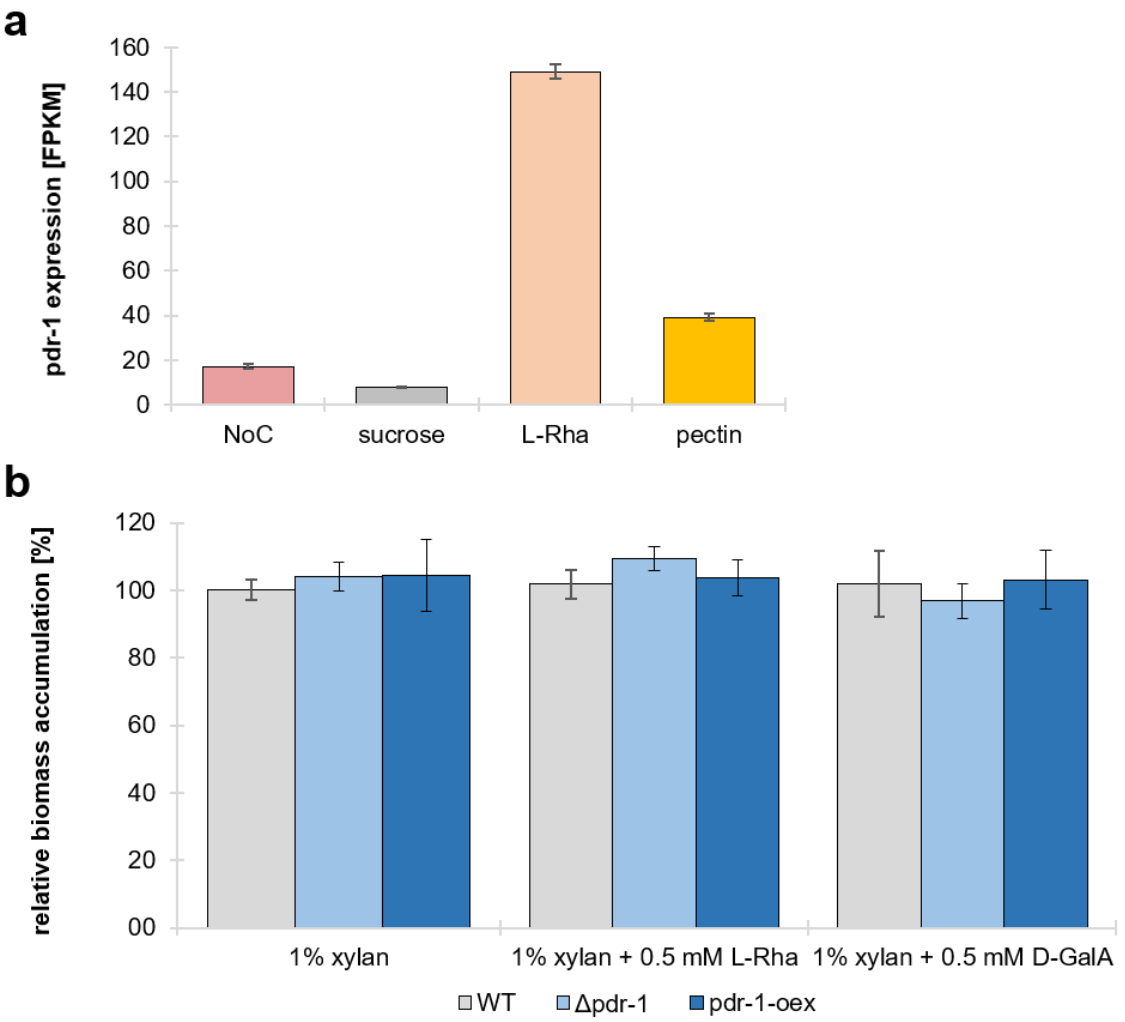

SFigure 6-4: Expression profile of *pdr-1* and biomass accumulation of the *pdr-1-oex* strain. **a)** RNA-Seq expression profile of *pdr-1*. After a 16 h pre-incubation on 2% sucrose, biomass of the WT strain was washed three times with 1x Vogel's solution and transferred to a medium of either no carbon source (NoC), 2% sucrose, 2 mM rhamnose or 1% pectin. The strain was incubated for an additional 4 h. Error bars represent standard deviation (n = 2 for 1% pectin, n = 3 for NoC, 2% sucrose and 2 mM rhamnose). **b)** Determination of accumulated biomass. Strains were grown on 1% xylan with 0.5 mM rhamnose or galacturonic acid. A medium containing 1% xylan was used as control. Biomass was determined by dry weight. Error bars represent standard deviation (n = 3). L-Rha = rhamnose, D-GalA = galacturonic acid.

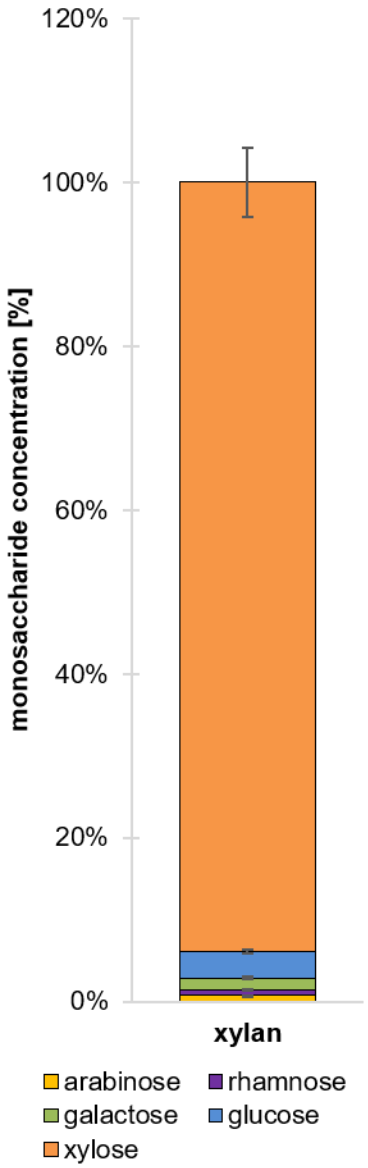

SFigure 6-5: Compositional analysis of the xylan used in this study.
3 µg of xylan were dissolved by acidic hydrolysis and the concentration of the released monosaccharides was measured by HPAEC-PAD. Error bars represent standard deviation (n = 3).

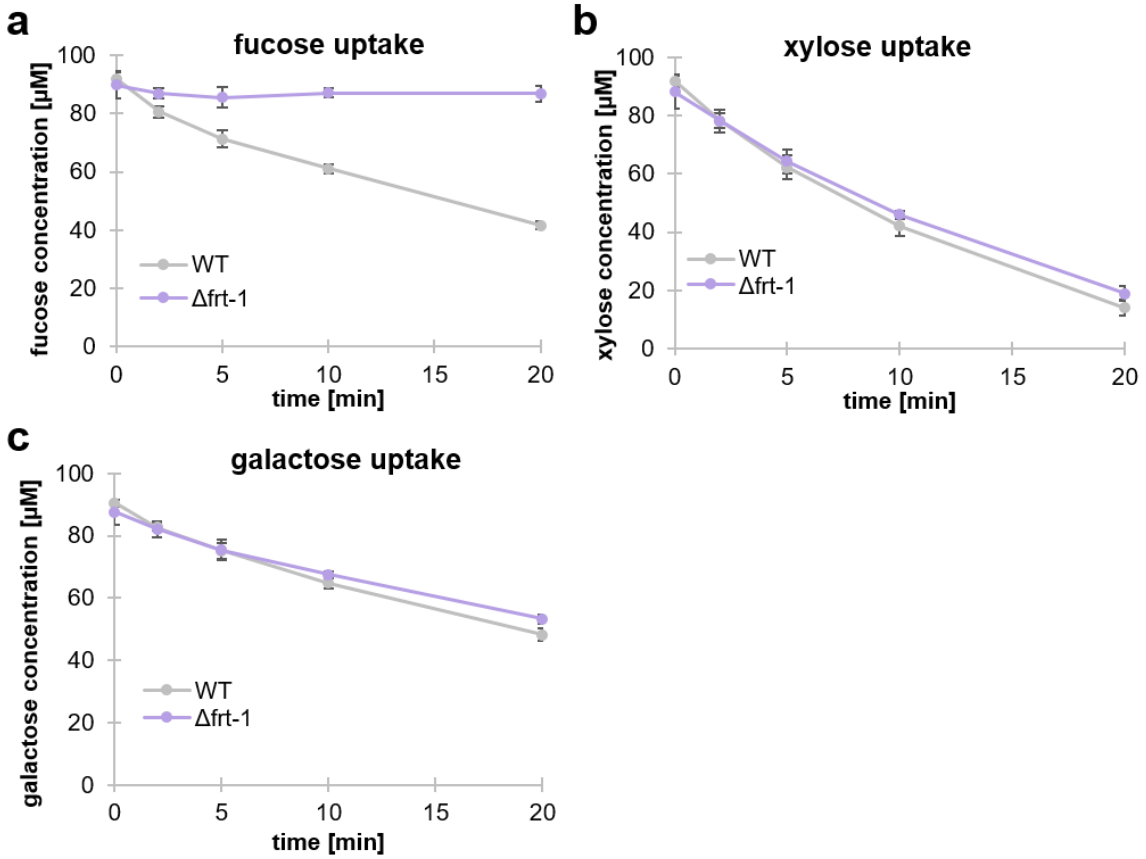

SFigure 6-6: Uptake assays of WT and Δ*frt-1* strains.
Both strains were pre-incubated for 16 h in 2% sucrose, washed and transferred to 0.5% xylan medium to induce gene expression. After 4 h of induction, the biomass was transferred to 90 µM of **a)** fucose, **b)** xylose or **c)** galactose and sample supernatant were taken at defined time points. The monosaccharide content of the supernatants was measured using HPAEC-PAD. Error bars represent standard deviation (n = 3).

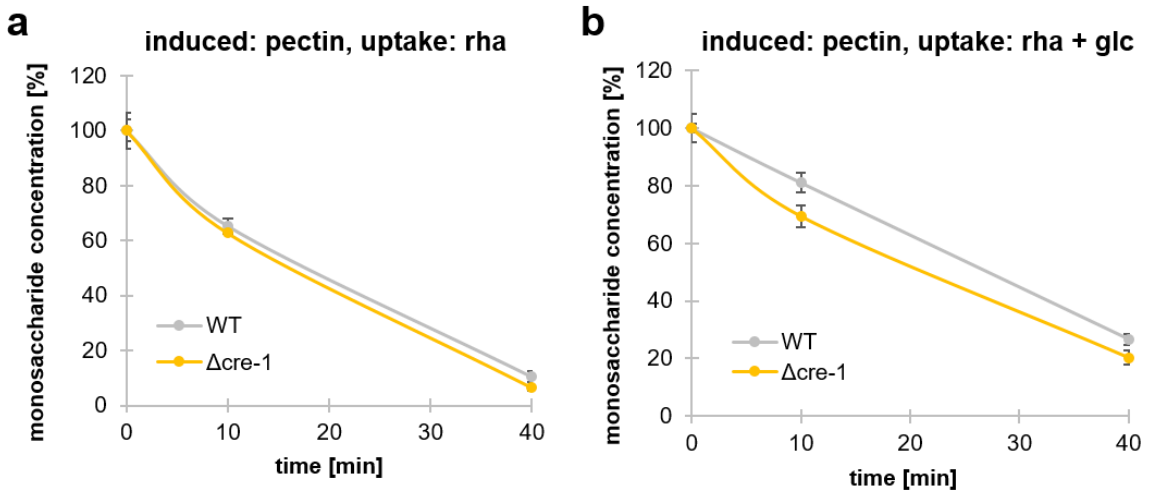

SFigure 6-7: Uptake assays of WT and Δ*cre-1* strains.
Both strains were pre-incubated for 16 h in 2% sucrose, washed and transferred to 0.5% pectin medium to induce gene expression. After 4 h of induction, the biomass was transferred to **a)** 100 µM rhamnose or **b)** 100 µM rhamnose plus 2% glucose and sample supernatant were taken at defined time points. The monosaccharide content of the supernatants was measured using HPAEC-PAD. Error bars represent standard deviation (n = 3).

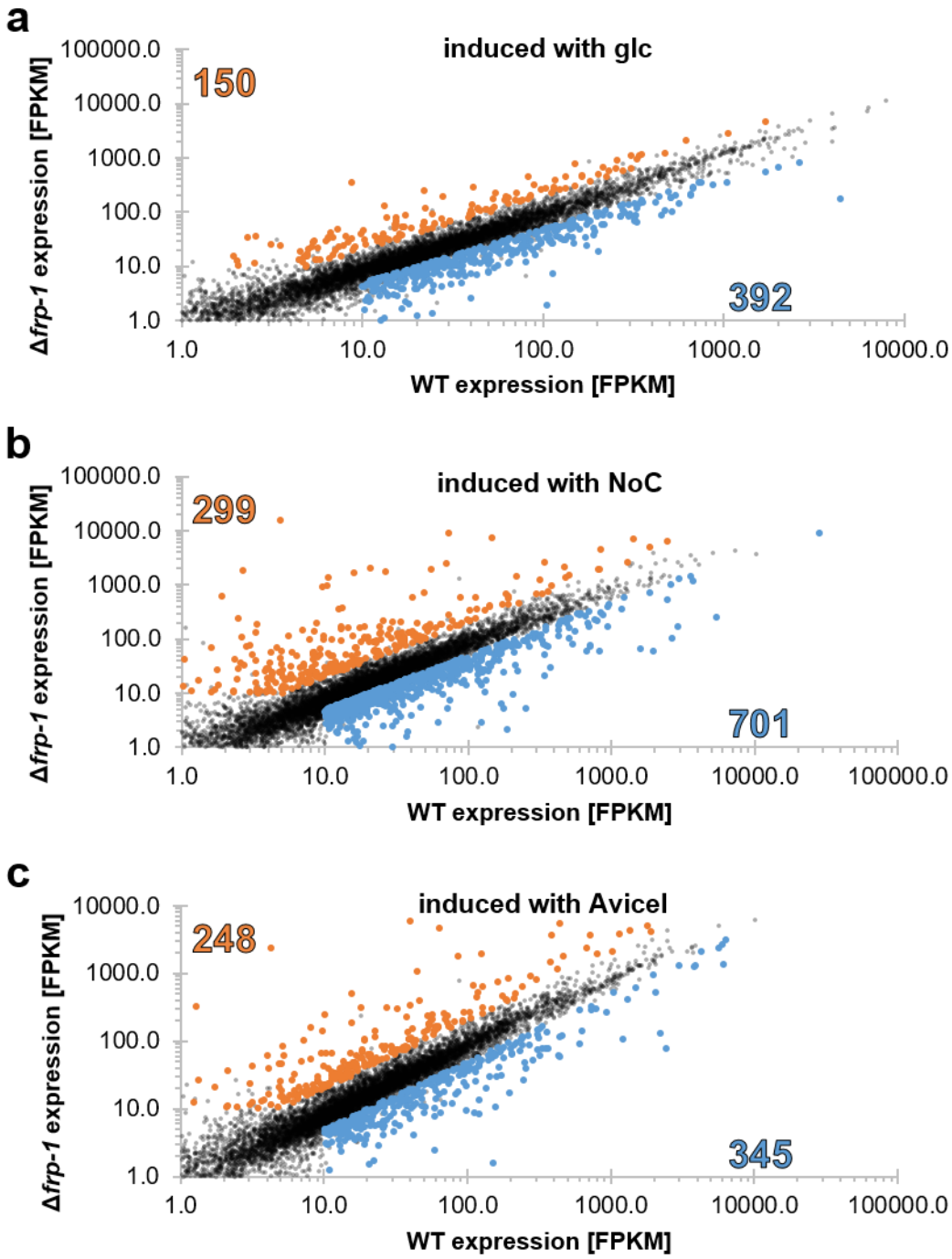

SFigure 6-8: Scatterplots of gene expression in the Δ*frp-1* strain versus the WT strain on glucose, NoC and Avicel medium.
RNA-Seq data of the WT and Δ*frp-1* strains induced for 16 h with either **a)** glucose (glc), **b)** NoC or **c)** Avicel were plotted against each other (black dots). Genes that were significantly mis-regulated (CuffDiff), had more than 10 FPKMs and were either at least a 2-fold up- or down-regulated are marked in the diagram as orange or blue dots, respectively. Axes are log_{10}-scaled.

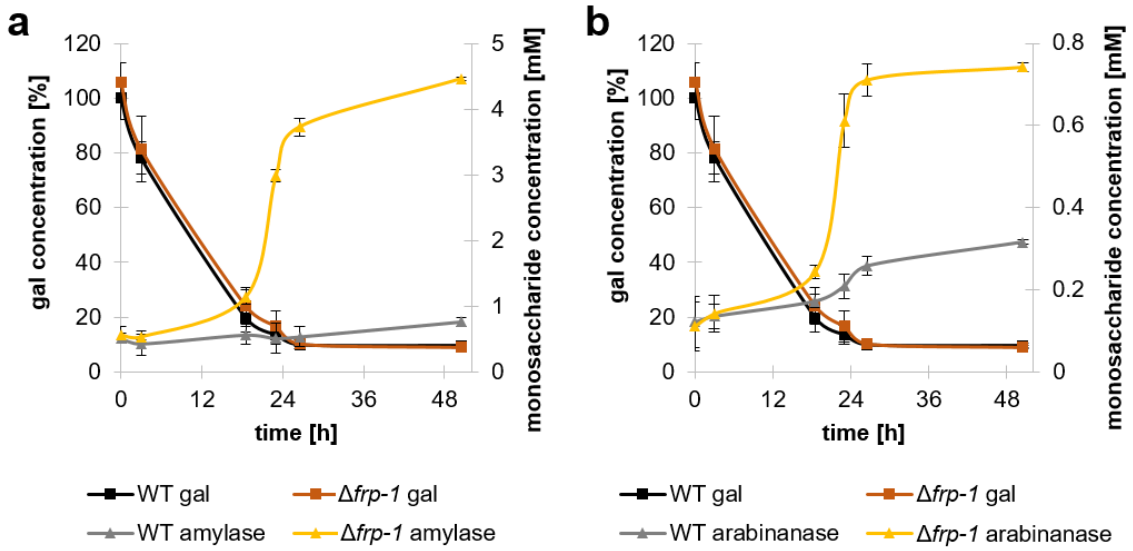

SFigure 6-9: Carbon source depletion induces secretion of α-amylases and arabinanases in the Δ*frp-1* strain.

The WT and Δ*frp-1* strains were pre-grown for 16 h in 2% sucrose and then transferred to 25 mM galactose (gal) medium for an additional two days of incubation. Sample supernatants were taken ir regular intervals. The supernatants were used to determine the galactose concentration and either **a)** α-amylase or **b)** arabinanase activity in the sample supernatants. Error bars represent standard deviation (n = 3).

6.5. Plasmid cards

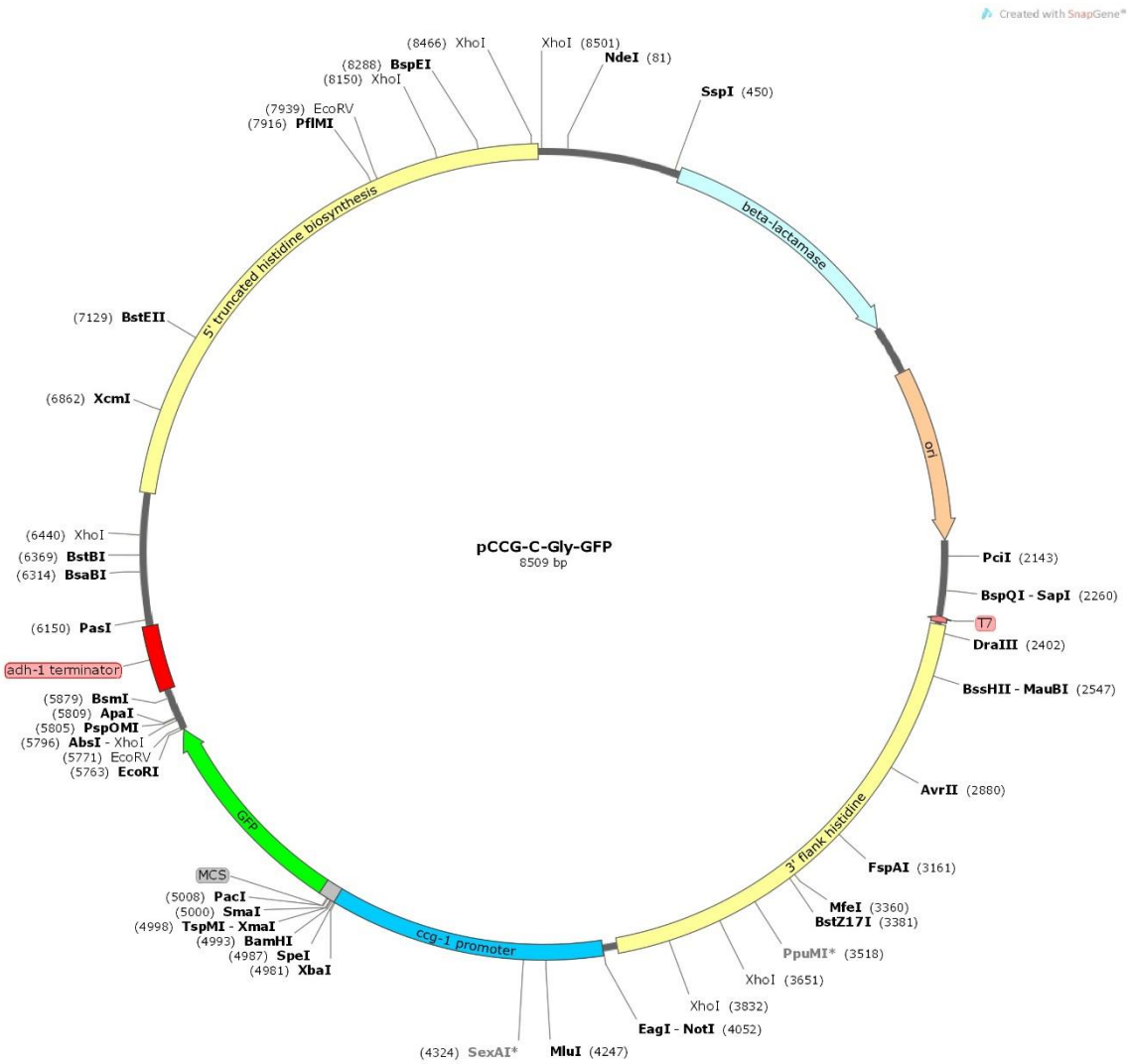

SFigure 6-10: Plasmid map of pCCG-C-Gly-GFP.
This plasmid contains 5' and 3' flanking regions that locate the cloning cassette into the *his-3* locus by homologous recombination. The 5' flank restores the point mutation in the *his-3* gene to WT sequence, removing the histidine auxotrophy from the recipient strain. Between these flanks lie the constitutive promoter *ccg-1*, the MCS, the *gfp* gene as a fluorescent marker and the *adh-1* terminator. The β-lactamase gene conveys Ampicillin resistance to *E. coli* strains.

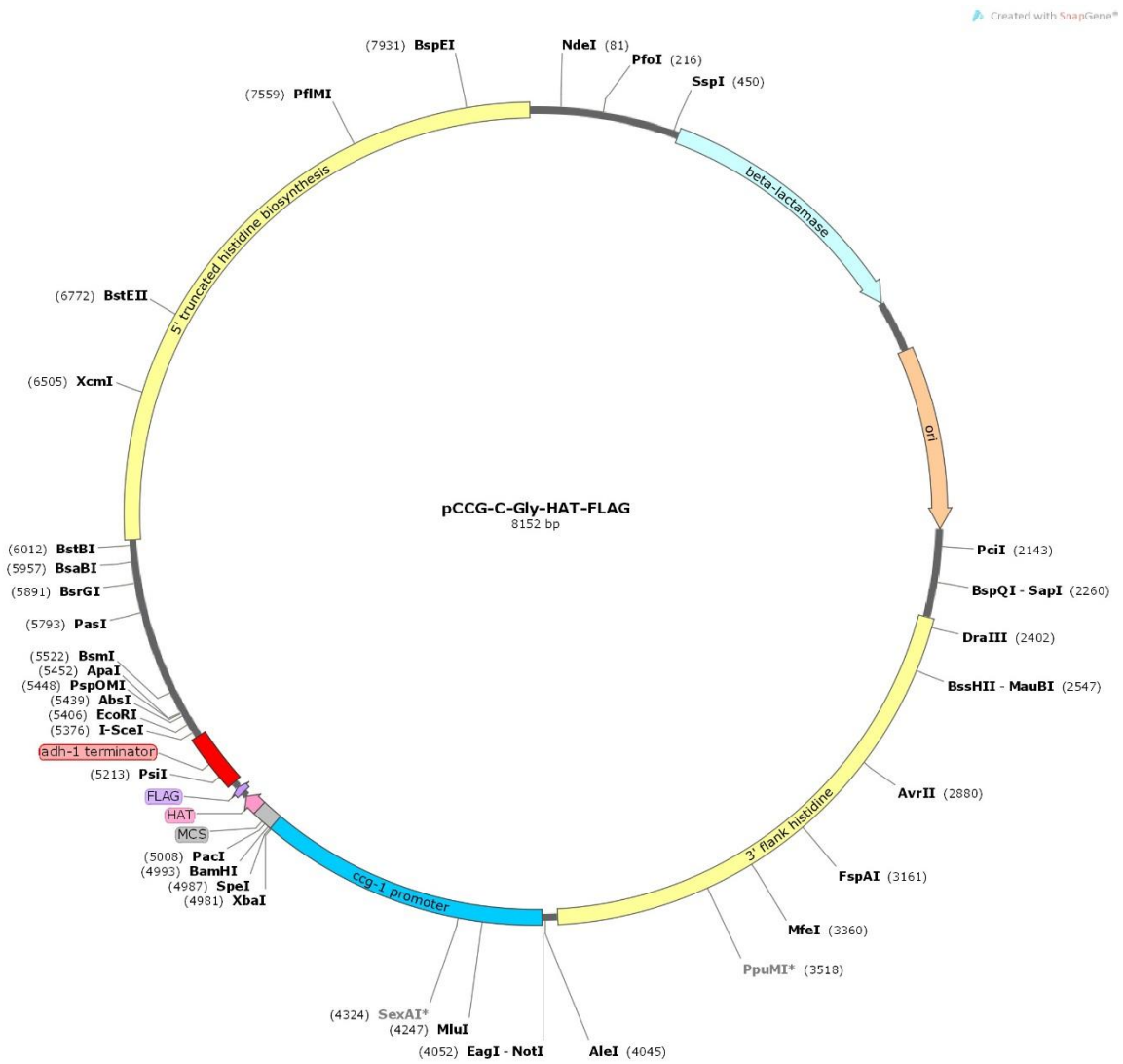

SFigure 6-11: Plasmid map of pCCG-C-Gly-HAT-FLAG.

The 5' and 3' flanking regions locate the cloning cassette into the *his-3* locus by homologous recombination. The flanking regions restore histidine auxotrophy from the recipient strain. Between these flanks lie the constitutive promoter *ccg-1*, the MCS, a HAT and a FLAG tag, as well as the *adh-1* terminator. The β-lactamase gene conveys Ampicillin resistance to *E. coli* strains.

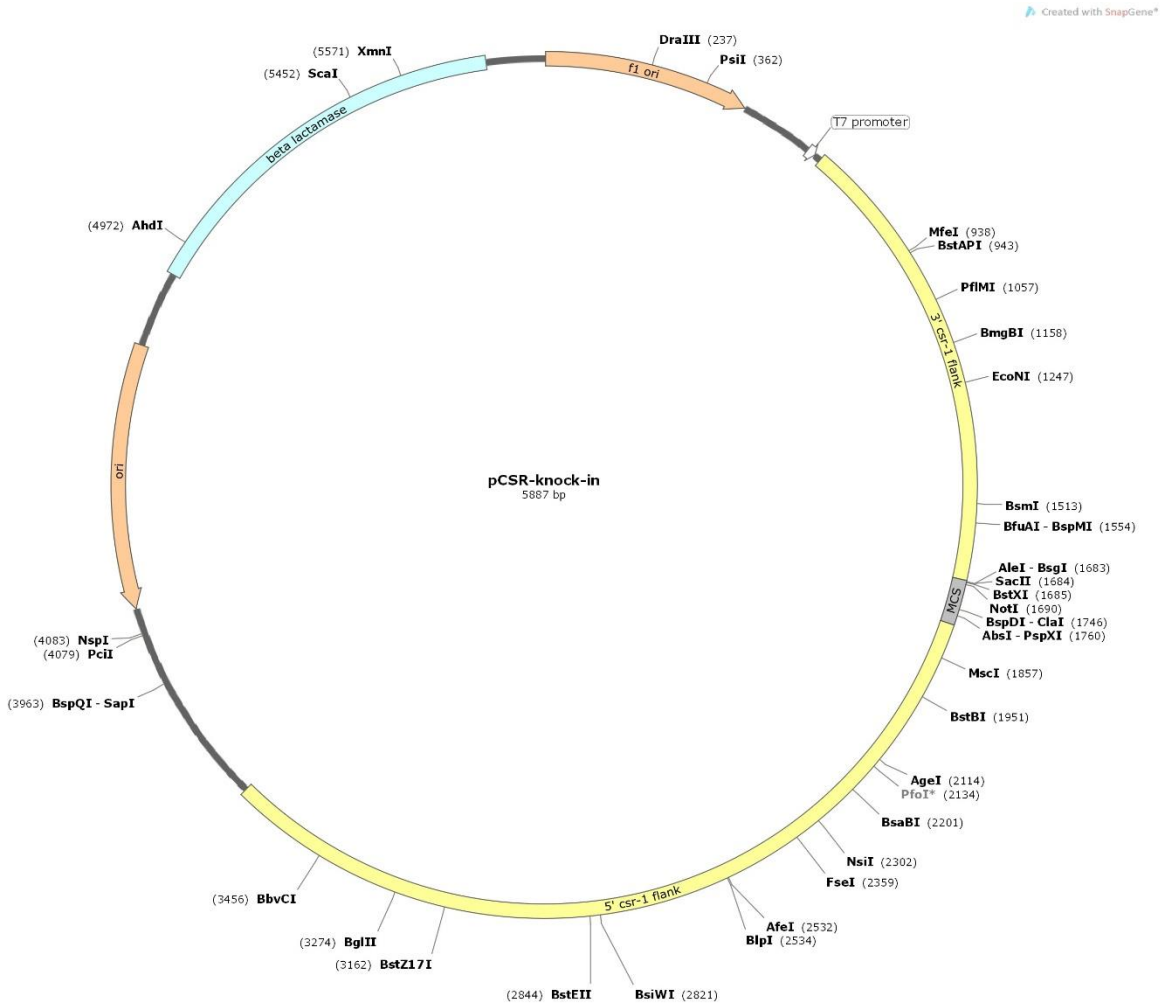

SFigure 6-12: Plasmid map of pCSR-knock-in.
The 5' and 3' flanking regions locate the cloning cassette into the *csr-1* locus by homologous recombination. Resistance to Cyclosporin A is transferred to *N. crassa* by disruption of the *csr-1* gene. Between these flanks lies the MCS. The β-lactamase gene conveys Ampicillin resistance to *E. coli* strains.

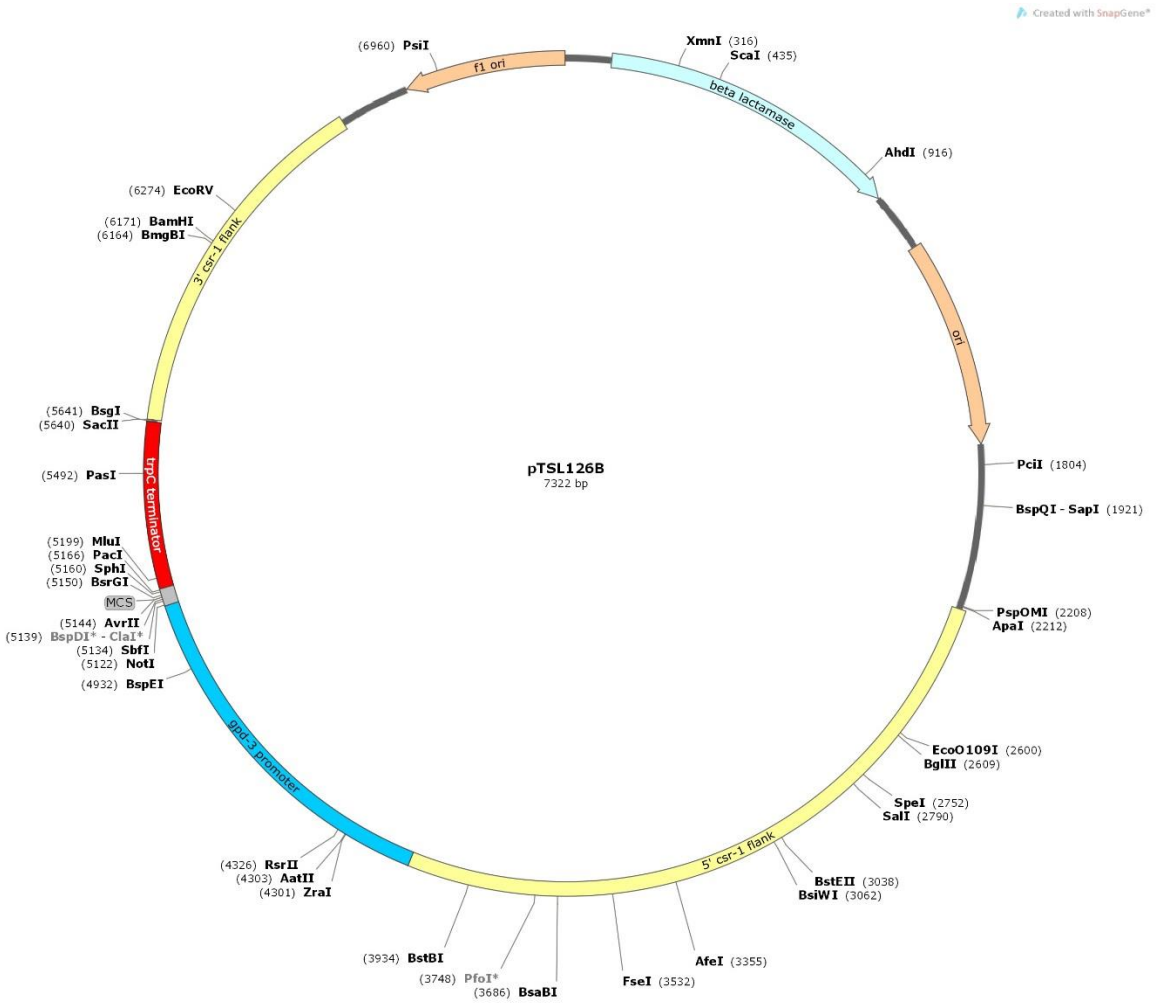

SFigure 6-13: Plasmid map of pTSL126B.

The 5' and 3' flanking regions locate the cloning cassette into the *csr-1* locus by homologous recombination. Resistance to Cyclosporin A is transferred to *N. crassa* by disruption the of the *csr-1* gene. Between these flanks lie the constitutive promoter *gpd-3*, the MCS and the *trpC* terminator. The β-lactamase gene conveys Ampicillin resistance to *E. coli* strains.

References

Agarwal UP, Reiner RR, Ralph SA. Cellulose Crystallinity of Woods , Wood Pulps , and Agricultural Fibers By FT-Raman Spectroscopy. Proc 16th ISWFPC 2011:69–75.

Alam MA, Kamlangdee N, Kelly JM. The CreB deubiquitinating enzyme does not directly target the CreA repressor protein in *Aspergillus nidulans*. Curr Genet 2017;63:647–67. doi:10.1007/s00294-016-0666-3.

Alazi E, Khosravi C, Homan TG, du Pré S, Arentshorst M, Di Falco M, *et al.* The pathway intermediate 2-keto-3-deoxy-L-galactonate mediates the induction of genes involved in D-galacturonic acid utilization in *Aspergillus niger*. FEBS Lett 2017;591:1408–18. doi:10.1002/1873-3468.12654.

Alazi E, Niu J, Kowalczyk JE, Peng M, Aguilar Pontes MV, van Kan JAL, *et al.* The transcriptional activator GaaR of *Aspergillus niger* is required for release and utilization of D-galacturonic acid from pectin. FEBS Lett 2016;590:1804–15. doi:10.1002/1873-3468.12211.

Alazi E, Niu J, Otto SB, Arentshorst M, Pham TTM, Tsang A, *et al.* W361R mutation in GaaR, the regulator of D-galacturonic acid-responsive genes, leads to constitutive production of pectinases in *Aspergillus niger*. Microbiologyopen 2018:e732. doi:10.1002/mbo3.732.

Alazi E, Ram AFJ. Modulating Transcriptional Regulation of Plant Biomass Degrading Enzyme Networks for Rational Design of Industrial Fungal Strains. Front Bioeng Biotechnol 2018;6:133. doi:10.3389/fbioe.2018.00133.

Albersheim P, Darvill AG, O'Neill MA, Schols HA, Voragen AGJ. An hypothesis: The same six polysaccharides are components of the primary cell walls of all higher plants, 1996, p. 47–55. doi:10.1016/S0921-0423(96)80245-0.

Altschul SF, Gish W, Miller W, Myers EW, Lipman DJ. Basic local alignment search tool. J Mol Biol 1990;215:403–10. doi:10.1016/S0022-2836(05)80360-2.

Anders S, Pyl PT, Huber W. HTSeq--a Python framework to work with high-throughput sequencing data. Bioinformatics 2015;31:166–9. doi:10.1093/bioinformatics/btu638.

Anderson CT. We be jammin': an update on pectin biosynthesis, trafficking and dynamics. J Exp Bot 2016;67:495–502. doi:10.1093/jxb/erv501.

Andrews S. FASTQC. A quality control tool for high throughput sequence data. 2016. http://www.bioinformatics.babraham.ac.uk/projects/fastqc/ (accessed October 25, 2017).

Aranda E. Promising approaches towards biotransformation of polycyclic aromatic hydrocarbons with Ascomycota fungi. Curr Opin Biotechnol 2016;38:1–8. doi:10.1016/j.copbio.2015.12.002.

Aro N, Pakula T, Penttilä M, Penttila M. Transcriptional regulation of plant cell wall degradation by filamentous fungi. FEMS Microbiol Rev 2005;29:719–39. doi:10.1016/j.femsre.2004.11.006.

Ashburner M, Ball CA, Blake JA, Botstein D, Butler H, Cherry JM, *et al.* Gene Ontology: tool for the unification of biology. Nat Genet 2000;25:25–9. doi:10.1038/75556.

Bailey C, Arst HN. Carbon Catabolite Repression in *Aspergillus nidulans*. Eur J Biochem 1975;51:573–7. doi:10.1111/j.1432-1033.1975.tb03958.x.

Bastawde KB. Xylan structure, microbial xylanases, and their mode of action. World J Microbiol Biotechnol 1992;8:353–68. doi:10.1007/BF01198746.

Battaglia E, Hansen SF, Leendertse A, Madrid S, Mulder H, Nikolaev I, *et al.* Regulation of pentose utilisation by AraR, but not XlnR, differs in *Aspergillus nidulans* and *Aspergillus niger*. Appl Microbiol Biotechnol 2011a;91:387–97. doi:10.1007/s00253-011-3242-2.

Battaglia E, Visser L, Nijssen A, van Veluw GJ, Wösten HAB, de Vries RP. Analysis of regulation of pentose utilisation in *Aspergillus niger* reveals evolutionary adaptations in Eurotiales. Stud Mycol 2011b;69:31–8. doi:10.3114/sim.2011.69.03.

Beadle GW, Tatum EL. Genetic Control of Biochemical Reactions in *Neurospora*. Proc Natl Acad Sci U S A 1941;27:499–506.

Beeson WT, Phillips CM, Cate JH, Marletta MA. Oxidative cleavage of cellulose by fungal copper-dependent polysaccharide monooxygenases. J Am Chem Soc 2012;134:890–2.

doi:10.1021/ja210657t.

Benocci T, Aguilar-Pontes MV, Zhou M, Seiboth B, de Vries RP. Regulators of plant biomass degradation in ascomycetous fungi. Biotechnol Biofuels 2017;10:152. doi:10.1186/s13068-017-0841-x.

Benocci T, Aguilar- Pontes MV, Kun RS, Seiboth B, de Vries RP, Daly P. ARA1 regulates not only L-arabinose but also d-galactose catabolism in *Trichoderma reesei*. FEBS Lett 2018;592:60–70. doi:10.1002/1873-3468.12932.

Benz J, Protzko RJ, Andrich JM, Bauer S, Dueber JE, Somerville CR. Identification and characterization of a galacturonic acid transporter from *Neurospora crassa* and its application for *Saccharomyces cerevisiae* fermentation processes. Biotechnol Biofuels 2014;7:20. doi:10.1186/1754-6834-7-20.

Benz JP, Chau BH, Zheng D, Bauer S, Glass NL, Somerville CR. A comparative systems analysis of polysaccharide-elicited responses in *Neurospora crassa* reveals carbon source-specific cellular adaptations. Mol Microbiol 2014;91:275–99. doi:10.1111/mmi.12459.

Bertani G. Studies on lysogenesis. I. The mode of phage liberation by lysogenic *Escherichia coli*. J Bacteriol 1951;62:293–300.

Bertaud F, Holmbom B. Chemical composition of earlywood and latewood in Norway spruce heartwood, sapwood and transition zone wood. Wood Sci Technol 2004;38:245–56. doi:10.1007/s00226-004-0241-9.

Beyer HM, Gonschorek P, Samodelov SL, Meier M, Weber W, Zurbriggen MD. AQUA Cloning: A Versatile and Simple Enzyme-Free Cloning Approach. PLoS One 2015;10:e0137652. doi:10.1371/journal.pone.0137652.

Blankenberg D, Gordon A, Von Kuster G, Coraor N, Taylor J, Nekrutenko A. Manipulation of FASTQ data with Galaxy. Bioinformatics 2010;26:1783–5. doi:10.1093/bioinformatics/btq281.

Bonnin E, Garnier C, Ralet MC. Pectin-modifying enzymes and pectin-derived materials: applications and impacts. Appl Microbiol Biotechnol 2014;98:519–32. doi:10.1007/s00253-013-5388-6.

Boratyn GM, Schäffer AA, Agarwala R, Altschul SF, Lipman DJ, Madden TL. Domain enhanced lookup time accelerated BLAST. Biol Direct 2012;7:12. doi:10.1186/1745-6150-7-12.

Borkovich KA, Alex LA, Yarden O, Turner GE, Read ND, Seiler S, *et al.* Lessons from the Genome Sequence of *Neurospora crassa*: Tracing the Path from Genomic Blueprint to Multicellular Organism. Microbiol Mol Biol Rev 2004;68:1–108. doi:10.1128/mmbr.68.1.1-108.2004.

Bradford MM. A rapid and sensitive method for the quantitation of microgram quantities of protein utilizing the principle of protein-dye binding. Anal Biochem 1976;72:248–54. doi:10.1016/0003-2697(76)90527-3.

Brameier M, Krings A, MacCallum RM. NucPred Predicting nuclear localization of proteins. Bioinformatics 2007;23:1159–60. doi:10.1093/bioinformatics/btm066.

van den Brink J, de Vries RP. Fungal enzyme sets for plant polysaccharide degradation. Appl Microbiol Biotechnol 2011;91:1477–92. doi:10.1007/s00253-011-3473-2.

Brown NA, Ries LNA, Goldman GH. How nutritional status signalling coordinates metabolism and lignocellulolytic enzyme secretion. Fungal Genet Biol 2014;72:48–63. doi:10.1016/j.fgb.2014.06.012.

Bubner P, Plank H, Nidetzky B. Visualizing cellulase activity. Biotechnol Bioeng 2013;110:1529–49. doi:10.1002/bit.24884.

Caffall KH, Mohnen D. The structure, function, and biosynthesis of plant cell wall pectic polysaccharides. Carbohydr Res 2009;344:1879–900. doi:10.1016/j.carres.2009.05.021.

Cai P, Gu R, Wang B, Li J, Wan L, Tian C, *et al.* Evidence of a Critical Role for Cellodextrin Transporte 2 (CDT-2) in Both Cellulose and Hemicellulose Degradation and Utilization in *Neurospora crassa*. PLoS One 2014;9:e89330. doi:10.1371/journal.pone.0089330.

Camacho C, Coulouris G, Avagyan V, Ma N, Papadopoulos J, Bealer K, *et al.* BLAST+: architecture and applications. BMC Bioinformatics 2009;10:421. doi:10.1186/1471-2105-10-421.

Cantarel BL, Coutinho PM, Rancurel C, Bernard T, Lombard V, Henrissat B. The Carbohydrate-Active EnZymes database (CAZy): an expert resource for Glycogenomics. Nucleic Acids Res 2009;37:D233-8. doi:10.1093/nar/gkn663.

Carpita NC, Gibeaut DM. Structural models of primary cell walls in flowering plants: consistency of molecular structure with the physical properties of the walls during growth. Plant J 1993;3:1–30. doi:10.1111/j.1365-313X.1993.tb00007.x.

Christensen U, Gruben BS, Madrid S, Mulder H, Nikolaev I, de Vries RP. Unique Regulatory Mechanism for D-Galactose Utilization in *Aspergillus nidulans*. Appl Environ Microbiol 2011;77:7084–7. doi:10.1128/AEM.05290-11.

Chung D, Pattathil S, Biswal AK, Hahn MG, Mohnen D, Westpheling J. Deletion of a gene cluster encoding pectin degrading enzymes in *Caldicellulosiruptor bescii* reveals an important role for pectin in plant biomass recalcitrance. Biotechnol Biofuels 2014;7:147. doi:10.1186/s13068-014-0147-1.

Colot H V, Park G, Turner GE, Ringelberg C, Crew CM, Litvinkova L, *et al.* A high-throughput gene knockout procedure for *Neurospora* reveals functions for multiple transcription factors. Proc Natl Acad Sci U S A 2006;103:10352–7. doi:10.1073/pnas.0601456103.

Coradetti ST, Craig JP, Xiong Y, Shock T, Tian C, Glass NL. Conserved and essential transcription factors for cellulase gene expression in ascomycete fungi. Proc Natl Acad Sci 2012;109:7397–402. doi:10.1073/pnas.1200785109.

Coradetti ST, Xiong Y, Glass NL. Analysis of a conserved cellulase transcriptional regulator reveals inducer-independent production of cellulolytic enzymes in *Neurospora crassa*. Microbiologyopen 2013;2:595–609. doi:10.1002/mbo3.94.

Cosgrove DJ. Growth of the plant cell wall. Nat Rev Mol Cell Biol 2005;6:850–61. doi:10.1038/nrm1746.

Cosgrove DJ, Jarvis MC. Comparative structure and biomechanics of plant primary and secondary cell walls. Front Plant Sci 2012;3:204. doi:10.3389/fpls.2012.00204.

la Cour T, Kiemer L, Mølgaard A, Gupta R, Skriver K, Brunak S. Analysis and prediction of leucine-rich nuclear export signals. Protein Eng Des Sel 2004;17:527–36. doi:10.1093/protein/gzh062.

Craig JP, Coradetti ST, Starr TL, Glass NL. Direct Target Network of the *Neurospora crassa* Plant Cell Wall Deconstruction Regulators CLR-1, CLR-2, and XLR-1. MBio 2015;6:e01452-15. doi:10.1128/mBio.01452-15.

Crotti LB, Jorge JA, Terenzi HF, Polizeli MLTM. Purification and characterization of galactose-induced pectinases from the exo-1 mutant strain of *Neurospora crassa*. Prog. Biotechnol., vol. 14, 1996, p. 787–92. doi:10.1016/S0921-0423(96)80317-0.

Crotti LB, Terenzi HF, Jorge JA, Polizeli MDLTM. Regulation of pectic enzymes from the exo-1 mutant strain of *Neurospora crassa*: effects of glucose, galactose, and galacturonic acid. J Basic Microbiol 1998a;38:181–8. doi:10.1002/(SICI)1521-4028(199807)38:3<181::AID-JOBM181>3.0.CO;2-N.

Crotti LB, Terenzi HF, Jorge JA, Polizeli MLTM. Characterization of galactose-induced extracellular and intracellular pectolytic activities from the exo-1 mutant strain of *Neurospora crassa*. J Ind Microbiol Biotechnol 1998b;20:238–43. doi:10.1038/sj.jim.2900519.

Culleton H, McKie V, de Vries RP. Physiological and molecular aspects of degradation of plant polysaccharides by fungi: What have we learned from *Aspergillus*? Biotechnol J 2013;8:884–94. doi:10.1002/biot.201200382.

Cziferszky A, Mach RL, Kubicek CP. Phosphorylation Positively Regulates DNA Binding of the Carbon Catabolite Repressor Cre1 of *Hypocrea jecorina* (*Trichoderma reesei*). J Biol Chem 2002;277:14688–94. doi:10.1074/jbc.M200744200.

Daher FB, Braybrook SA. How to let go: pectin and plant cell adhesion. Front Plant Sci 2015;6:523. doi:10.3389/fpls.2015.00523.

Damasio AR de L, Rubio MV, Gonçalves TA, Persinoti GF, Segato F, Prade RA, *et al.* Xyloglucan breakdown by endo-xyloglucanase family 74 from *Aspergillus fumigatus*. Appl Microbiol Biotechnol 2017;101:2893–903. doi:10.1007/s00253-016-8014-6.

Danquah MK, Forde GM. Growth Medium Selection and Its Economic Impact on Plasmid

DNA Production. J Biosci Bioeng 2007;104:490–7. doi:10.1263/jbb.104.490.

Davis RH. *Neurospora*: Contributions of a Model Organism. Oxford University Press; 2000.
Delmas S, Pullan ST, Gaddipati S, Kokolski M, Malla S, Blythe MJ, *et al.* Uncovering the genome-wide transcriptional responses of the filamentous fungus *Aspergillus niger* to lignocellulose using RNA sequencing. PLoS Genet 2012;8:e1002875. doi:10.1371/journal.pgen.1002875.

Demain AL. Biosolutions to the energy problem. J Ind Microbiol Biotechnol 2009;36:319–32. doi:10.1007/s10295-008-0521-8.

Dementhon K, Iyer G, Glass NL. VIB-1 is required for expression of genes necessary for programmed cell death in *Neurospora crassa*. Eukaryot Cell 2006;5:2161–73. doi:10.1128/EC.00253-06.

Denton JA, Kelly JM. Disruption of *Trichoderma reesei* cre2, encoding an ubiquitin C-terminal hydrolase, results in increased cellulase activity. BMC Biotechnol 2011;11:103. doi:10.1186/1472-6750-11-103.

Dereeper A, Audic S, Claverie J-M, Blanc G. BLAST-EXPLORER helps you building datasets for phylogenetic analysis. BMC Evol Biol 2010;10:8. doi:10.1186/1471-2148-10-8.

Dereeper A, Guignon V, Blanc G, Audic S, Buffet S, Chevenet F, *et al.* Phylogeny.fr: robust phylogenetic analysis for the non-specialist. Nucleic Acids Res 2008;36:W465–9. doi:10.1093/nar/gkn180.

Derntl C, Gudynaite-Savitch L, Calixte S, White T, Mach RL, Mach-Aigner AR. Mutation of the Xylanase regulator 1 causes a glucose blind hydrolase expressing phenotype in industrially used *Trichoderma* strains. Biotechnol Biofuels 2013;6:62. doi:10.1186/1754-6834-6-62.

Dick-Pérez M, Zhang Y, Hayes J, Salazar A, Zabotina OA, Hong M. Structure and Interactions of Plant Cell-Wall Polysaccharides by Two- and Three-Dimensional Magic-Angle-Spinning Solid-State NMR. Biochemistry 2011;50:989–1000. doi:10.1021/bi101795q.

Dietschmann A. Deciphering L-rhamnose mediated pectin degradation signaling in the model filamentous fungus *Neurospora crassa*. Technical University Munich, 2015.

Ding S-Y, Liu Y-S, Zeng Y, Himmel ME, Baker JO, Bayer EA. How Does Plant Cell Wall Nanoscale Architecture Correlate with Enzymatic Digestibility? Science (80-) 2012;338:1055–60. doi:10.1126/science.1227491.

Dogaris I, Mamma D, Kekos D. Biotechnological production of ethanol from renewable resources by *Neurospora crassa*: an alternative to conventional yeast fermentations? Appl Microbiol Biotechnol 2013;97:1457–73. doi:10.1007/s00253-012-4655-2.

Dowzer CE, Kelly JM. Analysis of the creA gene, a regulator of carbon catabolite repression in *Aspergillus nidulans*. Mol Cell Biol 1991;11:5701–9. doi:10.1128/MCB.11.11.5701.

Dowzer CEA, Kelly JM. Cloning of the creA gene from *Aspergillus nidulans*: a gene involved in carbon catabolite repression. Curr Genet 1989;15:457–9. doi:10.1007/BF00376804.

Dragovic Z, Tan Y, Görl M, Roenneberg T, Merrow M. Light reception and circadian behavior in “blind” and “clock-less” mutants of *Neurospora crassa*. EMBO J 2002;21:3643–51. doi:10.1093/emboj/cdf377.

Dunlap JC, Borkovich KA, Henn MR, Turner GE, Sachs MS, Glass NL, *et al.* Enabling a Community to Dissect an Organism: Overview of the *Neurospora* Functional Genomics Project. Adv Genet, vol. 57. 2007/03/14, 2007, p. 49–96. doi:10.1016/S0065-2660(06)57002-6.

Dunlap JC, Loros JJ. How fungi keep time: circadian system in *Neurospora* and other fungi. Curr Opin Microbiol 2006;9:579–87. doi:http://dx.doi.org/10.1016/j.mib.2006.10.008.

Ebbole DJ. Carbon Catabolite Repression of Gene Expression and Conidiation in *Neurospora crassa*. Fungal Genet Biol 1998;25:15–21. doi:10.1006/fgbi.1998.1088.

Edwards MC, Doran-Peterson J. Pectin-rich biomass as feedstock for fuel ethanol production. Appl Microbiol Biotechnol 2012;95:565–75. doi:10.1007/s00253-012-4173-2.

El-Gebali S, Mistry J, Bateman A, Eddy SR, Luciani A, Potter SC, *et al.* The Pfam protein families database in 2019. Nucleic Acids Res 2019;47:D427–32. doi:10.1093/nar/gky995.

Emri T, Szilágyi M, László K, M-Hamvas M, Pócsi I. PepJ is a new extracellular proteinase

of *Aspergillus nidulans*. Folia Microbiol (Praha) 2009;54:105–9. doi:10.1007/s12223-009-0015-8.

Englesberg E. GLUCOSE INHIBITION AND THE DIAUXIE PHENOMENON. Proc Natl Acad Sci U S A 1959;45:1494–507.

Ewels P, Magnusson M, Lundin S, Käller M. MultiQC: summarize analysis results for multiple tools and samples in a single report. Bioinformatics 2016;32:3047–8. doi:10.1093/bioinformatics/btw354.

Fan LT, Lee Y-H, Beardmore DR. The influence of major structural features of cellulose on rate of enzymatic hydrolysis. Biotechnol Bioeng 1981;23:419–24. doi:10.1002/bit.260230215.

Fengel D, Grosser D. Chemische Zusammensetzung von Nadel- und Laubhölzern. Holz Als Roh- Und Werkst 1975;33:32–4. doi:10.1007/BF02612913.

Fernando S, Adhikari S, Chandrapal C, Murali N. Biorefineries: Current Status, Challenges, and Future Direction. Energy & Fuels 2006;20:1727–37. doi:10.1021/ef060097w.

Fleissner A, Simonin AR, Glass NL. Cell fusion in the filamentous fungus, *Neurospora crassa*. Methods Mol Biol 2008;475:21–38. doi:10.1007/978-1-59745-250-2_2.

Freitag M, Selker EU. Controlling DNA methylation: many roads to one modification. Curr Opin Genet Dev 2005;15:191–9. doi:10.1016/j.gde.2005.02.003.

Frey-Wyssling A. The Fine Structure of Cellulose Microfibrils. Science (80-) 1954;119:80–2. doi:10.1126/science.119.3081.80.

Fujino T, Sone Y, Mitsuishi Y, Itoh T. Characterization of Cross-Links between Cellulose Microfibrils, and Their Occurrence during Elongation Growth in Pea Epicotyl. Plant Cell Physiol 2000;41:486–94. doi:10.1093/pcp/41.4.486.

Fulton LM, Lynd LR, Körner A, Greene N, Tonachel LR. The need for biofuels as part of a low carbon energy future. Biofuels, Bioprod Biorefining 2015;9:476–83. doi:10.1002/bbb.1559.

Gabriel R, Thieme N, Schuerg T, McCluskey K, Baker SE, Hart S, *et al.* Reverse Engineering CAZy Hypersecretion in Filamentous Fungi (manuscript in preparation) 2019.

Galagan JE, Calvo SE, Borkovich KA, Selker EU, Read ND, Jaffe D, *et al.* The genome sequence of the filamentous fungus *Neurospora crassa*. Nature 2003;422:859–68. doi:10.1038/nature01554.

Galagan JE, Selker EU. RIP: the evolutionary cost of genome defense. Trends Genet 2004;20:417–23. doi:10.1016/j.tig.2004.07.007.

Galazka JM, Tian C, Beeson WT, Martinez B, Glass NL, Cate JHD. Cellodextrin transport in yeast for improved biofuel production. Science 2010;330:84–6. doi:10.1126/science.1192838.

Gancedo JM. Yeast Carbon Catabolite Repression. Microbiol Mol Biol Rev 1998;62:334–61.

Garna H, Mabon N, Nott K, Wathelet B, Paquot M. Kinetic of the hydrolysis of pectin galacturonic acid chains and quantification by ionic chromatography. Food Chem 2006;96:477–84. doi:10.1016/j.foodchem.2005.03.002.

Garna H, Mabon N, Wathelet B, Paquot M. New Method for a Two-Step Hydrolysis and Chromatographic Analysis of Pectin Neutral Sugar Chains. J Agric Food Chem 2004;52:4652–9. doi:10.1021/jf049647j.

Gielkens MMC, Dekkers E, Visser J, de Graaff LH. Two Cellobiohydrolase-Encoding Genes from *Aspergillus niger* Require D-Xylose and the Xylanolytic Transcriptional Activator XlnR for Their Expression. Appl Environ Microbiol 1999;65:4340–5.

Glass NL, Dunlap J, Selker E, Bell-pedersen D, Sachs M, Taylor J, *et al.* Joint Genome Institute Community Sequencing Project ID 982 2013a:1–22.

Glass NL, Schmoll M, Cate JHDD, Coradetti S. Plant cell wall deconstruction by ascomycete fungi. Annu Rev Microbiol 2013b;67:477–98. doi:10.1146/annurev-micro-092611-150044.

Gratzner H, Sheehan DN. *Neurospora* mutant exhibiting hyperproduction of amylase and

invertase. J Bacteriol 1969;97:544–9.

Gratzner HG. Cell wall alterations associated with the hyperproduction of extracellular enzymes in *Neurospora crassa*. J Bacteriol 1972;111:443–6.

Green MM, Blankenhorn G, Hart H. Which starch fraction is water-soluble, amylose or amylopectin? J Chem Educ 1975;52:729. doi:10.1021/ed052p729.

Griffiths AJF, Collins RA, Nargang FE. Mitochondrial Genetics of *Neurospora*. In: Kück U, editor. Genet. Biotechnol., vol. 2, Springer Berlin Heidelberg; 1995, p. 93–105. doi:10.1007/978-3-662-10364-7_7.

Grimmler C, Held C, Liebl W, Ehrenreich A. Transcriptional analysis of catabolite repression in Clostridium acetobutylicum growing on mixtures of D-glucose and D-xylose. J Biotechnol 2010;150:315–23. doi:10.1016/J.JBIOTEC.2010.09.938.

Gruben BS, Mäkelä MR, Kowalczyk JE, Zhou M, Benoit-Gelber I, De Vries RP. Expression-based clustering of CAZyme-encoding genes of *Aspergillus niger*. BMC Genomics 2017;18:900. doi:10.1186/s12864-017-4164-x.

Gruben BS, Zhou M, de Vries RP. GalX regulates the D-galactose oxido-reductive pathway in *Aspergillus niger*. FEBS Lett 2012;586:3980–5. doi:10.1016/j.febslet.2012.09.029.

Gruben BS, Zhou M, Wiebenga A, Ballering J, Overkamp KM, Punt PJ, *et al. Aspergillus niger* RhaR, a regulator involved in L-rhamnose release and catabolism. Appl Microbiol Biotechnol 2014;98:5531–40. doi:10.1007/s00253-014-5607-9.

Ha S, Galazka JM, Rin S, Choi J, Yang X, Seo J. Engineered *Saccharomyces cerevisiae* capable of simultaneous cellobiose and xylose fermentation. Proc Natl Acad Sci 2010:1–6. doi:10.1073/pnas.1010456108/-/DCSupplemental.www.pnas.org/cgi/doi/10.1073/pnas.1010456108.

Haffner FB, Mitchell VD, Arundale RA, Bauer S. Compositional analysis of M*iscanthus giganteus* by near infrared spectroscopy. Cellulose 2013;20:1629–37. doi:10.1007/s10570-013-9935-1.

Hanahan D. Studies on transformation of *Escherichia coli* with plasmids. J Mol Biol

1983;166:557–80. doi:10.1016/S0022-2836(83)80284-8.

Harholt J, Suttangkakul A, Vibe Scheller H. Biosynthesis of Pectin. PLANT Physiol 2010;153:384–95. doi:10.1104/pp.110.156588.

Harris P V, Welner D, McFarland KC, Re E, Navarro Poulsen JC, Brown K, *et al.* Stimulation of lignocellulosic biomass hydrolysis by proteins of glycoside hydrolase family 61: structure and function of a large, enigmatic family. Biochemistry 2010;49:3305–16. doi:10.1021/bi100009p.

Harris PJ, Smith BG. Plant cell walls and cell-wall polysaccharides: structures, properties and uses in food products. Int J Food Sci Technol 2006;41:129–43. doi:10.1111/j.1365-2621.2006.01470.x.

Hasper AA. Functional analysis of the transcriptional activator XlnR from *Aspergillus niger*. Microbiology 2004;150:1367–75. doi:10.1099/mic.0.26557-0.

Hassan L, Lin L, Sorek H, Goudoulas T, Germann N, Tian C, *et al.* Cross-talk of cellulose and mannan perception pathways leads to inhibition of cellulase production in several filamentous fungi. BioRxiv 2019:520130. doi:10.1101/520130.

Hassan L, Reppke MJ, Thieme N, Schweizer SA, Mueller CW, Benz JP. Comparing the physiochemical parameters of three celluloses reveals new insights into substrate suitability for fungal enzyme production. Fungal Biol Biotechnol 2017;4:10. doi:10.1186/s40694-017-0039-9.

Have A ten, Mulder W, Visser J, van Kan JAL. The Endopolygalacturonase Gene Bcpg1 Is Required for Full Virulence of *Botrytis cinerea*. Mol Plant-Microbe Interact 1998;11:1009–16. doi:10.1094/MPMI.1998.11.10.1009.

Herold S, Bischof R, Metz B, Seiboth B, Kubicek CP. Xylanase Gene Transcription in *Trichoderma reesei* Is Triggered by Different Inducers Representing Different Hemicellulosic Pentose Polymers. Eukaryot Cell 2013;12:390–8. doi:10.1128/EC.00182-12.

Himmel ME, Ding S-Y, Johnson DK, Adney WS, Nimlos MR, Brady JW, *et al.* Biomass Recalcitrance: Engineering Plants and Enzymes for Biofuels Production. Science (80-) 2007;315:804–7. doi:10.1126/science.1137016.

Hsiao HY, Chiang LC, Ueng PP, Tsao GT. Sequential utilization of mixed monosaccharides by yeasts. Appl Environ Microbiol 1982;43:840–5.

Huberman LB, Coradetti ST, Glass NL. Network of nutrient-sensing pathways and a conserved kinase cascade integrate osmolarity and carbon sensing in *Neurospora crassa*. Proc Natl Acad Sci 2017;114:E8665–74. doi:10.1073/pnas.1707713114.

Huberman LB, Liu J, Qin L, Glass NL. Regulation of the lignocellulolytic response in filamentous fungi. Fungal Biol Rev 2016;30:101–11. doi:10.1016/j.fbr.2016.06.001.

Hunter AJ, Morris TA, Jin B, Saint CP, Kelly JM. Deletion of creB in *Aspergillus oryzae* Increases Secreted Hydrolytic Enzyme Activity. Appl Environ Microbiol 2013;79:5480–7. doi:10.1128/AEM.01406-13.

Hurley JM, Dasgupta A, Emerson JM, Zhou X, Ringelberg CS, Knabe N, *et al.* Analysis of clock-regulated genes in *Neurospora* reveals widespread posttranscriptional control of metabolic potential. Proc Natl Acad Sci 2014;111:16995–7002. doi:10.1073/pnas.1418963111.

Ilmén M, Thrane C, Penttilä M. The glucose repressor gene cre1 of *Trichoderma*: Isolation and expression of a full-length and a truncated mutant form. MGG Mol Gen Genet 1996;251:451–60. doi:10.1007/BF02172374.

Jäger G, Büchs J. Biocatalytic conversion of lignocellulose to platform chemicals. Biotechnol J 2012;7:1122–36. doi:10.1002/biot.201200033.

Janus D, Hortschansky P, Kück U. Identification of a minimal cre1 promoter sequence promoting glucose-dependent gene expression in the β-lactam producer *Acremonium chrysogenum*. Curr Genet 2008;53:35–48. doi:10.1007/s00294-007-0164-8.

Jarvis MC, Forsyth W, Duncan HJ. A Survey of the Pectic Content of Nonlignified Monocot Cell Walls. PLANT Physiol 1988;88:309–14. doi:10.1104/pp.88.2.309.

Jiang Z, Fei B, Chen X, Jayanetti L. Wood properties of the global important tree species. Beijing: Science Press Beijing; 2013.

Juhász R, Salgó A. Pasting Behavior of Amylose, Amylopectin and Their Mixtures as Determined by RVA Curves and First Derivatives. Starch - Stärke 2008;60:70–8. doi:10.1002/star.200700634.

Kačuráková M, Capek P, Sasinková V, Wellner N, Ebringerová A, Kacuráková M. FT-IR study of plant cell wall model compounds: pectic polysaccharides and hemicelluloses. Carbohydr Polym 2000;43:195–203. doi:10.1016/S0144-8617(00)00151-X.

Kars I, Krooshof GH, Wagemakers L, Joosten R, Benen JAE, Van Kan JAL. Necrotizing activity of five Botrytis cinerea endopolygalacturonases produced in *Pichia pastoris*. Plant J 2005;43:213–25. doi:10.1111/j.1365-313X.2005.02436.x.

Kavakli IH, Slattery CJ, Ito H, Okita TW. The conversion of carbon and nitrogen into starch and storage proteins in developing storage organs: an overview. Funct Plant Biol 2000;27:561. doi:10.1071/PP99176.

Keegstra K. Plant Cell Walls. PLANT Physiol 2010;154:483–6. doi:10.1104/pp.110.161240.
Keller NP, Turner G, Bennett JW. Fungal secondary metabolism — from biochemistry to genomics. Nat Rev Microbiol 2005;3:937–47. doi:10.1038/nrmicro1286.

Kim D, Pertea G, Trapnell C, Pimentel H, Kelley R, Salzberg SL. TopHat2: accurate alignment of transcriptomes in the presence of insertions, deletions and gene fusions. Genome Biol 2013;14:R36. doi:10.1186/gb-2013-14-4-r36.

Kim H, Lee WH, Galazka JM, Cate JH, Jin YS. Analysis of cellodextrin transporters from *Neurospora crassa* in *Saccharomyces cerevisiae* for cellobiose fermentation. Appl Microbiol Biotechnol 2014;98:1087–94. doi:10.1007/s00253-013-5339-2.

Kim Y, Islam N, Moss BJ, Nandakumar MP, Marten MR. Autophagy induced by rapamycin and carbon-starvation have distinct proteome profiles in *Aspergillus nidulans*. Biotechnol Bioeng 2011;108:2705–15. doi:10.1002/bit.23223.

Klaubauf S, Zhou M, Lebrun M-H, de Vries RP, Battaglia E. A novel <scp>l</scp> -arabinose-responsive regulator discovered in the rice-blast fungus *Pyricularia oryzae* (*Magnaporthe oryzae*). FEBS Lett 2016;590:550–8. doi:10.1002/1873-3468.12070.

Koivistoinen OM, Arvas M, Headman JR, Andberg M, Penttilä M, Jeffries TW, *et al.*

Characterisation of the gene cluster for L-rhamnose catabolism in the yeast Scheffersomyces (Pichia) stipitis. Gene 2012;492:177–85. doi:10.1016/j.gene.2011.10.031.

Krebs EG, Beavo JA. Phosphorylation-Dephosphorylation of Enzymes. Annu Rev Biochem 1979;48:923–59. doi:10.1146/annurev.bi.48.070179.004423.

Kruger NJ, von Schaewen A. The oxidative pentose phosphate pathway: structure and organisation. Curr Opin Plant Biol 2003;6:236–46. doi:10.1016/S1369-5266(03)00039-6.

Kubicek CP, Mikus M, Schuster A, Schmoll M, Seiboth B. Metabolic engineering strategies for the improvement of cellulase production by *Hypocrea jecorina*. Biotechnol Biofuels 2009;2:19. doi:10.1186/1754-6834-2-19.

Kulmburg P, Mathieu M, Dowzer C, Kelly J, Felenbok B. Specific binding sites in the alcR and alcA promoters of the ethanol regulon for the CREA repressor mediating carbon cataboiite repression in *Aspergillus nidulans*. Mol Microbiol 1993;7:847–57. doi:10.1111/j.1365-2958.1993.tb01175.x.

Kumar A, Henrissat B, Arvas M, Syed MF, Thieme N, Benz JP, *et al.* De Novo Assembly and Genome Analyses of the Marine-Derived *Scopulariopsis brevicaulis* Strain LF580 Unravels Life-Style Traits and Anticancerous Scopularide Biosynthetic Gene Cluster. PLoS One 2015;10:e0140398. doi:10.1371/journal.pone.0140398.

Kuo H-C, Hui S, Choi J, Asiegbu FO, Valkonen JPT, Lee Y-H. Secret lifestyles of *Neurospora crassa*. Sci Rep 2014;4:5135. doi:10.1038/srep05135.

Lagunas R. Sugar transport in *Saccharomyces cerevisiae*. FEMS Microbiol Rev 1993;10:229–42.

Lameiras F, Ras C, ten Pierick A, Heijnen JJ, van Gulik WM. Stoichiometry and kinetics of single and mixed substrate uptake in *Aspergillus niger*. Bioprocess Biosyst Eng 2018;41:157–70. doi:10.1007/s00449-017-1854-3.

Lamond AI, Spector DL. Nuclear speckles: a model for nuclear organelles. Nat Rev Mol Cell Biol 2003;4:605–12. doi:10.1038/nrm1172.

Lattanzio V, Lattanzio VMT, Cardinali A. Phytochemistry: Advances in Research. vol. 661.

2006.

Lechner E, Achard P, Vansiri A, Potuschak T, Genschik P. F-box proteins everywhere. Curr Opin Plant Biol 2006;9:631–8. doi:10.1016/j.pbi.2006.09.003.

Li J, Lin L, Li H, Tian C, Ma Y. Transcriptional comparison of the filamentous fungus *Neurospora crassa* growing on three major monosaccharides D-glucose, D-xylose and L-arabinose. Biotechnol Biofuels 2014;7:31. doi:10.1186/1754-6834-7-31.

Li W, Cowley A, Uludag M, Gur T, McWilliam H, Squizzato S, *et al.* The EMBL-EBI bioinformatics web and programmatic tools framework. Nucleic Acids Res 2015;43:W580-4. doi:10.1093/nar/gkv279.

Lian J, Li Y, HamediRad M, Zhao H. Directed evolution of a cellodextrin transporter for improved biofuel production under anaerobic conditions in *Saccharomyces cerevisiae*. Biotechnol Bioeng 2014;111:1521–31. doi:10.1002/bit.25214.

Lichius A, Seidl-Seiboth V, Seiboth B, Kubicek CP. Nucleo-cytoplasmic shuttling dynamics of the transcriptional regulators XYR1 and CRE1 under conditions of cellulase and xylanase gene expression in *Trichoderma reesei*. Mol Microbiol 2014;94:1162–78. doi:10.1111/mmi.12824.

Linden H, Ballario P, Macino G. Blue light regulation in *Neurospora crassa*. Fungal Genet Biol 1997;22:141–50. doi:10.1006/fgbi.1997.1013.

Liu B, Zhang Y, Zhang X, Yan C, Zhang Y, Xu X, *et al.* Discovery of a rhamnose utilization pathway and rhamnose-inducible promoters in *Pichia pastoris*. Sci Rep 2016;6:27352. doi:10.1038/srep27352.

Liu Q, Li J, Gao R, Li J, Ma G, Tian C. CLR-4, a novel conserved transcription factor for cellulase gene expression in ascomycete fungi. Mol Microbiol 2018;0:1–22. doi:10.1111/mmi.14160.

Lombard V, Golaconda Ramulu H, Drula E, Coutinho PM, Henrissat B. The carbohydrate-active enzymes database (CAZy) in 2013. Nucleic Acids Res 2014;42:D490-5. doi:10.1093/nar/gkt1178.

Loomis WF, Magasanik B. Glucose-lactose diauxie in *Escherichia coli*. J Bacteriol 1967;93:1397–401.

Love MI, Huber W, Anders S. Moderated estimation of fold change and dispersion for RNA-seq data with DESeq2. Genome Biol 2014;15:550. doi:10.1186/s13059-014-0550-8.

Lynd LR, Liang X, Biddy MJ, Allee A, Cai H, Foust T, *et al.* Cellulosic ethanol: status and innovation. Curr Opin Biotechnol 2017;45:202–11. doi:10.1016/j.copbio.2017.03.008.

MacPherson S, Larochelle M, Turcotte B. A fungal family of transcriptional regulators: the zinc cluster proteins. Microbiol Mol Biol Rev 2006;70:583–604. doi:10.1128/MMBR.00015-06.

Mäkelä MR, Aguilar-Pontes MV, van Rossen-Uffink D, Peng M, de Vries RP. The fungus *Aspergillus niger* consumes sugars in a sequential manner that is not mediated by the carbon catabolite repressor CreA. Sci Rep 2018;8:6655. doi:10.1038/s41598-018-25152-x.

Mallinson SJB, Machovina MM, Silveira RL, Garcia-Borràs M, Gallup N, Johnson CW, *et al.* A promiscuous cytochrome P450 aromatic O-demethylase for lignin bioconversion. Nat Commun 2018;9:2487. doi:10.1038/s41467-018-04878-2.

Mansfield SD, Mooney C, Saddler JN. Substrate and Enzyme Characteristics that Limit Cellulose Hydrolysis. Biotechnol Prog 1999;15:804–16. doi:10.1021/bp9900864.

Marchler-Bauer A, Bo Y, Han L, He J, Lanczycki CJ, Lu S, *et al.* CDD/SPARCLE: functional classification of proteins via subfamily domain architectures. Nucleic Acids Res 2017;45:D200–3. doi:10.1093/nar/gkw1129.

Marchler-Bauer A, Bryant SH. CD-Search: protein domain annotations on the fly. Nucleic Acids Res 2004;32:W327–31. doi:10.1093/nar/gkh454.

Marchler-Bauer A, Derbyshire MK, Gonzales NR, Lu S, Chitsaz F, Geer LY, *et al.* CDD: NCBI's conserved domain database. Nucleic Acids Res 2015;43:D222–6. doi:10.1093/nar/gku1221.

Marchler-Bauer A, Lu S, Anderson JB, Chitsaz F, Derbyshire MK, DeWeese-Scott C, *et al.* CDD: a Conserved Domain Database for the functional annotation of proteins. Nucleic

Acids Res 2011;39:D225–9. doi:10.1093/nar/gkq1189.

Martens-Uzunova ES, Schaap PJ. Assessment of the pectin degrading enzyme network of *Aspergillus niger* by functional genomics. Fungal Genet Biol 2009;46 Suppl 1:S170–9.

Matera AG, Izaguire-Sierra M, Praveen K, Rajendra TK. Nuclear Bodies: Random Aggregates of Sticky Proteins or Crucibles of Macromolecular Assembly? Dev Cell 2009;17:639–47. doi:10.1016/j.devcel.2009.10.017.

Mathieu M, Felenbok B. The *Aspergillus nidulans* CREA protein mediates glucose repression of the ethanol regulon at various levels through competition with the ALCR-specific transactivator. EMBO J 1994;13:4022–7. doi:10.1002/j.1460-2075.1994.tb06718.x.

Matthews JF, Skopec CE, Mason PE, Zuccato P, Torget RW, Sugiyama J, *et al.* Computer simulation studies of microcrystalline cellulose Iβ. Carbohydr Res 2006;341:138–52. doi:10.1016/j.carres.2005.09.028.

McCann M, Wells B, Roberts K. Direct visualization of cross-links in the primary plant cell wall. J Cell Sci 1990;96:323–34.

McCluskey K, Wiest a., Plamann M. The Fungal Genetics Stock Center: a repository for 50 years of fungal genetics research. J Biosci 2010;35:119–26. doi:10.1007/s12038-010-0014-6.

McWilliam H, Li W, Uludag M, Squizzato S, Park YM, Buso N, *et al.* Analysis Tool Web Services from the EMBL-EBI. Nucleic Acids Res 2013;41:W597-600. doi:10.1093/nar/gkt376.

Meerts P. Mineral nutrient concentrations in sapwood and heartwood: a literature review. Ann For Sci 2002;59:713–22. doi:10.1051/forest:2002059.

Mehra A, Baker CL, Loros JJ, Dunlap JC. Post-translational modifications in circadian rhythms. Trends Biochem Sci 2009;34:483–90. doi:10.1016/j.tibs.2009.06.006.

Mitchell VD, Taylor CM, Bauer S. Comprehensive Analysis of Monomeric Phenolics in Dilute Acid Plant Hydrolysates. BioEnergy Res 2014;7:654–69. doi:10.1007/s12155-013-9392-6.

Mohnen D. Pectin structure and biosynthesis. Curr Opin Plant Biol 2008;11:266–77. doi:http://dx.doi.org/10.1016/j.pbi.2008.03.006.

Mojzita D, Herold S, Metz B, Seiboth B, Richard P. L- xylo -3-Hexulose Reductase Is the Missing Link in the Oxidoreductive Pathway for D-Galactose Catabolism in Filamentous Fungi. J Biol Chem 2012;287:26010–8. doi:10.1074/jbc.M112.372755.

Moreira LRS, Filho EXF. An overview of mannan structure and mannan-degrading enzyme systems. Appl Microbiol Biotechnol 2008;79:165–78. doi:10.1007/s00253-008-1423-4.

Morre DJ. Cell wall dissolution and enzyme secretion during leaf abscission. Plant Physiol 1968;43:1545–59.

Mountfort DO, Asher RA. Role of catabolite regulatory mechanisms in control of carbohydrate utilization by the rumen anaerobic fungus *Neocallimastix frontalis*. Appl Environ Microbiol 1983;46:1331–8.

Mylin LM, Johnston M, Hopper JE. Phosphorylated forms of GAL4 are correlated with ability to activate transcription. Mol Cell Biol 1990;10:4623–9. doi:10.1128/MCB.10.9.4623.

Nafisi M, Stranne M, Zhang L, van Kan JAL, Sakuragi Y. The Endo-Arabinanase BcAra1 Is a Novel Host-Specific Virulence Factor of the Necrotic Fungal Phytopathogen *Botrytis cinerea*. Mol Plant-Microbe Interact 2014;27:781–92. doi:10.1094/MPMI-02-14-0036-R.

Naik SN, Goud V V., Rout PK, Dalai AK. Production of first and second generation biofuels: A comprehensive review. Renew Sustain Energy Rev 2010;14:578–97. doi:10.1016/j.rser.2009.10.003.

Nehlin JO, Ronne H. Yeast MIG1 repressor is related to the mammalian early growth response and Wilms' tumour finger proteins. EMBO J 1990;9:2891–8.

Nishitani K, Masuda Y. Auxin-induced changes in the cell wall structure: Changes in the sugar compositions, intrinsic viscosity and molecular weight distributions of matrix polysaccharides of the epicotyl cell wall of *Vigna angularis*. Physiol Plant 1981;52:482–94. doi:10.1111/j.1399-3054.1981.tb02720.x.

Niu J, Alazi E, Reid ID, Arentshorst M, Punt PJ, Visser J, *et al.* An Evolutionarily Conserved Transcriptional Activator-Repressor Module Controls Expression of Genes for D-Galacturonic Acid Utilization in *Aspergillus niger*. Genetics 2017;205:169–83. doi:10.1534/genetics.116.194050.

Noguchi Y, Tanaka H, Kanamaru K, Kato M, Kobayashi T. Xylose Triggers Reversible Phosphorylation of XlnR, the Fungal Transcriptional Activator of Xylanolytic and Cellulolytic Genes in *Aspergillus oryzae*. Biosci Biotechnol Biochem 2011;75:953–9. doi:10.1271/bbb.100923.

O'Neill M a., Ishii T, Albersheim P, Darvill AG. Rhamnogalacturonan II: structure and function of a borate cross-linked cell wall pectic polysaccharide. Annu Rev Plant Biol 2004;55:109–39. doi:10.1146/annurev.arplant.55.031903.141750.

Ogawa M, Kobayashi T, Koyama Y. ManR, a Transcriptional Regulator of the β-Mannan Utilization System, Controls the Cellulose Utilization System in *Aspergillus oryzae*. Biosci Biotechnol Biochem 2013;77:426–9. doi:10.1271/bbb.120795.

Ogawa M, Kobayashi T, Koyama Y. ManR, a novel Zn(II)2Cys6 transcriptional activator, controls the β-mannan utilization system in *Aspergillus oryzae*. Fungal Genet Biol 2012;49:987–95. doi:10.1016/j.fgb.2012.09.006.

Orejas M, MacCabe AP, Perez Gonzalez JA, Kumar S, Ramon D. Carbon catabolite repression of the *Aspergillus nidulans* xlnA gene. Mol Microbiol 1999;31:177–84. doi:10.1046/j.1365-2958.1999.01157.x.

Oribe Y, Funada R, Kubo T. Relationships between cambial activity, cell differentiation and the localization of starch in storage tissues around the cambium in locally heated stems of *Abies sachalinensis* (Schmidt) Masters. Trees 2003;17:185–92. doi:10.1007/s00468-002-0231-1.

Orłowski A, Róg T, Paavilainen S, Manna M, Heiskanen I, Backfolk K, *et al.* How endoglucanase enzymes act on cellulose nanofibrils: role of amorphous regions revealed by atomistic simulations. Cellulose 2015;22:2911–25. doi:10.1007/s10570-015-0705-0.

Ortiz GE, Guitart ME, Albertó E, Fernández Lahore HM, Blasco M. Microplate assay for endo-polygalacturonase activity determination based on ruthenium red method. Anal

Biochem 2014;454:33–5. doi:10.1016/j.ab.2014.02.028.

Pardo E, Orejas M. The *Aspergillus nidulans* $Zn(II)_2Cys_6$ transcription factor AN5673/RhaR mediates L-rhamnose utilization and the production of α-L-rhamnosidases. Microb Cell Fact 2014;13:161. doi:10.1186/s12934-014-0161-9.

Peciulyte A, Anasontzis GE, Karlström K, Larsson PT, Olsson L. Morphology and enzyme production of *Trichoderma reesei* Rut C-30 are affected by the physical and structural characteristics of cellulosic substrates. Fungal Genet Biol 2014;72:64–72. doi:10.1016/j.fgb.2014.07.011.

van Peij NN, Gielkens MM, de Vries RP, Visser J, de Graaff LH. The transcriptional activator XlnR regulates both xylanolytic and endoglucanase gene expression in *Aspergillus niger*. Appl Environ Microbiol 1998;64:3615–9.

Pettersen RC. The Chemical Composition of Wood. U.S. Dep. Agric. For. Serv. For. Prod. Lab. Madison, WI 53705, 1984, p. 57–126. doi:10.1021/ba-1984-0207.ch002.

Phillips CM, Beeson WT, Cate JH, Marletta MA. Cellobiose dehydrogenase and a copper-dependent polysaccharide monooxygenase potentiate cellulose degradation by *Neurospora crassa*. ACS Chem Biol 2011;6:1399–406. doi:10.1021/cb200351y.

Pinto I, Pereira H, Usenius A. Heartwood and sapwood development within maritime pine (*Pinus pinaster* Ait.) stems. Trees - Struct Funct 2004;18:284–94. doi:10.1007/s00468-003-0305-8.

Polizeli M d. LTM, Jorge JA, Terenzi HF. Pectinase production by *Neurospora crassa*: purification and biochemical characterization of extracellular polygalacturonase activity. J Gen Microbiol 1991;137:1815–23. doi:10.1099/00221287-137-8-1815.

Popper ZA, Michel G, Herve C, Domozych DS, Willats WG, Tuohy MG, *et al.* Evolution and diversity of plant cell walls: from algae to flowering plants. Annu Rev Plant Biol 2011;62:567–90. doi:10.1146/annurev-arplant-042110-103809.

Portnoy T, Margeot A, Linke R, Atanasova L, Fekete E, Sándor E, *et al.* The CRE1 carbon catabolite repressor of the fungus *Trichoderma reesei*: a master regulator of carbon assimilation. BMC Genomics 2011;12:269. doi:10.1186/1471-2164-12-269.

Protzko RJ, Hach CA, Coradetti ST, Hackhofer MA, Magosch S, Thieme N, *et al.* Genome-wide and enzymatic analysis reveals efficient D-galacturonic acid metabolism in the basidiomycete yeast Rhodosporidium toruloides (manuscript in submission). MBio 2019.

Qi X, Behrens BX, West PR, Mort AJ. Solubilization and Partial Characterization of Extensin Fragments from Cell Walls of Cotton Suspension Cultures (Evidence for a Covalent Cross-Link between Extensin and Pectin). Plant Physiol 1995;108:1691–701. doi:10.1104/pp.108.4.1691.

Ragauskas AJ, Williams CK, Davison BH, Britovsek G, Cairney J, Eckert C a, *et al.* The path forward for biofuels and biomaterials. Science (80-) 2006;311:484–9. doi:10.1126/science.1114736.

Dos Reis TF, Menino JF, Bom VLP, Brown NA, Colabardini AC, Savoldi M, *et al.* Identification of glucose transporters in *Aspergillus nidulans*. PLoS One 2013;8:e81412. doi:10.1371/journal.pone.0081412.

Richard P, Hilditch S. d-Galacturonic acid catabolism in microorganisms and its biotechnological relevance. Appl Microbiol Biotechnol 2009;82:597–604. doi:10.1007/s00253-009-1870-6.

Ries L, Pullan ST, Delmas S, Malla S, Blythe MJ, Archer DB. Genome-wide transcriptional response of *Trichoderma reesei* to lignocellulose using RNA sequencing and comparison with *Aspergillus niger*. BMC Genomics 2013;14:541. doi:10.1186/1471-2164-14-541.

Riquelme M, Yarden O, Bartnicki-Garcia S, Bowman B, Castro-Longoria E, Free SJ, *et al.* Architecture and development of the *Neurospora crassa* hypha -- a model cell for polarized growth. Fungal Biol 2011;115:446–74. doi:10.1016/j.funbio.2011.02.008.

Roche CM, Loros JJ, McCluskey K, Glass NL. *Neurospora crassa*: Looking back and looking forward at a model microbe. Am J Bot 2014;101:2022–35. doi:10.3732/ajb.1400377.
Ronne H. Glucose repression in fungi. Trends Genet 1995;11:12–7. doi:10.1016/S0168-9525(00)88980-5.

Ruepp A. The FunCat, a functional annotation scheme for systematic classification of proteins from whole genomes. Nucleic Acids Res 2004;32:5539–45.

doi:10.1093/nar/gkh894.

Ruijter GJ., Visser J. Carbon repression in *Aspergilli*. FEMS Microbiol Lett 1997;151:103–14. doi:10.1111/j.1574-6968.1997.tb12557.x.

Ruijter GJG, Vanhanen SA, Gielkens MMC, van de Vondervoort PJI, Visser J. Isolation of *Aspergillus niger* creA mutants and effects of the mutations on expression of arabinases and L-arabinose catabolic enzymes. Microbiology 1997;143:2991–8. doi:10.1099/00221287-143-9-2991.

Saier MH, Reddy VS, Tsu B V, Ahmed MS, Li C, Moreno-Hagelsieb G. The Transporter Classification Database (TCDB): recent advances. Nucleic Acids Res 2016;44:D372–9. doi:10.1093/nar/gkv1103.

Samal A, Craig JP, Coradetti ST, Benz JP, Eddy JA, Price ND, *et al.* Network reconstruction and systems analysis of plant cell wall deconstruction by *Neurospora crassa*. Biotechnol Biofuels 2017;10:225. doi:10.1186/s13068-017-0901-2.

Sánchez OJ, Cardona C a, Sánchez ÓJ. Trends in biotechnological production of fuel ethanol from different feedstocks. Bioresour Technol 2008;99:5270–95. doi:10.1016/j.biortech.2007.11.013.

Sauter JJ, van Cleve B. Storage, mobilization and interrelations of starch, sugars, protein and fat in the ray storage tissue of poplar trees. Trees 1994;8:297–304. doi:10.1007/BF00202674.

Schmitz K, Protzko R, Zhang L, Benz JP. Spotlight on fungal pectin utilization—from phytopathogenicity to molecular recognition and industrial applications. Appl Microbiol Biotechnol 2019:1–18. doi:10.1007/s00253-019-09622-4.

Seibert T, Thieme N, Benz JP. Gene Expression Systems in Fungi: Advancements and Applications. 1st ed. Cham: Springer International Publishing; 2016. doi:10.1007/978-3-319-27951-0.

Seiboth B, Metz B. Fungal arabinan and L-arabinose metabolism. Appl Microbiol Biotechnol 2011;89:1665–73. doi:10.1007/s00253-010-3071-8.

Selker EU. Premeiotic instability of repeated sequences in *Neurospora crassa*. Annu Rev Genet 1990;24:579–613. doi:10.1146/annurev.ge.24.120190.003051.

Shiu S-H, Shih M-C, Li W-H. Transcription factor families have much higher expansion rates in plants than in animals. Plant Physiol 2005;139:18–26. doi:10.1104/pp.105.065110.

Sievers F, Wilm A, Dineen D, Gibson TJ, Karplus K, Li W, *et al.* Fast, scalable generation of high-quality protein multiple sequence alignments using Clustal Omega. Mol Syst Biol 2011;7:539. doi:10.1038/msb.2011.75.

Sims REH, Mabee W, Saddler JN, Taylor M. An overview of second generation biofuel technologies. Bioresour Technol 2010;101:1570–80. doi:10.1016/j.biortech.2009.11.046.

Skowyra D, Craig KL, Tyers M, Elledge SJ, Harper JW. F-Box Proteins Are Receptors that Recruit Phosphorylated Substrates to the SCF Ubiquitin-Ligase Complex. Cell 1997;91:209–19. doi:10.1016/S0092-8674(00)80403-1.

Sloothaak J, Odoni DI, Martins dos Santos VAP, Schaap PJ, Tamayo-Ramos JA. Identification of a Novel L-rhamnose Uptake Transporter in the Filamentous Fungus *Aspergillus niger*. PLOS Genet 2016;12:e1006468. doi:10.1371/journal.pgen.1006468.

Smith AM, Denyer K, Martin CR. What Controls the Amount and Structure of Starch in Storage Organs? Plant Physiol 1995;107:673–7.

Somerville C. Toward a Systems Approach to Understanding Plant Cell Walls. Science (80-) 2004;306:2206–11. doi:10.1126/science.1102765.

Somerville C, Youngs H, Taylor C, Davis SC, Long SP. Feedstocks for lignocellulosic biofuels. Science (80-) 2010;329:790–2. doi:10.1126/science.1189268.

Spinelli LBB, Lourdes T.M. Polizeli M, Terenzi HF, Jorge JA. Biochemical characterization of glucoamylase from the hyperproducer exo -1 mutant strain of *Neurospora* erassa. FEMS Microbiol Lett 1996;138:173–7. doi:10.1111/j.1574-6968.1996.tb08152.x.

Sternberg D, Sussman AS. Hyperproduction of some glycosidases in *Neurospora crassa*. Arch Microbiol 1974;101:303–20. doi:10.1007/BF00455947.

Stormo GD. DNA binding sites: representation and discovery. Bioinformatics 2000;16:16–23. doi:10.1093/bioinformatics/16.1.16.

Strauss J, Horvath HK, Abdallah BM, Kindermann J, Mach RL, Kubicek CP. The function of CreA, the carbon catabolite repressor of *Aspergillus nidulans*, is regulated at the transcriptional and post-transcriptional level. Mol Microbiol 1999;32:169–78. doi:10.1046/j.1365-2958.1999.01341.x.

Stricker AR, Grosstessner-Hain K, Würleitner E, Mach RL. Xyr1 (xylanase regulator 1) regulates both the hydrolytic enzyme system and D-xylose metabolism in *Hypocrea jecorina*. Eukaryot Cell 2006;5:2128–37. doi:10.1128/EC.00211-06.

Stricker AR, Steiger MG, Mach RL. Xyr1 receives the lactose induction signal and regulates lactose metabolism in *Hypocrea jecorina*. FEBS Lett 2007;581:3915–20. doi:10.1016/j.febslet.2007.07.025.

Stülke J, Hillen W. Carbon catabolite repression in bacteria. Curr Opin Microbiol 1999;2:195–201. doi:10.1016/S1369-5274(99)80034-4.

Sun J, Glass NL. Identification of the CRE-1 cellulolytic regulon in *Neurospora crassa*. PLoS One 2011;6:e25654. doi:10.1371/journal.pone.0025654.

Sun J, Phillips CM, Anderson CT, Beeson WT, Marletta MA, Glass NL. Expression and characterization of the *Neurospora crassa* endoglucanase GH5-1. Protein Expr Purif 2011;75:147–54. doi:http://dx.doi.org/10.1016/j.pep.2010.08.016.

Sun J, Tian C, Diamond S, Glass NL. Deciphering transcriptional regulatory mechanisms associated with hemicellulose degradation in *Neurospora crassa*. Eukaryot Cell 2012;11:482–93. doi:10.1128/EC.05327-11.

Syed K, Shale K, Pagadala NS, Tuszynski J. Systematic Identification and Evolutionary Analysis of Catalytically Versatile Cytochrome P450 Monooxygenase Families Enriched in Model Basidiomycete Fungi. PLoS One 2014;9:e86683. doi:10.1371/journal.pone.0086683.

Szilagyi M, Miskei M, Karanyi Z, Lenkey B, Pocsi I, Emri T. Transcriptome changes initiated by carbon starvation in *Aspergillus nidulans*. Microbiology 2013;159:176–90. doi:10.1099/mic.0.062935-0.

Tamayo-Ramos JA, Flipphi M, Pardo E, Manzanares P, Orejas M. L-Rhamnose induction of *Aspergillus nidulans* α-L-rhamnosidase genes is glucose repressed via a CreA-independent mechanism acting at the level of inducer uptake. Microb Cell Fact 2012;11:26. doi:10.1186/1475-2859-11-26.

Tamayo EN, Villanueva A, Hasper AA, Graaff LH de, Ramón D, Orejas M. CreA mediates repression of the regulatory gene xlnR which controls the production of xylanolytic enzymes in *Aspergillus nidulans*. Fungal Genet Biol 2008;45:984–93. doi:10.1016/j.fgb.2008.03.002.

Tan L, Eberhard S, Pattathil S, Warder C, Glushka J, Yuan C, *et al.* An Arabidopsis Cell Wall Proteoglycan Consists of Pectin and Arabinoxylan Covalently Linked to an Arabinogalactan Protein. Plant Cell 2013;25:270–87. doi:10.1105/tpc.112.107334.

Tani S, Kawaguchi T, Kobayashi T. Complex regulation of hydrolytic enzyme genes for cellulosic biomass degradation in filamentous fungi. Appl Microbiol Biotechnol 2014;98:4829–37. doi:10.1007/s00253-014-5707-6.

Tate CG, Muiry JAR, Henderson PJF. Mapping, cloning, expression, and sequencing of the rhaT gene, which encodes a novel L-rhamnose-H+ transport protein in *Salmonella typhimurium* and *Escherichia coli*. J Biol Chem 1992;267:6923–32.

Taylor AM, Gartner BL, Morrell JJ. Heartwood formation and natural durability - a review. Wood Fiber Sci 2002;34:587–611.

Team RC. R: A language and environment for statistical computing 2013.

Teramoto A, Fuchigami M. Changes in Temperature, Texture, and Structure of Konnyaku (Konjac Glucomannan Gel) During High-pressure-freezing. J Food Sci 2000;65:491–7. doi:10.1111/j.1365-2621.2000.tb16034.x.

The Gene Ontology Consortium. Expansion of the Gene Ontology knowledgebase and resources. Nucleic Acids Res 2017;45:D331–8. doi:10.1093/nar/gkw1108.

Thieme N, Wu VW, Dietschmann A, Salamov AA, Wang M, Johnson J, *et al.* The transcription factor PDR-1 is a multi-functional regulator and key component of pectin deconstruction and catabolism in *Neurospora crassa*. Biotechnol Biofuels 2017;10:149.

doi:10.1186/s13068-017-0807-z.

Thornber J, Northcote D. Changes in the chemical composition of a cambial cell during its differentiation into xylem and phloem tissue in trees. 2. Carbohydrate constituents of each main component. Biochem J 1961;81:455–64. doi:10.1042/bj0810455.

Tian C, Beeson WT, Iavarone AT, Sun J, Marletta MA, Cate JHD, *et al.* Systems analysis of plant cell wall degradation by the model filamentous fungus *Neurospora crassa*. Proc Natl Acad Sci U S A 2009;106:22157–62. doi:10.1073/pnas.0906810106.

Tian C, Li J, Glass NL. Exploring the bZIP transcription factor regulatory network in *Neurospora crassa*. Microbiology 2011;157:747–59. doi:10.1099/mic.0.045468-0.

Timell TE. Recent progress in the chemistry of wood hemicelluloses. Wood Sci Technol 1967;1:45–70. doi:10.1007/BF00592255.

Trapnell C, Hendrickson DG, Sauvageau M, Goff L, Rinn JL, Pachter L. Differential analysis of gene regulation at transcript resolution with RNA-seq. Nat Biotechnol 2012;31:46–53. doi:10.1038/nbt.2450.

Trapnell C, Williams BA, Pertea G, Mortazavi A, Kwan G, van Baren MJ, *et al.* Transcript assembly and quantification by RNA-Seq reveals unannotated transcripts and isoform switching during cell differentiation. Nat Biotechnol 2010;28:511–5. doi:10.1038/nbt.1621.

Vaheri M, Leisola M, Kauppinen V. Transglycosylation products of cellulase system of*Trichoderma reesei*. Biotechnol Lett 1979;1:41–6. doi:10.1007/BF01395789.

Varner JE, Lin L-S. Plant cell wall architecture. Cell 1989;56:231–9. doi:10.1016/0092-8674(89)90896-9.

Vashee S, Xu H, Johnston S, Kodadek T. How do "Zn_2 Cys_6" proteins distinguish between similar upstream activation sites? Comparison of the DNA-binding specificity of the GAL4 protein in vitro and in vivo. J Biol Chem 1993;268:24699–706.

Vincken J-P, Schols HA, Oomen RJFJ, McCann MC, Ulvskov P, Voragen AGJ, *et al.* If homogalacturonan were a side chain of rhamnogalacturonan I. Implications for cell wall architecture. Plant Physiol 2003;132:1781–9.

Vinuselvi P, Kim MK, Lee SK, Ghim CM. Rewiring carbon catabolite repression for microbial cell factory. BMB Rep 2012;45:59–70. doi:10.5483/BMBRep.2012.45.2.59.

Vogel HJ. A convenient growth medium for *Neurospora* (Medium N). Microb Genet Bull 1956;13.

de Vries RP, van den Broeck HC, Dekkers E, Manzanares P, de Graaff LH, Visser J. Differential expression of three alpha-galactosidase genes and a single beta-galactosidase gene from *Aspergillus niger*. Appl Environ Microbiol 1999;65:2453–60. doi:10.1094/PHYTO-96-0181.

de Vries RP, Jansen J, Aguilar G, Pařenicová L, Joosten V, Wülfert F, *et al.* Expression profiling of pectinolytic genes from *Aspergillus niger*. FEBS Lett 2002;530:41–7. doi:10.1016/S0014-5793(02)03391-4.

Wang B, Cai P, Sun W, Li J, Tian C, Ma Y. A transcriptomic analysis of *Neurospora crassa* using five major crop residues and the novel role of the sporulation regulator rca-1 in lignocellulase production. Biotechnol Biofuels 2015;8:21. doi:10.1186/s13068-015-0208-0.

Wang B, Li J, Gao J, Cai P, Han X, Tian C. Identification and characterization of the glucose dual-affinity transport system in *Neurospora crassa*: pleiotropic roles in nutrient transport, signaling, and carbon catabolite repression. Biotechnol Biofuels 2017;10:17. doi:10.1186/s13068-017-0705-4.

Weirauch MT, Yang A, Albu M, Cote AG, Montenegro-Montero A, Drewe P, *et al.* Determination and Inference of Eukaryotic Transcription Factor Sequence Specificity. Cell 2014;158:1431–43. doi:10.1016/j.cell.2014.08.009.

Werpy T, Petersen G, Aden A, Bozell J, Holladay J, White J, *et al.* Top Value Added Chemicals from Biomass Volume I—Results of Screening for Potential Candidates from Sugars and Synthesis Gas. 2004.

Westergaard M, Mitchell HK. *NEUROSPORA* V. A SYNTHETIC MEDIUM FAVORING SEXUAL REPRODUCTION. Am J Bot 1947;34:573–7. doi:10.1002/j.1537-2197.1947.tb13032.x.

Winderickx J, Holsbeeks I, Lagatie O, Giots F, Thevelein J, de Winde H. From feast to famine; adaptation to nutrient availability in yeast, Springer, Berlin, Heidelberg; 2003, p. 305–86. doi:10.1007/3-540-45611-2_7.

Wink M. Plant breeding: importance of plant secondary metabolites for protection against pathogens and herbivores. Theor Appl Genet 1988;75:225–33. doi:10.1007/BF00303957.

Wu VW-X. Lessons in Plant Cell Wall Degradation by the Ascomycete Model Fungus, *Neurospora crassa*. University of California, Berkeley, 2017.

Wu VW, Thieme N, Huberman LB, Dietschmann A, Bleek E, Kowbel DJ, *et al.* The plant biomass ENCODE of a filamentous fungi (manuscript in preparation) 2019.

Xiang Q, Glass NL. Identification of vib-1, a Locus Involved in Vegetative Incompatibility Mediated by het-c in *Neurospora crassa*. Genetics 2002;162:89–101.

Xiong Y, Sun J, Glass NL. VIB1, a Link between Glucose Signaling and Carbon Catabolite Repression, Is Essential for Plant Cell Wall Degradation by *Neurospora crassa*. PLoS Genet 2014;10:e1004500. doi:10.1371/journal.pgen.1004500.

Xiong Y, Wu VW, Lubbe A, Qin L, Deng S, Kennedy M, *et al.* A fungal transcription factor essential for starch degradation affects integration of carbon and nitrogen metabolism. PLOS Genet 2017;13:e1006737. doi:10.1371/journal.pgen.1006737.

Yoav S, Salame TM, Feldman D, Levinson D, Ioelovich M, Morag E, *et al.* Effects of cre1 modification in the white-rot fungus Pleurotus ostreatus PC9: altering substrate preference during biological pretreatment. Biotechnol Biofuels 2018;11:212. doi:10.1186/s13068-018-1209-6.

Yoshimura M, Takaya T, Nishinari K. Rheological studies on mixtures of corn starch and konjac-glucomannan. Carbohydr Polym 1998;35:71–9. doi:10.1016/S0144-8617(97)00232-4.

Zhang L, Lubbers RJM, Simon A, Stassen JHM, Vargas Ribera PR, Viaud M, *et al.* A novel Zn_2 Cys_6 transcription factor BcGaaR regulates D-galacturonic acid utilization in B otrytis cinerea. Mol Microbiol 2016;100:247–62. doi:10.1111/mmi.13314.

Zhong F, Yokoyama W, Wang Q, Shoemaker CF. Rice Starch, Amylopectin, and Amylose: Molecular Weight and Solubility in Dimethyl Sulfoxide-Based Solvents. J Agric Food Chem 2006;54:2320–6. doi:10.1021/jf051918i.

Znameroski E a, Glass NL. Using a model filamentous fungus to unravel mechanisms of lignocellulose deconstruction. Biotechnol Biofuels 2013;6:6. doi:10.1186/1754-6834-6-6.

Znameroski EA, Coradetti ST, Roche CM, Tsai JC, Iavarone AT, Cate JHD, *et al.* Induction of lignocellulose-degrading enzymes in *Neurospora crassa* by cellodextrins. Proc Natl Acad Sci U S A 2012;109:6012–7. doi:10.1073/pnas.1118440109.

Znameroski EA, Li X, Tsai JC, Galazka JM, Glass NL, Cate JHD. Evidence for Transceptor Function of Cellodextrin Transporters in *Neurospora crassa*. J Biol Chem 2014;289:2610–9. doi:10.1074/jbc.M113.533273.

Acknowledgements

Zuallererst möchte ich mich bei Prof. Dr. J. Philipp Benz bedanken, dass ich diese Doktorarbeit in seiner Arbeitsgruppe durchführen und schreiben durfte. An meiner Doktorarbeit zuarbeiten und nebenbei ein Labor von Grund auf mit aufbauen war teilweise anstrengend, aber auch sehr lehrreich und erfüllend.
Des Weiteren möchte ich mich bei Prof. Dr. Wolfgang Liebl für die Übernahme meines Mentorats bedanken und dafür, dass er diese Arbeit als mein Zweitprüfer kontrolliert. Mein weiterer Dank gilt außerdem Prof. Dr. Klaus Richter für die Übernahme des Prüfungsvorsitzes und die interessanten und stets freundlichen Gespräche während der Arbeit. Danke möchte ich auch Prof. Dr. André Fleißner sagen, nicht nur dafür, dass er sich bereit erklärt hat mein Drittprüfer zu sein, sondern auch dafür, dass er mich damals auf die offene Stelle bei Prof. Benz aufmerksam gemacht hat.
Meinem Freund und Kollegen Vincent Wu schulde ich auch ein großes Dankeschön für die Anfertigung der Proben des ENCODE Projekts, sowie die geduldige Beantwortung meiner Fragen zu RNA-Seq und Datenauswertung. Ohne dich und deinen Einsatz wäre diese Arbeit (wortwörtlich) nur halb so gut. An dieser Stelle möchte ich mich daher auch bei Raphael Gabriel bedanken, der mit vollem Herzen beim EXO-1 Projekt dabei ist!
Es war eine tolle Zeit in der Arbeitsgruppe Holz-Bioprozesse, die ich im Leben nicht missen möchte. Von den „bescheidenen“ Anfängen, als nur Tanja, Petra und ich im Labor waren, bis heute war es immer eine angenehme Zeit. Daher möchte ich mich hier auch bei allen Mitgliedern der Arbeitsgruppe für die gute Zusammenarbeit und das entspannte Miteinander bedanken.
Ein besonderer Dank geht an Petra und Sabrina für ihre technische und organisatorische Unterstützung im Alltag der Arbeitsgruppe, ohne die schon längst alles im Chaos versunken wäre. Des Weiteren möchte ich herzlich bei Lara bedanken für die stets gute Zusammenarbeit und Unterstützung von Anfang an bis zum Ende. Auch den neusten Mitgliedern der Arbeitsgruppe Holz-Bioprozesse gilt mein Dank. Maria, Kevin, Christina, Yuxin und Lisa: Es war immer schön mit euch über die Arbeit oder auch einfach alles andere zu reden. Ich hoffe ihr habt eine großartige Zeit und dass eure Projekte immer gut laufen!
Ich möchte an dieser Stelle auch meinen ehemaligen Masteranden Axel, Chris und Magdalena danken. Es hat viel Spaß gemacht mit euch zusammen zu arbeiten und ich wünsche euch weiterhin viel Erfolg bei euren eingeschlagenen Lebenswegen.
Da das Leben nicht nur aus Arbeit besteht möchte ich mich hier auch kurz bei meinen Freunden für ihre Unterstützung und die immer spaßige Zeit zusammen bedanken! Und zu guter Letzt möchte ich mich bei meiner Familie, insbesondere meinen Eltern, bedanken. Danke, dass ihr immer hinter mir gestanden und mich bei allem unterstützt habt!